Enhancement of the conceptual aircraft design process through certification constraints management and full mission simulations

Peter Schmollgruber

Université Fédérale

Toulouse Midi-Pyrénées

THÈSE

En vue de l'obtention du

DOCTORAT DE L'UNIVERSITÉ DE TOULOUSE

Délivré par :

Institut Supérieur de l'Aéronautique et de l'Espace (ISAE)

Présentée et soutenue par :
Peter SCHMOLLGRUBER
le vendredi 7 décembre 2018

Titre :

Enhancement of the conceptual aircraft design process through certification constraints management and full mission simulations

Amélioration du processus de conception avion en prenant en compte les contraintes de certification et des simulations de mission complètes

---

École doctorale et discipline ou spécialité :
ED Aéronautique et Astronautique

Unité de recherche :
Équipe d'accueil ISAE-ONERA MOIS

Directeur(s) de Thèse :

Pr. Yves GOURINAT (ISAE-SUPAERO, ICA), Advisor
Dr. Nathalie BARTOLI (ONERA), Co-Advisor

Jury :

Pr. Marcel MONGEAU	ENAC	President
Pr. Eric FERON	Georgia Institute of Technology	External Referee
Pr. Giulio ROMEO	Politecnico di Torino	External Referee
Mr. Darold CUMMINGS	Aerospace consultant	Examiner
Pr. Timothy TAKAHASHI	Arizona State University	Examiner
Pr. Yves GOURINAT	ISAE-SUPAERO, ICA	Advisor
Dr. Nathalie BARTOLI	ONERA	Co-Advisor

Université de Toulouse
Institut Supérieur de l'Aéronautique et de l'Espace

Enhancement of the aircraft design process through certification constraints management and full mission simulations

Doctoral Thesis

prepared by: Peter Schmollgruber

Supervisors: Nathalie Bartoli
Yves Gourinat

Reviewers: Eric Feron
Giulio Romeo

Examiners: Darold Cummings
Marcel Mongeau
Timothy Takahashi

Toulouse

December 2018

To Chiara, Heiko and Alessandro

Contents

Acknowledgements

This PhD has been an incredible journey that would not have been possible without the help and support of many persons:

Thank you Nathalie Bartoli for accepting from start without any questions to be my co-advisor for an unconventional PhD. Your continuous guidance during the entire research and your thorough comments on the manuscript were key to the final result.

Thank you Yves Gourinat for accepting to be my co-advisor and for reactivating my PhD project in 2012. You turned the idea into a reality. Also, the addition of certification aspects was spot on.

Thank you Darold Cummings, Pr. Eric Feron, Pr. Marcel Mongeau, Pr. Giulio Romeo and Pr. Tim Takahashi. I was truly honored to have you as members of my PhD jury.

Thank you Judicaël Bedouet for your important help with GAMME in the development of the Certification Constraints Module and your computations of flight trajectories following real routes;

Thank you Sébastien Defoort for the efficient and appreciated collaboration towards the development of FAST and the review of the manuscript;

Thank you Rémi Lafage for your full revision of FAST to meet computer science standards;

Thank you Alessandro Sgueglia, Julien Mariné, Antony Delclos, Antoine Dompnier and Li Yan for your specific work on FAST and on the modules of the expanded MDAO process;

Thank you Sylvain Dubreuil for your contribution on the sensitivity analyses;

Thank you Thierry Lefebvre for sharing the early battles in trying to develop the aircraft design and advanced method activities;

Thank you Emmanuel Benard for your efforts in the promotion of FAST at ISAE-SUPAERO;

Thank you to the JSBSim community and Bill Galbraight for their work and availability;

Thank you to the late Ray Whitford for the exchanges during the final manuscript rush;

Thank you to ONERA collegues who offered kind encouragments all through the years;

Thank you to the girls for their motivation with a thought to dad;

Thank you to Heiko and Alessandro for being such an endless source of joy and energy;

Grazie, Chiara for always being a positive force in my life and for taking care of many many things that are needed to run our wonderful family.

Summary

The design of a new aircraft is initiated at the conceptual design phase. In an initial step, aircraft designers, disciplinary and subsystems experts identify a set of potential concepts that could fulfill the customer requirements. To select the most promising candidates, aircraft designers carry out the sizing process through a Multidisciplinary Design Analysis. Nowadays, in the field of civil transport aircraft, environmental constraints set challenging goals in terms of fuel consumption for the next generations of airplanes. With the "tube and wing" configuration offering low expectations on further improvements, disruptive vehicle concepts including new technologies are investigated. However, little information on such architectures is available in the early phases of the design process. Thus, in order to avoid mistakenly selecting or eliminating a wrong concept, a key objective in Aircraft Design research is to add knowledge in the Multidisciplinary Design Analysis.

Nowadays, this objective is achieved with different approaches: implementation of Multidisciplinary Design Optimization, addition of accuracy through high fidelity analyses, introduction of new disciplines or systems and uncertainty management. The role of the aircraft designer is then to combine these options in a multidisciplinary design process to converge to the most promising concept meeting certification constraints. To illustrate this process, the optimization of a transport aircraft featuring ground based assistance has been performed. Using monolithic optimization architecture and advanced structural models for the wing and fuselage, this study emphasized the impact of certification constraints on final results. Further review of the regulatory texts concluded that aircraft simulation capabilities are needed to assess some requirements. The same need has been identified in the field of Air Traffic Management that provides constraints for aircraft operations. This research proposes then to add knowledge through an expansion of the Multidisciplinary Design Analysis and Optimization with a new Certification Constraint Module and full simulation capabilities.

Following the development of the Certification Constraint Module (CCM), its capabilities have been used to perform four optimization problems associated to a conventional civil transport aircraft based on the ONERA / ISAE-SUPAERO sizing tool called FAST. Facilitated by the Graphical User Interface of the CCM, the setup time of these optimizations has been reduced and the results clearly confirmed the necessity to consider certification constraints very early in the design process in order to select the most promising concepts.

To achieve full simulation capabilities, the multidisciplinary analysis within FAST had to be enhanced. First, the aerodynamics analysis tool has been modified so that necessary coefficients for a 6 Degrees-of-Freedom model could be generated. Second, a new module computing inertia properties has been added. Last, the open source simulator JSBSim has been used including different control laws for stability augmentation and automated navigation. The comparison between flight trajectories obtained with FAST and real aircraft data recorded with ADS-B antenna confirmed the validity of the approach.

Résumé

La conception d'un nouvel avion est initiée durant la phase avant-projet. Dans un premier temps, les concepteurs d'aéronefs identifient un ensemble de concepts potentiels pouvant répondre aux exigences du client en s'appuyant sur des informations fournies par les spécialistes disciplinaires et experts système. Ensuite, les solutions sont évaluées via un processus de dimensionnement basé sur une analyse multidisciplinaire. Dans le domaine des avions de transport civil, les objectifs ambitieux en termes de consommation de carburant amènent à étudier des configurations innovantes incluant de nouvelles technologies. Cependant, peu de données sur de telles architectures sont disponibles dans les phases amont de la conception. Ainsi, afin d'éviter une sélection ou élimination erronnée d'une solution, un objectif clé de la recherche en conception d'aéronefs est l'ajout de connaissances dans l'analyse multidisciplinaire.

Aujourd'hui, cet objectif est atteint avec différentes approches: application d'optimisations multidisciplinaires, ajout de précision grâce aux analyses haute fidélité, introduction de nouvelles disciplines ou systèmes et enfin, gestion de l'incertitude. Le rôle du concepteur est alors de combiner ces options dans un processus de conception multidisciplinaire afin de converger vers le concept le plus performant tout en répondant aux contraintes de certification. Afin d'illustrer ce processus, l'optimisation d'un avion de transport avec assistance au sol pour le décollage qui a mis en évidence l'impact des contraintes de certification sur la conception du véhicule a été effectuée. La revue successive des textes réglementaires et de recherches associées de la gestion du trafic aérien ont conclu à la nécessité d'inclure des simulations au sein de l'analyse multidisciplinaire. Tenant compte de ces conclusions, la recherche effectuée dans le cadre de cette thèse propose alors d'ajouter des connaissances en développant l'analyse et l'optimisation de la conception multidisciplinaire avec un nouveau module de contrainte de certification et des fonctionnalités de simulation complètes.

Développé dans le cadre de la thèse, le module de contraintes de certification (CCM) a été utilisé pour résoudre quatre problèmes d'optimisation associés à un avion de transport civil classique basé sur l'outil de dimensionnement ONERA / ISAE-SUPAERO appelé FAST. Grâce à l'interface utilisateur du CCM, un gain de temps au niveau de la mise en place de ces optimisations a constaté. De plus, les résultats ont confirmé la nécessité de définir au mieux et dès que possible les contraintes de certification.

Pour atteindre des capacités de simulation complètes, l'analyse multidisciplinaire au sein de FAST a été améliorée. Premièrement, l'outil d'analyse aérodynamique a été modifié afin de générer la base de données complète pour alimenter un modèle à 6 degrés de liberté. Ensuite, un nouveau module de calcul des propriétés d'inertie a été ajouté. Enfin, le simulateur open source JSBSim a été utilisé avec différentes lois de contrôle pour augmenter la stabilité et permettre la navigation automatisée. La comparaison entre les trajectoires de vol obtenues avec FAST et les données réelles sur les avions enregistrées avec une antenne ADS-B a confirmé la validité de l'approche.

Acronyms

ACODE	Airliner COnceptual DEsign
AGILE	Aircraft 3rd Generation MDO for Innovative coLlaboration of heterogeneous teams of Experts
AMC	Acceptable Means of Compliance
ANS	Air Navigation Services
APM	Aircraft Performance Model
ATC	Air Traffic Control
ATS	Air Transportation System
BADA	Base of Aircraft DAta
BWB	Blended Wing Body
CAD	Computer Aided Design
CAH	Cruise Altitude Hold
CAM	Computer Aided Manufacturing
CCM	Certification Constraints Module
CDR	Critical Design Review
CFD	Computational Fluid Dynamics
CoG	Center of Gravity
COMPACT	Code d'Optimisation Multi Paramétrique adapté aux Avions Civils de Transport
CVCH	Cruise VC Hold
DEP	Distributed Electric Propulsion
DoF	Degree(s)-of-Freedom
EASA	European Aviation Safety Agency
EIS	Entry Into Service
EU	European Union
FAA	Federal Aviation Administration
FAST	Fixed wing Aircraft Sizing Tool
FCS	Flight Control System
FEA	Finite Element Analysis
FW	Fuel Weight
GABRIEL	integrated Ground And on-Board system for support of the aircraft safe take-off and Landing
GUI	Graphical User Interface
IATA	International Air Transport Association
FOD	Foreign Object Damage
HWB	Hybrid Wing Body
MDA	Multidisciplinary Design Analysis
MDAO	Multidisciplinary Design Analysis and Optimization
MDF	Multi-Disciplinary Feasible

MoM	Measure of Merit
MLW	Maximum Landing Weight
MTOW	Maximum Take Off Weight
MZFW	Maximum Zero Fuel Weight
NLF	Natural Laminar Flow
NPSS	Numerical Propulsion System Simulation
OEI	One Engine Inoperative condition
OWE	Operating Weight Empty
PID	Proportional Integral Derivative
PDR	Preliminary Design Review
RANS	Reynolds Averaged Navier Stokes
RoC	Rate of Climb
SAS	Stability Augmentation System
SBW	Strut-Braced Wing
SRR	System Requirements Review
SSA	Single-aiSle Aircraft
TRL	Technology Readiness Level
TWA	Transcontinental and Western Air
VTP	Vertical Tail Plane
XDSM	eXtended Design Structure Matrix

Nomenclature

$^{(0)}$	Initial guess for a given variable
^{t}	Fixed value for an iteration
*	Optimized value
α	Angle of attack
β	Angle of sideslip
δ_a	Aileron deflection (angle)
$\delta_{a\ norm}$	Aileron deflection (normalized)
δ_e	Elevator deflection (angle)
$\delta_{e\ norm}$	Elevator deflection (normalized)
δ_r	Rudder deflection (angle)
δ_{stab}	Stabilizer deflection (angle)
$\delta_{throttle\ norm}$	Engine throttle position (normalized)
ΔCAS	Difference between the target CAS and the actual aircraft CAS
Δh	Difference between the target altitude and the actual aircraft altitude
ΔM	Difference between the target Mach number and the actual aircraft Mach number
$\Delta\phi$	Difference between the target roll angle and the actual aircraft roll angle
$\Delta\psi$	Difference between the target heading and the actual aircraft heading
$\phi_{aircraft}$	Actual roll angle of the aircraft during simulations
ϕ_{target}	Target value for the aircraft roll angle
$\psi_{aircraft}$	Actual heading of the aircraft during simulations
ψ_{target}	Target value for the aircraft heading
A/C	Vector of data describing the aircraft geometry
$C_{D0\ correction}$	Zero lift Drag coefficient due to Vertical Tail Plane, nacelles and pylones
$C_{D\ compressibility}$	Drag coefficient due to compressibility effects
$C_{D\ \delta_e}$	Drag coefficient due to elevator deflection
$C_{D\ gear}$	Drag coefficient due to landing gear
$C_{D\ wbh}$	Drag coefficient of the wing, fuselage and Horizontal Tail Plane
$C_{L\ \dot{\alpha}}$	Variation of the Lift coefficient with respect to rate of change of angle of attack
$C_{L\ \delta_e}$	Lift coefficient generated by elevator deflection
$C_{L\ q}$	Variation of the Lift coefficient with respect to pitch rate
$C_{L\ wbh}$	Lift coefficient generated by the wing, body and Horizontal Tail Plane configuration
$C_{l\ \beta}$	Variation of Rolling moment coefficient with respect to sideslip angle
$C_{l\ \delta_a}$	Variation of Rolling moment coefficient with respect to aileron deflection
$C_{l\ \delta_r}$	Variation of Rolling moment coefficient with respect to rudder deflection

$C_{l\,p}$	Variation of Rolling moment coefficient with respect to roll rate
$C_{l\,r}$	Variation of Rolling moment coefficient with respect to yaw rate
$C_{m\,\dot{\alpha}}$	Variation of Pitching moment coefficient with respect to rate of change of angle of attack
$C_{m\,\delta_e}$	Pitching moment coefficient generated by elevator deflection
$C_{m\,q}$	Variation of Pitching moment coefficient with respect to Pitch rate
$C_{m\,wbh}$	Pitching moment coefficient generated by the wing, body and Horizontal Tail Plane configuration
$C_{n\,\beta}$	Variation of Yawing moment coefficient with respect to sideslip angle
$C_{n\,\delta_r}$	Variation of Yawing moment coefficient with respect to rudder deflection
$C_{n\,r}$	Variation of Yawing moment coefficient with respect to yaw rate
$C_{Y\,\beta}$	Variation of side force coefficient with respect to sideslip angle
$CAS_{aircraft}$	Actual Calibrated Air Speed of the aircraft during simulations
CAS_{target}	Target value for the aircraft Calibrated Air Speed
c_i	Constraints values calculated by the Certification and Operational constraints module
h	Altitude
$h_{aircraft}$	Actual altitude of the aircraft during simulations
h_{target}	Target value for the aircraft altitude
I_{xx}	Moment of inertia about x axis
I_{xz}	Product of inertia about x and z axes
I_{yy}	Moment of inertia about y axis
I_{zz}	Moment of inertia about z axis
k_d	Derivative gain associated to the PID controller
k_i	Integral gain associated to the PID controller
k_p	Proportional gain associated to the PID controller
M	Mach number
$M_{aircraft}$	Target value for the aircraft Mach number
M_{target}	Actual Mach number of the aircraft during simulations
$m_{f\,sizing}$	Mass of fuel for the sizing mission
$m_{f\,operational}$	Mass of fuel for the operational mission
LFBO	Toulouse-Blagnac airport
LFPO	Paris-Orly airport
N_{pax}	Number of passengers
OWE_m	Calculated Operating Weight Empty based on mission fuel estimation
$V_{approach}$	Approach speed
V_{FC} /M_{FC}	Maximum speed for stability characteristics
V_{FE}	Maximum flap extended speed
V_{LE}	Maximum landing gear extended speed
V_{LOF}	Lift-off speed

V_{REF}	Reference landing speed
V_{SR}	Reference stall speed
V_{SR0}	Reference stall speed in the landing configuration
$W_{payload}$	Weight of the payload

List of figures

List of tables

Introduction

The aeronautical industry has always been characterized by mergers and acquisitions driven by a very competitive environment. The US manufacturer Boeing for example, founded in 1916, merged with McDonnell Douglas in 1997. McDonnell Douglas was itself the result of a merger in 1967 between the Douglas Aircraft Company founded in 1921 and the Mc Donnell Aircraft Corporation founded in 1939. Today, this industry landscape features very large manufacturers whose revenues reach tens of billions (US $) with profits in the order of billions (US $). In the large jet airliner market, such business contest is well illustrated by the Airbus / Boeing rivalry that started in the 1990's. Within each company, the goal is then to develop a product that is superior to the one offered by competing entities in terms of performances and / or profitability. For civil transport aircraft, the main customers are airlines. From the point of view of these airplane operators, the goal is to maximize the revenue passenger miles metric so that the aircraft commercial flights become profitable. Thus, airlines primary interest is naturally an airplane with low acquisition cost and low operating costs. Looking at the Life Cycle Cost of an aircraft program, these latter essential elements are basically defined during the design stage. It is true that airlines can have specific internal procedures to reduce maintenance cost and maximize fuel savings to minimize Direct Operating Cost but such gains are small with respect to the ones that can be made through design.

Under the responsibility of the airplane manufacturer, the design step is divided into three phases identified as conceptual design, preliminary design and detail design. In conceptual design, aircraft designers explore a wide range of vehicle concepts that could meet the customer requirements. These concepts are analyzed through multidisciplinary tools that capture the possible compromises to be made between the key disciplines or subsystems. After possible optimization loops, the most promising design or family of designs is selected for further refinements. These improvements are carried out during preliminary design. At this stage, the preferred concept is deeply analyzed and revised through high fidelity computations and experimental tests. In parallel, evaluations are made to make sure that the aircraft can be built for a given budget and timeframe. It is at the end of this phase that the company commits to the program launch and the associated expenses. Following the decision to build the aircraft, the detail design is started. In this phase, the design of all components up to the smallest bolt is carried out considering all necessary details for manufacturing. Concurrent studies on the manufacturing plant are performed in order to prepare the industrialization phase. Large scale tests for certification purposes are also made to ensure the vehicle airworthiness.

As it is the first design step, decisions made during conceptual design strongly affect the entire program (about 65 % of program cost is fixed at the end of conceptual design) and from the beginning, customer requirements necessitate well-adjusted tradeoff analyses. A low acquisition cost for example would favor the use of proven technologies while the reduction of operating cost, directly associated to fuel burn, is pushing for the implementation of advanced technologies. On top of such customer requirements, airplane manufacturers have to meet stringent constraints in terms of safety and environmental impact. With the objective of making the best possible choices and defining the most promising concept, design engineers develop a Multidisciplinary Design Analysis (MDA) that allows

the sizing and performance assessment taking into account the key disciplines or systems. Implemented within a computerized process, this MDA relies on disciplinary analyses that supply many data so that a performance analysis over a reference mission can be made. More important, this MDA is supported by a large amount of historical data as vehicles result from a progressive integration of technologies. From the outcomes of this tool, designers can evaluate different options and assess possible technology scenario to identify an efficient and viable concept for a given Entry Into Service (EIS) date.

For civil transport aircraft, following the introduction of the Boeing 707 in 1958, the classical "tube and wing" configuration has been developed and optimized taking into account essential improvements of the turbofan engine. Today, 60 years have passed and the latest generation of aircraft reaches the impressive fuel burn value of 2.23 liters per 100 km per seat. In comparison, cars can reach a metric fuel mileage of 3.2 liters per 100 km. However, market shares and environmental constraints are continuously pulling for further improvements that are hardy attainable with an aircraft configuration and associated engine technology that have been optimized for decades. For this reason, many studies at conceptual design level explore unconventional vehicles that feature disruptive configurations or technologies (e.g. Blended Wing Body, aircraft with High Aspect Ratio Truss-Braced Wing, Hybrid Electric Distributed Propulsion concepts…). Unfortunately, for the definition and sizing of such radically different concepts, there is a key problem: the Multidisciplinary Design Analysis that is the core of the evaluation and tradeoff process cannot rely on historical data or available knowledge. For research in Aircraft Design, it becomes mandatory to answer the following question: "**How to add knowledge in the Multidisciplinary Design Analysis at aircraft conceptual design level?**"

This question not being new, many approaches have been followed in order to introduce more knowledge to the aircraft MDA. First, the introduction of a Multidisciplinary Design Optimization enables aircraft designers to first explore the design space and secondly to mathematically identify the best aircraft or the best family of aircraft. Such information is key to make sure that the best design decision are taken and that they are not affected by historical habits. In addition, such an optimization process provides additional information about active and non-violated constraints that help in possible review of key requirements. A second option to add knowledge is obviously to increase the accuracy and reliability of the disciplinary analyses so that the Multidisciplinary Design Analysis and Optimization (MDAO) process can converge to a solution on which designers have a certain level of confidence. Computational Fluid Dynamics approaches and Finite Element Method are examples of tested solutions that add key information early in the design process with some issues that are associated to setup and computational time. The third option for designers is to add new disciplinary or system analyses within the MDA to open the design space. A recent example to illustrate such a solution is related to Hybrid Electric propulsion: in the classical design of a civil transport aircraft, electrical systems were often considered as having a low impact on the overall aircraft sizing. Thus, the MDA was simply taking into account a weight penalty associated to such systems based on historical data. For vehicles designed around a Hybrid Electric chain supplying thrust, the impact on sizing is radically different. Thus, new models of electrical components must be added to the MDA as

well as thermal analyses to make sure that the overall integrated system is viable. The fourth option that is offered to design engineers is uncertainty management. This approach takes as starting point the fact that the aircraft design process is subject in any case to uncertainties. These uncertainties can be caused by approximations made through analysis models or they can be introduced within the MDA as some parameters values are not exactly known. Relying mainly on mathematical methods, uncertainty management allows designers to better estimate possible errors, to possibly reduce these uncertainties and finally to identify the success probability of key performance metrics. The role of the aircraft designers then consists in tailoring the conceptual design MDA so that the required options to add knowledge are taken into account with the final objective of assessing as best as possible one or many airplane concepts.

One additional responsibility of the designer is to ensure that the aircraft meets certification requirements. Through the MDAO of an aircraft using an innovative ground based system improving performances, it is verified that basic certification constraints can strongly affect the outcomes of a design space exploration. Further analysis of the European Certification Specifications for Large Aeroplanes highlights at first the necessity to perform aircraft simulations based on a six Degrees-of-Freedom model to verify some constraint thresholds. Second, the complexity of some sections of the regulatory text is underlined: there is a real need for a tool or interface that helps aircraft designers in the handling of certification constraints within a Multidisciplinary Design Analysis and Optimization. Following checks related to airworthiness, designers also have to consider that the aircraft under development will be one day operated within the Air Transportation System. Among the stakeholders of this global and complex system affecting the global economy, Air Traffic Management has a key role as it organizes the planning and the monitoring of all flights. In this field, aircraft trajectories are still determined using performance models calibrated on true operational values. Aiming for better accuracy and the possibility to simulate trajectories based solely on the aircraft characteristics, there is a strong demand within ATM research for a six Degrees-of-Freedom simulator with control and navigation loops. At the center of two important needs, simulation capabilities within the MDAO give the opportunity to link regulatory texts, the vehicle sizing, and its operational trajectories subject to specific limitations. Such full assessment capability could well be applied during the development of disruptive operational integrated systems such as Urban Air Mobility for which certification and operations must still be defined.

In this research, it is therefore proposed to add knowledge in the Multidisciplinary Design Analysis and Optimization at aircraft conceptual design level through the development of a Certification Constraints Module and the implementation of full simulation capabilities.

This PhD has been carried out in parallel to the work performed as Research Engineer in Aircraft Design at ONERA. On one hand, such part time organization required much more time to complete the necessary investigations with respect to the usual period of three years. On the other hand, technical contributions, proposal writing and coordination role on topics such as future concepts design, Multidisciplinary Design Optimization, Scaled Flight Testing have been a unique chance to broaden, to evolve and consolidate the research activity. In addition, continuous international

exchanges with research establishments, universities and industrial partners led to a balanced work between design and methods.

The first chapter of this dissertation starts with a review of Life Cycle Cost and the aircraft design phases within a program in order to have a clear understanding of the aircraft design context. Subsequently, the analysis of the challenges faced by aircraft designers towards the definition of the next generation of aircraft leads to the definition of the research problem. To close this chapter, the existing solutions to the research problem are presented. In order to initiate the second chapter, an extended preliminary sizing of an unconventional aircraft showing the impact of certification constraints at conceptual design level is detailed. Then, a review of the regulatory texts and the observation of a specific Air Traffic Management requirement lead to the identification of supplementary needs that must be taken into account in the conceptual design multidisciplinary tools. Based on these needs, a solution to the research problem corresponding to an expansion of the Multidisciplinary Design Analysis and Optimization is proposed. To begin with, chapter 3 describes the development of the Certification Constraint Module (CCM), a tool that simplifies the coupling between the Certification Specifications and the aircraft sizing iterations. Subsequently, to verify its capabilities, the CCM is implemented in an aircraft optimization process based on the code FAST (Fixed wing Aircraft Sizing Tool) shared by ISAE-SUPAERO and ONERA. Considering four different scenarios, the optimization results show the added value of the CCM in terms of knowledge gain. Last, chapter 4 focuses on the required modifications to the classical MDA to achieve full simulations capabilities. To this end, a dedicated section describes the implementation of the new aerodynamics module that provides static coefficients, dynamic derivatives and control effectiveness along and around the three aircraft axes. Next, the inertia estimation module as well as the control and navigation system are presented. To validate the simulation model generated by the new version of FAST, resulting trajectories as well as initial cruise phases are compared with real flight traces recorded with an ADS-B antenna.

Chapter 1

Adding knowledge at aircraft conceptual design stage

Roadmap of the chapter

- The important impact of the design phase on aircraft Life Cycle Cost is identified
- The three design phases and their characteristics are described
- Aviation goals to lower environmental impact are presented
- Challenges faced by aircraft designers toward the design of next generation airplanes are detailed
- The research problem is stated
- Existing solutions to the research problem are reviewed

Résumé du chapitre

La configuration classique de l'avion de transport civil a été définie par Boeing pour le B707 à la fin des années 50. Après des décennies d'optimisation, cette configuration et les technologies associées semblent avoir atteint un plateau au niveau des performances. Cependant, pour la conception des prochaines générations d'avions de transport civil, les constructeurs sont incités à améliorer leurs performances afin de tenir compte de la forte concurrence et à respecter des exigences de sécurité et des contraintes environnementales strictes. La seule solution pour atteindre ces objectifs consiste alors à explorer des concepts d'avions caractérisés par des changements radicaux au niveau de la configuration et/ou la prise en compte de technologies innovantes. Initiée lors de la phase d'avant-projet, la définition de ces concepts s'appuie sur une analyse de conception multidisciplinaire (MDA) qui permet de dimensionner les avions et d'estimer leurs performances. Dans cette phase initiale, l'un des principaux atouts de la MDA est la possibilité de bien identifier les compromis possibles entre les principales disciplines ou composants de l'aéronef. Le problème est que l'actuelle MDA n'est pas conçue pour prendre en compte les spécificités de configurations non conventionnelles ou de nouvelles technologies pour lesquelles très peu d'informations sont disponibles. Après un examen de différents cas associés à des conceptions de véhicules innovants, ce chapitre a permis d'identifier la problématique de Conception Avion à résoudre : "Comment ajouter des connaissances dans l'analyse de conception multidisciplinaire lors de la phase d'avant-projet ?".

Dans ce chapitre, les solutions disponibles pour ajouter des connaissances ont été examinées et classées en quatre catégories : optimisation multidisciplinaire (MDO), amélioration de la précision grâce à des analyses haute fidélité, ajout de nouvelles disciplines dans le processus de conception et enfin gestion des incertitudes. Pour chacune d'entre elles, des exemples concrets sont proposés afin de quantifier les gains potentiels au niveau du processus de Conception Avion.

Au cours de la défintion de futurs avions non conventionnels, les concepteurs ont pour pour rôle de sélectionner la ou les options disponible(s) et adaptée(s) et de les mettre en œuvre au sein de la MDA. Avec ce processus consolidé, il est alors possible d'identifier le concept ou bien la famille de concepts les plus prometteurs. Les défis à relever lors de cette activité sont : (i) la gestion d'un grand nombre de paramètres (variables de conception, contraintes…) ; (ii) l'organisation des boucles de conception en tenant compte des temps de calcul importants ; (iii) une exploration efficace de l'espace de conception à partir d'une paramétrisation pertinente ; (iv) la collecte de données pour orienter les étapes initiales de conception ou bien pour valider des résultats. Le rôle du concepteur d'aéronef ne se limite cependant pas à cette tâche. En effet, il doit s'assurer que le futur concept est conforme aux exigences de certification et qu'il sera un jour capable de voler en toute sécurité en respectant les contraintes liées à la gestion du trafic aérien. Ces sujets sont traités dans le chapitre suivant.

1.1. Introduction

With the design and Entry Into Service of the B707 in 1958, Boeing defined the configuration of large jet airliners for the next 60 years. Although the “tube and wing” architecture remains unchanged, the last decades brought continuous improvements at disciplinary level as well as at system level. Wind tunnel tests and numerical simulations lead to an improvement of aerodynamics, progress in engine technologies resulted in Thrust Specific Fuel Consumption reduction and the use of Carbon Fiber Reinforced Polymer decreased airframe weight. Nevertheless, competition and mostly stringent environmental constraints are constantly pulling for large fuel burn reductions. As the conventional configuration and its associated turbofan offer limited gains, such reduction in fuel consumption will be achieved through future aircraft presenting disruptive architecture or technology.

In industry, the design of the next generation of aircraft occurs during the conceptual design phase and it is carried out by aircraft designers. In this chapter, the goal is thus to acquire a thorough vision of the Aircraft Design context with respect to the airplane program, an accurate understanding of aircraft designers activities, and a grasp of associated analysis tools that are used in the early phases of the airplane definition. With such a full view, the challenges associated to the design of unconventional configuration are identified and subsequently translated into a research question in the field of Aircraft Design.

The first section of the chapter is then dedicated to Aircraft Life Cycle Cost in order to highlight the importance of the design phase. Subsequently, the different phases of aircraft design are detailed to better comprehend the decision process and the exploration needs. The third and key part of the chapter identifies the research problem through a step-by-step approach: with the stringent environmental constraint well identified, key enablers for fuel burn reduction are identified. Next, the Multidisciplinary Design Analysis used to size the airplane is described and challenges associated to the design of future aircraft are reported. As conclusion, chapter 1 lists the currently available options to solve this research problem.

1.2. Aircraft Life Cycle Cost

When looking at the life cycle of an aircraft, two distinct parts can be recognized. The first one is dedicated to the airplane development and manufacturing up to flight tests prior to customer delivery while the second one concerns operations up to aircraft disposal. In terms of parties involved, the first part is carried out by the manufacturer with crucial inputs from the customers. For the second part, operations are clearly performed by airlines with key involvements from manufacturers. In his book dedicated to Airplane Cost Estimation [1], Roskam provides a refined decomposition into 6 phases of such program life cycle. Phase 1, identified as “Planning and Conceptual Design”, englobes the customer requirements analysis, initial design, preliminary sizing and many iterative loops to downselect one or several promising designs. In Phase 2 “Preliminary Design and System Integration”, engineers refine the various disciplinary estimations, complete cost estimations and

converge to the final configuration. With the configuration frozen, Phase 3 “Detail Design and Development” is started: the manufacturer or its suppliers carries out the design of all aircraft components, integrates all required systems, and prepares the necessary documents or Computer Aided Design (CAD) models for manufacturing. During Phase 4 “Manufacturing and Acquisition”, the airplane maker is building the aircraft and delivers it to its customers after validation flights. It must be noted that during this phase, there is a shift in the aircraft’s ownership as it enters into service. For the entire next phase called “Operation and Support” (Phase 5), airlines operate the aircraft within a flight envelope and given operational conditions. In order to ensure the aircraft airworthiness, maintenance programs defined for each type of aircraft and operations are scheduled. During this operational life, the aircraft configuration can be modified by following service bulletin instructions for different scopes ranging from airworthiness (mandatory Service Bulletin) to pure performance oriented changes [2]. Finally, when the aircraft is no more economically viable or is outperformed by newer products for a given mission, its operational life is terminated and Phase 6 “Disposal” is initiated. For civil airplanes, operations are organized to dismantle the airframe and reuse some material. Regarding military vehicles, storage can be also a viable option (e.g. Davis-Monthan Air Force Base).

For a better understanding of the tasks executed by the airplane manufacturer in Phases 1 to 4, details about the milestones sequencing are given by Pardessus [3] (Airbus generic view) and Morales [4] with a specific view of A380 program, illustrated in Figure 1. In this description, maturity gates associated to expected engineering contents monitor advancement and decompose the main program into 5 phases that match the breakdown by Roskam (disposal is not considered): Feasibility (M0 - M3), Concept (M3 - M5), Definition (M5 - M7), Development (M7 - M13) and Post Entry Into Service (M13 - M14). Naturally, M3 “Definition of Basic A/C Concept”, M5 “End of Concept Phase”, M7 “Definition Phase Complete” and M13 “Entry Into Service” are key milestones that trigger the completion of one phase and the start of the next one.

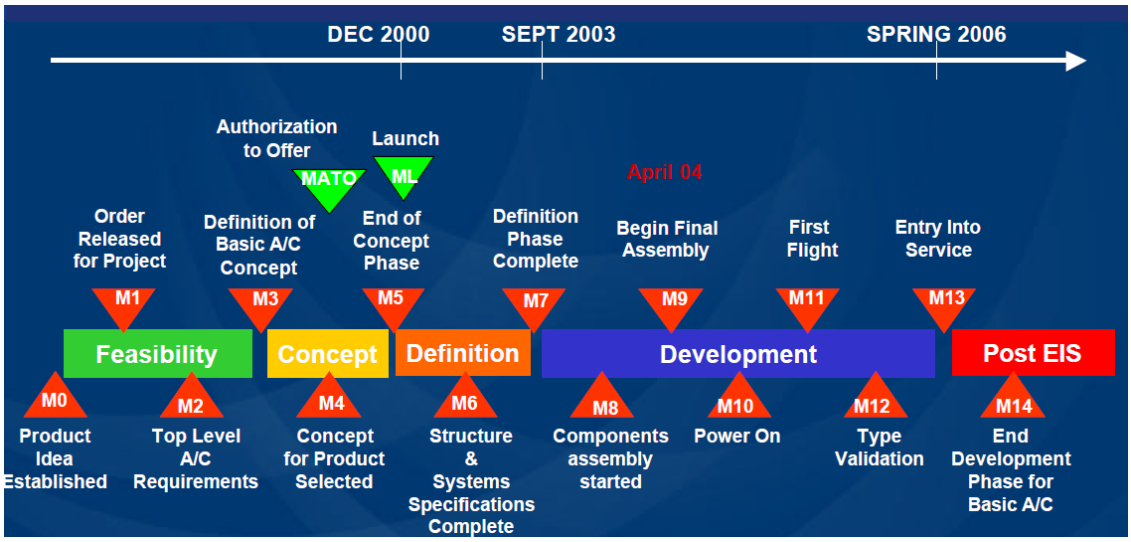

Figure 1: Airbus A380 program with milestones [4]

Among these, M5 corresponds to the “go / no go” decision for the program which commits the company to an important financial investment. To emphasize the importance of this turning point taken at the end of the preliminary design phase, both Raymer [5] and Anderson [6] indicate that this is the moment when “you bet your company” with the latest stressing the risk taken by Boeing with the launch of the B747 program. Last but not least, Figure 1 places this entire program sequence with respect to a time frame so that durations of the phases can be considered.

In the previous paragraphs providing an overview of the airplane life cycle, two stakeholders with profitability objectives are considered. On the one hand, there is the aircraft manufacturer that has to sell a product meeting stringent requirements with a certain margin to generate revenues. On the other hand, the airline is seeking to buy a system with reduced operating costs so that aircraft operations are profitable taking into account the acquisition cost. As the aeronautical industry involves many airplane manufacturers and many airlines, there is an environment driven by competition which is “the genesis of many airplane designs” [7]. In order to support this statement, a good example provided by Anderson [6] about the background leading to the design of the Douglas DC-3 is described hereafter. In 1932, Boeing was finalizing the 247, its latest civil transport aircraft featuring advanced characteristics such as a single low wing, full metal airframe, NACA cowling and retractable landing gear. With a passenger capacity of 10 passengers, a cruise speed of 300 km/h and a 1200 km range, this aircraft was naturally highly demanded by airlines. However, as Boeing and United Airlines were both members of the United Aircraft Group, there was an agreement that the first 70 Boeing 247 would go to United Airlines. To counter this unfavorable situation, Jack Frye, vice president of Transcontinental and Western Air sent to different manufacturers asking about their interest in the design of a transport plane according to a given set of performance specifications. After several iterations between the two companies, especially about the number of engines, the contract to build the DC-1 (Douglas Commercial 1) was signed on 20th September 1932. At the end of the design process that included wind tunnel tests at the California Institute of Technology, Douglas proposed a pioneering high efficiency aircraft that was the combination of different proven technologies. After the first and only DC-1, Douglas designed and built 156 DC-2, thus paving the way to the famous DC-3. With a larger cabin carrying up to 21 passengers and a maximum lift-to-drag ratio of 14.7, the DC-3 instantly became an airline favorite with a 40% reduction in cents per available seat-mile over the Boeing 247 (1.27 versus 2.11). For Douglas, the efforts put in the design phase resulted in the production of 803 civil aircraft and more than 10000 military versions. This key role of cost in an airplane program is again emphasized by Raymer stating that “the final contractor selection will probably hinge on cost” [5].

When looking at the life cycle cost of a program, it is known that incurred costs are subject to an important increase during the production phase, when material and resources must be allocated for manufacturing. In contrast, committed costs follow an extremely rapid growth during the design phase. For this reason, Dieter indicates that “Decisions made in the design process cost very little in terms of the overall product cost but have a major effect on the cost of the product” [8]. If concentrating on airplanes, it is estimated that only about 5% of the life cycle cost can be affected by

changes made after the detail design phase [1][9]. Looking at this analysis the other way around, it means that 95% of life cycle costs are determined during the aircraft design phases. The next section of this chapter then aims at detailing the activities and the design choices that are carried out during this fundamental step of the program.

1.3. The aircraft design phases

The design of an aircraft starts with a set of requirements based on a military need [10], a commercial market outlook [11] or simply a vision [12] and ends when the last CAD models and drawing for the assembly line are issued. During this challenging task that takes several years to completion, thousands of engineers and scientists with various expertise contribute in defining, sizing, optimizing a design subject to various constraints (regulations, environmental impact, economics, manufacturing,..). Carried out following three distinct phases, the design process starts with conceptual design that results in a feasible design (Technology Readiness Level or TRL 2-3). This feasible design is subsequently refined during preliminary design to obtain a mature design (TRL 4-5). In the third and last step, the detail design, every single element of the airplane up to rivet size is defined leading up to shop designs (TRL 6-7) [13]. As stated by McDonald, these design phases are thus about what decisions are being made, not how they are made [14].

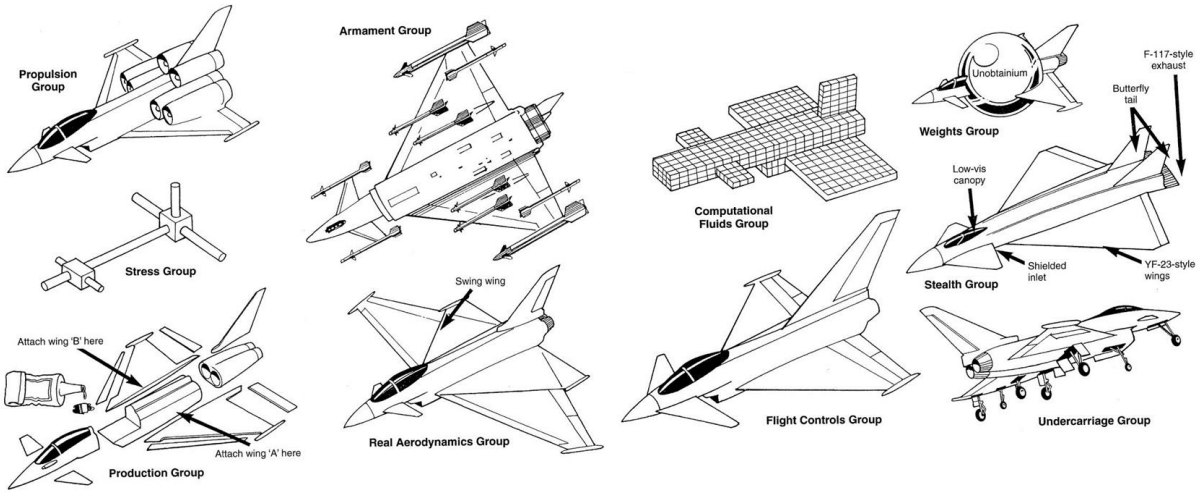

Figure 2: How specialists would have designed the Eurofighter Typhoon if given a free hand, courtesy of Ray Whitford [15]

In order to lead this multidisciplinary team effort, a chief engineer with aircraft design expertise synchronizes the activity of all disciplinary experts to make sure that the final product matches the specifications. In case of conflicting disciplinary solutions, the chief engineer has to act as the "referee" [13] and after an assessment of the possible trade-offs, he decides the way forward. As the objectives and the required skills for each design phase are different, personnel involved in the process might change and some priorities might shift as well. At this point, it is up to the chief engineer to both

avoid that a single discipline or group takes over the design (Figure 2) and make sure the aircraft is the best blend of compromises.

Such interactions between specialists and the chief engineer are well illustrated by Rich [16] who shares details about the SR-71 development lead by Kelly Johnson. In 1958, the Lockheed Advanced Development Projects group called the Skunk Works started the design of a spyplane that would fly higher than the U-2 at a cruise speed of Mach 3. To match these extremely stringent requirements, weight reduction was key. Towards this goal, the structure specialist Henry Combs proposed the use of titanium knowing that such unproven technology was a risk. Kelly Johnson was clearly interested in such option ("any material that can cut our gross weight nearly in half is damned tempting") but the adaptation of the production line to titanium was a problem. Ben Rich, at the time in charge of thermodynamics and propulsion then proposed to paint the whole aircraft in black. Basically, the black paint would radiate away some heat and thus enable to lower the temperature on the aircraft surface. With fewer constraints regarding the temperature, softer titanium could be used. Initially against this idea because of the impact on fuel consumption ("the weight of your black paint will cost me about eighty pounds of fuel"), Kelly Johnson outweighed possible benefits at manufacturing level and known drawbacks in performance and on the next day, he approved the proposal from Ben Rich. From this compromise, the SR-71 became the Blackbird. In the next sections, the three sequential design phases are detailed.

1.3.1. Conceptual design

The product of the conceptual design phase is a feasible aircraft concept under the form of 3 view drawings or a 3D model that meets with a certain margin a given set or requirements and constraints. Its characteristics in terms of overall configuration, geometry, internal layout, performances are determined with "a certain somewhat fuzzy latitude" [6] through the use of low computational time tools tailored to design space exploration. In terms of size and duration, the conceptual design of an airplane involves about 15 to 40 persons for about one year depending on the company and the type of program (military or civil). The team in charge of the conceptual studies starts its activities by a thorough requirement analysis to make sure that the customer need is well translated into measurable metrics used in the engineering process. In order to maximize the chances of winning a contract, Nicolai suggests adding as a key requirement the Measure of Merit (MoM): it is a characteristics of the aircraft that is really important to the customer even though it may not be underlined. The rationale is that all competitors will match the requirements and the aircraft manufacturer has to design its aircraft for the criterion that will be used as "tie-breaker" [17]. While reviewing the requirements, the design team has also to identify the list of potential new technologies or subsystems (such as the engines) that would be available for the specified Entry Into Service (EIS). As too optimistic estimations can lead to critical program delays (Lockheed L-1011, Dassault Falcon 5X), the design team has to take various scenarios into account. To conclude this Systems Requirements Definition that can successfully drive the design of a new airplane (Boeing 777 [17]), a System Requirements Review (SRR) that will set the design guidelines takes place [18]. At this point, brainstorming sessions

within the design team identify a number of possible configuration layouts wrapping the payload. Identified as concepts or configuration sketches, these layouts that used to be 2D sketches are nowadays defined with 3D tools such as OpenVSP [19] giving access to additional useful data (e.g. total wetted area). In the case of civil transport aircraft, the configuration exploration can either be limited to lifting surfaces shape and position or expanded to disruptive shapes depending on the choices for the cabin layout. An example of such a concept generation phase is illustrated in Figure 3, where it is interesting to see that some of the selected configurations are taking into account technology choices made earlier in the requirement definition phase (open rotor in this case).

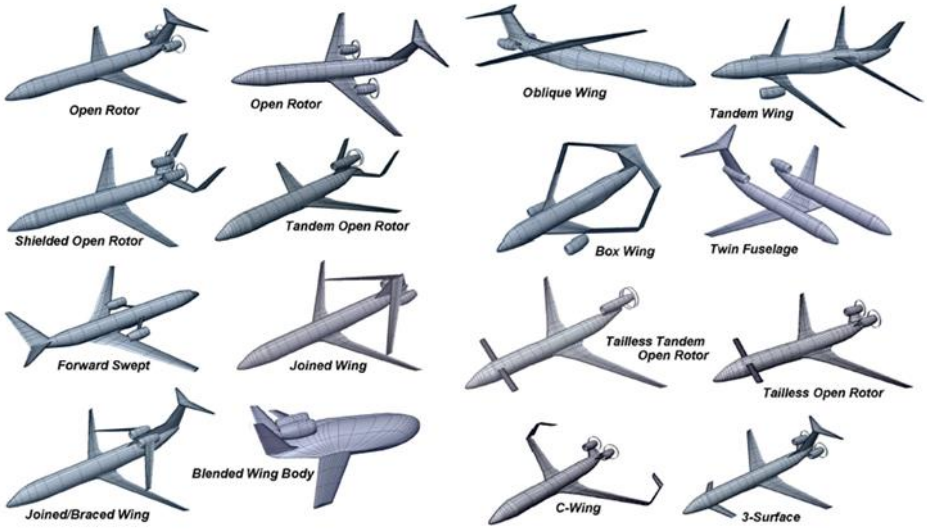

Figure 3: Proposed configurations during the conceptual design of a civil transport aircraft [20]

In parallel to this task, it is good practice to perform constraint diagram analyses with various hypotheses [21]. This simple approach provides quantitative values in terms of wing loading and thrust-to-weight ratio that help the designers in assessing the new concepts with respect to existing or competing designs. Then comes the central step of the conceptual design phase: it is the aircraft sizing process that converges to an airframe capable of carrying a payload and the necessary fuel to complete the mission including some reserves. Based on a point mass approach, computations rely on analytical models of the main flight physics disciplines: aerodynamics, propulsion, weight and performance [22][23][24]. To this end, a Multidisciplinary Design Analysis (MDA) estimates the fuel consumption over the mission for a given geometry. After some iterations, designers are able to estimate with a certain margin of error the size and weight of the major aircraft components (fuselage, wing, empennage) and they can derive the fuel or energy consumption for the different mission segments. For the estimation of the fuel consumption along the mission, first estimations can rely on the Breguet equation [5][13][25][26] but more reliable results are obtained with time-step integrating simulations [27]. A fundamental feature of this sizing process is its capability to assess the impact of different engines on global performances. It is indeed key for designers to estimate in the early phases if fuel consumption targets and thrust requirements can be met with an existing engine or if a tailored engine is necessary. To strengthen the concept definition, an important step consists in assessing risks and opportunities associated to new technologies. As written earlier, estimations on available technologies for a given EIS are associated with some uncertainty. Through the use of “k factors” [28] to simulate a

technology impact, parametric studies and sensitivity studies are completed. The design team ends up with a good knowledge about the required performances variations with respect to the best and worst case scenarios for each technology impacting the disciplines. At the end of the conceptual design, these aeronautical science studies are assisted by early cost estimations based on simplified models [1] in order to better guide the selection of the preferred configuration.

1.3.2. Preliminary design

At the end of the preliminary design, the airplane manufacturer must be confident that the proposed concept can fulfill the customer requirements and that it can be produced within a certain schedule at a given cost. Starting from the output of the conceptual design phase, 100 persons or more will work several years [13] to provide all necessary information for the Preliminary Design Review (PDR) [18], a key decision gate for the program. Knowing that flight physics characteristics have been estimated through analytical methods in the previous phase, it becomes mandatory for the design team to use higher fidelity methods to consolidate the performance level. For structure, after a structural layout is selected [29], Finite Elements Analysis providing data on stress and deflections is now used to size the various elements under given loads. With the diverse elements accurately sized, engineers can subsequently provide better weight estimations. In the case of aerodynamics, Computational Fluid Dynamics (CFD) codes are utilized to accurately predict the coefficients and identify local flow issues. Today's state of the art allows to directly perform aerostructural analyses and optimizations to converge to the best combination of airfoil shape, wing twist and structural components size [30]. Also related to aerodynamics / structure interactions, flutter issues can significantly affect a program success [31]. Such studies are then carried out early in the preliminary design phase to avoid costly redesign loops. The other crucial data that needs to be improved for better fuel burn estimations are engine performances. To achieve the required level of fidelity, propulsion specialists rely on dedicated software that simulate the complete thermodynamic cycle within a turbine engine taking into account the performance of all components, from inlet to nozzle [32][33]. Fully described by Mattingly [21], this approach generates the necessary database consisting in thrust and thrust specific fuel consumption as function of Mach, Altitude and power setting [27]. Once the performances are validated, the design team has to certify that the vehicle has the required handling qualities over the entire flight domain. This verification is achieved through 6 Degrees of Freedom (DoF) simulations (more degrees of freedom if the vehicle is highly flexible) that necessitate aerodynamic coefficients for the 3 forces, the 3 moments, associated dynamic derivatives, movable surfaces effectiveness and vehicle inertia. Based on this simulation environment, the flight control system that can have different loops is subsequently designed [34]. Concurrently to these disciplinary assessments, groups of specialists are involved to develop the landing gear, fuel system, hydraulic system, electrical system, environment control system and de/anti-icing [35] considering maintenance constraints as well as redundancy options to meet safety criteria. With all these systems to be added within the airframe, the use of CAD systems becomes mandatory to limit integration issues and recent methods offer better assessment of systems allocation within the airframe [36]. When the local environment of each subsystem is known, physicists can simulate thermal exchanges and stress critical areas where opening

would be required if no other options are available. At this stage, the design team has sufficient data about the aircraft airframe, engines, subsystems and global layout to carry out lofting (see example in Figure 4) and freeze the concept outer surface shapes.

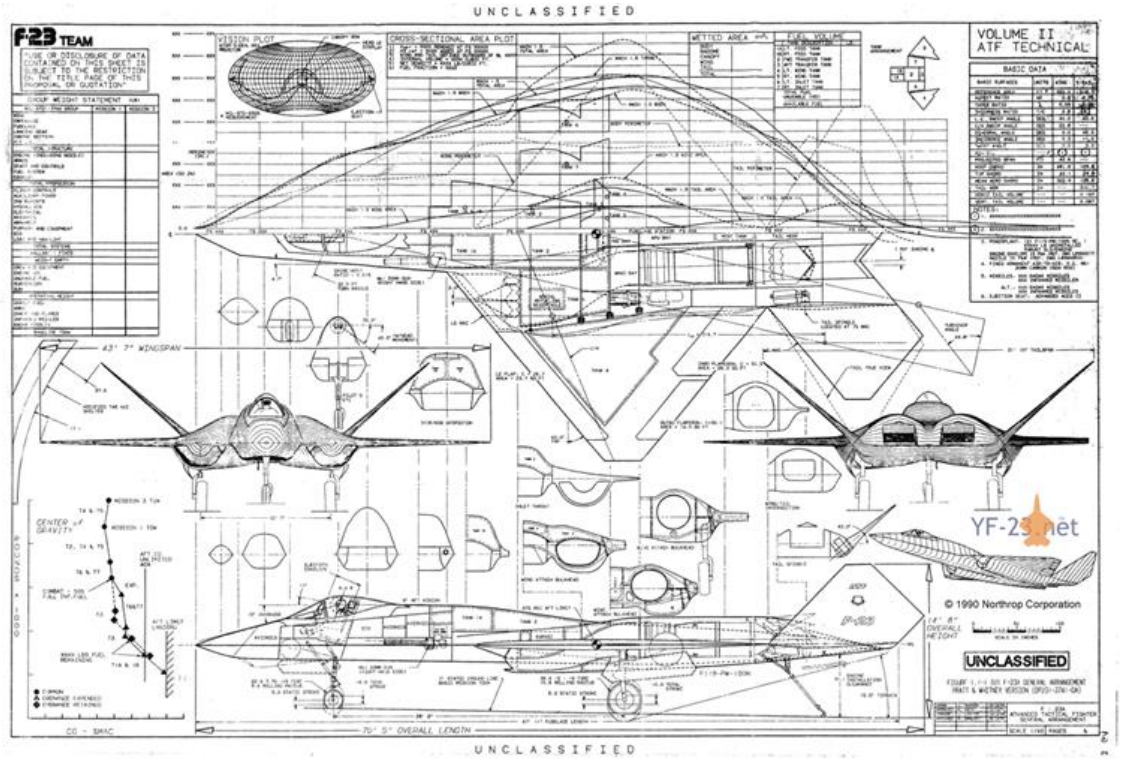

Figure 4: Lofting of the YF-23 [37]

In parallel to paper studies and simulations described so far, the design team can launch ground tests to validate and complete the concept multidisciplinary database. Generally, these experiments are wind tunnel tests that provide drag polars for the different flight regimes with high accuracy. At high speed, measurements confirm that fuel consumption or speed targets can be achieved while at low speed, they give information about high lift capabilities and control power. For some high maneuverability aircraft, specific wind tunnel tests in different facilities are executed to populate the aerodynamic database in the corners of the flight domain so that simulations at high angle of attack [38] can be made. However, aerodynamics is not the only discipline that benefits from wind tunnel tests. For some configurations with high aspect ratio wings, flutter is a real concern. To limit risks, wind tunnels tests are carried out to validate the numerical chain that is used to perform the calculations [39]. Last in this description but not least important, the design team has to supplement all this work concentrated on the vehicle with assembly line preparation and accurate cost predictions. Such topics are indeed key to assess the feasibility and viability of the airplane program [31] during the PDR.

1.3.3. Detail design

After a successful PDR and the decision of the aircraft manufacturer to build the aircraft, the detail design phase is started. As the configuration is consolidated, the work to be performed aims at having

a full engineering description of a tested and producible aircraft. Each part of the aircraft up to the last bolt has to be designed with information on dimensions, tolerances, surfaces properties, material and associated manufacturing process [8]. With all this supplementary information, the design office can now have full CAD models of the airframe as the one illustrated in Figure 5 in order to better prepare required experimental validations for certification purposes. As an example, such full scale wing static test illustrated in Figure 6 is virtually achieved through the use of a 68 million Degrees of Freedom Finite Element Model [40].

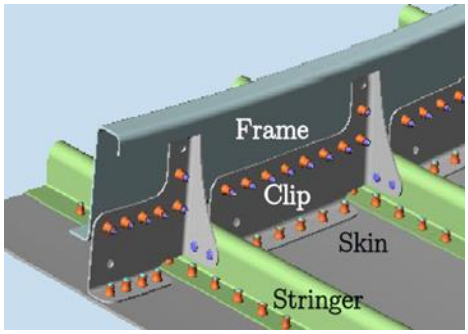

Figure 5: Detailed CAD model showing all necessary components for production [41]

Figure 6: Airbus A350 full scale wing static test [42]

Full scale mock-ups of the aircraft are also necessary to test key components such as landing gear, hydraulic lines, fuel systems, electrical architecture and Environmental Control System. An important portion of the company resources are committed to the design of these test facilities that can be very large. An example is the “Iron bird” illustrated in Figure 7 where real components of the electrical architecture, hydraulics system and actuators are coupled to the control system as planned in the real aircraft. Virtual flights based on simulator data are carried out to verify that the assembled complex system behave as expected. In addition to these final verifications regarding the aircraft, many tasks focus on the final assembly line definition that must be tailored to reach a production rate expressed in aircraft per month. After the main production stream is consolidated, working stations including jigs are designed by the production group with specific Computer Aided Design and Manufacturing software as illustrated in Figure 8.

Figure 7: Airbus A350 Iron Bird with folded wings to save space [43]

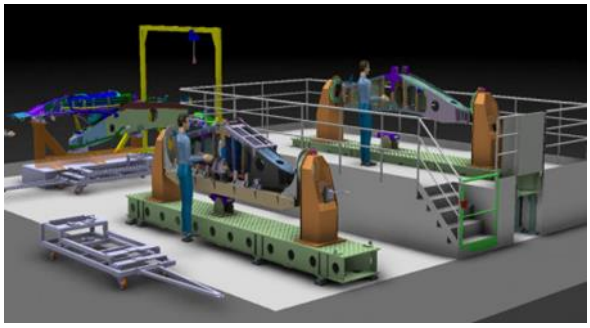

Figure 8: CAD model of assembly line station [44]

Details on the industrial implementation of an aircraft assembly line are provided in [45] with a focus on the A400M program. With the work carried out during preliminary design about the aircraft performance and fulfillment of customer requirements, issues detected at the detail design phase should normally not affect the program. However, in such a scenario, the chief engineer and the design team have to coordinate the recovery plan to make sure that the final product will still be viable [46]. A practical example of such emergency plan in the frame of the F-35 program is described in [47]. Progresses made towards the final product design are verified during the Critical Design Review that gives permission to proceed with the next program phase [18]. Overall, as the detail phase englobes final design aspects, production definition, test benches preparation and analysis, it results in being the most demanding design step in terms of resources and budget. For the entire phase, depending of the program type, about thousands of persons are involved for a period that can last several years.

1.4. Research problem

1.4.1. Aviation goals to lower environmental impact

A decade after the first flight in 1903 of a vehicle heavier than air (Wright Flyer), the aircraft designer T. W. Benoist and his business associate P. Fansler started an air transportation service between St-Petersburg and Tampa in Florida. The aircraft, a Benoist XIV, was a flying boat with a capacity of 1 passenger sitting next to the pilot. Charging 5 US$ for the trip, the company transported 1205 persons between January and March 1914 when the service become unprofitable as city subsidy ran out. At the same time in Russia, Sikorsky designed the first airplane dedicated to passenger transport with the first true cabin with a capacity of 16 passengers (the Sikorsky Ilya Muromets). In 2018, after a century of constant developments in many domains, the Air Transport System (ATS) that includes aircraft manufacturers, Air Traffic Management, airports and airlines is a key pillar of global economy. The next numbers are given for a given year:

- Generation of 709 billion US$ of revenues (cargo and passengers) with a net profit of 34.2 billion US$ [48];
- Transportation of 3.8 billion passengers and 57 million freight tons [48];
- Employment of 8.9 million people through airlines, airports and air navigation service providers [49];
- Employment of 1.1 million people by the civil aerospace sector [49];
- Direct and indirect employment of 36.3 million persons through air transport's impact on tourism [49].

However, the values provided by the International Air Transport Association (IATA) also indicate that in 2016, 812 million tons of CO_2 emissions have been produced by ATS. The environmental impact of aviation is a known issue to the International Civil Aviation Organization (ICAO) whose role is to find consensus between its Member States on Standards and Recommended Practices towards "a safe, efficient, secure, economically sustainable and environmentally responsible civil aviation sector" [50]. To address the specific issues on aircraft noise and emissions policies, ICAO established in 1983 the

Committee on Aviation Environmental Protection (CAEP). In 2013, CAEP proposed an ambitious plan shown in Figure 9 in order to limit CO_2 emissions of civil aviation with the overall goal to reach a carbon-neutral growth from 2020.

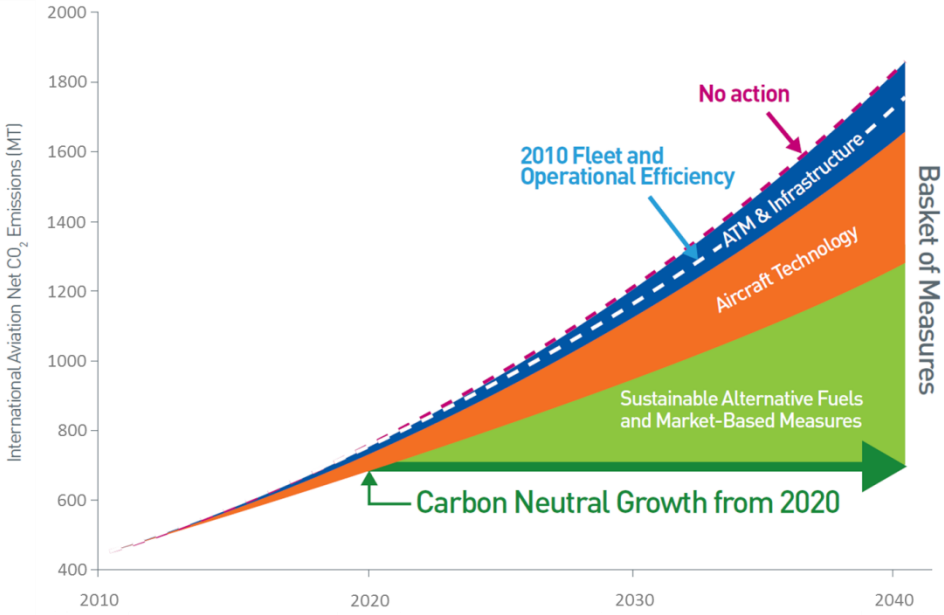

Figure 9: Contribution of measures for reducing international aviation net CO_2 emissions [51]

Taking into account an annual growth rate of 5% for passenger traffic (expressed as revenue passenger kilometers), the CO_2 emission reduction would be achieved through improvements in Air Traffic Management (ATM) and infrastructures, implementation of new aircraft technology, use of sustainable alternative fuels and market-based measures [52]. Focusing on the expected improvements at the single aircraft level, the European initiative Flightpath 2050 [53] fixed an objective of 75% reduction in fuel burn through technologies and procedures with respect to new aircraft entering their operational life in 2000. With a similar approach towards improving CO_2 emissions, NASA proposed a more stringent set of subsonic transport system level metrics setting a decrease in fuel burn of 50% in 2020 and 60% in 2025 with respect to a 2005 best-in-class aircraft [54]. These targets naturally become the drivers of future transport aircraft designs.

1.4.2. Key enablers to decrease aircraft fuel burn

With fuel burn reduction identified as the top level requirement, the next step consists in understanding how it can be achieved at aircraft design level. To this end, a basic analysis of a steady flight is carried out starting with the review of the different forces acting on the aircraft. First, pressure distribution and shear stress around and along the aircraft surface create an aerodynamic force that is divided into lift (component that is perpendicular to the airspeed) and drag (component that is parallel to the airspeed). Second, as this aircraft has a certain mass, gravity generates an additional force towards the ground called weight. Last, the engine installed on the vehicle is providing a certain thrust. Considering a point mass approach, the airplane is now represented by its center of gravity and these 4

forces acting on the airplane are applied to this same point. Figure 10 illustrates such a representation of the aircraft flying at constant altitude and airspeed:

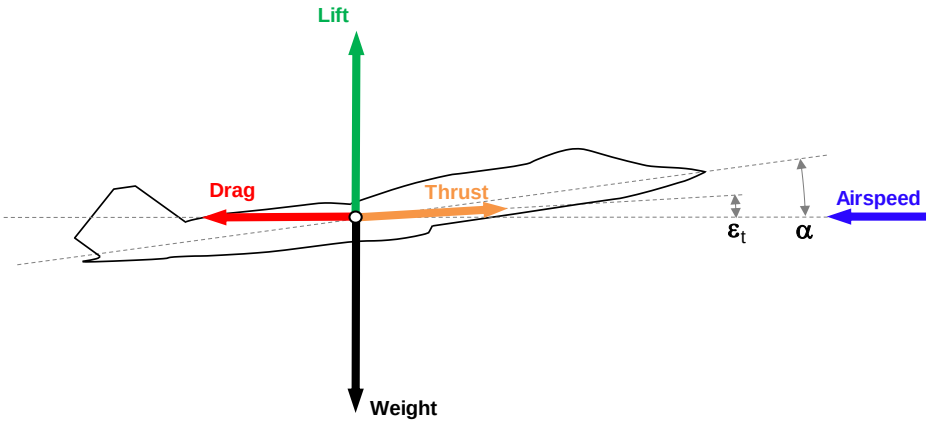

Figure 10: Forces applied during steady flight

- The airplane is flying at a certain angle of attack α;
- The airplane lift is perpendicular to the airspeed (or flight path);
- The airplane drag is parallel to the airspeed (or flight path);
- The airplane weight is oriented vertically towards the ground;
- The engine Thrust forms a certain angle ε_t with the airspeed (or flight path).

Regarding Lift and Drag, a dimensional analysis carried out by Anderson [55] demonstrates that both are directly proportional to dynamic pressure, a reference surface (generally the project wing area of the airplane), and a non-dimensional lift and drag coefficient influenced by the angle of attack α, the Mach number M, the Reynolds number $\mathcal{R}e$ and obviously the shape of the aircraft. The resulting equations are given here below:

$$L = qSC_L$$
$$D = qSC_D$$

where L is the Lift force in N;
D is the Drag force in N;
q is the dynamic pressure at the flight altitude and speed in $kg/(m.s^2)$;
S is the reference wing surface in m^2;
C_L is the Lift coefficient that is a function of α, M and $\mathcal{R}e$;
C_D is the Drag coefficient that is a function of α, M and $\mathcal{R}e$.

This decomposition is a clear asset that facilitates preparation of experimental sessions in wind tunnels and allows direct comparisons between aerodynamic properties of vehicles that may not have the same size nor fly at the same speed or altitude. Such wind tunnel tests confirmed theoretical findings that the Lift coefficient and the Drag coefficient are related through a parabolic function: the curve called "Drag Polar" illustrated in Figure 11.

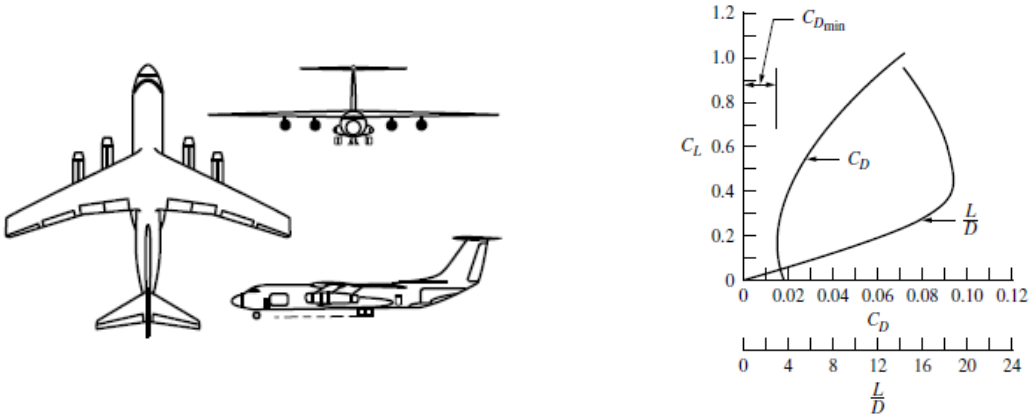

Figure 11: View of the Lockheed C141 and its associated drag polar [55]

This curve is one of the fundamental ingredients for aircraft performance as it translates the penalty (drag) associated to the lifting capability. An aerodynamic efficient aircraft is typically characterized by a high Lift-to-Drag ratio implying a capability to lift with reduced drag.

With this latter information about the essential relationship between Lift and Drag, let's review what happens to this aircraft in Figure 10 making the realistic assumption that the angle of attack α and the engine orientation ε_t are negligible. As the aircraft is in steady flight, when applying Newton's second law, the sum of all forces along the same axis must be equal to zero. As the primary need of the airplane is to remain in the air, forces along the vertical axis are considered first: in this case, the airplane flying at a given speed needs to generate through its wings a level of lift that is equal to its weight. However, lift cannot be generated without creating an amount of drag, the force that decelerates the aircraft along the horizontal axis. To have the complete system at equilibrium, the installed propulsion system must then provide the required thrust to counter drag. With the engine running with a thrust specific fuel consumption corresponding to the given altitude and airspeed, a certain amount of fuel is spent. Even if very simple, this performance analysis highlights the three fundamentals enablers in aircraft design leading to fuel consumption reduction:

- Thrust Specific Fuel Consumption (TSFC)
  As the engine is the aircraft component that consumes fuel, any improvement regarding its efficiency would directly translate into a lower fuel burn for the complete aircraft.
- Lift-to-Drag ratio
  A higher lift-to-drag ratio implies a reduction of the required thrust to maintain level flight. The same flight condition can thus be achieved with a lower throttle level or a smaller engine: the overall aircraft fuel burn is reduced.
- Aircraft weight
  The primary goal of lift is to counter the aircraft weight. Any reduction of weight at aircraft level translates automatically in less severe lifting capabilities requirements. Given the shape of the drag polar, such decrease in lift leads to a reduction of drag that in the end results in fuel burn savings.

In the aeronautical industry, there are a few examples showing how changes on a key enabler directly or indirectly resulted in fuel burn reduction. The simplest case is illustrated by the UPS fleet upgrade to take place in 2018 [56]. Basically, Boeing 757s and 767s are scheduled to receive an upgrade to lighter cockpit displays eliminating 80 pounds per aircraft. This weight reduction should translate directly into a saving of 208000 liters of fuel per year at fleet level. The second example concerns industry's recent NEO [57] and MAX [58] programs leaning on new engines and their TSFC improvement. Given the turbofan architecture, it is known that an increase of the by-pass ratio provides a higher propulsive efficiency and thus a better TSFC. Considering this design driver, engine manufacturers developed new high by-pass ratio turbofans that went through successful ground tests in 2008. With respect to the previous generation, the fuel burn reduction purely associated to the engine was about 14%. However, these new engines are characterized by an increase of weight and given their bigger size, they increase the total drag of the aircraft. Thus, when considering all aspects, the expected benefit associated to the new engine option is about 11% [59]. This case illustrates that the key enablers are always at the origin of aircraft changes but benefits go along with penalties that must be taken into account by the design engineers.

A first solution to identify possible trade-offs at aircraft level is to use the Breguet range equation [6]. Derived from the weight variation due to TSFC, this equation is both simple and powerful as the three key enablers are taken into account and a global performance metric (range) is calculated. This is the reason why this equation is often used as the objective function of Multidisciplinary Design Optimization problems [60].

$$R = \frac{V_\infty}{g.c_t}\frac{L}{D}ln\frac{W_0}{W_1}$$

where R is the aircraft range in m;
V_∞ is is the aircraft speed in m/s;
g is is the gravitational acceleration in m/s^{-2};
c_t is the Thrust Specific Fuel Consumption in $g/kN.s$;
L/D is the Lift-to-Drag ratio;
W_0 is the aircraft weight with full fuel tank in kg;
W_1 is the aircraft weight with empty fuel tank in kg.

However, overall performances calculated with the Breguet equation may lead to significant deviation when considering all mission segments (takeoff, climb, descent…) and real operational mission profiles with short cruise segments [27]. In order to limit risk at the conceptual design phase that is responsible for 65% of the aircraft life cycle costs [1], it becomes mandatory to apply a Multidisciplinary Design Analysis (MDA) simulating a complete mission profile during the vehicle sizing process. Such implementation is the only way to maximize benefits from the key enablers taking into accounts penalties so that the final design would be superior to the competition. The next section focuses on the key Multidisciplinary Design Analysis.

1.4.3. Multidisciplinary Design Analysis at conceptual design level

The conceptual design phase is characterized by many multidisciplinary design loops to assess the performances of potential promising concepts. In various text books about aircraft design, each author proposes its description of these iterative sequences [1][5][6][13][18][24][46]. A preliminary review of all these flowcharts reported in Appendix 1 rightfully points out the non-uniform nature of the design process: iterative loops are not made at the same time, the number and type of aircraft parameters to be considered are different and disciplines to be addressed are not the same. Indeed, each design follows a specific mission, requirements are translated into design decisions following company policies and Measure of Merit will differ [61]. Besides, it is worth noting that all authors propose to initiate the sizing process only after the definition of a first drawing or 3D model of the concept. As it can be quite difficult to have an estimation of the aircraft high level characteristics when starting from scratch, one effective solution is to build the constraint diagram following the approach detailed by Mattingly [21].

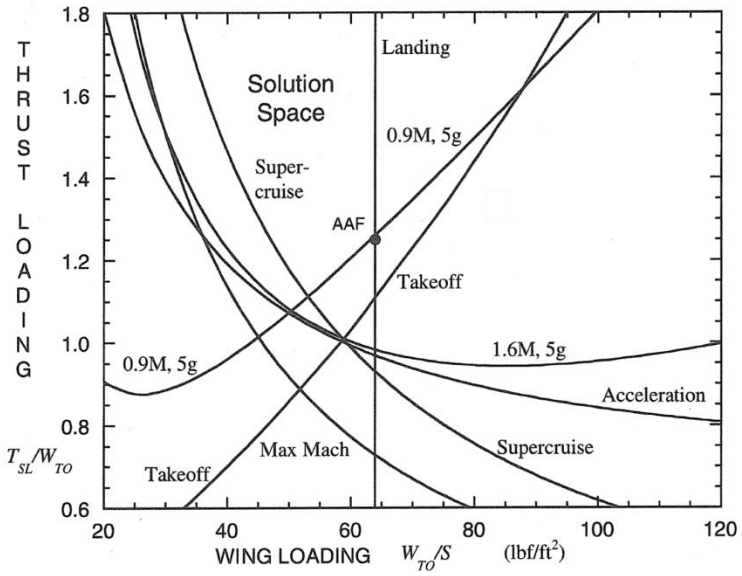

Figure 12: Thrust loading and wing loading derived from the constraint analysis [21]

This approach consists in translating all the various segments of the mission into constraints related to the thrust loading and wing loading (see Figure 12). Design engineers can then identify a feasible point for which the maximum thrust at sea level, the wing area and the maximum takeoff weight are related. Assumptions on weight or maximum thrust at sea level (existing engines provide a good starting point) lead to an estimated value of the wing area so that an initial wing layout can be generated.

A subsequent thorough analysis reveals an additional common backbone between all diagrams regarding the airplane sizing process. The calculation of the fuel consumption over a reference mission is based on three disciplinary analyses associated to both fundamental aeronautical sciences and key enablers: propulsion, aerodynamics and structure. In order to enable the computation of all

engineering characteristics, this common process equally relies on a geometry module that provides all information about the airframe shape as well as the components and systems position within the airframe [62]. To describe this generic Multidisciplinary Design Analysis at conceptual design, it has been decided to use the eXtended Design Structure Matrix (XDSM) proposed by Lambe and Martins [63]. In the field of Aircraft Design, the need of iterative loops rapidly led to computer based synthesis codes [64][65] and recent books [18][46] center their rationale on such computer based approach. The XDSM format is thus well tailored to detail a Multidisciplinary Design Analysis that can be programmed later. Illustrated in Figure 13, the sequence of operations is as follows:

Input:	Engine specifications (based on constraint analysis), initial sketch (based on constraint analysis), approach speed, number of passengers, empennage volumes, required static margin, sizing mission specifications
Output:	Engine deck, aircraft geometry, aerodynamic characteristics, weight breakdown, sizing mission performances

0. Propulsion. The propulsion module takes as input the engine specifications and computes its performance (Thrust, TSFC).

1. First estimate. With an initial sketch of the vehicle, the engine performances and assumptions regarding the mission, a first iterative loop is computed to derive an initial guess for MTOW, MLW, MZFW and the wing area (based on Breguet and aerodynamics data based on historical data).

repeat

2. The Multidisciplinary Design Analysis is started;

3. Geometry. In this module, given a certain number of inputs (approach speed, number of passengers, empennage volumes and static margin), aircraft parameters (fuel weight, maximum landing weight, maximum lift coefficient) and engine geometry, the complete geometry of the aircraft is computed and the main subsystems are positioned. In the generic case, data are stored in the vector identified as *A/C* but a dedicated CAD model can be used instead [19].

4. Aerodynamics. Taking into account the aircraft geometry defined during the previous step, the Aerodynamics module computes the drag polar and other aerodynamics coefficients with respect to the angle of attack, the angle of sideslip and the flight condition.

5. Structure and Weight. Using the engine weight as input, the aircraft geometry and the MTOW value defined at the beginning of the step 2, this module computes the masses of the different aircraft components.

6. Performance. Based on a point mass analysis, the performance module computes the aircraft fuel consumption for the sizing mission based on the engine performances calculated in step 0, the MTOW value defined at the beginning of the step 2 and the aerodynamics properties of the aircraft calculated in step 4. In this module, the segment simulations based on sizing mission specifications use time step integration to better represent real trajectories.

7. Update MTOW. The objective of this function is to calculate the difference between the Operating Weight Empty taking as input the estimated fuel consumption calculated at step 6 $\left(OWE_m = MTOW - FW - W_{payload}\right)$ and the value of OWE resulting from the weight breakdown (step 5). If the difference between these 2 values is higher than a given tolerance, MTOW is updated.

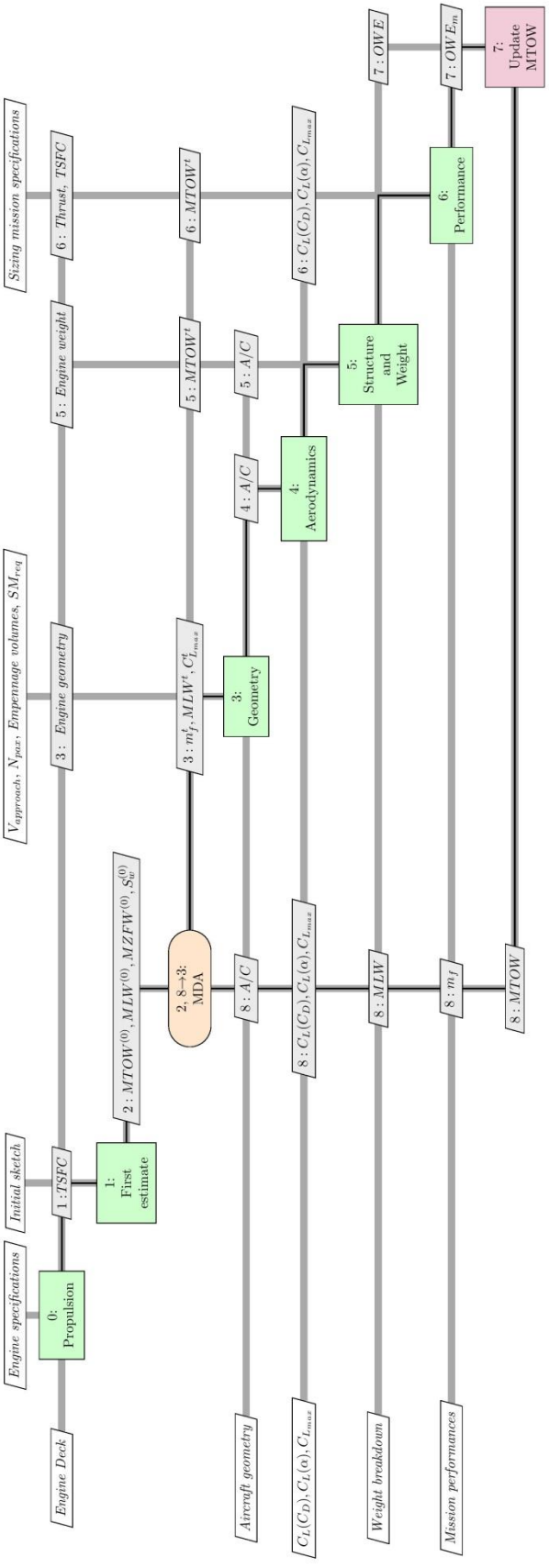

Figure 13: Generic Multidisciplinary Design Analysis at conceptual design (XDSM)

8. Iteration loop. All values calculated by the different modules are returned to the MDA so that a comparison with the target values is made (superscript t in Figure 13).

until 8-2 MDA has converged.

This step-by-step process can be easily traced in Figure 13 following XDSM's guidelines: each green rectangular box represents an analysis while the pink box symbolizes a function. Input variables related to the analysis are placed vertically and outputs are placed horizontally. The thick gray lines trace data dependencies and the thin black lines indicate the data flow. Numbers are provided for each component and each input / output to represent the order of execution previously described.

As stated in Section 1.3.1., the goal of conceptual design is to downselect among many possible combinations a feasible concept that best matches a set of requirements. Through the sizing process based on the MDA, designers can have a good estimate of the vehicle viability by looking at main parameters such as MTOW, wing area or total thrust at sea level. For the downselection, it is necessary to compare more data obtained through one or more disciplinary modules and the performance level for the different mission segments (speed, fuel consumption…). Also, depending on the type of vehicle, different weights can be affected to the selection criteria to finally choose the design to be refined at preliminary level [66]. A key constraint at this stage is the necessity for an unbiased evaluation: key metric values must be calculated with the same sizing logic and identical analysis models so that differences are purely related to the aircraft concept. This implies that the disciplinary modules used in the MDA must feature: (i) the capability to capture the main phenomena, (ii) robustness with respect to design space exploration, (iii) reduced computational time because of the number of concepts to be evaluated. Referring to the competence level for disciplinary analyses [67] reported in Table 1, the MDA is carried out with Level 0 models resting upon statistical data of former products and design rules [68][69]. Proposed by many authors [5][22][25] with some focusing on a particular type of airplane [24][70], such models including "k factors" to simulate technology effects allow a good first scan of the design space.

Table 1: Competence levels of disciplinary analyses [67]

Level	Modeling Details	Physics Representation	Phenomena Type
0	No geometry	Empirical	Design rule
1	Reference quantities	Linear	Static, Steady
2	Analytical	Non linear	Dynamic, Unsteady
3	Numerical	Non isentropic	Transient

As illustrated in the various conceptual design sequences in Appendix 1, the MDA is repeated with refined disciplinary analyses so that a revised layout can be better evaluated. To be classified as Level 1, such models are proposed by Torenbeek [46] for the estimation of the wing structural weight and by Roskam [71] for the definition of a complete aerodynamics characteristics dataset. With the core

process of the conceptual design phase and the associated analysis tool capabilities well defined, the next section provides insights about the design of the next generation of aircraft.

1.4.4. Designing future transport aircraft

The design of future transport aircraft is directly driven by the need to reduce fuel burn so that the product can match the environmental constraints as well as the customer requirement of lower Direct Operating Costs. Thus, during the conceptual design phase, engineers concentrate their work on identifying specific designs or technologies that will improve one or more fundamental enabler without critical penalties. Considering the high level characteristics, such future vehicle would feature a compromise between flight physics disciplines: propulsion (reduced TSFC), aerodynamics (better Lift-to-Drag ratio) and structure (lighter airframe). With the objective of assessing possible options in these three areas, it is interesting to see the progress made so far in the last decades.

Limiting the discussion to turbine engines, the first transport aircraft including this type of propulsion was the British de Havilland Comet (entered service in 1952) featuring the Ghost 50, a pure turbojet. In the 60's, the introduction of low-bypass turbofan engines on the Boeing 727 provided a first significant improvement regarding TSFC and, naturally, such technology became the new norm. Then, in 1970, engine manufacturers enabled another step change in fuel consumption through the introduction of high-bypass ratio turbofans (Pratt & Whitney JT9D, General Electric CF6). Benefits associated to these engines paved the way for successful airplane programs such as the Boeing 747-100. Since then, all airliners have high-bypass ratio turbofans. Figure 14 reports the evolutions of TSFC in cruise for large transport jets and other aircraft type from 1955 to 2005.

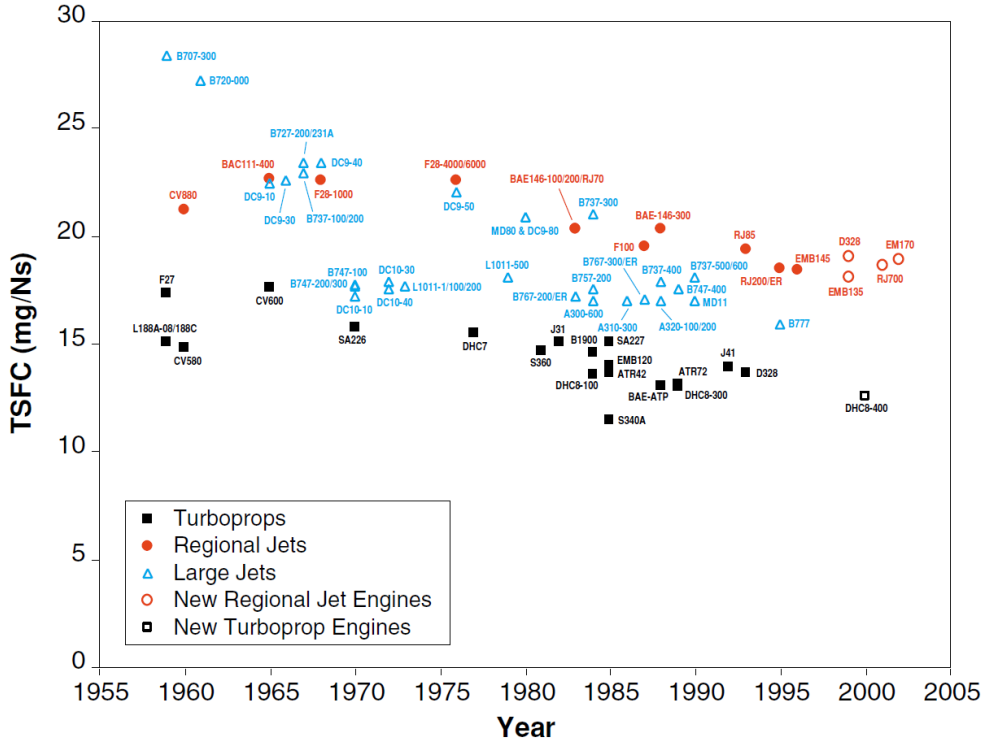

Figure 14: Evolution of Thrust Specific Fuel Consumption from 1955 to 2005 [73]

To illustrate today's level of performance, it is possible to refer to the Airbus A320 NEO aircraft that has the latest ultra-high bypass ratio engine designed by CFM international. This engine, with a bypass ratio of 11, provides a 15% reduction in fuel burn with respect to CFM56 [74]. It is possible to extend the historical view of Figure 14 by adding a point defined by a TSFC of about 14.5 mg/Ns in 2014 (A320 NEO Entry Into Service).

Regarding aerodynamics, the efficiency of the aircraft is represented by the Lift-to-Drag ratio. Historical improvements are then observed by looking at the maximum Lift-to-Drag ratio that has been achieved for given aircraft. As reported by Anderson [75], the first airplanes based on a strut-and-wire architecture reached values around 8. Later came the period of mature propeller-driven monoplanes with NACA cowling with efficiency about 12. In the 1950's, the period of modern jet planes started and the aerodynamic design allowed reaching higher Lift-to-Drag as presented by Babikian [73] and shown in Figure 15.

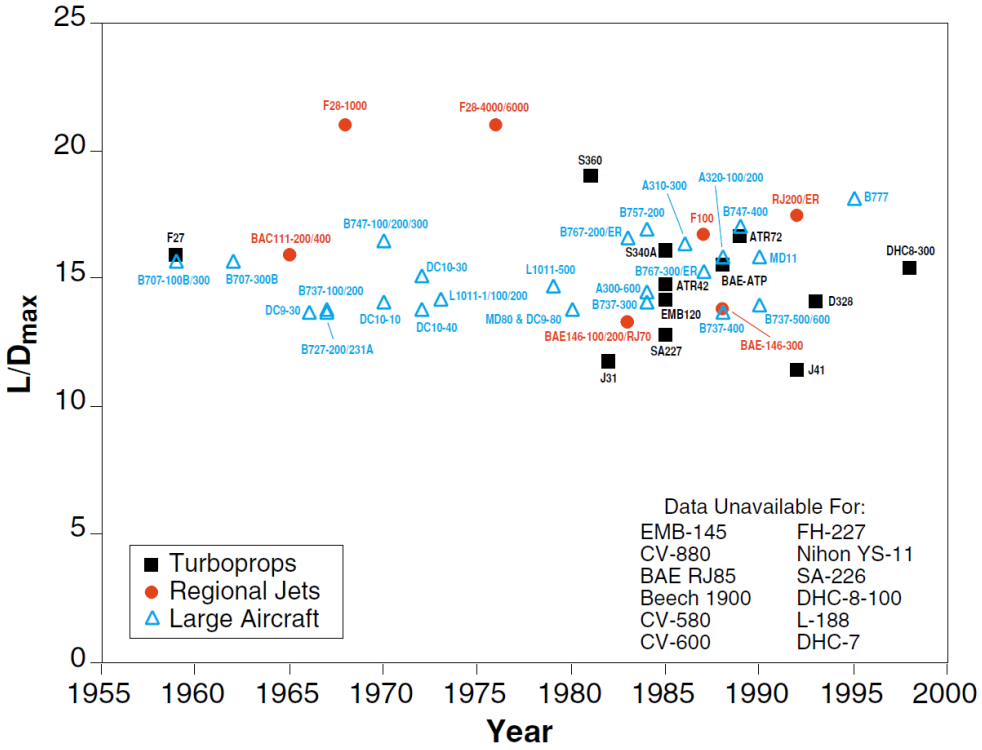

Figure 15: Evolution of maximum Lift-to-Drag ratio from 1955 to 2000 [73]

While observing trends, it is interesting to note that many airplanes introduced after the Boeing B707 (maximum Lift-to-Drag ratio of 15) had lower aerodynamic efficiency. In the 80's, because of the use of CFD during wing design, more efficient propulsion integration and better wind tunnel testing techniques, airplanes featured a better maximum lift-to-drag ratio [76]. Continuing on this positive trends, the Boeing B777 introduced in 1995 reaches a value of 17.5 and nowadays, the Boeing B787 has a maximum Lift-to-Drag ratio above 18 at Mach = 0.88 [77].

In order to estimate the progress made in aeronautical structure in the last decades, one criterion that can be easily monitored is the OWE over MTOW ratio. As MTOW corresponds to the sum of OWE,

payload weight and fuel weight, a lower value indicates a larger portion of the available weight for fuel (more range) or payload capability (more revenue). Figure 16 shows the evolution of OWE over MTOW from 1955 to 2000. Focusing on the values for large jets, the first point to be noted is the important data dispersion. With a more careful review, the different values can be regrouped into two clusters: the first one englobes airplanes up to 1975 with an average ratio OWE over MTOW of about 0.49. The second set considers vehicles that entered into service around 1985 with an average ratio of about 0.51. So, overall, there is a tendency to slightly increase the ratio OWE over MTOW.

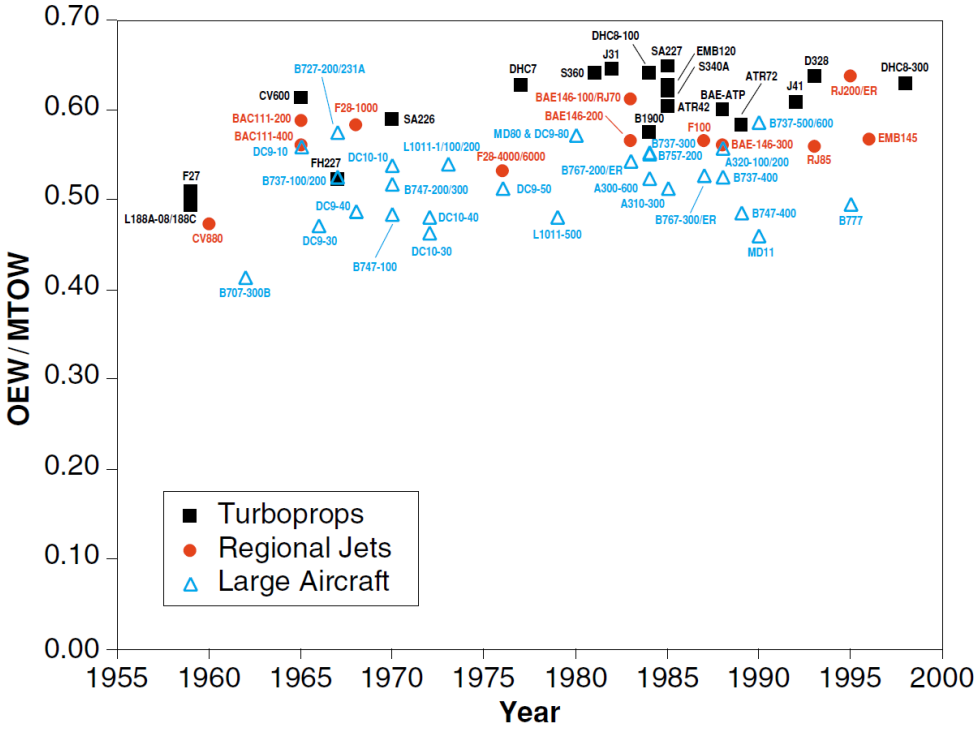

Figure 16: Evolution of OEW over MTOW from 1955 to 2000 [73]

At the end of the 80's, airplane manufacturers started to introduce composites on civil transport aircraft with the objective of reducing weight. Little by little, the proportion of composites increased and nowadays, airplanes such as the Boeing B787 are 50 percent composite by weight [78]. Unfortunately, data provided in [73] do not offer view on such products because of the limited time scale. Thus, additional public domain data [79] have been gathered on aircraft introduced after 1985. Reported in Figure 17, the values show a clearly smaller dispersion around a constant value of 0.52.

In order to understand this trend, it must be recalled that OWE corresponds to the complete airframe weight, including structural weight, engine weight and systems weight. Thus, any penalty in weight associated to the implementation of a technology is captured by the OWE over MTOW ratio. Such losses probably cancel benefits associated to improvements regarding pure structural efficiency [80]. In Figure 17, the values are therefore the result of both the integration of very high by-pass ratio engines characterized by a higher weight and the adaptation of composites for airframe structures (a possible increase of weight due to new systems such as Flight Entertainment should be also considered). To trace progress in structural efficiency solely (with reference to one of the three key

enablers), it is recommended to trace the ratio of structural weight over MTOW for all aircraft of interest.

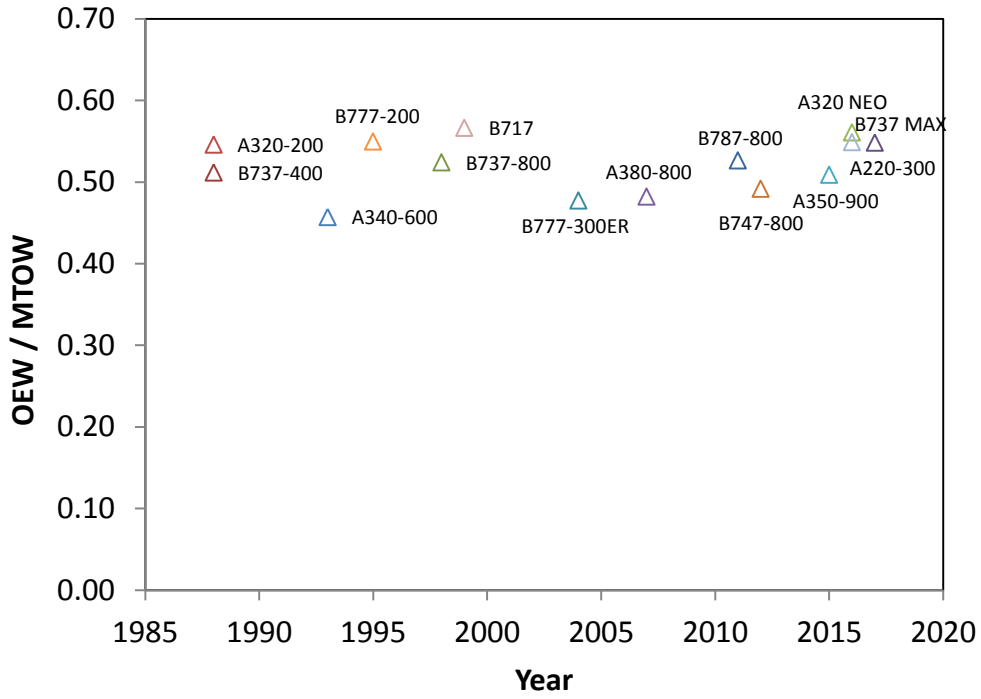

Figure 17: Evolution of OEW over MTOW from 1985 to 2020

This historical review shows that over the last decades, many improvements affecting key enablers have been implemented on transport aircraft. The result is an overall reduction of fuel burn about 45% between 1968 and 2014 [81]. This outstanding progress is the result of a 50 years long continuous optimization of both the classical “tube and wing” configuration defined by Boeing with the B707 and its associated turbofans. Looking further into the disciplines, the maximum Lift-to-Drag ratio has now reached very high values. For propulsion, the turbofans already went through step changes and the use of ultra-high bypass ratio engines could be limited by their size [82]. Regarding airframe structure, manufacturers already used composites on the main components (wing, fuselage, empennage, belly fairing) leaving reduced margins for improvements. Recalling now the stringent requirements in fuel burn fixed by ACARE [53] and NASA [54] for the future generation of transport aircraft, there is an obvious risk that they won’t be attainable with the classical “tube and wing” configuration and its propulsion system.

Researchers and engineers involved in the conceptual design phase must then explore radically new configurations as well as airplane concepts based on disruptive technology to find a design with step performances. Such advanced concepts are illustrated in the figures here below. First, Figure 18 illustrates the Hybrid Wing Body configuration proposed by Lockheed Martin for a military cargo mission [83]. For this aircraft, the idea is to combine most of the benefits associated to a flying wing while decreasing the inherent risks. Besides, the position of the engines allows large bypass ratios and cancels Foreign Object Damage (FOD) issues. As a second example, the Transonic Truss-Braced Wing suggested by Boeing [83] is shown in Figure 19. Here, the key element is a very high aspect

ratio wing that is supported by a truss brace. This structural layout should help in increasing the wing span so that a very high lift-to-Drag ratio can be achieved. From an operational point of view, once on the ground, wings would fold in order to match the aircraft category wingspan limit.

Figure 18: Hybrid Wing Body configuration proposed by Lockheed Martin [83]

Figure 19: Transonic Truss-Braced Wing suggested by Boeing [83]

When looking at innovative technology implementation, hybrid electric propulsion architecture offers different options [84]. As chosen by ESAero, the availability of many electric fans enables distributed propulsion. Applied on the ECO-150 (Figure 20) this technology features positive aero-propulsive effects that lead to an efficient short range aircraft. Also relying on a hybrid electric architecture, the STARC-ABL concept defined by NASA (Figure 21) is characterized by two large turbofans coupled to generators. These generators supply power to a large electric fan located at the rear of the fuselage. Because of its position, this fan subsequently ingests the boundary layer that has formed over the entire fuselage resulting in an overall positive thrust / drag balance with a lower power setting.

Figure 20: Distributed propulsion concept designed by ESAero [85]

Figure 21: Boundary Layer Ingestion concept considered by NASA [86]

In the design process, such novel aircraft must be evaluated at conceptual design stage against other potential candidates including evolutions of the conventional “tube & wing” configurations. However, these airplanes are characterized by new shapes, whose aerodynamics properties cannot relate to previous studies. In addition, their new geometry also implies strong and complex coupling between disciplines, and in some cases, important airframe/engine interactions must be considered because of key aero-propulsive effects. With respect to these new technical challenges, the generic Multidisciplinary Design Analysis as it is detailed in Section 1.4.3. is no more sufficient to carry out a reliable sizing process. In the next section, the goal is to identify the limitations to be solved.

1.4.5. Problem statement

To better point out the issue, it is interesting to have a deeper appraisal of the previous studies on disruptive concepts. Regarding the Hybrid Wing Body represented in Figure 18, Hooker and Wick provide valuable information about the analyses that have been performed [87]. First, because of the innovative shape, Navier-Stokes based CFD have been used at conceptual design for aerodynamic performance and design. Coupled with optimization loops, the accurate calculations provided key information in cruise conditions that have a profound impact on sizing. Second, CFD and thrust-to-drag bookkeeping methods have been used to assess different engine options (current turbofan, Ultra High Bypass Ratio engine, Open Rotor) and various locations around the HWB. For structure, as structural layouts of Blended Wing Body concepts are still an open discussion, semi-empirical equations calibrated through high fidelity codes have limited applications. Thus, as expressed in an ONERA publication [89], it is recommended to use FEA as soon as possible to take into account the fuselage shape and cabin / luggage hold layout. Considering now the Truss-Braced Wing concept illustrated in Figure 19, Chakraborty [90] details a design study based on a multidisciplinary process. As this concept fully relies on a very high aspect ratio wing, the interactions between aerodynamics and structure must be considered within the MDA. To this end, a specific physics-based analysis tool has been developed by Gur [91] as the classical methods are not tailored to capture such complex phenomena. Based on a FEA approach, the disciplinary module sizes the structure according to 19 load cases and calculates the weight that is used for mission performance assessment. With more reliable structural assessments, the design team can then explore solutions with thinner airfoils so that the sweep angle can be reduced. This is an important high level criterion to enable the Natural Laminar Flow (NLF) technology to further reduce drag. In this case, CFD becomes mandatory to accurately predict the aerodynamics performance of the NLF wing [92]. Last but not least, the high aspect ratio value on a Truss-Braced Wing concept hypothesizes a higher risk of flutter. To mitigate such problems, aeroelastic evaluations are key to support downselection decisions [92]. When looking at hybrid electric aircraft, design details of the ECO-150 (Figure 20) based on distributed propulsion are given by Schiltgen [93]. Unsurprisingly, the sizing process is based on a detailed analysis of the propulsion system that includes ducted fans, gearboxes, motors/generators and their controllers, power cables and turboshaft engines. Because of their power level, components of the hybrid electric chain generate some heat. Therefore, a thermal management system under the form of a liquid cooling system with ducted radiators has been designed. As such element is essential towards the feasibility of the entire concept, it becomes mandatory to consider it early in the design process. To confirm aerodynamics in cruise condition and at low speed, the design team also ran many CFD simulations. For the latter, focus was put on calculating the powered lifting capabilities obtained through the aero-propulsive effects and their impact on operational aspects. Finally, as the number of components of the hybrid electric chain is quite high, there has been an important effort in integrating all systems within the airframe to identify potential blocking points (CAD model). For the Boundary Layer Ingestion concept called STARC-ABL (Single-aisle Turboelectric AiRCraft with an Aft Boundary Layer propulsor) and shown in Figure 21, one of the crucial points to be analyzed is the rear fan performances when ingesting the Boundary Layer [94]. To this end, thanks to CFD simulations, a normalized map of the boundary layer has been calculated and used in the program NPSS (Numerical

Propulsion System Simulation [33]). Subsequently, performances of the complete propulsion system have been calculated and overall aircraft trade studies have been achieved. The other essential phenomenon that must be considered is that the positioning of the fan at the end of the fuselage allows a reduction of wasted kinetic energy [95]. Thus, to fully assess such configuration and estimate the possible reduction in required power for flight, Reynolds Averaged Navier Stokes (RANS) CFD simulations including a thermodynamic propulsion model must be performed [96].

In these various examples, design engineers had no reliable data about the configurations or technologies to be explored. Thus, to achieve valuable assessments and robust downselection of the concepts, there was a required search of additional details on the airframe and the propulsion system so that physics-based analyses could be performed. This clearly multidisciplinary effort has been made towards a unique goal: knowledge about the aircraft had to be generated.

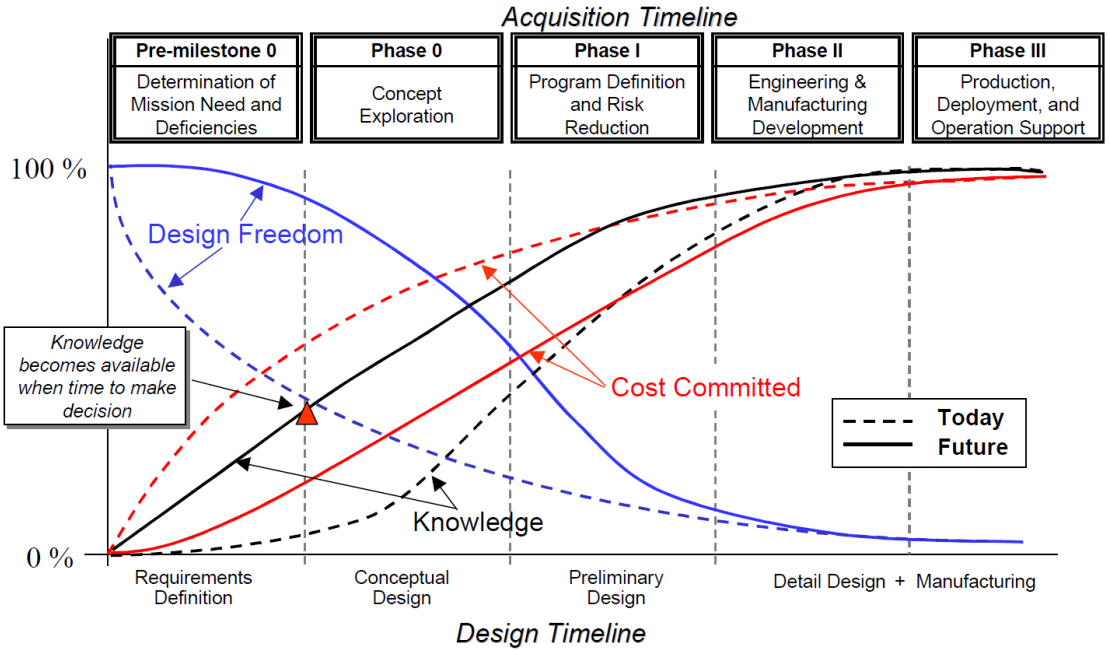

Figure 22: The relationship of design freedom, knowledge, and cost committed [9]

This idea is corroborated by Wood and Bauer in their research towards improving the efficiency and effectiveness of multidisciplinary design; they state that "we must focus on including ever greater amount of knowledge into the conceptual design" [97]. In Figure 22, benefits of knowledge addition in the early phases of the design process are shown. With additional knowledge available in the early phases, the design engineers have more options to consider which translates into an increase of design freedom for a longer period. With the design freedom expanded, cost commitment can be delayed. Thus, at a given step in the aircraft program, this is equivalent to a reduction in committed cost [9]. At industry level, such change is key for program management as decisions based on better knowledge would decrease major risks [98].

For research in Aircraft Design, the key question is now **"How to add knowledge in the Multidisciplinary Design Analysis at aircraft conceptual design level?"**

1.5. Available solutions for adding knowledge to the aircraft MDA

The addition of knowledge during the conceptual design phase is a twenty years old as confirmed by the publication date of some of the references previously cited [97]. In the last decades, advances in computing capabilities [99], progress in aeronautical disciplines and fundamental sciences provided many options to increase the level of knowledge in the first phase of the design process. In this research, the available solutions have been classified into four groups.
First, there is the possibility for the design engineers to add more knowledge through the application of Multidisciplinary Design Optimization (MDO) techniques as proposed in [5][18]. Second, higher accuracy and reliability in the disciplinary analyses can be achieved by using higher fidelity tools generally used at preliminary design stage. In other cases, the design of the airplane and/or a customer requirement could require the addition of new disciplines or aircraft subsystems that are not considered at all within the original MDA. By adding such new modules in the MDA, additional knowledge is available. To better appreciate the fourth method to add knowledge, it is important to recall that conceptual design is distinguished by a lack of data. This issue generates a level of uncertainty; the idea is then to enhance information by better quantifying, managing and reducing this uncertainty.

In the next sections, different examples are provided in order to illustrate these four different approaches knowing that the solutions are not exclusive. It is possible to combine them for further benefits at the cost of increasing the process complexity.

1.5.1. Multidisciplinary Design Optimization

Multidisciplinary Design Optimization has been acknowledged as a new field of research by Sobieszczanski-Sobieski in 1993. More specifically, he defines MDO as “a methodology for the design of complex engineering systems that are governed by mutually interacting physical phenomena and made up of distinct interacting subsystems” with a key capability that is the identification of “synergism of the disciplines and subsystems” [100]. Considering the aircraft MDA defined in the previous chapter, the fuel burn objectives and the conflicting requirements among disciplines, the design of an aircraft is a good use case for MDO. With many potential benefits associated to this research area, many efforts in the field of aeronautics took place [101]. In a work focusing on the application of MDO at conceptual design, Raymer states that “such MDO techniques can reduce the weight and cost of an aircraft design concept in the conceptual design phase by fairly minor changes to the key design variables, and with no additional downstream costs. In effect, we get a better airplane for free” [102]. For aircraft designers, the identification of the best aircraft or the best family of aircraft is of course a key output but the optimization process also provides important additional information about the design space exploration and active / non violated constraints. As stated by Martins [103], the fundamental step to carry out MDO is the accurate description of the problem that must be solved. First, the objective of the optimization must be defined. In some case, it is a simple

scalar to be minimized (e.g. fuel burn). In others cases, design engineers are required to consider multiobjectives (e.g. noise and range) knowing that the result will be a family of optimum designs. This MDO problem is also associated to Design Variables, the parameters that define the system of interest. During the optimization, the search of the best design explores the design space that is linked to these Design Variables and their upper/lower bounds. Depending on the problem, the Design Variables can be continuous (e.g. sweep angle of the main wing) or discrete (e.g. number of blades for a propeller). In most cases, the complex system to be optimized has to meet a certain number of constraints that are in fact functions of the Design Variables. If a function must be equal to a fixed value, the problem deals with an equality constraint. If the function has to be lower/greater that a certain threshold, it is said that the process manages inequality constraints. The convergence to the most promising set of design variables is driven by the optimization algorithm or optimizer. In this domain, engineers can select between gradient-based or gradient-free optimization, each one offering specific capabilities with inherent drawbacks [104]. Naturally, at the core of the optimization problem lays the Multidisciplinary Design Analysis that delivers the system responses to a given set of Design Variables. For MDO, such concurrent approach between the disciplines is key as it has been demonstrated that a sequential approach cannot capture the multidisciplinary optimum [105]. Considering all these information related to the optimization problem, the architecture or formulation of the MDO can be selected. This formulation is the organization of both the multidisciplinary analysis and the optimizer(s), and two options are available: monolithic architectures or distributed architectures [106]. It is not uncommon to have the formulation constrained by practical problems such as the availability of coupled high fidelity analysis tools or the structure of the aircraft design legacy code. In terms of performance, Martins concludes in 2013 that "the distributed architectures still seem to be more expensive than the monolithic architectures they are meant to supersede" [106]. Depending on the optimization problem, the objective function to be optimized may require analysis tools with a high computational cost. In order to reduce process time, there are many initiatives to use surrogate models to replace the analysis tool in the MDO [107]. It may also happen that the critical element in terms of computational cost is the evaluation of the constraint. As described by Bettebghor [108], the constraint (buckling factor) can be approximated by a surrogate model (mixture of experts).

The work carried out by Alonso [109] provides a complete example of the application of MDO for an unconventional airplane. In this work, the objective is to optimize a generic supersonic aircraft configuration for low ground sonic boom and longer range. As the aerodynamics and acoustics analysis tools are expensive in terms of CPU time, the authors decided to replace these analyses within the MDA by a surrogate model. Generated on the base of 300 high fidelity data points via Neural Networks [104], this approximation model of the aerodynamic properties and noise boom assessment is coupled with low fidelity weight estimations and the performance analysis tool. As it is a multiobjective problem and there is the risk of multiple local minima in the design space of interest, the gradient free optimizer NSGA II [110] has been selected. The result of the MDO is a Pareto front that provides much information to the design engineers (see Figure 23).

First, the tradeoffs to be made at configuration level towards the two objectives can be acknowledged. Especially, a purely low noise aircraft or a long range aircraft can be singled out. Second, the shape of

the Pareto with a clear discontinuity determines a value of perceived noise level (67.5 dBA) and a range (3000 nm) that is a good overall compromise. Indeed, any increase in range would be associated to an important weight growth and any decrease in noise would go along with a reduction in range capabilities.

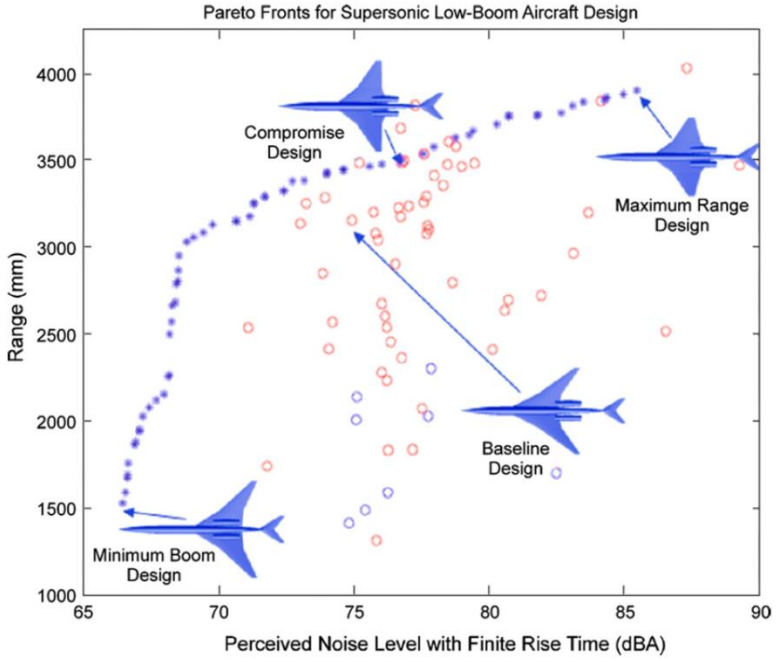

Figure 23: Resulting best family of generic supersonic aircraft configuration [109]

1.5.2. Addition of accuracy through higher fidelity disciplinary modules

The methods proposed in the following paragraphs are usually used in the preliminary design phase. In the case of unconventional configurations, there is an added value in applying them at conceptual design stage. The increase of accuracy and reliability of the results is counter balanced by longer setup time of the analysis and less design space exploration capabilities.

1.5.2.1 Finite Elements Method

For the sizing process and its MDA, one essential element when assessing unconventional configurations is the airframe weight calculation. Misuses of empirical equations can lead to important errors and wrong decisions. In such cases, the structure group initiates a detailed modeling of all components of the structural layout and proceeds with a real sizing process of the airframe. With the size of the elements fixed, accurate weight estimation is made. The steps of such a high fidelity analysis are provided by Mukhopadhyay [111] and listed here below:

1) Develop detailed geometry and finite element model of parts and assembly.
2) Apply material properties, loads, and boundary conditions.
3) Generate a finite-element mesh and perform FEM analyses of parts and assembly.
4) Plot stress, strain, displacement, and safety factor distributions.

5) Resize and redesign for stress and deformation reduction.
6) Repeat steps 1 through 5 for design feasibility and improvement.
7) Compute structural weight of each component and assembly.
8) Compare the computed weights with existing empirical estimates.

In order to visualize FEM analyses capabilities, results of the structural layout design of a distributed propulsion aircraft wing are illustrated in Figure 24. Moreover, Figure 24 provides a good view on the required level of details about the wing structure.

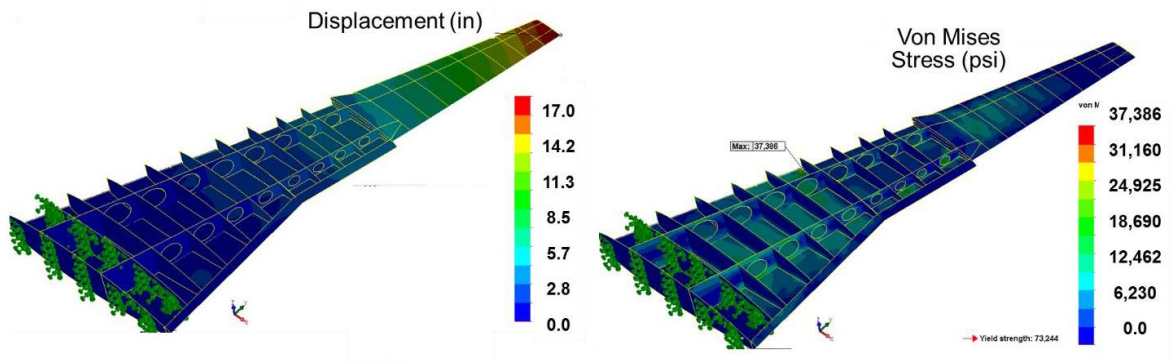

Figure 24: Deflection and stress distribution for a distributed propulsion aircraft [111]

Overall, the integration of FEM within the MDA is the only way to secure accurate estimations for the structural mass for an airframe with no historical database. However, because of the level of details that is required to carry out such analysis, a true expertise in structural layout is required. Besides, the parametrization of the finite element mesh is time consuming and its complexity may lead to robustness issues that limit the design space exploration. Thus, design engineers must then carefully select the configuration on which FEM must be applied during the conceptual design phase, also considering CPU time limitations.

1.5.2.2 Computational Fluid Dynamics

The Lift-to-Drag ratio is a key enabler towards the reduction of fuel consumption. Results of the sizing process through the MDA are thus totally related to the estimation of this aerodynamic efficiency ratio. For the "tube and wing" configuration, as there is a large database on existing vehicles, semi-empirical equations can provide accurate results [112] but such capability becomes very unreliable for unconventional shapes. In such condition, design engineers have to count on RANS CFD analyses performed by the aerodynamics group to accurately determine the Lift-to-Drag ratio. The first step consists in generating a 3D model of the configuration under investigation whose surfaces meet continuity requirements. Subsequently, the surface mesh and the volume mesh are generated so that the simulation with a given solver can be launched. The aerodynamic optimization depicted by Lyu [113] details the large amount of knowledge that can be gathered through high fidelity computations for a Blended Wing Body (Figure 25):

- Definition of the best airfoil shape and twist all along the span;

- Definition of the best airfoil shape and twist all along the span considering a constraint on trim;
- Definition of the best airfoil shape and twist all along the span as well as Center of Gravity (CoG) position considering constraints on trim and static margin;
- Definition of the best airfoil shape and twist all along the span considering various bending moment constraints;
- Definition of the best airfoil shape and twist all along the span as well as planform geometry considering various bending moment constraints;
- Definition of the best airfoil shape and twist all along the span considering a multipoint design for cruise conditions.

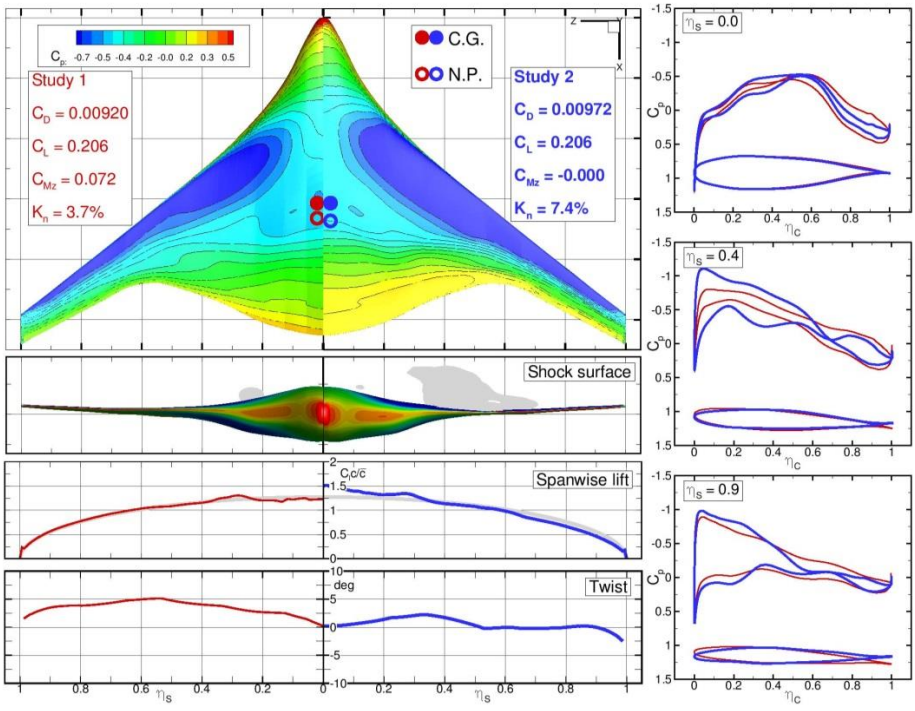

Figure 25: Results from RANS CFD analyses [113]

In terms of aircraft design, CFD studies can thus deliver not only accurate Lift-to-Drag ratio calculations but also data affecting structure, CoG positioning and stability that would contribute to the identification of the best overall configuration. However, "grid generation is a major problem in the CFD process and is the bottleneck with complex geometries" [114]. In addition, computational time for a complete aircraft (about 12 hours [115]) is not compatible with the other analyses within the MDA. Thus, it is difficult to include such simulations directly in the sizing process. As for the FEM applications, design engineers have to wisely choose the configuration and the runs to be performed with RANS CFD. It must be also noted that the 3D geometry for CFD studies requires a high finishing in all areas such as surfaces junctions with fairings. As it is difficult to standardize the definition of these elements, a fully parametrized 3D geometry may lead to robustness problems. A first step towards the direct use of high fidelity aerodynamic analyses is proposed by Defoort [116]. In this paper, the ONERA sizing code MYSTIC (MultidisciplinarY Sizing Tool for Integrated Concepts)

features an Aerodynamics analysis module based on Euler-CFD computations performed by the SU² code [117]. In order to limit mesh generation time, surface mesh and volume mesh are automatically generated through OpenVSP [19] and TetGen [118] respectively. The tradeoff is about the accuracy of the analysis as viscous effects are not captured.

1.5.2.3 Aerostructural coupling

Transport aircraft have relatively high aspect ratio wings. When subject to aerodynamic loads, the cantilever wing naturally deflects up to 12 feet at wing tip [119] in steady flight. Thus, the flight shape of the aircraft that defines the Lift-to-Drag ratio is the result of an equilibrium between the spanwise lift distribution and the wing structural properties. To investigate such interaction, structure and aerodynamics high fidelity analyses can be coupled. In such a scenario, design engineers would receive reliable values for: (i) aerodynamics coefficients calculated on the correct flight shape that depends on the structural design; (ii) the wing weight that is determined through a sizing process considering the loads depending on the aerodynamic design. To quantify the added value of the approach, Mader compares results on the D8 concept [120] obtained through high fidelity aerostructural optimization with faster tools used during the exploratory phase [121]. In the case of a cruise Mach of 0.84, the process converges to a disciplinary compromise with an improvement of 6% for the Lift-to-Drag ratio and an increase of the wing weight of 6%. Based on an rearrangement of the Breguet equation, the calculated fuel burn shows a gain of about 11.6% with the first design loop. In a downselection process, such differences cannot be neglected as they could lead to erroneous elimination of concepts. Obviously, computational time for these high fidelity bi-disciplinary analyses is very high. This is a hard point for a direct coupling with the conceptual design sizing loop. Studies such as the ones proposed by Lefebvre [122] and Variyar [123] are consequently looking towards multifidelity approaches in order to benefit from the data accuracy without penalizing the overall aircraft design loop.

Another area where the aerodynamics / structure interaction is critical is aeroelasticity, especially the determination of flutter conditions. As stated in Section 1.4.5, some unconventional configurations as the Strut-Braced Wing (SBW) configuration are naturally more affected by flutter. In the complete multidisciplinary design process carried out by DLR on a SBW airplane [124], a first loop based on low-level physics analyses computes a wing and strut mass of 11200 kg. The subsequent design step includes high fidelity aeroelastic computations so that flutter constraints could be taken into account with a reference dive speed of 180 m/s. In such conditions, the wing weight is increased by about 42% to reach 15900 kg. Thus, during the downselection process that takes place at conceptual design, the use of high fidelity method can be mandatory to validate the decision to select or eliminate an unconventional configuration.

1.5.3. Addition of more disciplines or systems in the design process

Taking the aircraft MDA presented in Section 1.4.3 as reference, it considers only three disciplinary analysis tools and performance calculations for a given mission as it is focused on the sizing of the airplane. However, additional disciplines or subsystems evaluations can be added to the MDA as their impact on unconventional configuration design can be critical.

1.5.3.1 Flying qualities

According to Anderson [7], during their journey towards the first powered flight, the Wright brothers focused "on the problem they felt was the most important to solve first – equilibrium and control of a flying machine". The result is that the Wright Flyer is characterized by a wing warping system enabling lateral control. In his classification scheme of flight mechanics, Chudoba [125] classifies all subjects related to stability, control qualities, vehicle response and pilot-vehicle interaction under the term Flying Qualities. The sizing of control surfaces to pilot the airplane around the three axes then falls under this discipline. For classical "tube and wing" configurations, as the decomposition of primary functions among the key components is well established, the location and size of the control surfaces is well known. Thus, in the early design stages, the size of control surfaces and their layout are usually based on a review of previous designs [68] and some basic design rules [5]. However, in the case of unconventional configurations such as the BWB concept illustrated in Figure 26, historical information is of little interest and, more importantly, the control surface location and size affect the overall design. In such cases, it is necessary to include flying qualities analyses in the MDA.

A first approach has been proposed by Kay [127] in order to assess the control authority earlier in the design process to avoid costly redesign iterations. In this work, the first key step has been the identification of the critical flight conditions and manoeuvres that will size movables (see Table 2): a set corresponds to equilibrium and performance aspects while the second group clearly focuses on dynamics considerations.

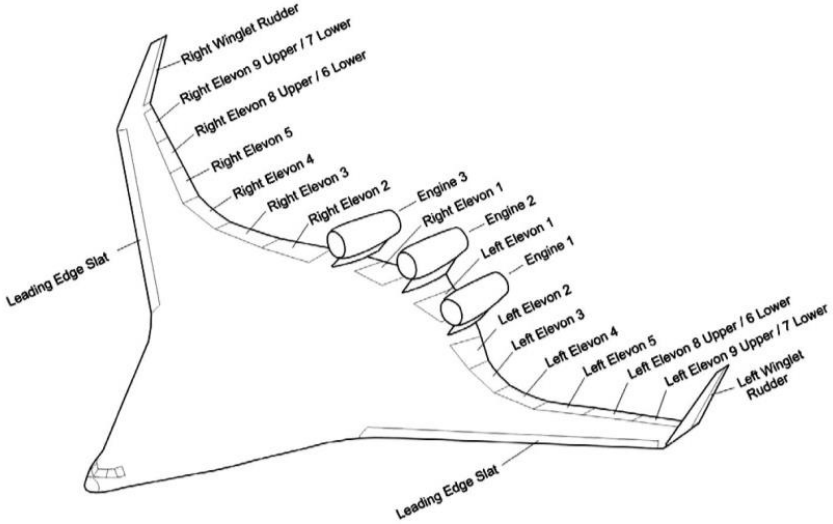

Figure 26: Example of control surfaces arrangement on a BWB [126]

Table 2: Critical flight conditions and manoeuvres [127]

Equilibrium/Performance Considerations	Dynamic Considerations
1) Normal Trimmed Flight	1) Takeoff and Landing Rotation
2) Classical 1G trim	2) Time-to-Bank
• Elementary Control Allocation	3) Inertia Coupling: Pitch Due to Velocity Axis Roll
• Longitudinal Manoeuvring Flight	4) Inertia Coupling: Yaw Due to Loaded Roll
• Steady Sideslip	5) Coordinated Velocity Axis Roll and Roll Acceleration
3) Engine-Out Trim	6) Short Period & CAP Requirements
	7) High Angle-of-Attack/Departure

Secondly, the necessity to have an aerodynamic analysis tool providing stability derivatives and control derivatives has been identified (it led the author to develop its own vortex lattice code [128]). With such database generated, control power is subsequently evaluated for the different control surfaces in all critical flight conditions and manoeuvres. If designers consider that the deflection of the control effector is too high, its size must be increased. In order to avoid many sizing loops with manual iterations, Chudoba [125] proposed a similar but more generic method called AeroMech to be implemented in a multidisciplinary Design Analysis. As it is non specific, the stability and control analysis tool can be applied to conventional "tube and wing" configuration but also to unconventional architectures such as three-surface configuration or oblique flying wing configuration. After the definition of both the constraints to be met by the aircraft (civil [129] or military specifications [130]) and the control allocation logic, the following sequence is proposed:

1) Full aerodynamic analysis (Chudoba selected VORSTAB [131] to perform this task);
2) Static 6 Degrees of Freedom equations of motion (trim conditions);
3) Trimmed aerodynamic data set for performance computations;
4) Analysis of the closed loop aircraft;
5) 6 Degrees of Freedom equations of motion (dynamic mode);
6) Reduced order model dynamic mode evaluation (to gain physical insights about key drivers);
7) Control power assessment and stability information are provided in an output file.

From the sizing process and MDA point of view, it must be noted that such additional disciplinary analysis automatically sets requirements for other modules. For example the weight and structure component shown in Figure 13 should now return inertia properties so that the dynamic manoeuvres can be properly assessed. In addition, the MDA must be adapted so that the information provided by the Flying Qualities analysis can be integrated within the sizing loop.

1.5.3.2 Flight Control System

Recalling the classical sequencing described at the beginning of this chapter, Flight Control System (FCS) is defined after the configuration is frozen to match the required manoeuvrability capabilities [34]. However, it is known that the Flight Control System and the overall aircraft configuration are

closely coupled [132]. Following the same notion, Carpenter stresses FCS benefits with respect to the weight breakdown: "One of the great benefits of a control-configured vehicle is the fact that its structure may be made substantially lighter that its conventional equivalent. A reduction in aircraft weight is one of the major advantages to be gained by relaxing the aircraft's longitudinal static stability" [133]. The work published by Sauvinet highlights the industry interest in such control configured vehicle [134]. Indeed, a reduced natural longitudinal dynamic stability compensated by a FCS allows the reduction of the horizontal tail plane and improves performances (reduced weight and drag). In terms of feasibility, the publication details that tailored control laws have been designed, implemented and flight tested on an Airbus A340 prototype. With positive feedback by the flight crew, the concept has been considered validated and it paved the way for future projects developments. Recognizing the need to perform the stability and control analysis including control laws in an aircraft MDA, Chudoba added in AeroMech the use of Equivalent Stability Derivatives in order to emulate the FCS [125]. Quantitative benefits associated to relaxed stability aircraft are estimated through the complete multidisciplinary optimization achieved by Perez [135]. In this study, output feedback controllers are added in the dynamics and control analysis of the MDA so that aircraft using Stability Augmentation System (SAS) can be sized. The commanded control surface deflections determining the aircraft motion are thus calculated through proportional gains applied on aircraft responses:

- For elevator, the feedback loop applies gains on the angle of attack α and the rotational speed along the lateral axis q;
- For ailerons, the feedback loop applies a gain on the rotational speed along the longitudinal axis p;
- For rudder, the feedback loop applies gains on the sideslip angle β and the rotational speed along the vertical axis r.

As there are many longitudinal and lateral-directional design constraining conditions and various Handling Qualities requirements [130] for the different mission segments, the MDA has been revised so that the aircraft sizing could be achieved through an optimization based on a Collaborative Optimization (CO), a distributed architecture. Figure 27 presents the resulting geometries of two aircraft sized and optimized with the same MDAO process. On the left, the shape corresponds to a "tube and wing" configuration following the traditional stability requirements (FCS has been disabled). On the right, the geometry shows changes on the layout for when the FCS allows relaxed stability. As expected, the airplane on the right presents a reduced horizontal tail plane. More significantly, this optimized aircraft reaches a range that is almost 10% higher than the one for the conventional aircraft with no FCS for the same MTOW.

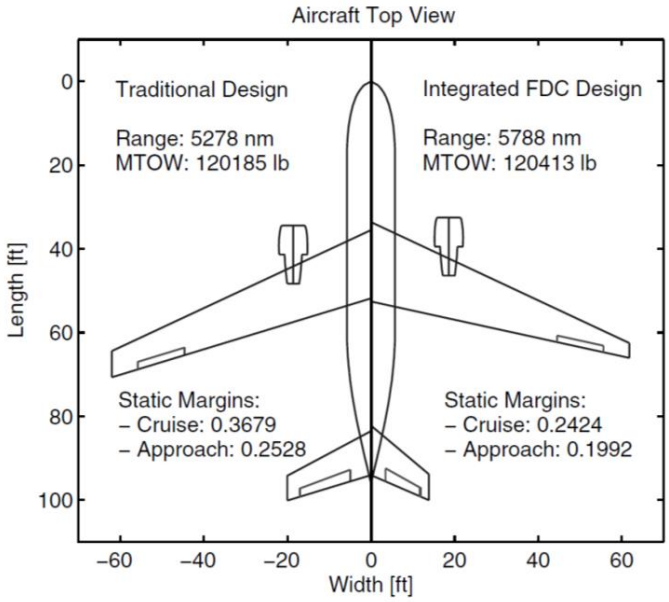

Figure 27: Impact of the Flight Control System on aircraft geometry [135]

The next step towards a more realistic assessment would be the identification and quantification of penalties at the aircraft level that are associated to the installation of more robust control systems to maintain the required safety level for control configured vehicles [136].

1.5.3.3 Thermal constraints

In the reference Aircraft Design textbooks [5][6][13][24][25][27], thermal analyses are rightfully not considered as for classical configuration using classical turbofans, they do not affect the sizing process. However, with the increase of By-Pass Ratio, the industry started to recognize thermal integration issues [137]. When considering future transport vehicles based on hybrid electric propulsion, this issue becomes critical. Indeed, in an electric propulsion concept, each component generates heat because of its inefficiency. With no monitoring of such thermal behavior, there is the risk of reaching very high operational temperatures that may affect not only the component integrity but also the one of surrounding subsystems. To mitigate this risk, MDA capabilities must be increased by adding analyses so that thermal aspects can be investigated earlier in the design process. In [93], the design approach used by ESAero to design a Turboelectric Distributed Propulsion Airliner identified as ECO-150 is described by Schiltgen. In this publication, details are given about the software (PANTHER - Propulsion Airframe iNTegration for Hybrid Electric Research) that has been used to design the propulsion system. Among the many disciplinary analyses within PANTHER, a specific thermal management system module is added to perform the mandatory verifications. With such capability, the design team estimated that the electrical components would produce nearly 1491 kW of heat at the top of climb flight condition. Such information provided at the beginning of the design phase allowed the engineer to include a recirculating liquid cooling system during the vehicle sizing process. Another example associated to thermal constraints is related to the NASA X-57 electric testbed [138]. Among the latest developments of electrical vehicles, this demonstrator is an exciting initiative as it will demonstrate through flight the various advantages associated to distributed electric

propulsion. However, because of the fully electric propulsion architecture that is considered, thermal characteristics must be monitored. To this end, Falck added within the classical Multidisciplinary Design Analysis dedicated to performance the necessary analysis capability so that the temperature evolution of the electrical components could be computed [139].

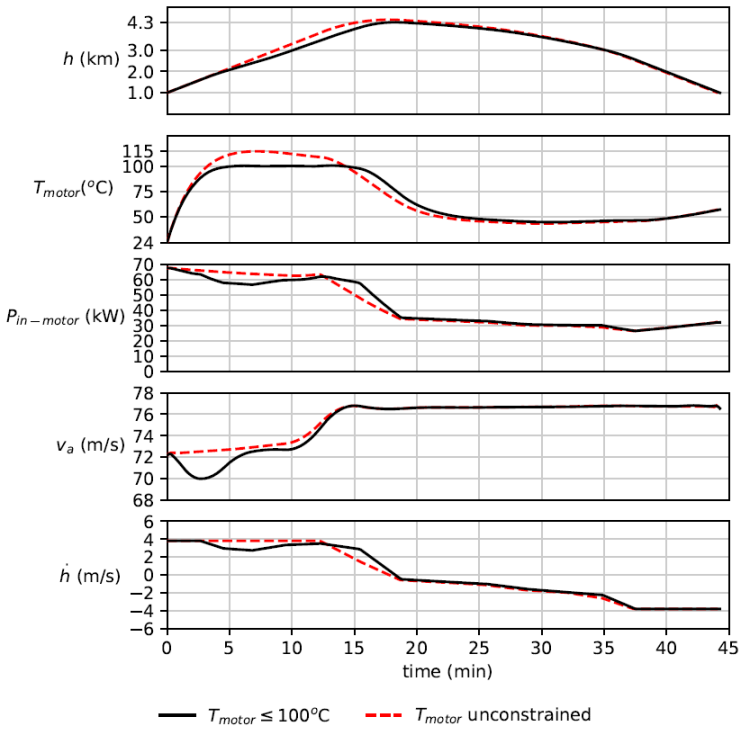

Figure 28: Optimized flight profiles with and without constraints on motor temperature [139]

The end result is the possibility to optimize the aircraft trajectory subject to thermal constraints. Results of such optimizations are illustrated in Figure 28 where it is seen that the limitation on engine temperature requires a reduction of the climb rate. After the climb phase, the aircraft can follow the nominal trajectory without reaching critical temperatures.

1.5.4. Uncertainty management

During the aircraft design process, two types of uncertainty can be identified [140]. First, there is aleatory uncertainty. It is associated with the fact that the values used for some parameters affecting the vehicle design are not known. An example is the cruise altitude of a civil transport aircraft to be used as a mission parameter in the MDA. Indeed, as this value changes according to operations, it is difficult to associate a single value. One aspect of aleatory uncertainty is that is cannot be reduced during the design process. This is why this type of uncertainty is also called irreducible uncertainty. Epistemic uncertainty, on the other hand, is associated with the models used in the design process. These analyses are in fact models representing a real phenomenon or a system. Naturally, approximations are made and thus, the outcomes of these models generate some errors. In the case of unconventional configurations, this scenario is often verified. With respect to aleatory uncertainty, epistemic uncertainty can be reduced while progressing in the design process. For example, the

prediction capabilities of a model can be enhanced following corrections based on high fidelity computations or experimental tests.

In the classical MDA, both uncertainty types are considered by introducing some margins within the design process. The problem is that such margins automatically penalize a potential good candidate in the downselection process. The classical approach for uncertainty analysis is presented by Sudret [141] where three steps are identified: definition of system model and identification of the design / assessment criteria, quantification of uncertainty sources and finally uncertainty propagation. In [142], Kirby illustrates the aleatory uncertainty management in the case of Aircraft Design so that probability of success to achieve a certain takeoff gross weight for different technology scenarios is assessed. For an investigation of epistemic uncertainty associated to Aircraft Design, an example is provided by Chakraborty [143].

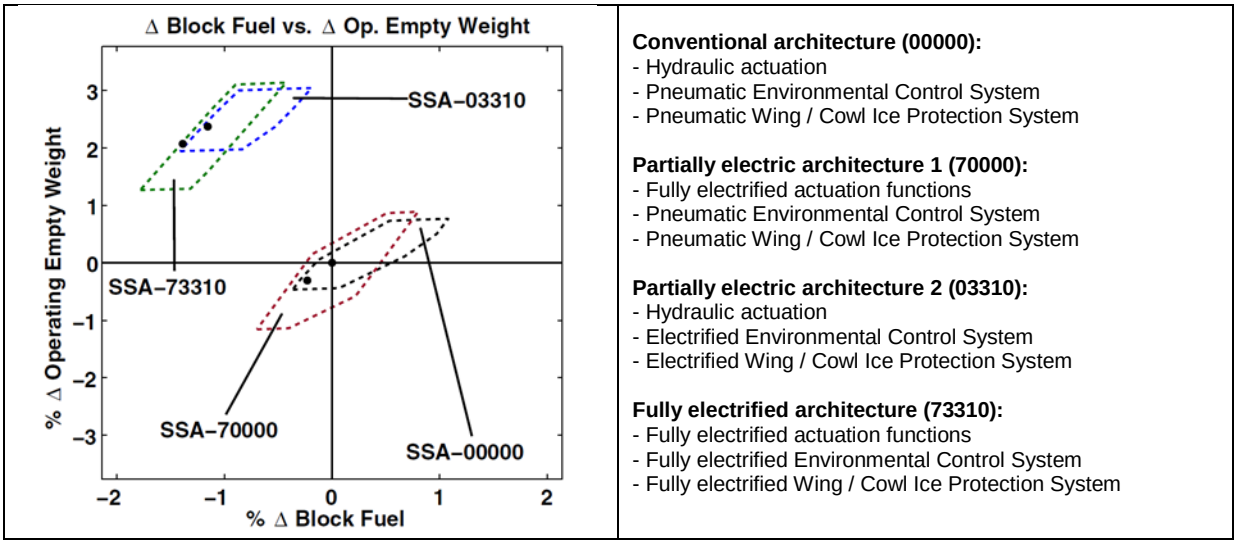

Figure 29: Sensitivity of different aircraft subsystem architectures [143]

In this study, four subsystem architectures to be compared are selected and defined within the multidisciplinary tool ISSAAC (Integrated Subsystem Sizing and Architecture Assessment Capability). As the component models may include simplifications, the impact of this uncertainty on subsystem architecture performances is estimated. Some outcomes of this work are illustrated in Figure 29 where aircraft sensitivities for a Single-aiSle Aircraft (SSA) are estimated. From an Aircraft designer point of view, such analysis is very valuable as it shows that two of the four selected architectures (SSA - 73310 and SSA - 03310) are more efficient than the reference one (SSA - 00000) when considering epistemic uncertainty. In fact, the fully electrified architecture and the partially electric architecture 2, even though they are heavier, offer a reduction on block fuel (upper left corner in the plot shown in Figure 29). Such knowledge is essential towards the downselection of the most promising vehicle or subsystem concept.

1.6. Conclusion

The classical “tube and wing” configuration and its associated technologies seems to have reached its plateau in terms of performance after decades of optimizations. Nevertheless, for the design of the next generation of civil transport aircraft, pressure is on the manufacturers to further improve performances to take into account strong competition and to match safety requirements as well as stringent environmental constraints. The only solution to reach these objectives is to explore aircraft concepts that present disruptive changes in terms of configuration and / or include innovative technologies. The definition of such concepts is initiated at conceptual design level where aircraft designers identify several configurations that would meet the requirements for a given reference mission. In order to downselect the most promising solution of family of vehicles, design engineers rely on a Multidisciplinary Design Analysis (MDA) that sizes the airplanes and estimates performances. In this early phase, a key asset of the MDA is the possibility to well identify the possible trades among the key disciplines or components of the aircraft. The problem is that the current MDA is not yet tailored to take into account specificities of unconventional configurations or new technologies for which very seldom information is available. After a review of different cases associated to advanced vehicle designs, this chapter identified the research problem in aircraft design and stated it as follow: “**How to add knowledge in the Multidisciplinary Design Analysis at aircraft conceptual design level?**”

In the last part of the chapter**,** the available solutions to add knowledge have been reviewed and classified into four categories: Multidisciplinary Design Optimization, addition of accuracy through higher fidelity analyses, addition of new disciplines in the design process and uncertainty management. The benefits of MDO are a mathematical (and thus unbiased) exploration of the design space and the identification of the best configuration (or best family of configurations) according to a well-defined, multidisciplinary and constrained problem. When using higher fidelity computations for disciplinary analyses, the accuracy and reliability of the results automatically increase the level of knowledge available to the designers. More importantly, for unconventional configurations, key phenomena are captured and can be included in the overall sizing tradeoffs that must be performed. For some design problems, it can happen that the MDA does not include a required disciplinary analysis or component sizing. In this case, specific modules must be added and coupled to the original design loop, inevitably bringing new knowledge. A good example is the required evolution of the MDA to fully assess hybrid electric airplanes and associated issues (thermal constraints). Knowing that the aircraft design process is characterized by many unknowns, the last approach consists in managing this uncertainty. Considering different types of uncertainty, different approaches allow an estimation of the possible errors, their propagation and possibly their reduction. In the end, the additional information used by designers to choose solutions translated into probabilities to reach some performance indicators or outcomes variability due to uncertainty.

During the design of unconventional vehicles, the role of the aircraft designer is then to select the available and adapted option(s) and to implement them within the MDA so that the outcomes will

support the downselection process. Challenges to be overcome during this activity are: (i) management of a large number of parameters (design variables, constraints,…); (ii) organization of the design loops taking into account large computational times; (iii) proper design exploration knowing the low robustness of complex shape parametrization; (iv) gathering of data to either guide the initial design step or to validate results. But this is not the only role of the Aircraft designer. Indeed, an additional crucial role consists in verifying the future concept is compliant with certification requirements and that one day it will be capable to fly safely following Air Traffic Management constraints. These subjects are considered in the next chapter.

Synthesis of the chapter

- The design of future aircraft takes place at conceptual design
- The vehicle sizing is performed through a Multidisciplinary Design Analysis
- The classical Multidisciplinary Design Analysis may lead to risky decisions in the downselection of the most promising options
- Knowledge must be added in the Multidisciplinary Design Analysis
- Current solutions to add knowledge in the Multidisciplinary Design Analysis are:
  - Multidisciplinary Design Optimization
  - Higher fidelity analyses
  - New disciplines or subsystems
  - Uncertainty management

➢ Aircraft designer's role is to both combine these different options within the Multidisciplinary Design Analysis according to the problem and verify compliance to certification constraints. An example of such process is provided in chapter 2.

Chapter 2

Expansion of the multidisciplinary design analysis

Roadmap of the chapter

- Within the EU project GABRIEL, the design of a transport aircraft featuring ground based assistance is requested
- A Multidisciplinary Design Analysis with higher fidelity structural models is defined
- A multiobjective optimization is completed
- The Pareto front with respect to constraints is analyzed
- Regulatory texts are reviewed
- Air Traffic Management need is identified
- An extension of the Multidisciplinary Design Analysis and Optimization to add knowledge in conceptual design is proposed

Résumé du chapitre

Dans le cadre de cette thèse, la conception et l'optimisation d'un avion utilisant le système GABRIEL ont été réalisées. Ce dispositif futuriste permet à l'avion de décoller à partir de, et d'atterrir sur, un chariot utilisant des rails électromagnétiques. Les avantages de ce système sont : une réduction de masse due à l'absence du train d'atterrissage, une réduction du carénage ventral et une poussée supplémentaire fournie par le système au sol. Afin d'évaluer les gains globaux au niveau de la consommation de carburant, un processus multidisciplinaire complet de dimensionnement et d'optimisation à été mis en place dans ModelCenter. Utilisant des modèles de type éléments finis pour l'estimation de la masse structurale, le processus est également en mesure de prendre en compte des données fournies lors d'analyses disciplinaires effectuées en parallèle. D'un point de vue Conception Avion, les itérations ont permis de converger vers un ensemble de véhicules adaptés au système au sol GABRIEL qui présentent une importante réduction de la consommation en carburant par rapport à un avion classique. Surtout, ce travail a souligné des aspects importants associés aux méthodes de conception des aéronefs. Premièrement, la valeur ajoutée de l'optimisation multidisciplinaire en termes d'acquisition de connaissances au cours de la conception est confirmée. En effet, les concepteurs non seulement explorent l'espace de conception, mais évaluent également les familles de véhicules et les compromis possibles au niveau des aéronefs. En outre, l'examen des contraintes actives fournit des informations supplémentaires pour d'éventuelles améliorations du système. Enfin, les travaux menés sur le concept GABRIEL ont mis en avant l'impact des contraintes de certification sur la forme du front de Pareto qui définit les meilleures options de conception. Suite à cette conclusion, un nouvel examen des spécifications de certification pour des avions de transport publiées par l'EASA (CS-25) et plus précisement la partie consacrée aux performances (SUBPART-B FLIGHT), a mis en évidence deux points importants. Tout d'abord, la structure du texte réglementaire est très complexe puisque les différentes contraintes détaillées dans les sections sont en réalité liées entre elles par des valeurs de référence. De plus, ces mêmes valeurs de référence font appel à différentes analyses disciplinaires au sein de l'optimsation. Cette situation amène donc à considérer une simplification de la gestion des contraintes de certification au niveau du processus de dimensionnment complet. Ensuite, il s'avère que certaines contraintes de certification nécessitent un modèle avion à 6 degrés de liberté pour calculer certains critères. Ce même besoin en termes d'outil a été identifié lors de l'analyse d'études récentes dans le domaine de la gestion du trafic aérien.

Suite à l'identification de ces besoins spécifiques en termes de connaissance lors de la phase avant-projet, cette thèse propose d'élargir les capacités du processus de conception et d'optimisation multidisciplinaire via l'ajout d'un module de contraintes de certification et d'un outil de simulation de trajectoires complètes. Grâce à cette extension du processus, les ingénieurs peuvent alors analyser, dimensionner et optimiser de nouveaux véhicules ainsi que des concepts opérationnels, depuis la certification jusqu'à la simulation de trajectoires en tenant compte des contraintes ATM.

Les développements de ces nouvelles briques du processus seront présentés dans les chapitres suivants.

2.1. Introduction

In the development cycle of an airplane, the aircraft takes shape at conceptual design following a set of requirements. Central to the success of this phase, the aircraft designer coordinates the activities of the disciplinary experts and sizes the airplane through a Multidisciplinary Design Analysis that can be coupled to an optimization formulation. Many efforts at this stage are made to tailor this MDA so that specific subsystems or disciplines can be assessed depending on the design problem. At the other end of the development cycle before customer delivery, the manufacturer needs about 15 to 20 months to certify an aircraft (including about 2500 flight hours) [183]. Certification is then a key step that requires the inclusion of specific constraints very early during the design process, in order to avoid costly redesigns. It is then not surprising to see publications on advanced concepts that feature specific layouts to meet key certification constraints [184].

The main risk for the design team during the early concept explorations is to erroneously keep or eliminate a design option. In order to find out if certification constraints affect outcomes of design process, the sensitivity of the Multidisciplinary Design Analysis (MDA) or the Multidisciplinary Design Analysis and Optimization (MDAO) with respect to basic regulatory limitations must be evaluated. With the impact properly assessed, it is mandatory to perform a review of the EASA (European Aviation Safety Agency) Certification Specifications to identify other important constraints that require specific analysis capabilities in the MDA or MDAO process. Finally, as an aircraft has to fly its mission following Air Traffic Management guidance, it is interesting to capture any needs of this technical field regarding aircraft data to find possible synergies. Following these investigations and considering the possible existing solutions listed in chapter 1, a solution to add knowledge within the Multidisciplinary Design Analysis at aircraft conceptual design level can be proposed.

In the first part of chapter 2, a Multidisciplinary Design Analysis and Optimization is carried out on an aircraft using an innovative ground based system to improve overall performances in the context of the EU project GABRIEL. This optimization process is solving a problem with different constraints that are associated to the EASA Certification Specifications for large aeroplanes. The analysis of results is then the opportunity to assess the effect of such constraints on the best family of designs. In a second section, further research is performed to identify supplementary needs related to the regulatory text and Air Traffic Management. In the last section, a synthesis of the findings made in this chapter proposes a four steps expansion of the Multidisciplinary Design Analysis and Optimization that will increase knowledge available to aircraft designers.

2.2. Preliminary assessment of the impact of certification constraints in conceptual design

2.2.1. Description of the use case

In order to assess the impact of certification constraints in conceptual design studies, this research starts with the sizing and optimization of an aircraft that is coupled to an innovative ground based system. For clarity, it must be noted that the work has been conducted within the EU project GABRIEL (Integrated Ground and on-Board system for Support of the Aircraft Safe Take-off and Landing) [144].

In this 4 years project (2011-2014) funded by the European Union [145], a consortium of 12 partners led by REA-Tech proposed an innovative ground-based system that would provide many benefits for future Air Transportation Systems. The main idea consists in using an electro-magnetic levitation system that would provide an extra thrust to the aircraft at take-off. To further enhance the benefits of the system, it is proposed to fully remove the landing gear of the aircraft. The proposed global system would then be decomposed into 4 main components: the aircraft, an electrically powered cart equipped with shock absorbers, the electromagnetic levitation track and its associated sledge. Figure 30 details ground and air operations based on the GABRIEL concept (left) and a 3D rendering of the concept (right).

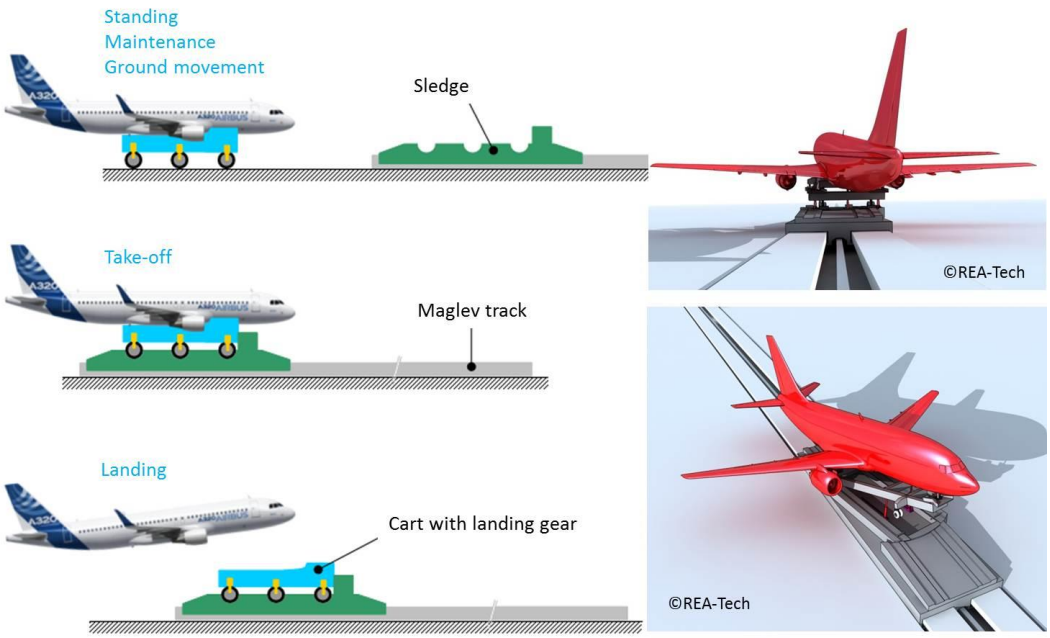

Figure 30: Illustration of the GABRIEL concept [146] (left) and 3D rendering of the system [147] (right)

When standing, for maintenance and ground movements, operations with the GABRIEL concept propose to have the aircraft fixed to an electrically powered cart that is able to provide the classical landing gear functions. For take-off, the aircraft on the cart is transferred along taxiways up to the Magnetic Levitation (MagLev) track following the Tower Ground Controller's guidance. At this point,

the cart (and the aircraft) moves into the sledge where a security system locks both systems together. When all checks are performed, the MagLev track provides a horizontal force to the sledge that allows the aircraft to reach lift-off speed. At the end of the mission, the objective is to have the aircraft landing on the cart and sledge. These two components are moving at a given speed that is adapted to the aircraft trajectory. It must be noted the sledge is designed to offer a Degree of Freedom along an axis that is parallel to the yaw axis to avoid the decrab maneuver. Given all parameters to be monitored during this flight phase, the GABRIEL concept aims for a fully autonomous control of the aircraft with the pilot (in agreement with Terminal Control Area and Tower Runway controllers) providing high level orders to the aircraft. More information is available in the conclusions of the GABRIEL project in [148].

When concentrating on the aircraft, the landing gear removal leads to weight savings and better aerodynamics as the belly fairing size can be reduced. In addition the extra thrust provided by the ground system offers an additional Degree of Freedom during operations. To assess the full benefits of this ground-based system, the sizing and optimization of a GABRIEL tailored aircraft following typical Airbus A320 mission requirements have been carried out. In the next section, the specific MDA that has been used is presented.

2.2.2. The GABRIEL Multidisciplinary Design Analysis

The GABRIEL concept affects different components and different disciplines on the aircraft. The objective at this point is to take these changes into account and to assess their impacts on aircraft sizing considering a reference mission. This sizing was based on the longstanding ONERA Multidisciplinary Design Analysis identified as ACODE (Airliner COnceptual DEsign) [122]. As for the classical MDA presented in chapter 1, the sizing of the GABRIEL aircraft is based on classical disciplinary modules described hereafter.

2.2.2.1 Propulsion module

At conceptual design, the identification of the best airframe / engine combination is one of the primary outcomes. Thus, the exploration of the design space needs a rubber engine model that has to provide many inputs for other modules following a set of specifications. For the aircraft geometry computations, the engine diameter and length are required while for the weight module, the mass of the engine is necessary. Obviously, for assessing the performances over the mission, thrust and TSFC must be available for different flight conditions (Mach, altitude). To generate the performance database, a complete engine components analysis [21] is considered too detailed for the first sizing loops of the GABRIEL aircraft. In addition, as no disruptive engine concepts are used in this study, it has been decided that the analytical method proposed by Roux would deliver reliable data [149]. In this case, the engine is described by high level design parameters such as the overall pressure ratio, the by-pass ratio and the maximum thrust at sea-level in static conditions (F_0). A first analysis carried by Roux allows to relate the engine design parameters to the Mach number and altitude effects on

maximum available thrust. Regarding the SFC estimation, Roux used a more complex physical approach as reference to identify within a simple analytical model the various interactions. Once these models have been coded, verification through published engine data [150] has been made showing good agreement for thrust calculations and conservative results for SFC. Further improvements have been then implemented to reach lower TSFC values, especially in cruise conditions. The second key output of the Propulsion module is the weight estimation. In her study, Roux also proposed a simple bi-linear formula resulting in small errors with respect to available data. However, in the GABRIEL project, the single aisle reference aircraft to be used as starting point for the design task has 2 turbofan engines of about 118 kN. Unfortunately, around such values, the bi-linear interpolation can generate some errors. For this reason, the Propulsion module uses the more general formula that is provided in the ISAE-Supaero handout on design of commercial transport aircraft [151]:

$$W_{engine} = N_{engine}.0.22.F_0^{0.939}$$

where W_{engine} is the installed engine mass in kg;
N_{engine} is the number of engines;
F_0 is the engine thrust at sea level in lbf.

To finalize the rubber engine model, the engine diameter and length for the given maximum thrust at sea-level must be estimated. As partners of the GABRIEL project already used the equations provided by Raymer [5] to compute these geometrical values for initial estimations, it has been decided to implement them in the Propulsion Module to maintain as much consistency as possible within the project.

2.2.2.2 Aerodynamics module

Aerodynamics assessments are performed using an analytical tool that relies on basic aerodynamics relationships and wind tunnel data. This tool is a proprietary ONERA code that has been revised and enhanced over many years [152]. For a given aircraft geometry and Mach number, the Aerodynamics module returns a complete drag polar that takes into account fuselage shape, airfoil and wing characteristics, empennage sizes and engine dimensions as well as high lift device effects. Subsequently, as the required lift is known, the corresponding Drag coefficient is calculated. Figure 31 provides an example of the drag breakdown generated by the Aerodynamics module with the total drag that takes compressibility effects into account. To cover all the needs requested by the sizing process, the Aerodynamics module automatically computes the low speed characteristics for different types of high lift devices. Also, as it is directly linked to the geometry module that receives data from the propulsion module, any change in the engine size is taken into account by the module and the overall drag polar is modified.

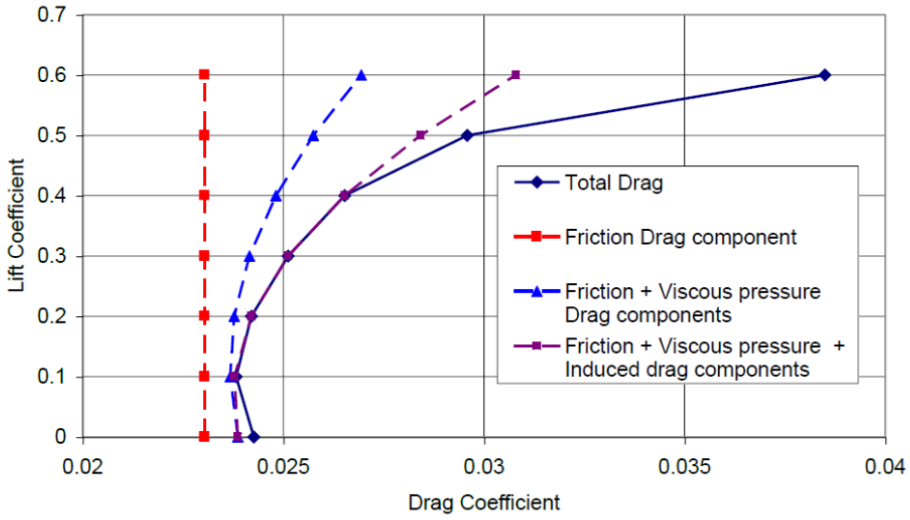

Figure 31: Drag breakdown used in the GABRIEL MDA

2.2.2.3 Structure / Weight module

The role of the Structure / Weight module used in the GABRIEL MDA is to calculate both the airframe weight as well as the subsystems weights (such as avionics) of the aircraft. As the MDA process aims at exploring unconventional configurations, it has been decided to use ONERA advanced physics-based mass estimation tools for the fuselage and the wing (the two heaviest elements in the aircraft mass breakdown). Thus, if unusual parameters lead to high aspect ratio wing, mass estimations would be more reliable than classical formulas. For other components of the airframe (horizontal tail, vertical tail, engine pylon...) and the aircraft subsystems, the module relies on ONERA's analytical models similar to these found in [5][13][22]. The fuselage weight estimation has been developed with the purpose of adding physics-based aspects into the conceptual design MDA. The approach identifies at first that the main components of the fuselage (skin, stiffeners, and spars) are used to withstand pressurization and bending moment. Thus, the module first calculates a structural mass due to pressurization. In a second step, the structural mass directly linked to bending is determined. In the end, a linear combination of the two models, including correction coefficients to match existing data, provides the total structural mass for the fuselage. In the case of the wing, the model takes into account the load generated by the lift over the span as well as those generated by the engines. These values are then used to compute the necessary thickness for different components for a fixed typical structural layout. Once this thickness is determined, the wing structural weight is calculated. For other masses associated to the wing such as high lift devices, estimations are based on classical empirical approaches [5][13][22]. As the GABRIEL aircraft has some specific characteristics regarding the components, the Structure / Weight module has been modified so that different scenarios could be taken into account during the sizing process: for example, the weight of the landing gear can be set to zero and an additional weight representing the supporting strut can be set.

2.2.2.4 Performance module

The Performance module used in the GABRIEL MDA is based on the analysis tool developed for the ONERA conceptual design code COMPACT [153]. It gathers the necessary outputs generated by the other disciplinary / systems modules and carries out the performance calculations for the reference sizing mission. This mission is described in a simple manner by various segments, each representing a phase of the flight. Of course, depending on the leg, the performance analysis is slightly different (for climb, calculations are made based on the available thrust while in cruise, fuel burn is computed through the required thrust). Figure 32 illustrates the mission breakdown that has been used in the GABRIEL project.

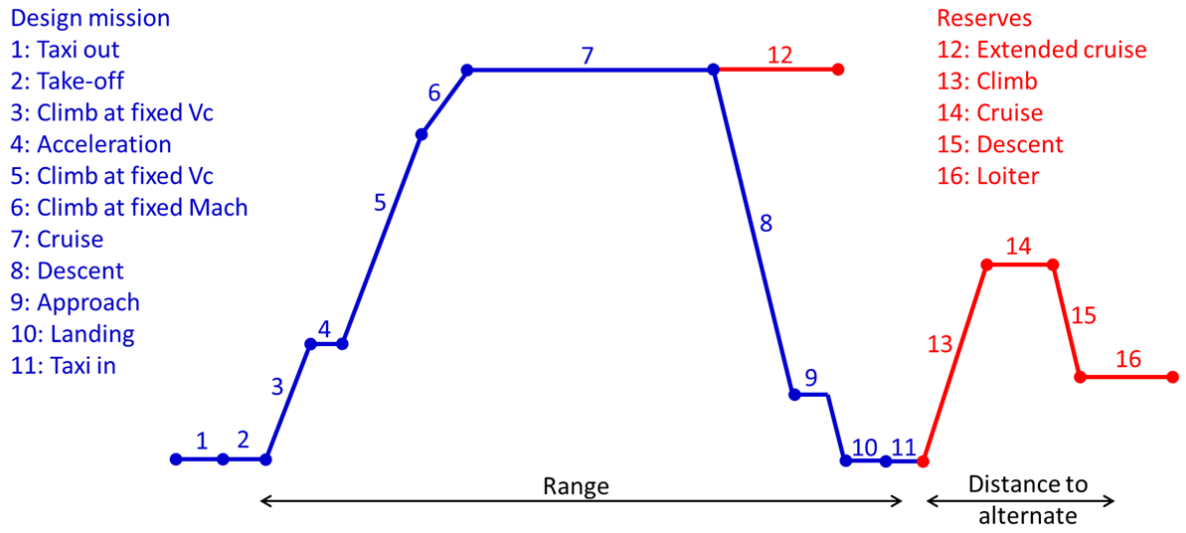

Figure 32: Reference Mission breakdown within the Performance module

To size the vehicle, design engineers have to consider both the reference sizing mission as well as some reserves when calculating fuel quantity. This is to make sure that even in case of aborted landing or re-routing, the aircraft has enough kerosene to reach an alternate airport. In the case of the GABRIEL project, these reserves shown in red in Figure 32 include an extended cruise portion (duration of 45 minutes) as well as a flight to an alternate airport that is 200 NM away from the initial airport. Regarding the reference mission, it features takeoff and 3 climb segments in different conditions and an acceleration at constant altitude as proposed in [154]. For the cruise segment, it has been decided to model it as a constant climb at fixed Mach with the aircraft flying at maximum Lift-to-Drag ratio. For taxi phases, the fuel consumption is determined considering a given duration and the engine TSFC at low regime. In order to provide more information about the aircraft performances, the GABRIEL Performance module also simulates an operational mission that corresponds to the most common mission for the vehicle class (800 NM for a small medium range aircraft). Last, different "k factors" [28] have been added to the input of the Performance module so that technology related improvements could be taken into account. In the case of the GABRIEL concept, it is useful to represent the aerodynamics benefits associated to the belly fairing removal.

2.2.2.5 Details of the GABRIEL MDA

The GABRIEL MDA is represented in Figure 33 following the XDSM format. With respect to the generic MDA presented in chapter 1, the main differences are:

- The approach speed is not an input anymore. It is an output of the performance module calculated considering the wing surface and the maximum lift coefficient in a landing configuration;
- The physics-based Structure and Weight Module requires load cases and the lift calculated from the Aerodynamics Module to perform the wing structural sizing;
- The performances of the aircraft for an operational mission are calculated.

The sequence of operations for the GABRIEL MDA is as follows (*changes in red*):

Input:	Engine specifications (based on constraint analysis), initial sketch (based on constraint analysis), number of passengers, empennage volumes, required static margin, *load cases*, sizing *and operational* mission specifications
Output:	Engine deck, aircraft geometry, aerodynamic characteristics, weight breakdown, sizing *and operational* mission performances including approach speed

0. Propulsion. The propulsion module takes as input the engine specifications and computes its characteristics (Thrust, TSFC, geometry and weight).

1. First estimate. With an initial sketch of the vehicle, the engine performances and assumptions regarding the mission, a first iterative loop is computed to derive an initial guess for MTOW, MLW, MZFW and the wing area (Breguet approach).

repeat

2. The Multidisciplinary Design Analysis is started;

3. Geometry. In this module, given a certain number of inputs (number of passengers, empennage volumes and required static margin), aircraft parameters (fuel weight, maximum landing weight, maximum lift coefficient) and engine geometry, the complete geometry of the aircraft is computed and the main subsystems are positioned. In the generic case, data are stored in the vector identified as *A/C* but a dedicated CAD model can be used instead [19].

4. Aerodynamics. Taking into account the aircraft geometry defined during the previous step, the Aerodynamics module computes the drag polar and other aerodynamics coefficients with respect to the angle of attack, the angle of sideslip and the flight condition.

5. Structure and Weight. Using as input *a set of load cases*, the engine weight, the aircraft geometry, the MTOW value defined at the beginning of the step 2 *and the lift calculated by the Aerodynamics module*, *this module sizes the wing and the fuselage and then* computes the masses of the different aircraft components.

6. Performance. Based on a point mass analysis, the performance module computes the aircraft fuel consumption for the sizing mission based on the engine performances calculated in step 0, the MTOW value defined at the beginning of the step 2 and the aerodynamics properties of the aircraft calculated in step 4. *The resulting approach speed for a given geometry and set of high lift devices is calculated.* In this module, the segment simulations based on sizing mission specifications use time step integration to better represent real trajectories.

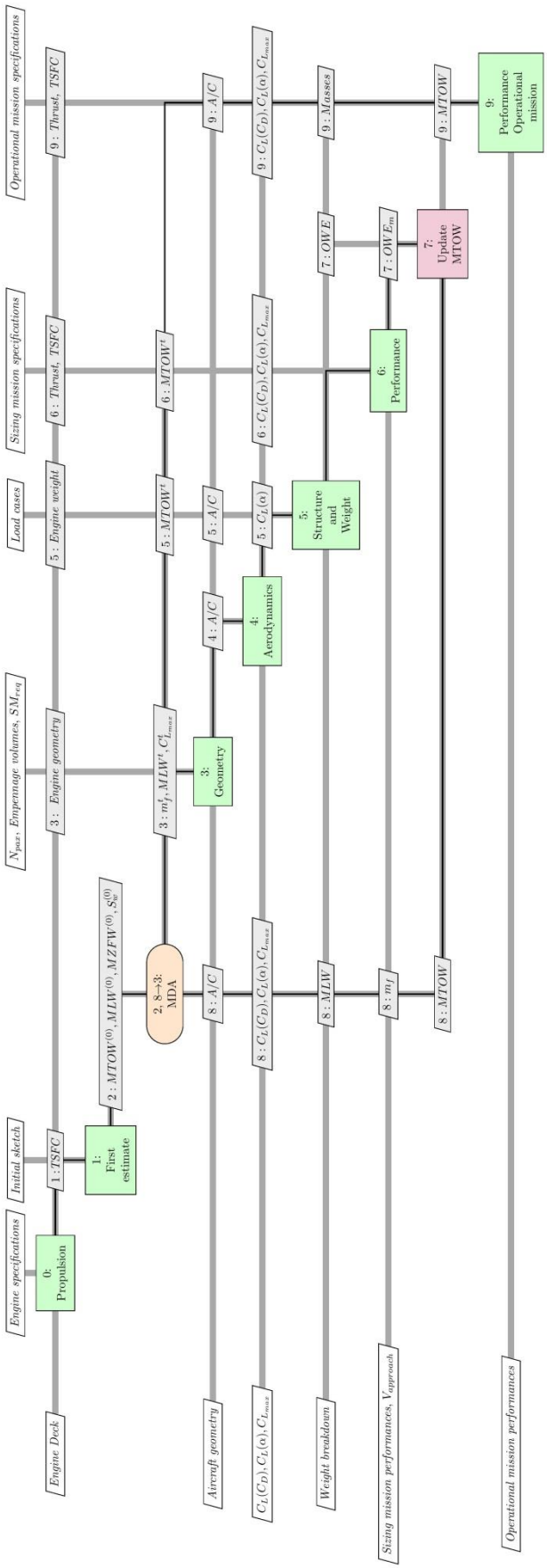

Figure 33: Multidisciplinary Design Analysis for the GABRIEL aircraft

7. Update MTOW. The objective of this function is to calculate the difference between the Operating Weight Empty taking as input the estimated fuel consumption calculated at step 6 $\left(OWE_m = MTOW - FW - W_{payload}\right)$ and the value of OWE resulting from the weight breakdown (step 5). If the difference between these 2 values is higher than a given tolerance, MTOW is updated.

8. Iteration loop. All values calculated by the different modules are returned to the MDA so that a comparison with the target values is made (superscript t in Figure 33).

until 8-2 MDA has converged.

9. *Performance Operational Mission. The aircraft that has been sized through the Multidisciplinary Design Analysis flies an operational mission to estimate the fuel consumption on a classical route. Thrust and SFC database are provided by the Propulsion module while masses, aircraft geometric parameters and aerodynamic characteristics are provided during the last loop of the disciplinary module.*

As it is set up, the GABRIEL MDA allows design engineers to size and judge the performances of an airplane with a given geometry and a given engine. However, the goal is to achieve MDO so that the design space can be explored and the most promising solutions identified. To fully setup this optimization process, some certification and operational constraints must be defined. These are detailed in the next section.

2.2.3. Definition of certification and operational constraints

For the sizing process, one fundamental aspect is the selection of the best airframe / engine combination. To this regard, the selection of the engine maximum thrust has to comply with certification constraints detailed in the regulatory text [129] and other operational requirements. At this stage of conceptual design, the limitations taken into account are:

- CS 25.119 Landing climb: all-engines operating;
- CS 25.121 (b) Climb: one-engine inoperative (Take-off; landing gear retracted);
- CS 25.121 (d) Climb: one-engine inoperative (Approach);
- Service ceiling of 500 ft/min at the highest cruise point [155].

All these constraints consider as threshold a climb gradient or vertical speed. A rapid point mass analysis is then performed for the climb condition represented in Figure 34;

- The airplane is climbing following the flight path angle γ;
- The airplane is flying at certain angle of attack α with respect to the airspeed;
- The airplane lift is perpendicular to the airspeed;
- The airplane drag is parallel to the airspeed;
- The airplane weight is oriented vertically towards the ground;
- The engine thrust forms a certain angle ε_t with the airspeed.

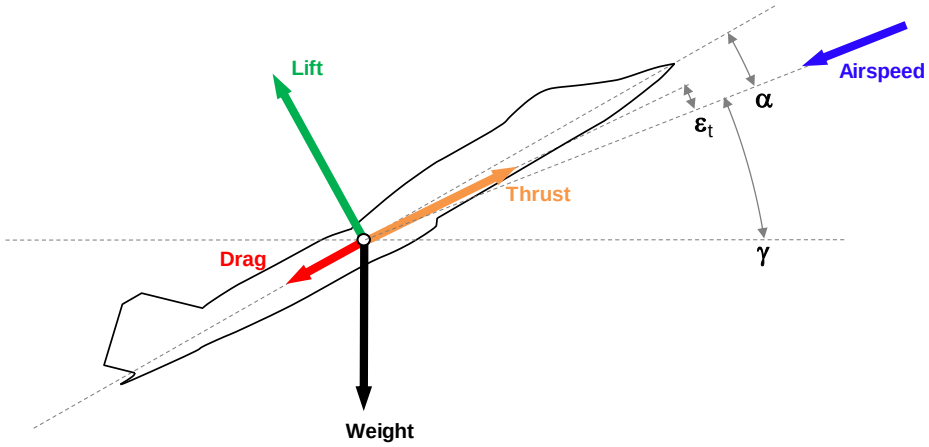

Figure 34: Forces applied during climb

Applying Newton's second law on the aircraft represented in Figure 34, the projection of the different forces on the reference frame associated to the airspeed, it is then possible to write the following equations:

$$D + mg\sin\gamma = T\cos\varepsilon_t$$
$$mg\cos\gamma = L + T\sin\varepsilon_t$$

where L is the Lift force in N and is a function of the angle of attack α;
D is the Drag force in N and is a function of the angle of attack α;
T is the Thrust in N;
m is the aircraft mass in kg;
g is is the gravitational acceleration in m/s^{-2};
γ is the flight path angle in rad or deg;
ε_t is the angle between the engine Thrust and the airspeed in rad or deg.

Knowing that for transport aircraft, ε_t is small, the two previous equations can be written as:

$$D + mg\sin\gamma = T$$
$$mg\cos\gamma = L$$

A new module solving this non-linear system has been subsequently developed for the MDA to calculate α and γ. In this manner, the flight path angle (and therefore the rate of climb) could be calculated for different flight conditions and aircraft configurations: thrust setting, flap configuration, landing gear (retracted or extended), airspeed, weight, and altitude. These additional values complement the definition of the MDO problem to be solved.

2.2.4. The GABRIEL Multidisciplinary Design Analysis and Optimization

The GABRIEL concept could see further developments if it demonstrates to airlines some possible economic benefits. As detailed in [1], civil transport aircraft should have affordable acquisition cost and low Direct Operating Cost (DOC). These two quantities are respectively directly linked to MTOW

and mission fuel burn [1][5]. Thus, for the GABRIEL aircraft, it is decided to carry out multiobjective optimization for these two latter outputs. As for the Design Variables, the choice has been to limit the exploration to both wing planform parameters and engine maximum thrust at sea level T_{SL} so that macroscopic geometry trends and promising airframe / propulsion couplings could be observed. In Figure 35, the three continuous parameters defining the wing planform are illustrated: (i) the wing span *b*, (ii) the leading edge sweep angle Λ_{LE}, (iii) the external taper ratio λ_{ext} that corresponds to the kink chord (C_{kink}) over the tip chord (C_{tip}). In the GABRIEL use case, these parameters are sufficient to define the complete wing planform as the root chord and the kink position are fixed.

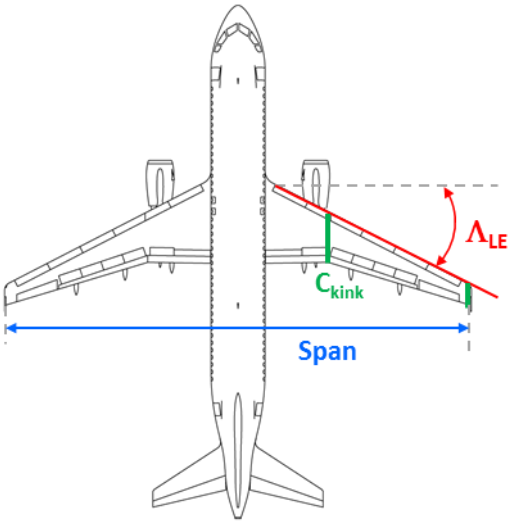

Figure 35: Wing planform Design Variables to be considered for the GABRIEL MDAO

For the constraints, five inequality constraints have been selected for this problem. Among them, four correspond to the ones defined in the previous section and related to certification and operational constraints. The fifth limitation corresponds to the approach speed: it must be noted indeed that in the GABRIEL MDA, the approach speed is an output of the analysis. Thus, if no constraint is given, the result of the optimization could be an aircraft requiring very long runway. One interesting point regarding constraints is that the wing span has not been limited while for such class of vehicle, airport constraints require a maximum span of 36 meters. The reasons for this choice are twofold: first, the GABRIEL system implies operations at airport level that are radically different with respect to today's system. Thus, it can be assumed that new arrangements allowing larger wing span could be found as benefits in terms of fuel consumption are obvious. Second, the structure / weight analysis tool depends on an accurate physics-based approach. Therefore, unreasonable wing spans cannot be obtained during the optimization loop as the structural weight penalty would be too high to provide any fuel gain. The optimization should in the end capture the most efficient wing planform from a pure flight physics point of view. It is also common practice to request a maximum takeoff distance to make sure that the aircraft can be used on many airports. In the case of the GABRIEL aircraft, as the ground based system using magnetic levitation provides additional thrust, the takeoff ground run is very short. Thus, the optimization problem does not consider a constraint on takeoff distances. As the optimization

problem centered on the GABRIEL MDA is now defined, the global process can be identified as the GABRIEL MDAO. It is summarized in Table 3.

Table 3: Description of the MDAO problem for the GABRIEL aircraft

	Function / Variable	Description
minimize	MTOW	Maximum TakeOff Weight
	Mfuel (sizing)	Mission fuel for the sizing mission
with respect to 4 design variables		
	b	Wing span
	Λ_{LE}	Sweep angle at leading edge
	λ_{ext}	External taper ratio
	T_{SL}	Maximum Thrust at sea level
subject to 5 inequality constraints		
	C119	Climb gradient [129]
	C121b	Climb gradient [129]
	C121d	Climb gradient [129]
	RoC	Service ceiling [155]
	V_{app}	Approach speed

Given the available MDA within ACODE, the selected formulation of the MDAO process is Multi-Disciplinary Feasible (MDF). Classified as monolithic formulation, this architecture ensures a feasible solution at each optimization loop. For the optimizer, as the objective is to minimize MTOW and Mfuel (sizing) of the GABRIEL aircraft, it has been decided to use the genetic algorithm NSGAII that can take into account inequality constraints and perform direct multiobjective optimization [110]. The ensuing GABRIEL MDAO is illustrated in Figure 36 following the XDSM guidelines. The associated algorithm is described here below (changes with respect to the GABRIEL MDA are highlighted in red).

Input: *Initial set of design variables (identified by $^{(0)}$)*, engine specifications (based on constraint analysis), initial sketch (based on constraint analysis), number of passengers, empennage volumes, required static margin, load cases, sizing and operational mission specifications

Output: *Optimal design variables, objective function, constraint values and aircraft data* (Engine deck, aircraft geometry, aerodynamic characteristics, weight breakdown, sizing and operational mission performances). *Optimal values are indicated by $^{(*)}$.*

0. *Initiation of the aircraft optimization*

repeat

1. Propulsion. The propulsion module takes as input the engine specifications and computes its characteristics (Thrust, TSFC, geometry and weight).

2. First estimate. With an initial sketch of the vehicle, the engine performances and assumptions regarding the mission, a first iterative loop is computed to derive an initial guess for MTOW, MLW, MZFW and the wing area (Breguet approach).

repeat

3. The Multidisciplinary Design Analysis is started;

4. Geometry. In this module, given a certain number of inputs (number of passengers, empennage volumes and required static margin), aircraft parameters (fuel weight, maximum landing weight, maximum lift coefficient) and engine geometry, the complete geometry of the aircraft is computed and the main subsystems are positioned. In the generic case, data are stored in the vector identified as A/C but a dedicated CAD model can be used instead [19].

5. Aerodynamics. Taking into account the aircraft geometry defined during the previous step, the Aerodynamics module computes the drag polar and other aerodynamics coefficients with respect to the angle of attack, the angle of sideslip and the flight condition.

6. Structure and Weight. Using as input a set of load cases, the engine weight, the aircraft geometry, the MTOW value defined at the beginning of the step 2 and the lift calculated by the Aerodynamics module, this module sizes the wing and the fuselage and then computes the masses of the different aircraft components.

7. Performance. Based on a point mass analysis, the performance module computes the aircraft fuel consumption for the sizing mission based on the engine performances calculated in step 0, the MTOW value defined at the beginning of the step 2 and the aerodynamics properties of the aircraft calculated in step 4. The resulting approach speed for a given geometry and set of high lift devices is calculated. In this module, the segment simulations based on sizing mission specifications use time step integration to better represent real trajectories.

8. Update MTOW. The objective of this function is to calculate the difference between the Operating Weight Empty taking as input the estimated fuel consumption calculated at step 7 $\left(OWE_m = MTOW - FW - W_{payload}\right)$ and the value of OWE resulting from the weight breakdown (step 6). If the difference between these 2 values is higher than a given tolerance, MTOW is updated.

9. Iteration loop. All values calculated by the different modules are returned to the MDA so that a comparison with the target values is made (superscript t in *Figure 36*).

until *9-4 MDA has converged.*

10. *Certification. The certification and operational constraints are calculated for the sized aircraft determined by the MDA (module 3). Inputs from the Propulsion module, the Geometry module, the Aerodynamics module, the Structure and Weight module are used.*

11. Performance Operational Mission. The aircraft that has been sized through the Multidisciplinary Design Analysis flies an operational mission to estimate the fuel consumption on a classical route. Thrust and SFC database are provided by the Propulsion module while masses, aircraft geometric parameters and aerodynamic characteristics are provided during the last loop of the disciplinary module.

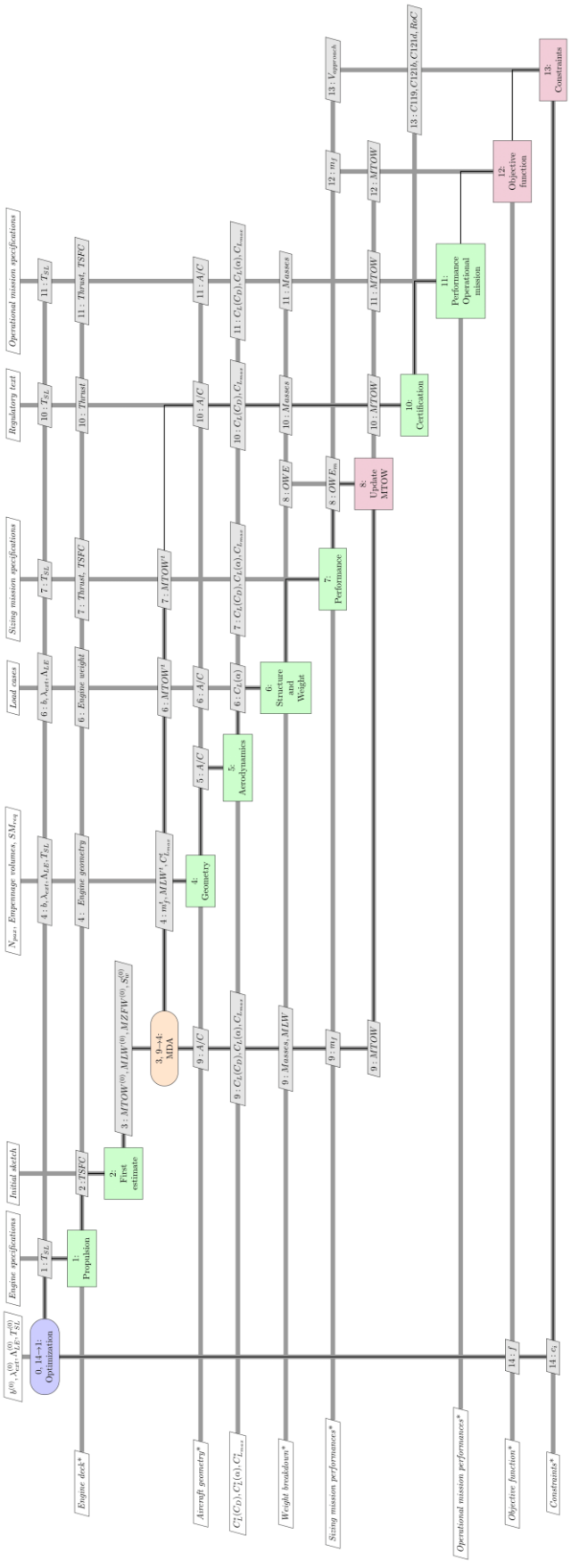

Figure 36: Multidisciplinary Design Analysis and Optimization for the GABRIEL aircraft

12. *Objective function. The objective of this function module is simply to manipulate the disciplinary outcomes that are used to compute the objective functions of the problem. In this case, the goal is to minimize both MTOW and sizing mission fuel weight* m_f.

13. *Constraints function. This function gathers the different constraint values that are computed by the disciplinary modules. In the case of the GABRIEL aircraft, constraints related to CS-25 are identified by their corresponding section number (C119, C121b, C121d) and the operational one is represented by the value of interest (RoC for Rate of Climb). With respect to conventional aircraft, no constraint is given for the Takeoff Field Length as the GABRIEL system provides sufficient additional thrust.*

14. *Feedback loop for the optimization with objective function (f) and constraints* (c_i) *values.*

until *14-1 Aircraft optimization has converged.*

2.2.5. Implementation of the GABRIEL MDAO

2.2.5.1 Implementation in ModelCenter

The process shown in Figure 36 is implemented in ModelCenter [156], a design environment that can easily couple executables programs, Python scripts and Excel spreadsheets. Figure 37 illustrates the representation of this GABRIEL MDAO process through the ModelCenter workflow where boxes with the symbol "+" represents a group of sub-modules. Some key analysis tool such as the sizing mission, the calculation of certification constraints and the performance estimation for an operational mission are clearly visible.

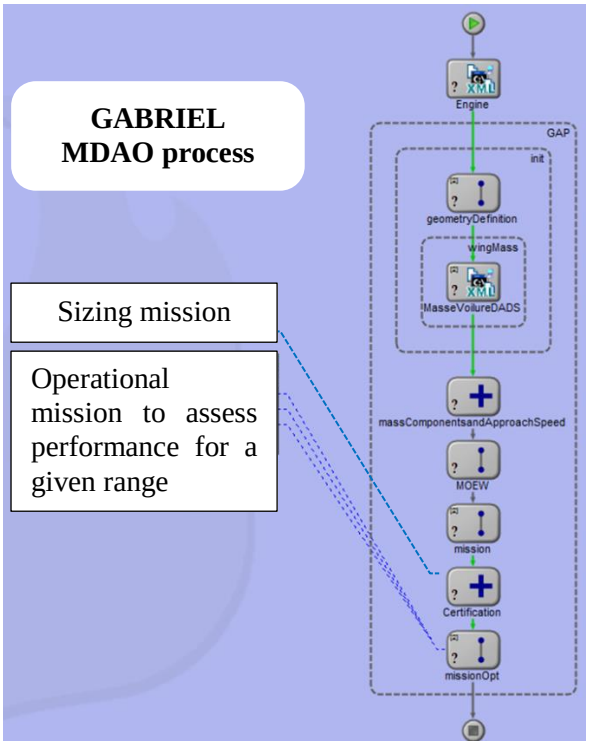

Figure 37: GABRIEL MDAO Process implemented in ModelCenter

Before launching the time consuming optimization process, a comparison of the data generated by the GABRIEL MDAO for the reference aircraft (Airbus A320) has been performed. The differences with the CeRAS public domain database [157] and the initial sizing loop performed by partners within the project are reported in Table 4. As they are below 5%, it is considered that the modeling capabilities within the MDA are providing enough accuracy on the design point. In addition, sizing sensitivities associated to fuel weight with respect to OWE provided consistent values with the CeRAS data [157]. Following these verifications, it is considered that the process is enough reliable to perform a first optimization loop.

Table 4: Verification of the GABRIEL MDA sizing process

		CeRAS [157]	GABRIEL (initial sizing)	GABRIEL MDAO
OWE	[kg]	42092	41914	40749
Maximum fuel weight	[kg]	18678	19159	19478
MTOW	[kg]	74378	73969	73771

During this verification test, the MDAO process also computed the values of the different constraints to be considered during the optimization. Unsurprisingly, the margin over the regulatory text threshold is very high (the calculation of certification constraints does not consider critical operational conditions such as hot day or high altitude airport). To avoid a comparison of two aircraft based on different constraints, it has been decided to use these same values, reported in Table 5, when optimizing the GABRIEL airplane.

Table 5: Lower bound values for the MDAO constraints

	Regulatory text limit	Value calculated for the reference single aisle aircraft	Value used for the optimization of the GABRIEL aircraft
CS 25.119	3.2%	16.55%	16.55%
CS 25.121(b)	2.4%	4.62%	4.62%
CS 25.121(c)	2.1%	4.23%	4.23%
Service ceiling	2.54 m/s	6.11 m/s at 37300 ft	6.11 m/s at 37300 ft

2.2.5.2 Optimization of the GABRIEL aircraft

As presented in Section 2.2.1., the GABRIEL ground based system positively affects the aircraft and its performances in different manners. To take these changes into account, and to assess their impact at overall aircraft level, changes must be made in the various analysis tools. First, as the aircraft is taxiing in and out on an autonomous cart, no fuel is consumed during these phases. The performance code is modified accordingly to consider this operational aspect. Second, the disruptive idea of the GABRIEL concept is the landing gear removal and its replacement by a simpler fixing system. Naturally, the landing gear weight (about 3000 kg) is no more considered in the aircraft weight breakdown analysis. On the other hand, FEA of the fixing system that connects the aircraft to the cart estimates a weight of about 1000 kg. Such mass is added to the weight breakdown so that globally, there is a weight

reduction of 2 tons. The last key point associated to aircraft performance is an important reduction of the belly fairing size. Indeed, without the necessity of an internal volume to store the retracted landing gear within the fuselage, it has been decided to minimize the belly fairing. CFD simulations carried out by a project partner resulted in a possible reduction in cruise conditions (M=0.76) of about 12.4 drag counts. This modification of the aerodynamic property is then coded within the performance analysis tool. Additional studies estimated the reduction in weight due to the belly fairing radical streamlining to be about 380 kg. This further gain in weight is also taken into account in the Structure & Weight module of the GABRIEL MDAO. With all parameters set, the optimization of the GABRIEL aircraft can be carried out according to the problem definition detailed in Table 6.

Table 6: Description of the MDAO problem for the GABRIEL aircraft

	Function / Variable	**Description**	**Range / Value**
minimize	MTOW	Maximum TakeOff Weight	
and	Mfuel (sizing)	Mission fuel for the sizing mission	
with respect to 4 design variables			
	b	Wing span	[28 : 45] meters
	Λ_{LE}	Sweep angle at leading edge	[22 : 40] °
	λ_{ext}	External taper ratio	[0.28 : 0.47]
	T_{SL}	Maximum Thrust at sea level	[85000 – 117000] N
subject to 5 inequality constraints			
	C119	Climb gradient [129]	0.1655 (min)
	C121b	Climb gradient [129]	0.0462 (min)
	C121d	Climb gradient [129]	0.0423 (min)
	RoC	Service ceiling [155]	6.11 (min)
	V_{app}	Approach speed	76.36 kt (max)

Relying on the NSGAII algorithm [110], the outcome of the GABRIEL MDAO is shown in Figure 38. It is the Pareto front showing the most promising family of aircraft. Within this set, that does not present large discontinuities, it is possible to highlight a few designs which characteristics are noted:

- Design 1 has the highest MTOW while the total fuel weight for the sizing mission is the lowest;
- Design 2 is an intermediate solution located in a discontinuous zone of the Pareto front;
- Design 3 has the lightest MTOW while the total fuel weight for the sizing mission is the highest;
- Design 4 is not considered, as improvements with respect to Design 3 are negligible while the increase of fuel weight is important.

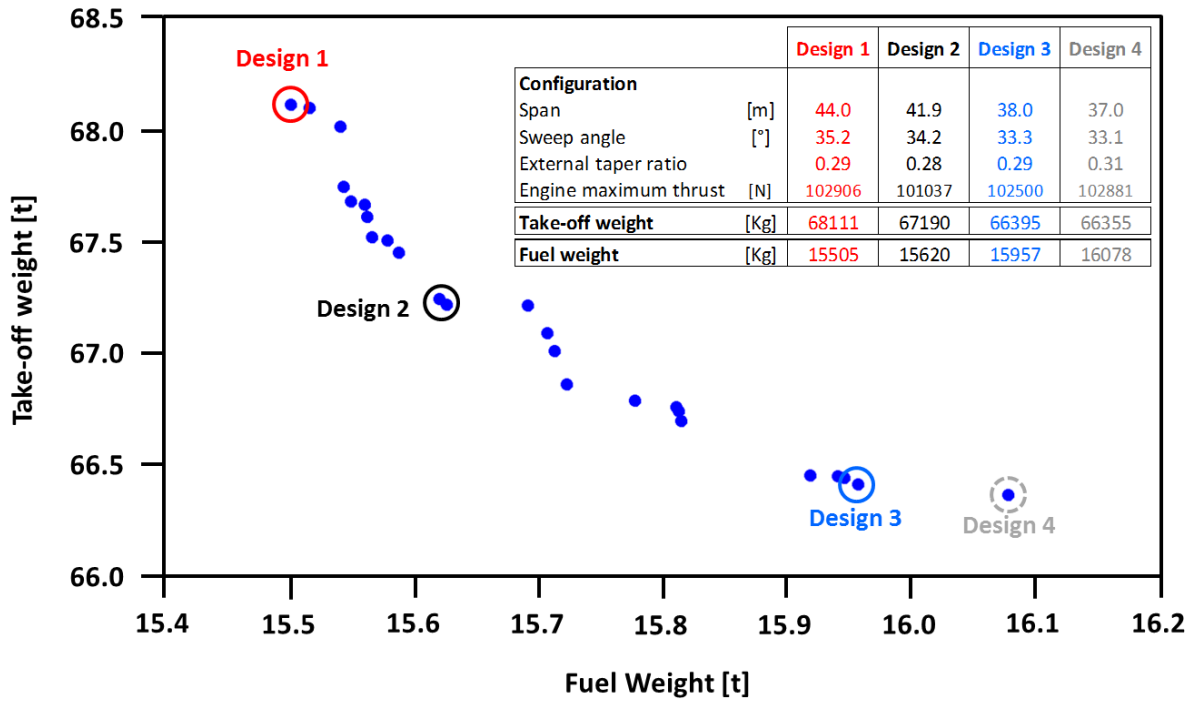

Figure 38: Optimization results of the GABRIEL MDAO showing the Pareto front

Looking at the corresponding geometries, the evolution of the Pareto front can easily be explained by the fact that the increase of wing span reduces the induced drag and thus the fuel weight. On the other hand, this span growth is associated with a higher structural weight that increases OWE and MTOW. For design 4, the problem is that structural weight benefits associated to a wing span of 37 meters (smallest in this set) are completely cancelled by the penalty due to a drag increase. The final Pareto front in Figure 38 can be approximated by two straight line segments joining at Design 2 (67.2 tons for MTOW and 15.6 tons for fuel weight). As the slope is steeper between Design 1 and Design 2, this implies that any mission fuel reduction below 15.6 tons would be achieved through higher penalty in weight. Consequently, the GABRIEL project members selected Design 2 as the most promising configuration. More information about the conclusions of the GABRIEL project is available in [148].

2.2.6. Results analysis

The Pareto front presented in Figure 38 is the useful outcome of the GABRIEL MDAO when focusing on the aircraft concept, as designers have a better understanding of the performance level that can be reached. When looking at the results in terms of Aircraft Design method, it is interesting to review the multiobjective optimization history. Illustrated in Figure 39, the plot provides all feasible (green stars) and infeasible designs (red squares) that have been explored during the optimization. Naturally, the density of tested designs is higher in the vicinity of the Pareto front, as the optimizer is converging towards the best solutions. Reviewing the optimization results for the infeasible designs that feature lower takeoff weight and require less mission fuel, it is possible to know the constraint that drives the infeasibility. Within these best infeasible designs, two categories are identified. The first one, characterized by dotted black circles in Figure 39, concerns designs that are discarded because they

meet neither the operational constraint V_{app} nor the certification requirements. The second group, highlighted by black circles in Figure 39 indicates designs that are eliminated solely because of the certification constraints. Even though these two black circled points are not enough to define a family of vehicles and their position is affected by uncertainty (the optimizer didn't converge for designs in this area), it is clear that only four basic certification constraints are sufficient to shift the Pareto front. At conceptual design stage, this is an important observation as the Pareto front can be used to select or eliminate a family of vehicles. It can be concluded that certification constraints must be embedded as soon as possible in the sizing process, to make sure that the optimization is converging to a viable vehicle. Logically, it becomes key for the designers to select the relevant regulatory constraints that are compatible with the aircraft available information.

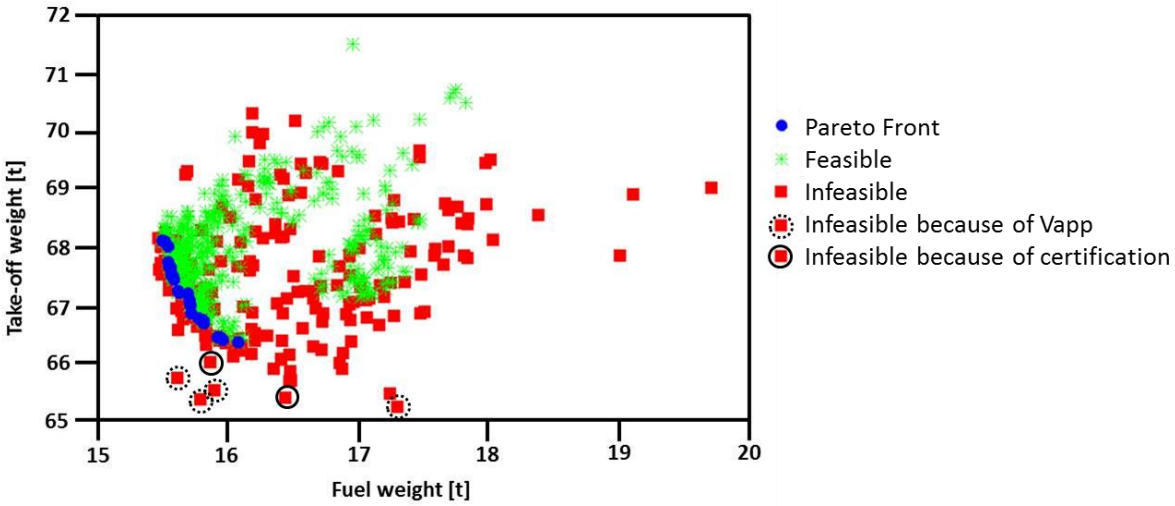

Figure 39: Optimization history for the GABRIEL aircraft

Regarding MDO aspects, the selection of the optimization objectives was directly related to cost (see Section 2.2.4.). However, from a mathematical point of view, such a choice can be challenged. The aircraft takeoff weight includes indeed the mission fuel weight. Thus, a reduction in mission fuel weight automatically leads to a MTOW decrease: the two objectives are not fully independent. For future optimizations, it is recommended to select OWE and fuel weight as objectives. With such choice, the relationship to cost is still maintained.

2.3. Supplementary need

2.3.1. Requirements associated to EASA CS-25

Aircraft airworthiness is established with a regulatory framework. In Europe and in the United States, airworthiness standards are defined respectively by the European Aviation Safety Agency (EASA) and the Federal Aviation Administration (FAA). For civil transport airplanes, these rules are detailed in the "CS-25 Certification Specifications and Acceptable Means of Compliance for Large Aeroplane" [129] for EASA while FAA publishes them under "CFR Part 25 – Airworthiness Standard: Transport Category Airplanes" [158]. Between the two documents, there are some differences to be noted but

they do not change the overall approach presented in this study. Thus, only sections referring to EASA CS-25 will be described.

Actually, CS-25 is made of two books: Book 1 presents all Certification Specifications while Book 2 details the Acceptable Means of Compliance. The decomposition of Book 1 reported in Figure 40 (left) shows the main disciplines and systems that are considered from a regulatory point of view. Many SUBPARTs refer to an area that is often under the responsibility of a specialist group, with required information usually used in the early phases of the project, or aspects rather considered during the detail design part. SUBPART B – STRUCTURE, for example, defines the flight manoeuvre envelope that is useful for initial sizing, as well as towing loads (CS 25.509) that will be used to design the single components of the landing gear. A parallel can be made with SUBPART E - POWERPLANT which provides not only constraints about high level aircraft characteristics (CS 25.925 propeller clearance) but also requirements on fuel system (CS 25.951 – CS 25.981) that should be investigated in the last phases of the design. SUBPART B – FLIGHT, on the other hand, relates to the aircraft as an integrated system. It is the part of the regulatory text that is naturally considered by the design engineers at conceptual level to ensure that the aircraft is flying according to a set of airworthiness rules. Topics within SUBPART B - FLIGHT are detailed in Figure 40 (right).

CS-25 Book 1

SUBPART A - GENERAL
SUBPART B - FLIGHT
SUBPART C -STRUCTURE
SUBPART D - DESIGN AND CONSTRUCTION
SUBPART E - POWERPLANT
SUBPART F - EQUIPMENT
SUBPART G - OPERATING LIMITATIONS AND INFORMATION
SUBPART H - ELECTRICAL WIRING INTERCONNECTION SYSTEM
SUBPART J - AUXILIARY POWER UNIT INSTALLATIONS
APPENDICES

SUBPART B - FLIGHT

GENERAL	CS 25.	20
	CS 25.	33
PERFORMANCE	CS 25.	101
	CS 25.	125
CONTROLLABILITY AND	CS 25.	143
MANOEUVRABILITY	CS 25.	149
TRIM	CS 25.	161
STABILITY	CS 25.	171
	CS 25.	181
STALLS	CS 25.	201
	CS 25.	207
GROUND HANDLING	CS 25.	231
CHARACTERISTICS	CS 25.	237
MISCELLANEOUS FLIGHT	CS 25.	251
REQUIREMENTS	CS 25.	255

Figure 40: Details of the CS-25 Book 1 decomposition (left) and the sections within SUBPART B - FLIGHT (right) [129]

As exposed by the study on the GABRIEL aircraft, many sections of SUBPART - B FLIGHT are dealing with performance. Essential elements such as speeds, path, critical conditions and threshold values are specified for the key mission segments (takeoff, en-route, and landing). For these sections between CS 25-101 and CS 25-125, from an analysis point of view, the point mass approach is sufficient to calculate the required criteria. A large part of the topics in SUBPART B -FLIGHT is directly related to flight mechanics aspects. Sections CS 25-143 to CS 25-149 are devoted to controllability and manoeuvrability, section CS 25-161 focuses on trim and sections CS 25-171 to CS 25-181 are dedicated to stability. Part of section CS 25.147 describing directional and lateral control

requirements is given as an example in Figure 41. In the presented paragraph (a), the requirement clearly states that an assessment of the moment around the Center of Gravity must be made to check yaw capabilities. From an analysis point of view, according to Chudoba [126], the verification of these constraints in the conceptual design phase requires a flying qualities / handling qualities (pilot skills are often mentioned) approach. Thus, to take into account many certifications constraints under SUBPART B - FLIGHT, it becomes mandatory to integrate within the MDAO process some simulation capabilities based on a six DoF model. Another point that has been observed during the review of CS 25 SUBPART B - FLIGHT is highlighted in the first paragraph of CS 25.145 (see Figure 42).

CS 25.147 Directional and lateral control
(See AMC 25.147)

(a) *Directional control; general.* (See AMC 25.147(a)) It must be possible, with the wings level, to yaw into the operative engine and to safely make a reasonably sudden change in heading of up to 15° in the direction of the critical inoperative engine. This must be shown at 1·3 V_{SR1}, for heading changes up to 15° (except that the heading change at which the rudder pedal force is 667 N (150 lbf) need not be exceeded), and with –

(1) The critical engine inoperative and its propeller (if applicable) in the minimum drag position;

(2) The power required for level flight at 1.3 V_{SR1}, but not more than maximum continuous power;

(3) The most unfavourable centre of gravity;

(4) Landing gear retracted;

(5) Wing-flaps in the approach position; and

(6) Maximum landing weight.

Figure 41: Information provided in section CS 25.147 (a) in SUBPART B - FLIGHT [129]

CS 25.145 Longitudinal control
(See AMC 25.145)

(a) (See AMC 25.145(a)) It must be possible at any point between the trim speed prescribed in CS 25.103(b)(6) and stall identification (as defined in CS 25.201(d)), to pitch the nose downward so that the acceleration to this selected trim speed is prompt with:

(1) the aeroplane trimmed at the trim speed prescribed in CS 25.103(b)(6);

(2) the most critical landing gear configuration;

(3) the wing-flaps (i) retracted and (ii) extended; and

(4) engine thrust or power (i) off and (ii) at go-around setting.

Figure 42: Contents of in section CS 25.145 (a) in SUBPART B - FLIGHT [129]

In this particular case, the complexity of the regulatory text is well illustrated as this single section refers not only to different disciplines but also to many other sections. To translate these different links within the current structure of the MDAO process where certification constraints and their associated parameters are described as inputs would require an important number of interdependencies. Also, updates related to section reference values (e.g. speed) would be difficult to be implemented during the resizing and optimization loops. Thus, there is a requirement in terms of tool or interface to be managed by the aircraft designer for an easier handling of the certification constraints at conceptual design level within a Multidisciplinary Design Analysis and Optimization process. In this research, the idea is the translation of a text-based complex document into a digital format. Section 2.4. provides more details on the proposed approach.

2.3.2. Need associated to Air Traffic Management

Each aircraft is designed to operate in a certain environment. For civil transport aircraft, the goal is to have seamless operations within the Air Transport System (ATS). In this research dedicated to Aircraft Design, it is then interesting to look at requests in terms of analysis capability from the operations side. As stated by Schmitt and Gollnick [159], the Air Transport System (ATS) is based on four main stakeholders: (i) Manufacturers who design, manufacture, integrate and sell airplanes; (ii) Airlines who operate the aircraft to carry passengers or freight; (iii) Air Navigation Services (ANS) who are responsible for Air Traffic Management; (iv) Airports, who manage and operate large ground infrastructures enabling both (de)boarding of passengers and (un)loading of freight on(from) airplanes. Thus, when this large scale ATS has to meet stringent constraints in terms of both environmental impacts (see chapter 1) and safety levels [160] for its future developments, improvement requirements are cascaded down to the key contributors. Recalling the fuel burn objectives of CAEP (Figure 9), it is then not surprising to observe required improvements not only at aircraft level but also on airports (infrastructures), ATM and airlines fleet operations.

At the ATM level, the goals set for the evolution of ATS lead to research activities in various domains. First, as the number of flights will increase, safety becomes a key issue [161]. As expected, environmental assessments in the vicinity of airports are of high interest and they cover noise evaluations as well as chemical emissions and air quality with high-fidelity analysis tools [162]. Other studies investigate the operational procedures to converge to an optimum use of Air Traffic Control (ATC) ressources [163]. For these studies and in general for ATM research, given the large number of flights to be considered, the simulation of each aircraft trajectory is based on the use of a fast Aircraft Performance Model (APM). Eurocontrol (the European Organization for the Safety of Air Navigation [164]), in collaboration with manufacturers and airlines defined the BADA (Base of Aircraft DAta) APM [165]. As explained by Nuic [166], BADA APM relies on a kinetic approach in which aerodynamic, propulsive and gravitational forces are applied to a point mass. With the performance model established, a parameter identification for each type of aircraft is performed using the Eurocontrol flight database. In the end, accurate trajectory simulations and predictions for existing aircraft can be obtained at reasonable computing cost. Yet, when looking at future ATM procedures, disruptive airplane concepts with new operational capabilities should be taken into account. In this scenario, as there is no database for such aircraft, the use of BADA APM could lead to uncertainties. There is thus a demand within ATM research for a 6 DoF simulator with control and navigation loops that would generate accurate trajectories based solely on the aircraft characteristics. In the case of existing aircraft, this capability offers the possibility to have directly a large amount of data concerning the trajectory, the speed, the thrust level and the aircraft attitude. If necessary, registered flight plans could be quickly verified in terms of feasibility. Section 2.4. takes this specific ATM need into account to define an extended MDAO.

2.4. Expanding the Multidisciplinary Design Analysis and Optimization process

In the previous sections of chapter 2, relevant observations have been made in order to select key knowledge to be added within the Multidisciplinary Design Analysis and Optimization. Considering also all previous studies presented in chapter 1, it is proposed in the present research to add knowledge at aircraft conceptual design through a consistent expansion of the MDAO process.

2.4.1. Step 1 - Including 6 Degrees of Freedom capabilities in the MDA

For future aircraft concepts, one promising area concerns hybrid electric propulsion and the development of airframes benefiting from aero-propulsive effects. At ONERA, configurations based on Distributed Electric Propulsion (DEP) have been studied for on-demand mobility purposes [167] and also for commercial applications [168]. A clear asset of this layout is the possibility to obtain an important increment of lift because of the blowing effect. However, as lift is highly affected by the level of thrust, the equilibrium of the aircraft has to be monitored over the complete flight domain. In terms of overall aircraft sizing and design process, this verification requires the capability to assess flight mechanics in the longitudinal plane as early as possible. Besides, given the large number of ducted fans that can be applied over the wing, DEP offers the possibility to generate yawing moments. Such additional degree of freedom allows designers to reduce the Vertical Tail Plane (VTP) size with positive effects on the overall performance level. As the calculation of the VTP area is a key step in the early design phases, there is then the need to expand the flight behavior evaluation capability to lateral directional motions. Besides, the verification of key certification constraints also requires the assessment of the aircraft behavior around its three axes. The first step towards the MDAO expansion is thus the addition of 6 Degrees of Freedom capabilities.

2.4.2. Step 2 - Taking into account a Stability Augmentation System

As detailed in chapter 1, aircraft designers and disciplinary experts involved during conceptual design have to downselect, from a set of various aircraft layouts or configurations, the most promising concept. In 1976, Walker [169] conducted a full preliminary design for a tanker aircraft with a fixed set of requirements. The interesting point in his work is that he aimed for a Control Configured Vehicle (CCV): basically, the design space has been opened by taking into account a control system enabling Reduced Static Stability and Flutter Mode Control in the sizing phase. The resulting feasible aircraft is a tailless configuration that is radically different from the conventional tanker layout characterized by important OWE reduction (see Figure 43). Among the different functions assigned to the control system, the stability augmentation is the one that has a profound impact “on the airplane configuration arrangement design and produces the largest reductions in weight and drag” [169]. Thus, in order to increase the exploration capabilities at conceptual design level, the second step towards the MDAO expansion is the addition of a Stability Augmentation System.

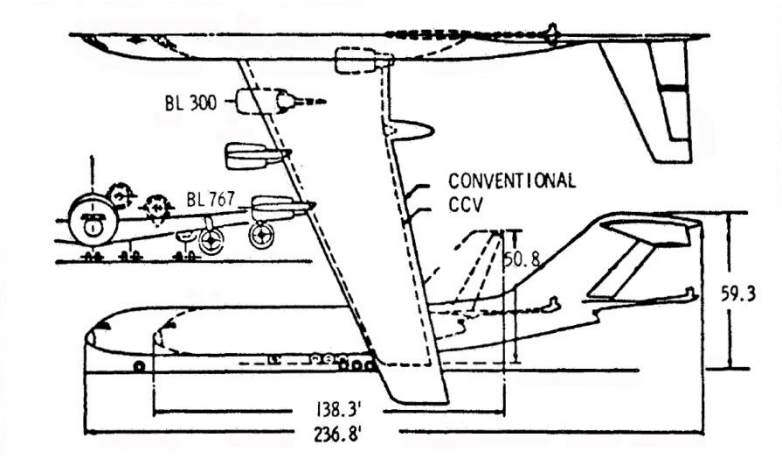

Figure 43: Comparison of a Control Configured Vehicle and a conventional tanker configuration based on the same requirements [169]

2.4.3. Step 3 - Implementing an automated full simulation in the MDA

With the ATM need expressed in Section 2.3.2., the third step towards the MDAO expansion consists in adding additional loops to the Flight Control System so that speed, altitude and heading can be maintained. An automated full simulation capability is then made available to aircraft designers at conceptual level. A good example of fuel burn reduction through ATM is formation flight. Demonstrated through a series of flights, the positive aerodynamics effects translate directly into required power reduction [170]. Carried out by Xu [171], the optimization of aircraft routes dedicated to formation flight illustrated in Figure 44 confirmed substantial fuel consumption reduction.

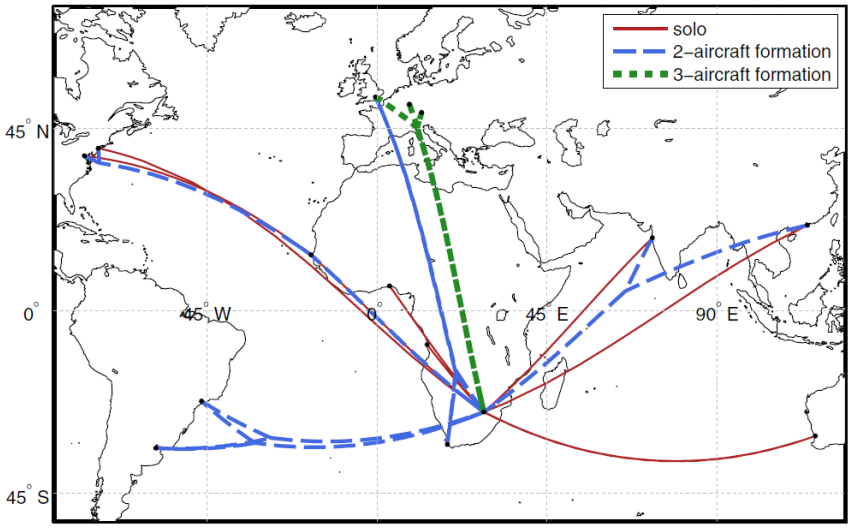

Figure 44: Example of formation flight routes for 2 or 3 aircraft [171]

Yet, with the flight segment analysis based on Breguet range equation and energy approach, some aspects of ATM constraints are not considered. It is clear that the availability of automated full simulation provides the necessary level of details to take vertical and horizontal flight track restriction into account. In addition, with a direct coupling between the aircraft sizing process and ATM

assessments through flight simulations, it is possible to envision a full optimization at aircraft and route level (with computation costs being a major issue). This global approach would avoid scenarios in which the direct combination of two advanced technologies (formation flight and advanced aircraft configuration), separately developed, would not translate in the expected overall benefits [172]. Driven by ATM need, the automated full simulation also offers advantages for the aircraft sizing process. Taking the case of the scaled demonstrator EOLE [173][174], this unmanned vehicle has to fly a very specific mission. Illustrated in Figure 45, it consists in a climbing spiral and two descending ones as the available operational volume is limited. In such case where the bank angle is not negligible, performance based analyses may lead to trajectory approximations. Thus, in order to increase the reliability of the fuel consumption estimation, the simulation tool can be used to fly the sizing mission.

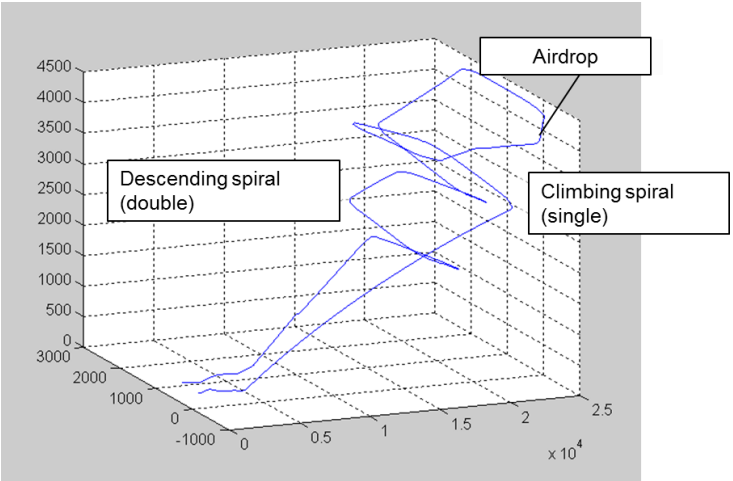

Figure 45: Reference mission for the EOLE demonstrator [175]

2.4.4. Step 4 - Adding a Certification Constraints Module

As demonstrated by the GABRIEL MDAO detailed in Section 2.2., the certification constraints can strongly affect conceptual studies results. They must therefore be considered in the sizing optimization process. However, as pointed out in the EASA CS-25 review carried out in Section 2.3, there is a clear need to facilitate the management of these certification constraints within the Multidisciplinary Design Analysis and Optimization. At this stage, it is also important to recall that next generation aircraft have to rely on disruptive technologies or configurations to meet fuel burn goals. The problem is that only guesses can be made about future certification requirement for such promising concepts featuring for example a large number of engines and different on-board energy sources [176]. Indeed, the standard addition of Critical Review Items for certification would not be suited for radically different airplanes. Consequently, the fourth step towards the MDAO expansion is the addition a Certification Constraints Module (CCM). This component enables the generation of a digital version of CS 25 SUBPART B - FLIGHT with active links between all parameters reported in the various sections when required. Directly coupled with the MDAO, this digital version of the regulatory text automatically updates data to be used for constraint verifications at each iteration of the process. It is believed that this CCM

gives an opportunity to designers to better map the certification constraints and facilitates exchanges with disciplinary or system modules within the MDAO. Equally important, this module paves the way for step by step Certification Specifications changes [177], an approach that seems in line with the revision of EASA CS-23 [178] to facilitate the introduction of disruptive vehicles.

In this research, it is therefore proposed to add knowledge in the Multidisciplinary Design Analysis and Optimization at aircraft conceptual design level through the development of a Certification Constraints Module and the implementation of full simulation capabilities.

2.5. Conclusion

The development of the GABRIEL Multidisciplinary Design Analysis and Optimization enabled a full exploration of the design space for an unconventional aircraft. Implemented within ModelCenter, the process using physics based models for structural weight estimation was also able to take into account input from disciplinary analyses performed by partners. From a vehicle sizing point of view, reliable results have been obtained showing the possible gains of an aircraft tailored to the GABRIEL ground based system with respect to a conventional one [148]. This work has been also valuable for Aircraft Design methods aspects. First, it is confirmed that MDO is a clear enabler for knowledge gain during conceptual design assessments. Indeed, designers not only explore the design space but also assess families of vehicles and possible tradeoff at aircraft level. In addition, the review of active constraints provides extra insight for possible further improvements. Last but not least, the work carried out in the frame of the project GABRIEL emphasized the impact of certification constraints on the Pareto front shape that defines the best design options. Following this first conclusion, further review of the EASA CS-25 and its dedicated section on performance (SUBPART-B FLIGHT [129]) highlighted two important points. First, the structure of the regulatory text features a large number of sections with many interconnections between them to define reference values. Besides, these same reference values must be computed by different disciplinary analyses. This background naturally pushes for a simplification of certification constraints at MDAO level. Second, certification constraints require the use of 6 Degrees-of-Freedom analyses to compute the exit criteria. The same need in terms of tool has been identified when looking at recent studies in the field of Air Traffic Management.

Following the identification of these specific needs in terms of additional knowledge, this PhD proposes to expand the Multidisciplinary Design Analysis and Optimization at aircraft conceptual design level through the coupling with a Certification Constraints Module and the implementation of full simulation capabilities. With such an expansion of the MDAO process, design engineers can investigate vehicle performances and sizing, from certification to operations with ATM constraints, and propose optimized solutions.

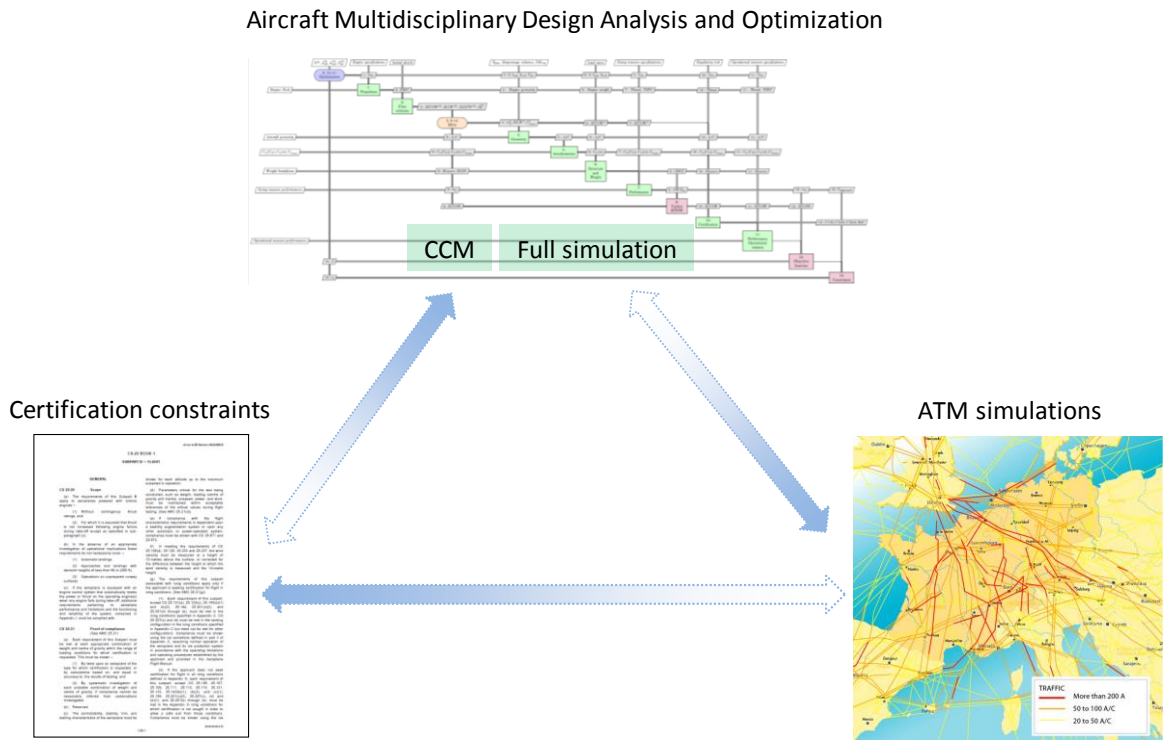

Figure 46: Overview of the MDAO expansion to certification constraints and ATM simulations

Illustrated in Figure 46, the possible exchanges feature many benefits:

- With the implementation of the CCM, certification constraints under a digital format can be easily connected to the various modules of the MDAO. There is then a notable gain in the setup of the optimization problem.
- During the certification process of an aircraft, authorities allow justified changes to regulatory text through Certification Review Items or Special Conditions. To mimic such a procedure, designers can easily assess the impact of threshold variations on the aircraft overall performances through the CCM [177].
- The full simulation capability within the MDAO process can supply a 6 Degrees-of-Freedom model for ATM simulations so that accurate trajectories can be computed. More importantly, advanced concepts defined through a complete design process can be integrated within the traffic.
- During operations, aircraft follow specific routes defined by ATM constraints. With such an expanded process, it is possible to take these constraints within the sizing and optimization process to assess the impact on overall performance level. Such direct coupling between aircraft design and ATM could further improve concurrent optimizations [179].
- Recently, there have been publications on radically new operational concepts that would increase air mobility [180][181]. However, for these scenarios, the regulatory framework may slow down developments [182]. The proposed expanded MDAO process, including the management of certification constraints, could help in the exploration of possible changes to

regulatory texts considering the characteristics of these new vehicles without compromising safety.

The proposed expansion is based on two distinct improvements: the Certification Constraints Module and full simulation capability. In the current research, benefits derived from these improvements are investigated in two distinct steps. Thus, chapter 3 is dedicated to the development of the CCM and its coupling with an existing aircraft sizing code to perform different optimization problems subject to certification constraints. In chapter 4, the Multidisciplinary Design Analysis is completed by specific modules so that full simulations can be achieved at the end of the sizing process. Subsequently, the same simulation model is used by ATM tools to simulate a real trajectory. To validate the simulation model generated by the sizing code, these ATM trajectories are compared with real flight traces recorded with an ADS-B antenna.

Synthesis of the chapter

- A multidisciplinary Design Analysis and Optimization process of an unconventional aircraft is implemented
- MTOW and Sizing mission fuel weight are minimized considering operational and certification constraints
- The shape of the Pareto front defining the best solutions is shifted because of certification constraints
- EASA Certification Specifications and Air Traffic Management studies both require simulation capabilities
- The Multidisciplinary Design Analysis and Optimization is expanded through the development of a Certification Constraints Module and the implementation of full simulation capabilities

➢ The Certification Constraints Module and its utilization for optimizations are described in chapter 3 while the implementation of simulation capabilities within the Multidisciplinary Design Analysis is detailed and verified in chapter 4

Associated conferences

- Schmollgruber P., Bartoli N., Gourinat Y., "Virtual flight testing in an aircraft sizing and optimization process", 15th AIAA Aviation Technology, Integration, and Operations Conference, AIAA AVIATION Forum, AIAA 2015-2546, Dallas, 2015

Chapter 3

Use of the Certification Constraints Module for Aircraft optimization

Roadmap of the chapter

- The interactions between the Certification Constraints Module and the Multidisciplinary Design Analysis and Optimization are described
- The development of the Certification Constraints Module is detailed
- The ONERA/ISAE aircraft sizing tool FAST is presented
- A sensitivity analysis with FAST is carried out
- A monolithic optimization architecture based on FAST is implemented
- Three different optimization algorithms to verify results and compare CPU time are selected
- Four different multiobjective optimizations on a conventional airplane considering operational and certification constraints are achieved

Résumé du chapitre

La première partie de ce chapitre détaille le développement du module de contraintes de certification (CCM). Développé à partir d'un modèle de données basé sur la structure des contraintes de certification (CS-25 SUBPART B - FLIGHT), ce module permet de générer une version numérique des contraintes utilisées lors du dimensionnement en phase avant-projet. Dans un premier temps, les concepteurs doivent définir, via une interface utilisateur graphique, les diverses contraintes à prendre en compte lors du processus de conception et d'optimisation. Un modèle prédéfini aide les utilisateurs à définir les conditions à vérifier et les critères de sortie. Par le biais d'une simple commande d'exportation, le CCM génère automatiquement l'ensemble des contraintes définies dans un fichier unique au format .XML. La digitalisation des contraintes de certifications permet alors une prise en compte simplifiée lors de la conception et optimisation multidisciplinaire d'un avion.

Afin d'évaluer les avantages du CCM pour les études de conception d'aéronefs, différents problèmes d'optimisation soumis à des contraintes de certification ont été réalisés. Pour effectuer les boucles de dimensionnement, l'outil FAST, développé conjointement par l'ONERA et l'ISAE-SUPAERO depuis 2015, est utilisé. Avant les optimisations, une analyse de sensibilité est effectuée afin de mieux évaluer la variance des résultats par rapport aux variables de conception. Comme prévu, le calcul des indices Sobol a confirmé que l'espace de conception, pour un avion de transport civil, est dominé par l'allongement de la voilure et la poussée maximale du moteur. Des vérifications ultérieures basées sur des données de référence ont démontré la capacité de FAST à reproduire fidèlement les facteurs d'échanges principaux entre les disciplines et les composants de l'aéronef. Au niveau des optimisations, il a été decidé de résoudre un problème multi-objectif en tenant compte des contraintes de certification (vérifications de la capacité de montée) ainsi que des contraintes opérationnelles (longueur de piste nécessaire au décollage et limitation de l'envergure de l'aile). Réalisées avec trois algorithmes différents, les optimisations ont tout d'abord mis en évidence l'efficacité de SEGOMOE puisque, pour des résultats équivalents, le temps de calcul a été divisé par 5. Par la suite, elles ont clairement exposé le fort impact des contraintes de certification et de leurs seuils sur les concepts les plus prometteurs. En phase avant-projet, le risque est d'éliminer un concept valable ou de sélectionner une mauvaise configuration. Aussi, en sachant que les contraintes de certification vont façonner l'aéronef et sa motorisation, il est important d'atténuer partiellement ce risque en prenant en compte le plus de contraintes de certification très tôt dans le processus de conception. À cet égard, le module de contraintes de certification offre des fonctionnalités uniques qui aident les concepteurs dans leur processus de prise de décision.

Dans ce chapitre, les optimisations multidisciplinaires ont pris en compte uniquement des contraintes de certification liées aux performances. Cependant, les textes réglementaires comportent également des contraintes associées à la dynamique de vol. Aussi, le processus de conception doit inclure des outils de simulation pour évaluer les mouvements de l'appareil autour de son centre de gravité. Des développements effectués en vue de cet objectif seront présentés dans le prochain chapitre.

3.1. Introduction

In this research, it is propounded to add knowledge in the Multidisciplinary Design Analysis and Optimization at the aircraft conceptual design level through the development of a Certification Constraints Module (CCM) and the implementation of full simulation capabilities. The idea of the Certification Module is to generate a digital version of important constraints extracted from Certification Specifications CS-25 SUBPART B - FLIGHT published by the European Aviation Safety Agency. As an initial step, designers have to define through a Graphical User Interface (GUI) the various constraints to be considered during the MDAO process. A predefined template helps users in defining the conditions to be verified and the exit criteria. Through a simple export command, the CCM automatically translates the constraints that have been defined in a single eXtensible Markup Language (.XML) file that contains all data related to certification constraints. Under this numerical format, it is then possible to have direct exchanges between certification constraints and the Multidisciplinary Design Analysis and Optimization. In some cases, the required information is stored in the CCM and the MDAO uses it to perform an analysis (engine throttle, landing gear position, high-lift configuration,…). In other cases, the MDAO process has to estimate a value that is subsequently passed to the CCM to store a reference value: it is the case of landing weight. This means that at each iteration of the sizing loop, certification constraints referring to landing weight will be estimated with the correct updated value. At the end of the process, the GUI is used to read information stored within the CCM including reference values that are specific to the converged aircraft. These exchanges between the CCM and the MDAO are illustrated in Figure 47.

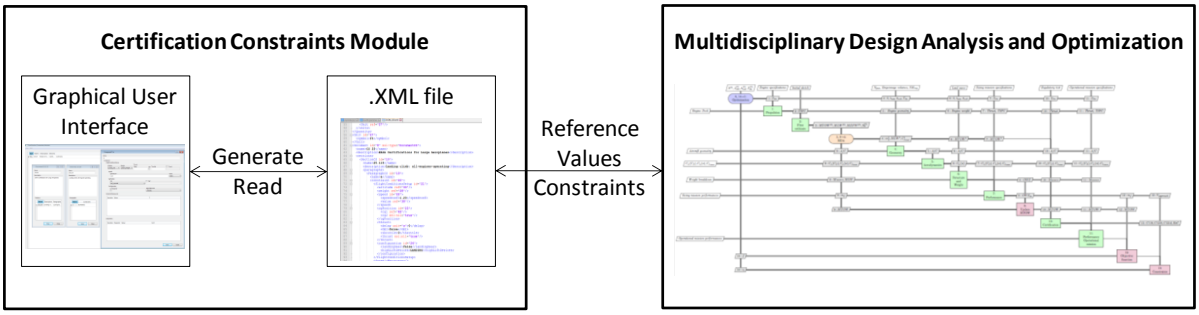

Figure 47: Exchanges between the components of the CCM and the MDAO

Following the development of this additional module, the objective is to test its capabilities within FAST (Fixed-wing Aircraft Sizing Tool), a tool dedicated to aircraft design studies jointly developed by ONERA and ISAE-SUPAERO. With the quality of FAST's results consolidated, a sensitivity analysis is carried out to better assess the system response with respect to a set of design variables. Subsequently, four optimizations taking into account certification and operational constraints are carried out to assess the benefits in terms of knowledge gain for the aircraft designer.

The first section of chapter 3 details the development of the Certification Constraints Module. Focus will be made on the necessary analysis of the regulatory texts and the extensive work on generating a robust data model enabling the description of many certification constraints. Subsequently, the sizing tool FAST is presented through a description of its Multidisciplinary Design Analysis. Naturally,

before the sensitivity analysis, the outcomes of FAST are compared to reference data to verify its capability to correctly size an aircraft for a given mission. Last, FAST is coupled to an optimizer within a monolithic architecture, so that different optimizations under certification and operational constraints can be completed.

3.2. Development of the Certification Constraints Module

3.2.1. General structure of regulatory constraints

The primary goal of the CCM is to generate an .XML file that is a digital version of CS 25 SUBPART B - FLIGHT (see Section 2.3.1) and the associated Acceptable Means of Compliance (AMC) [129]. Naturally, a detailed review of the different sections must be performed to identify the overall structure and understand the main logic. Following the topic separation proposed in the document, two sections detailed in Figure 48 are analyzed. One corresponds to a performance constraint (CS 25.119) while the other is a directional and lateral control constraint (CS 25.147).

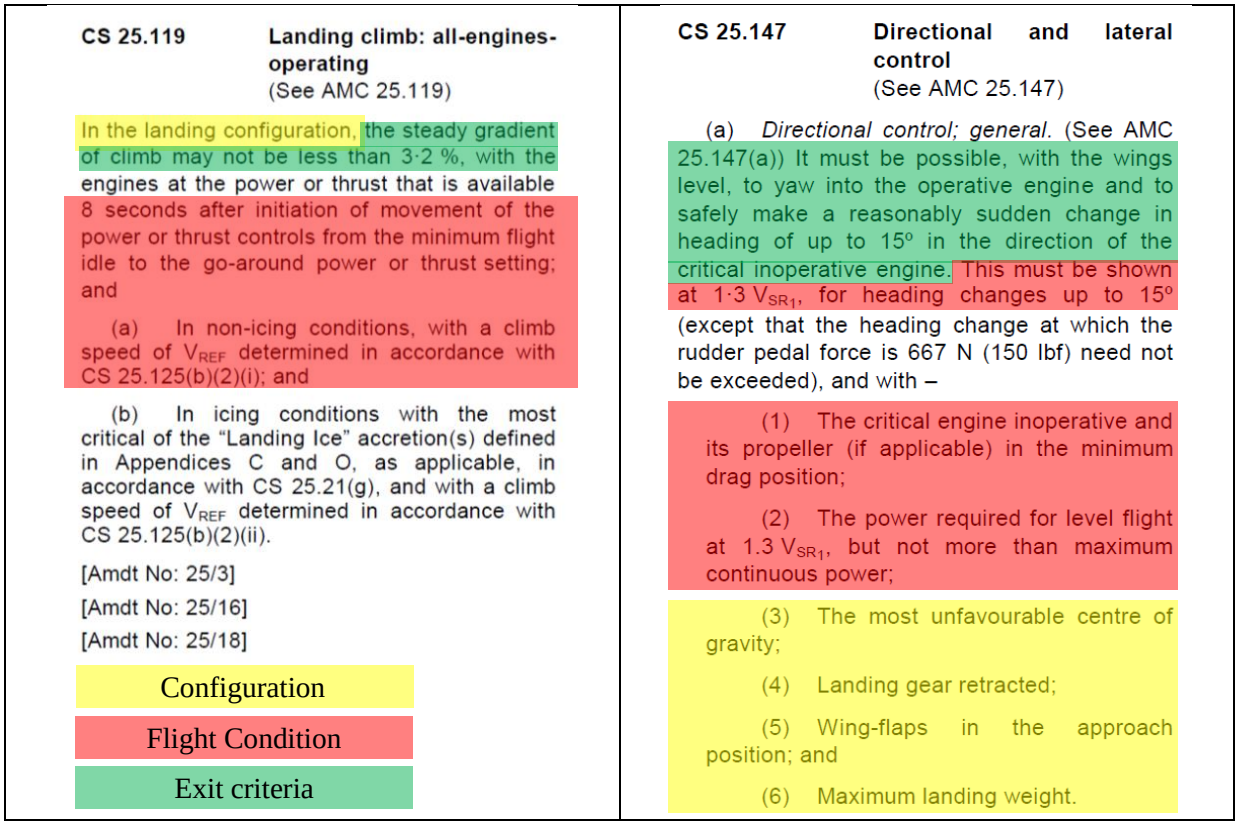

Figure 48: Analysis of CS-25 sections [129]

In both cases, the description of the certification constraint is defined by three common components: the aircraft configuration, a flight condition and an exit criterion. One difference is that in the case of the control constraint, there is additional information about the manoeuvre to be performed. This basic structure must be preserved in the CCM and the generated .XML file.

Concerning AMC related to CS 25 SUBPART B - FLIGHT [129], the sections provide different types of information. Some examples are given here below:

- In AMC 25.119(a), it is stated that "Engine acceleration tests should be conducted using the most critical combination of the following parameters: (i) Altitude, (ii) Airspeed, (iii) Engine bleed, (iv) Engine power off-take". All these parameters have a key impact on the engine performance.
- AMC 25.121 indicates that "In showing compliance with CS 25.121 it is accepted that bank angles of up to 2° to 3° toward the operating engine(s) may be used". This implies that the verification of CS 25.121 should be performed through both a point mass analysis and a flight mechanics assessment.
- In the case of AMC 25.147(a), the text doesn't specify a value. It is a clarification of the test objective: "The intention of the requirement is that the aircraft can be yawed as prescribed without the need for application of bank angle. Small variations of bank angle that are inevitable in a realistic flight test demonstration are acceptable".
- AMC 25.181 dedicated to Dynamic Stability, states that "The requirements of CS 25.181 are applicable at all speeds between the stalling speed and V_{FE}, V_{LE} or V_{FC}/M_{FC}, as appropriate". In this case, more reference speeds are provided to complement CS 25.181.

Looking at this disparate information, it is difficult to find a common structure similar to the one just observed for sections of CS 25 SUBPART B - FLIGHT. Nevertheless, in all cases, AMC is providing more information or an additional constraint about one or more aircraft parameters. Such logic must then be kept when defining the specifications of the Certification Constraints Module.

3.2.2. Specifications of the Certification Constraints Module

The CCM provides a Graphical User Interface (GUI) where the design engineers enter the various parameters of the constraints to be considered during MDAO. Following a certain template, all data are translated into a structured .XML file that is associated with the MDAO process. It is then essential to provide specifications on all data to be managed, their origin, type, hierarchy and possible dependencies.

The first specifications concern CS 25 SUBPART B - FLIGHT [129] and the decomposition of the constraints. To keep the data model as open and flexible as possible, it has been decided not to make a distinction between performance and control / stability / manoeuvrability constraints. Data have to be structured around the three categories identified earlier: aircraft configuration, flight conditions and exit criteria. Regarding stability and control requirements, supplementary data regarding the dynamic manoeuvre must be considered. For Acceptable Means of Compliance, there are simply too many different types of parameters to be managed by the CCM. After various tests, the most promising solution proposes a description of AMC sections through a variable number of parameters (no limitation) with each one associated to an operator type. This high level data decomposition allows taking into account other important AMC that affect the design phase. For example, when focusing on the engine integration, important limitations are indicated in AMC 20 "General Acceptable Means of

Compliance for Airworthiness of Products, Parts and Appliances" [185] and more specifically in section AMC 20-128A "Design Considerations for Minimizing Hazards caused by uncontained Turbine Engine and Auxiliary Power Unit Rotor Failure" [185]. In this document, geometric angles are indeed provided to place the engine in a certain position with respect to other aircraft components or subsystems. The structure considering parameters and operators is then perfectly applicable. As engines are discussed, it must be reminded that in CS 25 SUBPART B - FLIGHT [129], many sections refer to a thrust setting for all engines with additional information (e.g. CS 25.119 [129]) or the OEI - One Engine Inoperative - condition (e.g. CS 25.121 [129]). With the objective of having the most complete description of flight conditions including thrust cases, the Certification Constraints Module proposes a dedicated section with different options to be selected (Throttle level, OEI, time delay). To maintain flexibility, the possibility is given to designers to enter a direct value of the thrust if necessary.

To conclude the specifications of the certification data model, reference quantities are discussed. There are indeed several sections of CS 25 SUBPART B - FLIGHT [129] where standardized values describing flight conditions or aircraft configuration are used. For example, in CS 25.121(d)(1) [129], it is stated that "the steady gradient of climb may not be less than 2.1% with (i) the critical engine inoperative, the remaining engines at the go-around power or thrust setting; (ii) the maximum landing weight". In CS 25.147(a)(1) [129] dedicated to Directional and lateral control, the exit condition refers to the same "Maximum landing weight". Regarding speeds, many sections mention reference values such as V_{REF} (reference landing speed), V_{SR} (reference stall speed) or V_{SR0} (reference stall speed in the landing configuration). To ensure data consistency during the MDAO process, it is mandatory that the CCM defines these reference values once. The subsequent transcription of the constraints by the design team is made through a simple link to these reference values. This concept of reference values is extended to flight conditions set up and aircraft configuration: high lift configurations and Center of Gravity conditions must be selected from a reference list. In this case, the extreme CoG positions are identified in the CCM and can be used as desired later. By implementing such dependencies between the data, designers have to manage a single link between the MDAO and the CCM to ensure consistency of data during the iterative loops.

3.2.3. Data model of the Certification Constraints Module

Given the CCM specifications, a certification data model has been defined. In this section, various Unified Modeling Language (UML) class diagrams associated to the Certification Constraints Module are presented. The breakdown into three different diagrams has been performed for better understanding.

In the first one (Figure 49), the main structure of CCM is shown. As there was a request to manage regulatory constraints from Certification Specifications and Acceptable Means of Compliance, the user can select one of these two types of document. A document that inherits the properties of « DocumentCS » has a number of sections. Each section has a number of paragraphs. In each one of

these paragraphs, one constraint is defined. A document that inherits the properties of « DocumentAMC » has a number of sections. In these sections, paragraphs or key parameters can be defined. If necessary, constraints can also be included in a paragraph, depending on the structure of the reference document. Such open architecture matches the necessity to transcript as many Acceptable Mean of Compliance sections as possible, knowing that there is no clear and consistent structure.

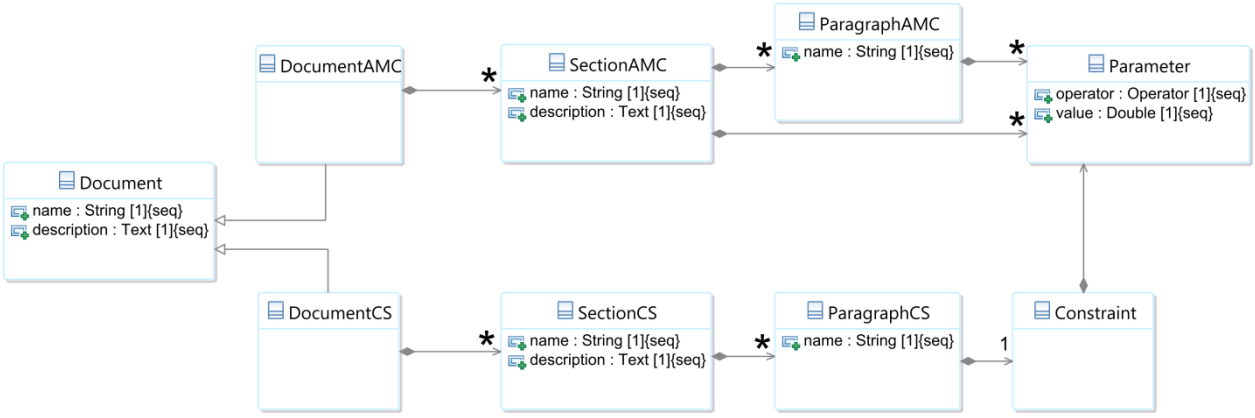

Figure 49: UML class diagram of the Certification Constraint Module – part 1

The central part of the Certification Constraint Module is obviously its capability to help the user to transcript in a formal manner the constraints that are described in the regulatory text. The second UML class diagram (Figure 50) reflects the selected logic to model the constraints that can be found in the CS 25 SUBPART B - FLIGHT [129]. To better understand the structure, it is proposed to review the information provided by CS 25.147(a) Directional and Lateral Control [129]. This regulatory text states at the beginning that "It must be possible, with the wings level, to yaw into the operative engine and to safely make a reasonably sudden change in heading of up to 15º in the direction of the critical inoperative engine". This is clearly the exit criteria defined by an operator and a threshold. Thus, the class diagram indicates that the element Constraint has Exit Criteria defined by the class Parameter that includes an operator and a value. Subsequently, CS 25.147(a) [129] indicates the following flight conditions: "This must be shown at 1.3 V_{SR1}, for heading changes up to 15º, […], and with (1) The critical engine inoperative and its propeller in the minimum drag position; (2) The power required for level flight at 1.3 V_{SR1}, but not more than maximum continuous power; (3) The most unfavourable centre of gravity; (4) Landing gear retracted; (5) Wing-flaps in the approach position; and (6) Maximum landing weight". In the CCM data model, there is then the necessity to associate with the flight condition all information related to the configuration (class Configuration in Figure 48 where information about the landing gear and the high lift devices is provided), the level of thrust, the speed and the CoG positions. Figure 50 rightfully illustrates that the class FlightConditions has information from classes Configuration, SpeedData and CoG Position. Regarding the definition of thrust level, the CCM must allow the transcription of many cases listed in CS 25 SUBPART B - FLIGHT [129]. For example, in CS 25.121(b) [129], the OEI condition must be considered, while CS 25.119(a) [129] states "engines at the power or thrust that is available 8 seconds after initiation of the movement of the power or thrust controls". This is the reason why the proposed class ThrustData (see Figure 50)

includes attributes such as delay, OEI, throttle and thrust. In CS 25.147(a) [129], many reference values such as "V_{SR1}" and "Maximum Landing Weight" can be identified. To manage such elements, the class StateReferenceValue has been created so that values of the flight conditions can be related to reference values. In the end, with the structure shown in Figure 50, users can select reference values for speed values, one or two CoG positions (fore and aft), Altitude and Weight. In many sections, CS 25 SUBPART B - FLIGHT [129] deals with time dependent manoeuvres requiring simulations to assess the exit criteria. For this reason, the class DynamicManoeuvre that features changes in the state vector of the airplane for a given time (attribute t to indicate the time at which the event happens and value) has been added to the constraint definition. In the case of CS 25.147(a) [129], users can then implement a change in the throttle level of one engine to simulate the failure case and monitor whether the changing in heading is achieved.

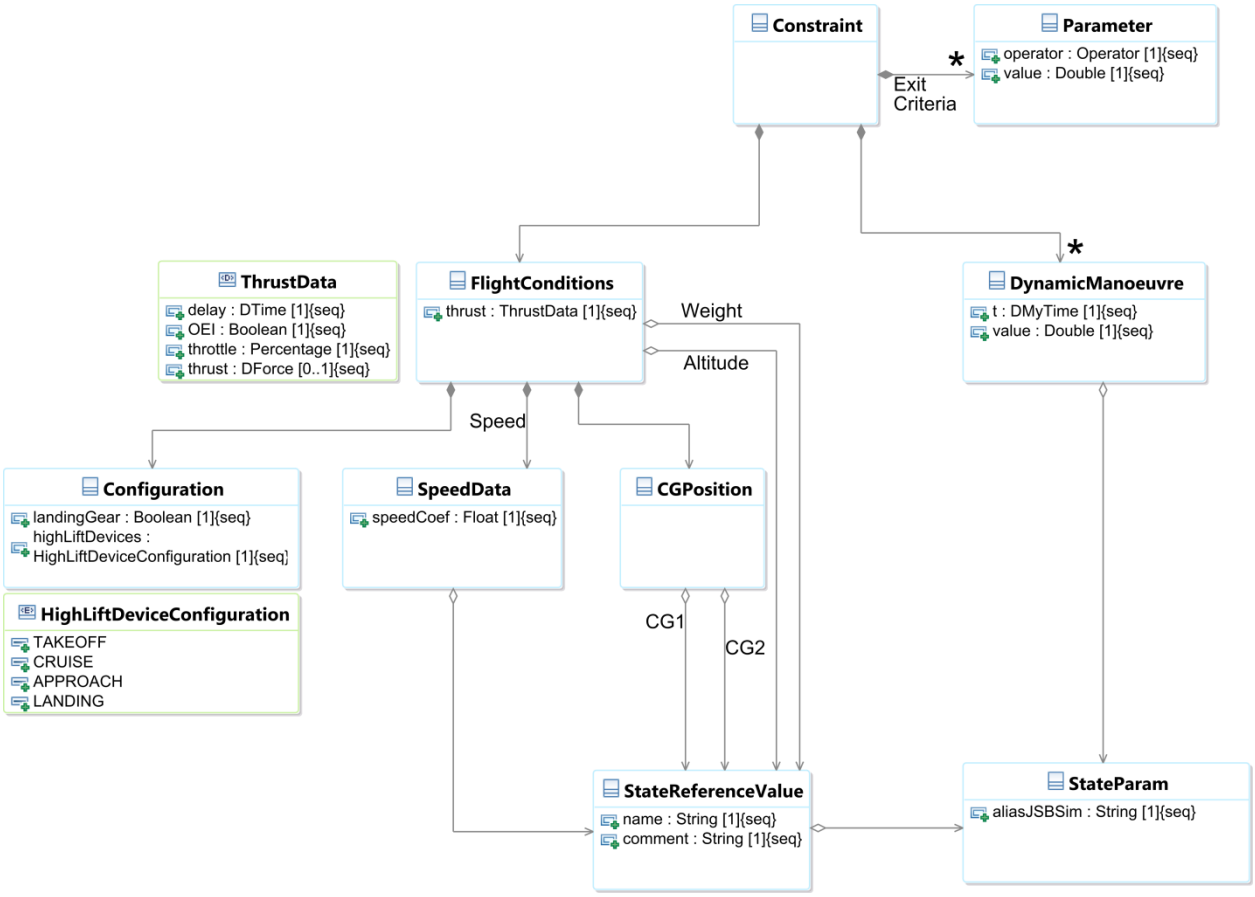

Figure 50: UML class diagram of the Certification Constraint Module – part 2

As described in the prior paragraphs, the Certification Constraints Module has to manage an important number of parameters that can be of different types. Therefore, there has been an important effort in structuring the various data. The last UML class diagram (Figure 51) focusing on these aspects can be interpreted as follows: in the upper left part where values are organized, the abstract class CValue has been introduced in order to define different types of values. For the moment, scalars (CDouble) and triplets (CDoubleTriplet, to deal with CoG coordinates) that can have units are identified. When

defining the CCM, the choice has been made to define a parameter (class Param) that can be associated to different types: (i) geometry (class GeometryParam) to consider constraints related to the position of components, such as the 15° angle used to avoid rotor burst issue described in AMC 20-128A [185]; (ii) analysis (class AnalysisParam) when the parameter of interest is a result of a post processing computation such as damping ratio; (iii) state vector (class StateParam). This parameter has then a quantity that can have a unit. To deal with exit criteria from Certification Specifications constraints and to describe information from AMC, the CCM includes the class Parameter (identified also in Figure 49 and Figure 50). Always in connection with AMC, Figure 51 details the options that can be selected regarding the attribute "Operator". Naturally, this class aggregates Param and Unit. Finally, the possibility of referencing key parameters is given through the class StateReferenceValue that related to CValue and StateParam.

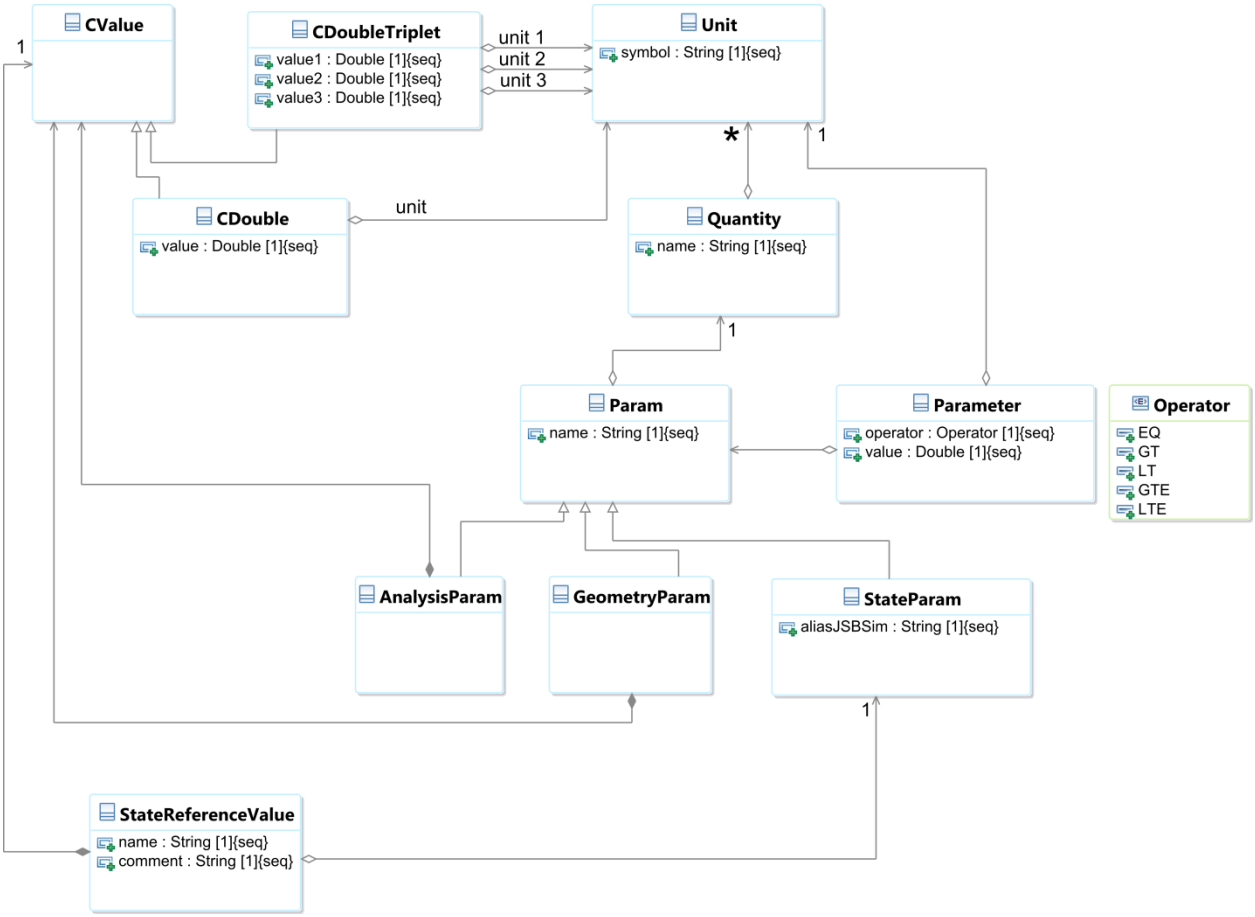

Figure 51: UML class diagram of the Certification Constraint Module – part 3

3.2.4. GAMME description

GAMME (Génération Automatique par Méta-Modèle Enrichi) is an ONERA in-house tool based on Model-Driven Engineering [186]. It has been developed to address the need for data unification in simulation modeling, especially in the field of complex systems where several forms of the same data may be used. At the core of GAMME, there is a metamodel that allows the description of data models in an object-oriented manner. Figure 52 illustrates the flow diagram in GAMME.

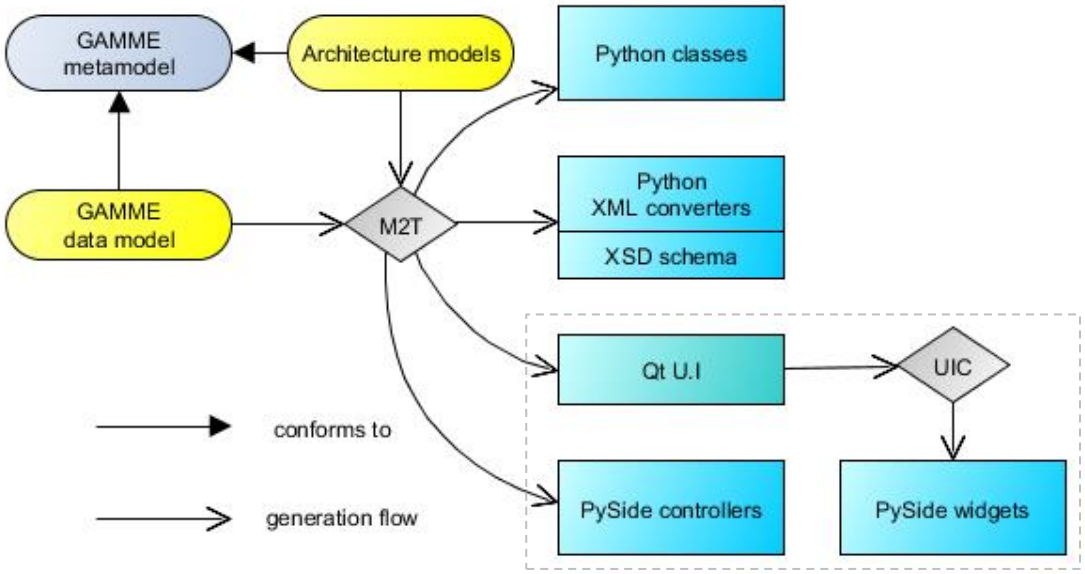

Figure 52: Overview of GAMME flows in the context of this research

First, the CCM data model is organized in order to conform to the GAMME metamodel [186]. In addition, Architecture models were defined to conform to GAMME metamodel also: they describe different software pieces to be integrated within a software application (for example: skill / competence classes, file writer / reader, Human Machine Interface). The data model and the Architecture model are subsequently woven through the Model to Text (M2T) [187] to generate the different software components such as Python classes, XML reader/writer or User Interface elements that can be combined to build the CCM application. One of the key assets is the automated update of all software components following changes in the data model and consequently the possibility of rapidly prototyping while ensuring consistency between the different components.

3.2.5. Graphical User Interface

From a software point of view, the code GAMME [186] is the enabler for the CCM generation. One of its key feature is the possibility to automatically generate a GUI depending on the data model structure. Although the CCM structure is complex, especially the management of data types (see Figure 49, Figure 50 and Figure 51) the resulting GUI is simple and it offers many possibilities for the users. This is very important as it is through this GUI that the certification constraints and information from the Acceptable Means of Compliance are defined. To better support the description of the GUI, a screenshot of the different windows is presented in Figure 53.

In the first window “Certification Constraints Module”, the user can import (open) or export (save) an .XML file that describes the constraints. Through the Edit command, it is possible to access the database where information related to Units, Geometry, State Vector, Analysis Parameters and Reference Values is stored. It is in this window that a document (CS or AMC) can be added. In Figure 53, it is decided to add a CS 25 constraint. Details of this document are given in the “DocumentCS CS 25” window that appears through a generic edit command used for all windows. If necessary, a text can be entered to provide additional information. In the section part, one can add a number of elements that correspond to the sections of the CS-25 [129]. In this example, CS 25.121 [129] is added.

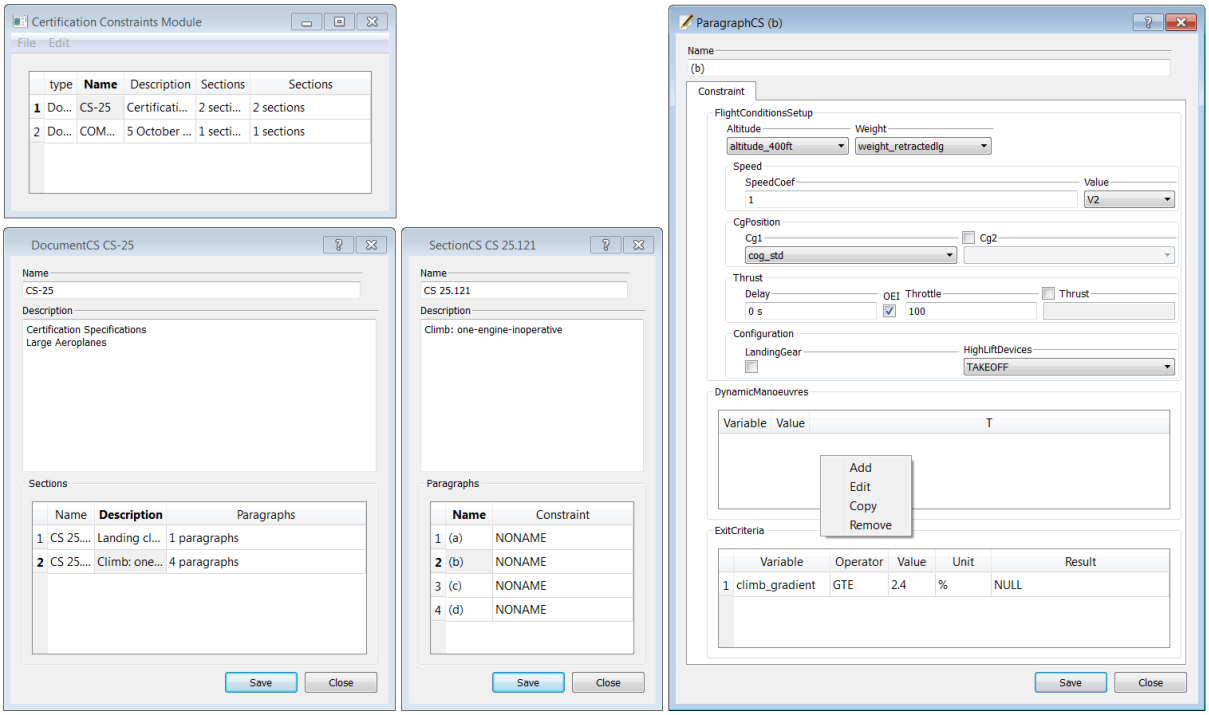

Figure 53: Graphical User Interface for the Certification Constraints Module

When editing the selected section, the associated window “Section CS 25.121” is opened. In this window, the name of the section is written and the number of paragraphs to be considered in the analysis can be added. For CS 25.121 [129], the four paragraphs are taken into account. This is why the GUI shows four paragraphs identified as in the regulatory text by (a), (b), (c) and (d). By right-clicking on the paragraph name, constraint window where all key parameters are entered is activated: reference altitude and reference weight are selected as they were already defined through the first window. For thrust information, a delay in seconds is provided and the level of throttle is indicated. If the box “Thrust” is not checked, the .XML file won’t have a dedicated tag where a value can be entered. In some cases as indicated previously, the value is determined by the MDAO (e.g. the thrust level can result from a trim condition). For the airspeed to be considered for the flight condition, a coefficient can be given with respect to a reference value always selected from the same initial list. In such manner, the CCM mimics regulatory texts. For configuration aspects, the GUI allows to indicate:

- one or different centers of gravity (usually fore and aft) which in case of steady performance constraints do not have an impact;

- if the landing gear must be extended by checking the dedicated box;
- the appropriate high lift devices configuration that can be selected from a list.

In CS 25.119(a), as the goal is to verify a steady performance check, there is no need to add Dynamic Manoeuvre information in the constraint window. Thus, the last elements to be added are the Exit Criteria which are detailed through a specific window named “Parameter”. Thanks to the operator value, users can define the thresholds indicating the success or the failure of the test.

Resulting from these various analyses and developments, the Certification Constraints Module is an innovative feature that provides designers with the possibility to digitalize some key constraints of EASA CS-25 in an .XML file to be used in a Multidisciplinary Design Analysis and Optimization. To illustrate its capabilities, it will be used for multiobjective optimizations based on FAST, the design code developed by ISAE-SUPAERO and ONERA.

3.3. The sizing tool FAST

3.3.1. The origin of FAST

The iterative nature of the aircraft sizing process promoted a quick development of computer codes dedicated to conceptual design explorations. A list of such historical codes can be found in the review made by Coleman [188]. At ONERA, aircraft design studies have been initiated in the late 80’s through COMPACT (Code d’Optimisation Multi Paramétrique adapté aux Avions Civils de Transport) which is a Fortran multi-parameters optimization code focused on Civil Transport Aircraft [153]. The Multidisciplinary Design Analysis includes the four key disciplines identified in section 1.4.3. and also an analysis of DOC. For the optimization, the objective function is usually DOC while the design variables define the wing geometry and also the reference mission parameters. Many aircraft configurations have been studied with COMPACT for more than a decade for given reference missions: short, medium and long range (1987-1992), long range and large capacity (1993-1998), long range supersonic (1994-2000) and flying wing (2000-2001). In 2000, ONERA started to perform Aircraft MDAO through ModelCenter [156] for internal research on High Altitude Long Endurance unmanned vehicles. This same process has been subsequently used in the European project CAPECON [189]. In 2008, COMPACT analysis capabilities have been integrated in ModelCenter [156] resulting in ACODE which has been used for the GABRIEL study [122]. Continuously improved since, this MDAO process is used to size unconventional configurations including higher fidelity disciplinary analyses and 3D layout arrangement [89]. With an overall positive feedback about its capabilities for conceptual design explorations, ACODE presents inherent limitations. First, as it is a commercial code, designers do not have the full control on the process and the available parameters nor the ability to include custom MDO algorithms. Second, as ACODE includes proprietary analysis codes (e.g. aerodynamics analysis considers wind tunnel results), it cannot be shared outside ONERA. Last and not least, commercial software has a cost that can be difficult to afford and limits the diffusion of the code even within the company. These latter points being true restrictions to activity

developments, initiatives in the United-States proposing open-source environments tailored for multidisciplinary design analyses and optimization such as OpenMDAO [190] or for aircraft design activities such as SUAVE [191] have been carefully followed.

In 2015, ONERA was granted resources to participate in both the European project AGILE dedicated to MDO enhancement [192] and the Clean Sky 2 program with activities in unconventional configuration / propulsive architectures exploration [193]. With the possibility to plan long term developments, it has been decided to launch the development of an enhanced Aircraft Design code benefiting from past experience in September 2015. The initial specifications were:

- The code shall not rely on commercial software or code;
- The code shall be easily shared among contributors to the design process;
- The programming language shall be Python;
- The code shall be modular enough to allow two types of expansion:
    - Higher fidelity analyses;
    - Additional disciplines;
- Input / Output shall be managed through an .XML file compatible with the CPACS format [194];
- Classical analyses as identified in Figure 13 for the MDA shall be included: propulsion, aerodynamics, structure and weight, performance;
- The mission analysis shall use a time step integration for all the different mission segments;
- The sizing of Horizontal Tail Plane and Vertical Tail Plane shall be based on simple analyses and not on volume coefficients;
- The resulting aircraft geometry shall be coupled with OpenVSP [19];
- The sizing logic for the overall aircraft shall be implemented first, considering that optimizations would be carried out in a second step.

In parallel, ONERA and ISAE-SUPAERO started to collaborate through many student projects on optimization and concept exploration. With the objective of capitalizing on the various and yearly advances in terms of multidisciplinary methods and aircraft design, it has been decided to jointly develop an aircraft sizing code. Based on ONERA disciplinary modules and initial parametrization, a TAS AERO Masters students from ISAE-SUPAERO developed the first version of the code FAST (Fixed wing Aircraft Sizing Tool) in 2015-2016. After a full standardization of the code by ONERA to follow best practices in computer science [195], FAST has since been used for different studies on conventional configurations [196], hybrid electric airplanes with distributed propulsion [168] [197] and disruptive configurations [198] (a detailed description of the code is given in [195]). The specification, development coordination and testing of FAST is inherently part of this PhD work.

3.3.2. The Multidisciplinary Design Analysis implemented in FAST

At ISAE-SUPAERO, students following the Aircraft Design classes dedicated to civil transport airplanes apply the approach proposed by Dupont and Colongo [151]. Considering the competence

levels of disciplinary analyses proposed by Ciampa and Nagel [67], the method features empirical laws for physics representation and design rules for Phenomena Type. Thus, it can be classified as Level 0. To maintain consistency between teaching material and FAST, it has been decided to integrate within the sizing MDA the same analyses and design logic, except when specifications listed previously required enhancements. At analysis level, the most notable modification with respect to [151] is the time step integration to simulate the reference missions. For disciplines, efforts have been made to improve aerodynamics estimations of the Oswald factor by implementing the formulas proposed by Scholz [199]. Regarding the Horizontal Tail Plane and Vertical Tail Plane geometries, rules proposed by Raymer [5] and Kroo [200] have been employed to give FAST better sizing capabilities with respect to empennage volume coefficient. More details about the input and output of the various analysis modules within the FAST MDA can be found in Appendix B. With the intention to introduce aircraft sizing logic to students, a first step has been to implement design rationales. The case of the wing sizing for a small medium range transport aircraft is detailed here as an example. For this type of aircraft, it is known that the main wing is sized according to two criteria: the approach speed (for a given maximum lift coefficient in a landing configuration) and the available fuel volume. In FAST, this same logic is coded within the MDA to reproduce the decision process. Of course, such loop can be challenged when a different type of aircraft is considered or if the configuration presents a discontinuity with the "tube and wing" layout. For this scenario, it is possible to introduce a constraint analysis in the logic. This is why, in a second step, it is planned to disconnect these design rules and to have the optimizer converging to the best solution taking a list of constraints into account. When comparing the FAST MDA and the one used in the GABRIEL project, a few differences can be noted:

- The analysis module "First estimate" uses a Thrust Specific Fuel Consumption estimation instead of the value provided by the module 0 "Propulsion";
- The analysis module "Geometry" does not take the span of the aircraft as a design variable. It is now through the Aspect Ratio value that the wing geometry is defined;
- The analysis module "Geometry" requires as input the taper ratio and thickness-to-chord of the Horizontal Tail Plane and Vertical Tail Plane. Volume coefficients are no more required;
- The analysis module "Geometry" requires the approach speed as additional input. As this parameter can have important effects on the resulting aircraft geometry (see Figure 39), it is preferred to use it as design driver. At the end of each MDA loop, design engineers are thus sure that this limitation is met;
- The engine geometry is directly calculated by the analysis module "Geometry" while for the GABRIEL MDA, it is determined by the Propulsion module.
- Following the guidelines provided in [151], the analysis module "Geometry" automatically increases the thickness-to-chord ratio of the main wing when sweep angle is increased. Pure effects associated to this sweep angle and the wing thickness-to-chord ratio cannot be captured;
- In FAST, module "Structure and Weight" is a Level 0 physics representation that does not consider aerodynamics and structure interaction (the wing sizing is associated to the maximum load factor and mass). Thus, contrary to the GABRIEL MDA, no input is needed from the module "Aerodynamics" to compute the wing mass.

- The engine weight is directly calculated by the analysis module "Structure and Weight", while for the GABRIEL MDA, it is computed in the Propulsion module.

In this research, the original FAST MDA has been extended through the addition of a Certification and Operational Constraints module that is directly linked to the capabilities of the CCM (step 9 in Figure 57). This analysis module interfaces with the digital version of the regulatory text that is an .XML file to gather all requested parameters to verify the exit criteria. To illustrate the capabilities of the CCM, performance constraints of CS 25 SUBPART B - FLIGHT [129] have been considered. In addition, requirements given in CAT.POL.A.410 (a) "En-route - all engines operating" are taken into account [201]. This regulatory text states that "the aeroplane shall be capable of a rate of climb of at least 300 ft per minute with all engines operating". Thus, this required Rate of Climb (RoC) threshold is taken as reference instead of the 500 ft/min used for the GABRIEL concept study of chapter 2. Table 7 details all constraints related to regulatory texts that have been implemented in the CCM and automatically taken into account in the FAST MDA.

Table 7: Constraints extracted from regulatory texts [129] [201] and implemented in FAST through the Certification Constraints Module

Section	Altitude [ft]	Speed	Weight	High lift configuration	Landing gear	OEI	Exit criteria
CS-25.119 (a)	1000	1.3 x V_{SO}	Max. Landing Weight	Landing	Yes	No	Climb grad. ≥ 3.2%
CS-25.121 (a)	35	V_{LOF}	Weight at the start of initial climb	Takeoff	Yes	Yes	Climb grad. ≥ 0%
CS-25.121 (b)	400	V_2	Weight at Landing gear retractation	Takeoff	No	Yes	Climb grad. ≥ 2.4%
CS-25.121 (c)	1500	V_{FTO}	Weight at the end of the takeoff path	Cruise	No	Yes	Climb grad. ≥ 1.2%
CS-25.121 (d)	2000	1.4 x $V_{SRapproach}$	Weight at the end of descent	Approach	No	Yes	Climb grad. ≥ 2.1%
CAT.POL.A.410 (a)	TOC	Cruise Mach	Weight at TOC	Cruise	No	No	RoC ≥ 300 ft/min
CAT.POL.A.410 (a)	TOP	Cruise Mach	Weight at TOD	Cruise	No	No	RoC ≥ 300 ft/min

The transcription of these different constraints via the CCM Graphical User Interface has to follow the logic represented in Figure 51. Thus, designers have at first to identify a series of quantities that will be considered in the analysis. Subsequently, parameters of the aircraft state vector to be used during computations are defined. For the certification constraints considered in Table 7, the corresponding set of state vector parameters is shown in Figure 54. In the GUI, these six parameters are associated to a quantity (to manage units) and a category (to facilitate selections of reference values). Furthermore, it is possible to associate to each state vector parameter its corresponding name in another analysis tool to facilitate variables coupling in the MDA. In the present research, the simulator JSBSim is used to carry out flight simulations. Thus, the last column of the GUI screenshot shown in Figure 54 lists the equivalent name of the parameter of interest under the label "Alias JSBSim". An application of this feature is detailed in chapter 4.

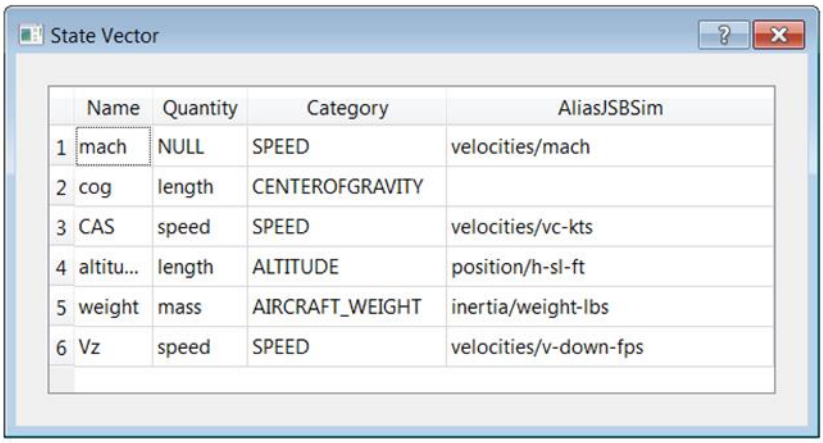

Figure 54: State vector parameters entered in the GUI to be considered in the FAST MDA

Once the required state vector parameters are stored, CCM users have to enter all reference values related to the six certification constraints of Table 7 and their attributes through the dedicated interface illustrated in Figure 55. At this stage of the certification constraint definition, some reference values are known while other must still be calculated by the MDA. Users can trace this difference through the interface by simply checking the tick box "Value" that opens a new dedicated field where the unit can be selected.

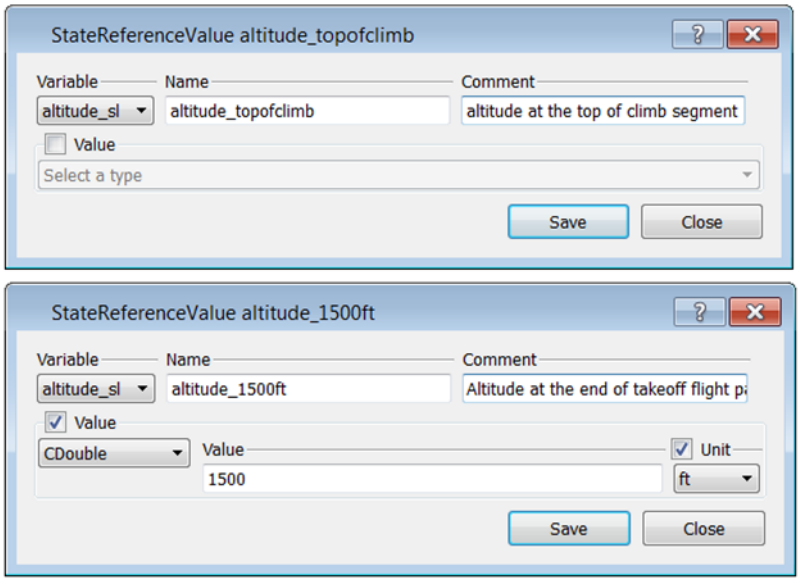

Figure 55: CCM interface to specify the reference values attributes

For the six constraints (seven cases) listed in Table 7, a total of twenty-one reference values have been defined and stored in the CCM (see Figure 56). In this figure, "NONAME" indicates that a value has been provided by the user. When the value column indicates "NULL", it means that the value is computed by the Multidisciplinary Design Analysis and Optimization and subsequently stored in the .XML.

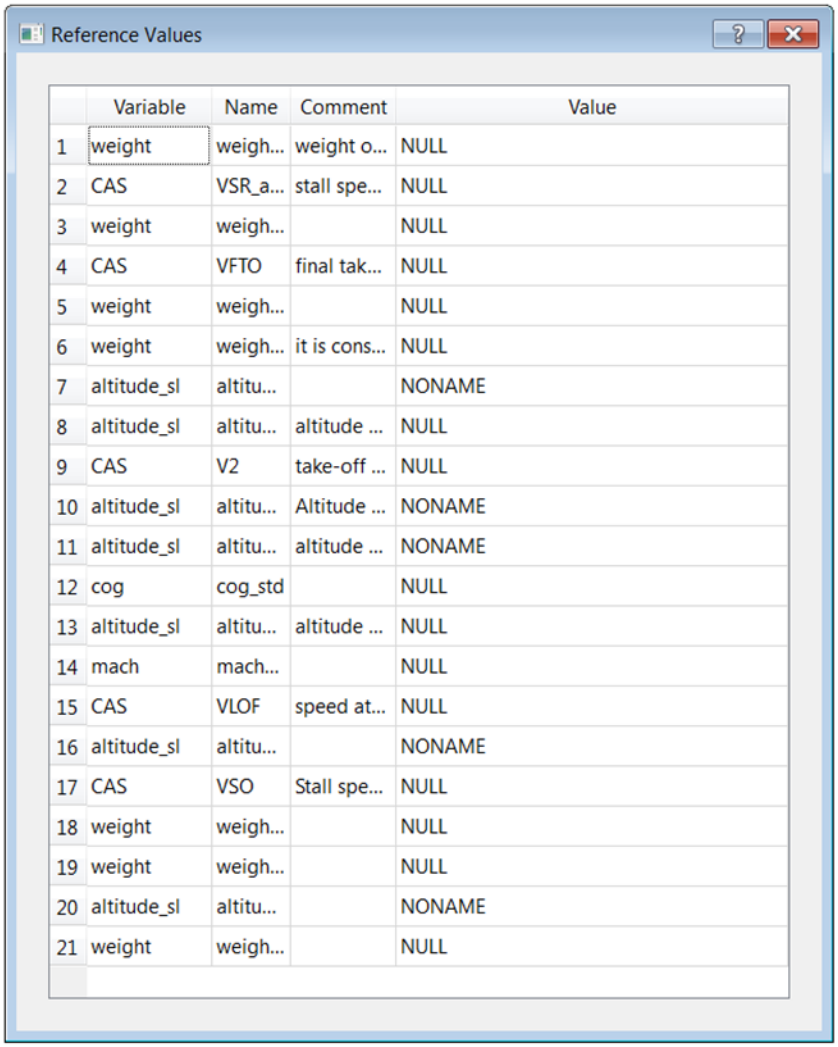

	Variable	Name	Comment	Value
1	weight	weigh...	weight o...	NULL
2	CAS	VSR_a...	stall spe...	NULL
3	weight	weigh...		NULL
4	CAS	VFTO	final tak...	NULL
5	weight	weigh...		NULL
6	weight	weigh...	it is cons...	NULL
7	altitude_sl	altitu...		NONAME
8	altitude_sl	altitu...	altitude ...	NULL
9	CAS	V2	take-off ...	NULL
10	altitude_sl	altitu...	Altitude ...	NONAME
11	altitude_sl	altitu...	altitude ...	NONAME
12	cog	cog_std		NULL
13	altitude_sl	altitu...	altitude ...	NULL
14	mach	mach...		NULL
15	CAS	VLOF	speed at...	NULL
16	altitude_sl	altitu...		NONAME
17	CAS	VSO	Stall spe...	NULL
18	weight	weigh...		NULL
19	weight	weigh...		NULL
20	altitude_sl	altitu...		NONAME
21	weight	weigh...		NULL

Figure 56: Reference values entered in the GUI to be considered in the FAST MDA

The associated XDSM is shown in Figure 57 and the sequence of operations for the FAST MDA is as follows (changes with respect to the GABRIEL MDA are highlighted in red).

Input:	Engine specifications (based on constraint analysis), initial sketch (based on constraint analysis), *empennage data (taper ratio and thickness-to-chord ratio),* required static margin, *approach speed*, sizing and operational mission specifications
Output:	Engine deck, aircraft geometry *(including wing span)*, aerodynamic characteristics, weight breakdown, sizing and operational mission performances *(including takeoff field length), Certification constraints 119a, 121a, 121b, 121c, RoC at Top of Climb (TOC), RoC at Top of Descent (ToD)*

0. Propulsion. The propulsion module takes as input the engine specifications and *computes its performances in the flight domain for Mach and altitude (Thrust, TSFC)*.

1. First estimate. With an initial sketch of the vehicle *and assumptions on the engine performances and mission segments*, a first iterative loop is computed to derive an initial guess for MTOW, MLW, MZFW and the wing area (Breguet approach).

repeat

2. The Multidisciplinary Design Analysis is started;

3. Geometry. In this module, given a certain number of inputs (number of passengers, *empennage data*, required static margin *and approach speed*), aircraft parameters (fuel weight, maximum landing weight, maximum lift coefficient) *and engine thrust*, the complete geometry of the aircraft is computed and the main subsystems are positioned. The wing is sized according to the most critical constraint between approach speed and available fuel quantity. In the generic case, data are stored in the vector identified as *A/C* but a dedicated CAD model can be used instead [19]. *The wing span that can be a constraint is calculated in this module.*

4. Aerodynamics. Taking into account the aircraft geometry defined during the previous step, the Aerodynamics module computes the drag polar and other aerodynamics coefficients with respect to the angle of attack, the angle of sideslip and the flight condition.

5. Structure and Weight. *Using the aircraft geometry as input, the MTOW value defined at the beginning of the step 2 and the engine thrust* calculated by the propulsion module 0, the module "Structure and Weight" sizes the wing and the fuselage and then computes the masses of the different aircraft components.

6. Performance. Based on a point mass analysis, the performance module computes the aircraft fuel consumption for the sizing mission based on the engine performances calculated in step 0, the MTOW value defined at the beginning of the step 2 and the aerodynamics properties of the aircraft calculated in step 4. In this module, the segment simulations based on sizing mission specifications use time step integration to better represent real trajectories. *The takeoff field length, which can be used as a constraint, is calculated in this module.*

7. Update MTOW. The objective of this function is to calculate the difference between the Operating Weight Empty taking as input the estimated fuel consumption calculated at step 6 $\left(OWE_m = MTOW - FW - W_{payload}\right)$ and the value of OWE resulting from the weight breakdown (step 5). If the difference between these 2 values is higher than a given tolerance, MTOW is updated.

8. Iteration loop. All values calculated by the different modules are returned to the MDA so that a comparison with the target values is made (superscript t in Figure 33).

until 8-2 MDA has converged.

9. *Certification and Operational Constraints. Certifications and Operational constraints defined in the CCM are assessed with the aircraft that has been sized through the Multidisciplinary Design Analysis. Thrust is provided by the Propulsion module while masses, aircraft geometric parameters and aerodynamic characteristics, are provided during the last loop of the disciplinary module.*

10. Performance Operational Mission. The aircraft that has been sized through the Multidisciplinary Design Analysis flies an operational mission to estimate the fuel consumption on a standard route. Thrust and SFC database are provided by the Propulsion module while masses, aircraft geometric parameters and aerodynamic characteristics, are provided during the last loop of the disciplinary module.

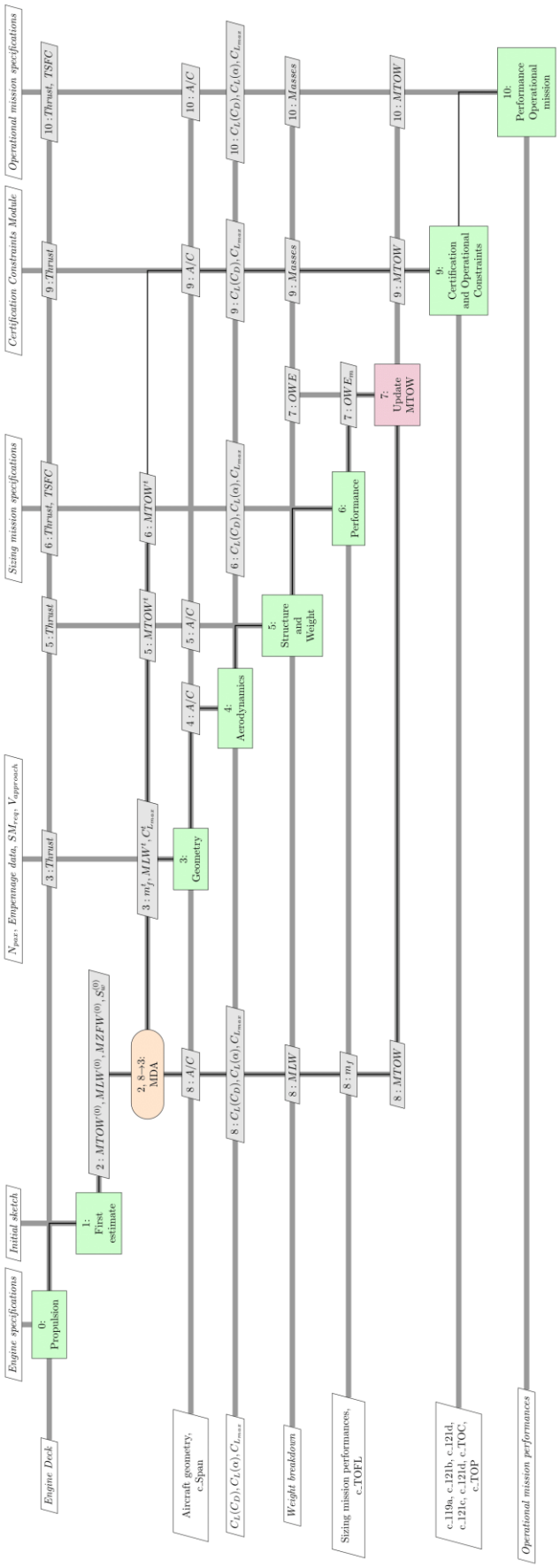

Figure 57: Multidisciplinary Design Analysis of FAST (XDSM)

3.3.3. Comparison with a reference aircraft

In this section, the results generated by FAST for a reference aircraft are compared with data available in the public domain. For Small Medium Range aircraft, the selected reference aircraft is an Airbus A320 for which a valuable database is the one proposed by the University of Aachen under the CeRAS initiative [157]. To have a valid comparison, assumptions made for the CeRAS aircraft are reported in the FAST .XML input file. In some cases, values have been replaced if more reliable data was available. In Figure 58, the values for the FAST variables defining the A320 model are reported. With respect to the GABRIEL study presented in chapter 2, it must be noted that the taper ratio taken into account by FAST is the ratio between the root chord (C_{root} in Figure 58) and tip chord (C_{tip} in Figure 58). For the Horizontal Tail Plane (HTP) and the Vertical Tail Plane (VTP), sweep angles are also necessary to define the geometry but FAST implemented basic design rules described in [151]. Theses sweep angles are then directly defined as a function of the main wing sweep angle value. For this reason, they are not reported in Figure 58.

Top Level Aircraft Requirements		
Number of passengers		150
Passenger weight	[lbs]	200
Design Range	[NM]	2750
Operational Range	[NM]	800
Cruise Mach number		0.78
Approach speed	[kts]	132
Geometry		
Aspect ratio		9.48
Taper ratio		0.38
Wing break	[%]	0.4
Sweep angle at 25%	[deg]	25
HTP Taper ratio		0.3
HTP Thickness-to-chord ratio		0.1
VTP Taper ratio		0.3
VTP Thickness-to-chord ratio		0.1
Propulsion		
Maximum thrust at sea level	[N]	117880

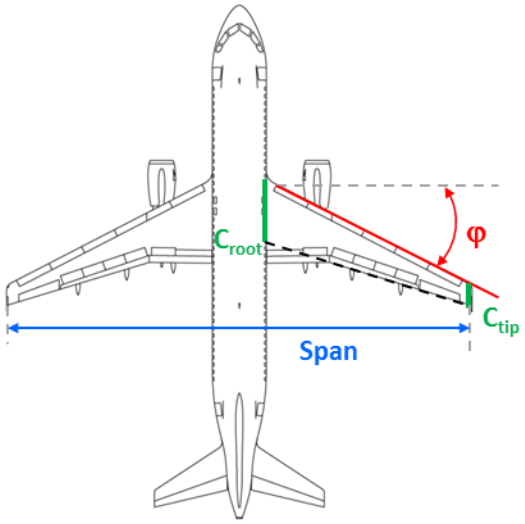

Figure 58: FAST variables defining the A320 model and the corresponding geometry

Regarding the mission to be considered during the sizing process, the key parameters for each segment are reported in Table 8.

Table 8: Mission parameters in FAST for the A320 model

Phase	Key parameters		
Taxi out	Duration	9	[min]
Takeoff	Friction coefficient	0.03	
	Throttle setting	100	[%]
	Flap angle	10	[deg]
	Slat angle	18	[deg]
Initial climb to 400 ft	Gear	Up	
Acceleration to 250 kts CAS	Level flight	400	[ft]
Climb to 1500 ft	Thrust setting	0.93	[%]
	Constant CAS	250	[kts]
	Flap angle	0	[deg]
	Slat angle	0	[deg]
Climb to 10000 ft	Constant CAS	250	[kts]
Acceleration to 300 kts CAS	Level flight	10000	[ft]
Climb up to M=0.78	Constant CAS	300	[kts]
Climb to cruise altitude	Constant Mach	0.78	
Cruise	Cruise climb at best Lift-to-Drag ratio		
Descent to 300 kts CAS	Throttle setting	Idle	
	Constant Mach	0.78	
Descent to 10000 ft	Constant CAS	300	[kts]
Decceleration to 250 kts	Level flight	10000	[ft]
Descent to 2000 ft	Constant CAS	250	[kts]
Landing	Friction coefficient with brakes on	0.3	
	Flap angle	30	[deg]
	Slat angle	20	[deg]
	Gear	Down	
Taxi in	Duration	5	[min]

When sizing an aircraft, fuel reserves are an important element that can lead to non-negligible differences, especially for small-medium range missions. The hypotheses taken for the A320 model with FAST are [151]:

- For alternate climb: the aircraft climbs from 2000 ft to 22000 ft following the same regular climb procedure detailed in Table 8 with a constraint on altitude;
- Alternate cruise: the aircraft flies at a constant altitude at the Mach number that is obtained at the end of the alternate climb;
- Alternate descent: the aircraft descends from 22000 ft to 2000 ft following the same regular descent procedure detailed in Table 8;
- Holding: the holding pattern is fixed at an altitude of 1500 ft at a fixed CAS of 230 kts for a duration of 45 minutes;
- A contingency fuel quantity equivalent to 3% of trip fuel is added.

With the TLARs fixed, the geometry parameters selected and the mission segments defined, the complete FAST MDA is carried out. Within 1 minutes, FAST computes the full process and generates the following outcomes:

- Updated .XML file in which all results are stored;
- Two .txt files in which the aircraft performances for the sizing and operational missions are written;
- Various plots to illustrate the aircraft characteristics over the mission (see Appendix C);

- The payload range diagram for the sized aircraft;
- A 3D model of this same airplane in the OpenVSP format [19].

The result is a sized aircraft whose geometry is shown in Figure 59 (with respect to the Airbus A320 [202]) and which weight breakdown is reported (comparison with CeRAS data [157]).

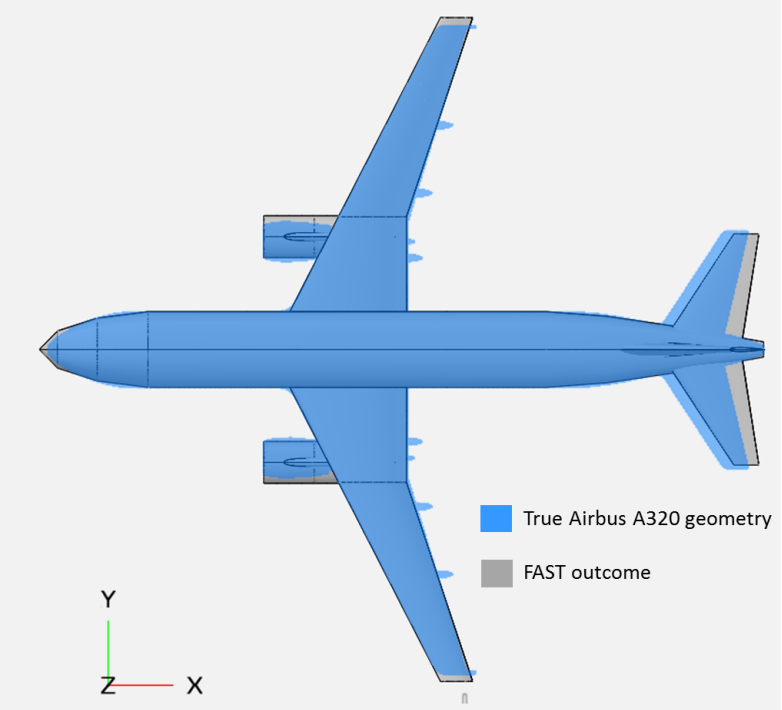

Figure 59: Geometry of the Airbus A320 and the geometry resulting from FAST

Table 9: Weight breakdown of the reference aircraft obtained with FAST

		FAST	CeRAS	[%]
OWE	[kg]	**42242**	**42092**	**-0.4**
Airframe	[kg]	23106	22018	4.9
Propulsion	[kg]	7732	7751	-0.2
Systems	[kg]	7822	8847	-11.6
Furnishing	[kg]	3112	3006	3.5
Crew	[kg]	470	470	0.0
Mission fuel	[kg]	**18248**	**18678**	**-2.3**
Taxi-out	[kg]	268	276	-2.9
Trip fuel	[kg]	14879	14992	-0.8
Taxi-in	[kg]	149	153	-2.6
Reserve fuel	[kg]	2952	3257	-9.4
Design Payload	[kg]	**13608**	**13608**	**0.0**
MTOW	[kg]	**74098**	**74378**	**-0.4**

The most notable difference on the geometries illustrated in Figure 59 concerns the position of the Horizonal Tail Plane. With respect to the real Airbus A320 geometry, the FAST sizing process shifts the stabilizer less than a meter further back on the fuselage. This difference is due to the positioning of the Horizontal Tail Plane that is fixed in the Geometry module. For the main wing area, FAST estimation is close to the real aircraft as the calculated value (124.4 m²) is about 1.6% higher than the one of the Airbus A320 (122.4 m² [203]).

Regarding the Operating Weight Empty (OWE) breakdown, discrepancies between FAST estimations and CeRAS can be observed for airframe weight, systems weight and furnishing. A difficulty to better trace the origins of these differences is that the element descriptions used in both cases are not accurate enough and components may end up in a category or another. However, as the variations compensate one another, the overall difference is small. For mission fuel, the main difference comes from the reserve fuel calculation. With the purpose of better understanding the causes, CeRAS indicates that the margins on kerosene are calculated after OPS 1.255 [204]. However, this regulatory text only provides guidelines with no quantitative information. It is then preferred not to modify the assumptions presented earlier as they are consistent with most of the sizing process considered in FAST [151]. Looking deeper into the fuel consumption, one can notice that the CeRAS aircraft is consuming more fuel that the one modeled in FAST for climb, whereas in cruise, this trend is inverted. The key reason for this difference in the most important segment is that the aerodynamics model results in different Lift-to-Drag ratios: in the case of FAST, the A320 cruise efficiency is about 16.6 while the CeRAS aircraft's one is about 17.43. As for OWE, these dissimilarities in fuel consumption cancel each other leading to a global MTOW that is very similar for both aircraft.

As comparisons in geometry and performance at the design point are positive, it is then interesting to verify the aircraft capabilities with different payload configurations. To this end, the payload / range diagram calculated by FAST for the reference aircraft is compared to both Airbus [205] and CeRAS data [157].

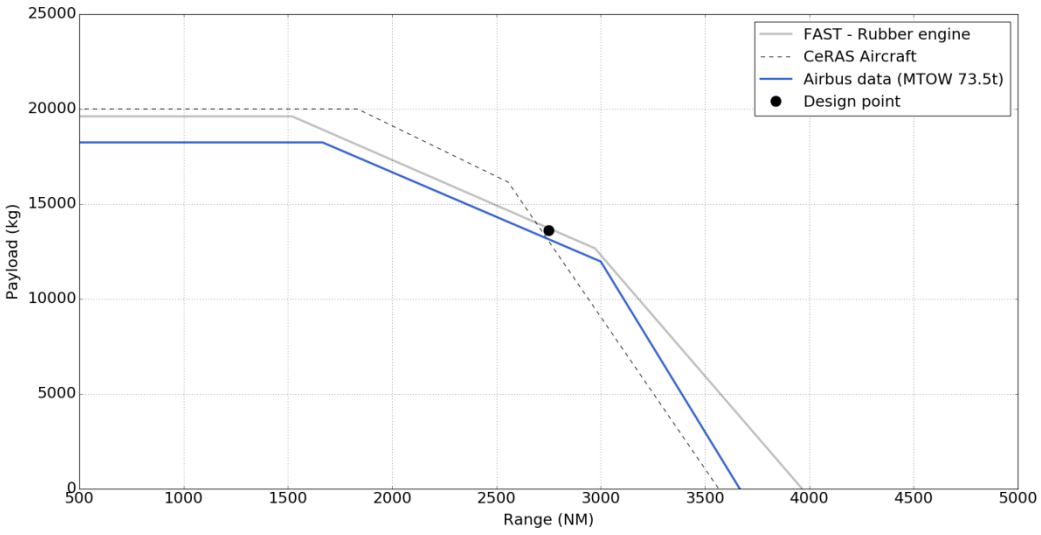

Figure 60: Payload / Range diagram comparison

All diagrams are illustrated in Figure 60 to better visualize differences. First, the differences on the top left size of the figure are directly due to different assumptions regarding the maximum payload weight. In the case of FAST, this value is calculated considering an additional 40 kg of luggage for all 150 passengers, for a total of 19608 kg [151]. For the first break point, Airbus data are considering almost the same MTOW as FAST but with lower mass corresponding to payload. Naturally, there is more fuel to go further (about 1700 NM vs 1500 NM). About the last segment that is associated to Maximum Fuel Weight, FAST offers more range as there is more volume available within the wing (the wing area is a 1.6% larger).

As expected, there are variations among the outcomes of FAST, the CeRAS reference aircraft and public domain data on the real Airbus A320. Most causes can be explained and, in case of remaining uncertainties, they could be reduced only through a large effort that is not in the scope of the present work. More importantly, these verifications made on the FAST outcomes showed that the sizing process is capable to converge not only to a very comparable geometry but also to very similar performances and weight breakdown. It is then considered as an efficient and reliable aircraft design process, capturing the right sizing trends on which optimization can be applied.

3.3.4. Sensitivity analysis

The optimization to be carried out with the FAST MDAO process is very similar to the one that has been completed for the GABRIEL project. The goal is to define a series of best aircraft given an objective function, a set of constraints and a list of design variables. Thus, a sensitivity analysis is carried out to better assess the system responses in terms of objective function and constraints for a given design space set by the design variable range. Table 10 details the setup of the sensitivity analysis, considering that design variable values corresponding to the reference aircraft have been used as central point for the range definition.

For the constraints listed in Table 10, their values are calculated so that they are considered valid for negative values. Thus, outputs of the analysis module c_i (i varying from 1 to 9) are combined with the threshold values available in the regulatory texts. Such standard format has been used so that the outputs of the FAST MDA could be directly used by optimization algorithms. When assessing the outcomes of the sensitivity analysis, such format allows to quickly identify constraints that may be always satisfied.

Table 10: Setup of the sensitivity analysis to be applied on the FAST MDA

	Variable	Description	Range / Inequality
Design variables			
	AR	Aspect Ratio	[8 : 12]
	λ	Taper ratio	[0.2 : 0.6]
	$\Lambda_{25\%}$	Sweep angle at 25%	[20 : 30] °
	T_{SL}	Maximum Thrust at sea level	[85000 – 135000] N
FAST performance outputs			
	MTOW	Maximum TakeOff Weight	
	OWE	Operating Weight Empty	
	M_{fuel} S	Mission fuel weight for the sizing mission	
	M_{fuel} Op	Mission fuel weight for the operational mission	
	$(L/D)_{max}$	Maximum Lift-to-Drag ratio	
FAST constraints outputs			
	c_TOFL	Takeoff field length [157]	$c_1 - 2200 \leq 0$
	c_Span	Span [206]	$c_2 - 36 \leq 0$
	c_119a	Climb gradient [129]	$0.032 - c_3 \leq 0$
	c_121a	Climb gradient [129]	$- c_4 \leq 0$
	c_121b	Climb gradient [129]	$0.024 - c_5 \leq 0$
	c_121c	Climb gradient [129]	$0.012 - c_6 \leq 0$
	c_121d	Climb gradient [129]	$0.021 - c_7 \leq 0$
	c_TOC	Rate of Climb [201]	$300 - c_8 \leq 0$
	c_TOD	Rate of Climb [201]	$300 - c_9 \leq 0$

The exploration of the design space is carried out for 200 runs of FAST with the design variable inputs sampled by a Latin Hypercube Sampling [104]. The results of these computations are reported in Figure 61 and Figure 62. Figure 61 focuses on the evolution of MTOW, OWE, M_{fuel} S, M_{fuel} Op, $(L/D)_{max}$, c_TOFL and c_Span with respect to the design variables AR, λ, $\Lambda_{25\%}$ and T_{SL}. Figure 62 is dedicated on the observation of certification constraint values (c_119a, c_121a, c_121b, c_121c, c_121d, c_TOC and c_TOD) with respect to the design variables AR, λ, $\Lambda_{25\%}$ and T_{SL}.

From these plots, a first qualitative analysis of FAST outcomes with respect to the design variables can be performed:

- The value of MTOW is fully driven by the thrust level of the engine;
- The value of OWE is primarily affected by the engine thrust level and then by the aspect ratio;
- The necessary fuel weight for the sizing mission is primarily affected by the aspect ratio and then by the engine thrust level;
- Regarding the fuel weight required for the operational mission, drivers are inverted: the outcome is indeed primarily affected by the engine thrust level and then by the aspect ratio;

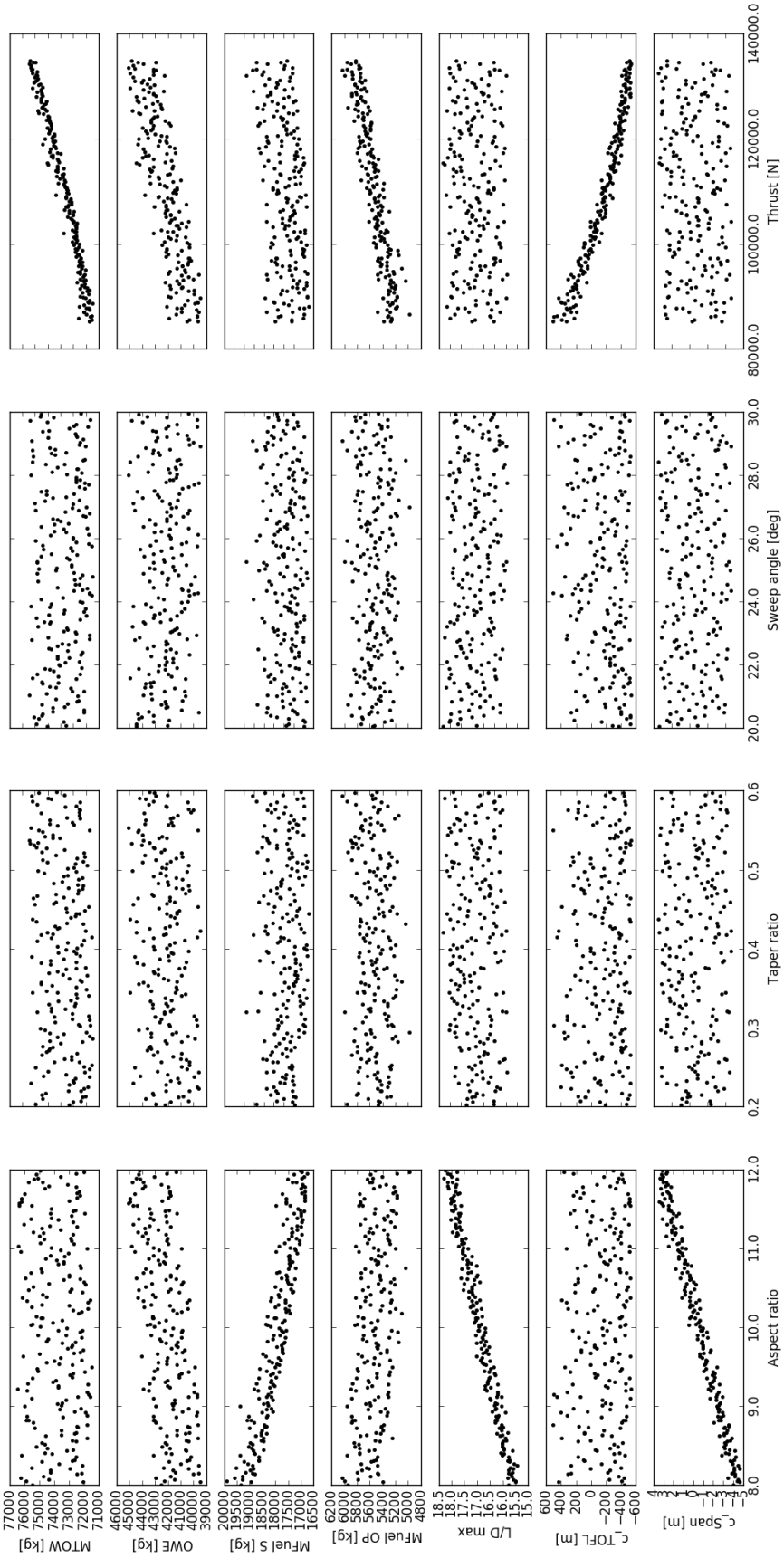

Figure 61: Results of the sensitivity analysis - Part I

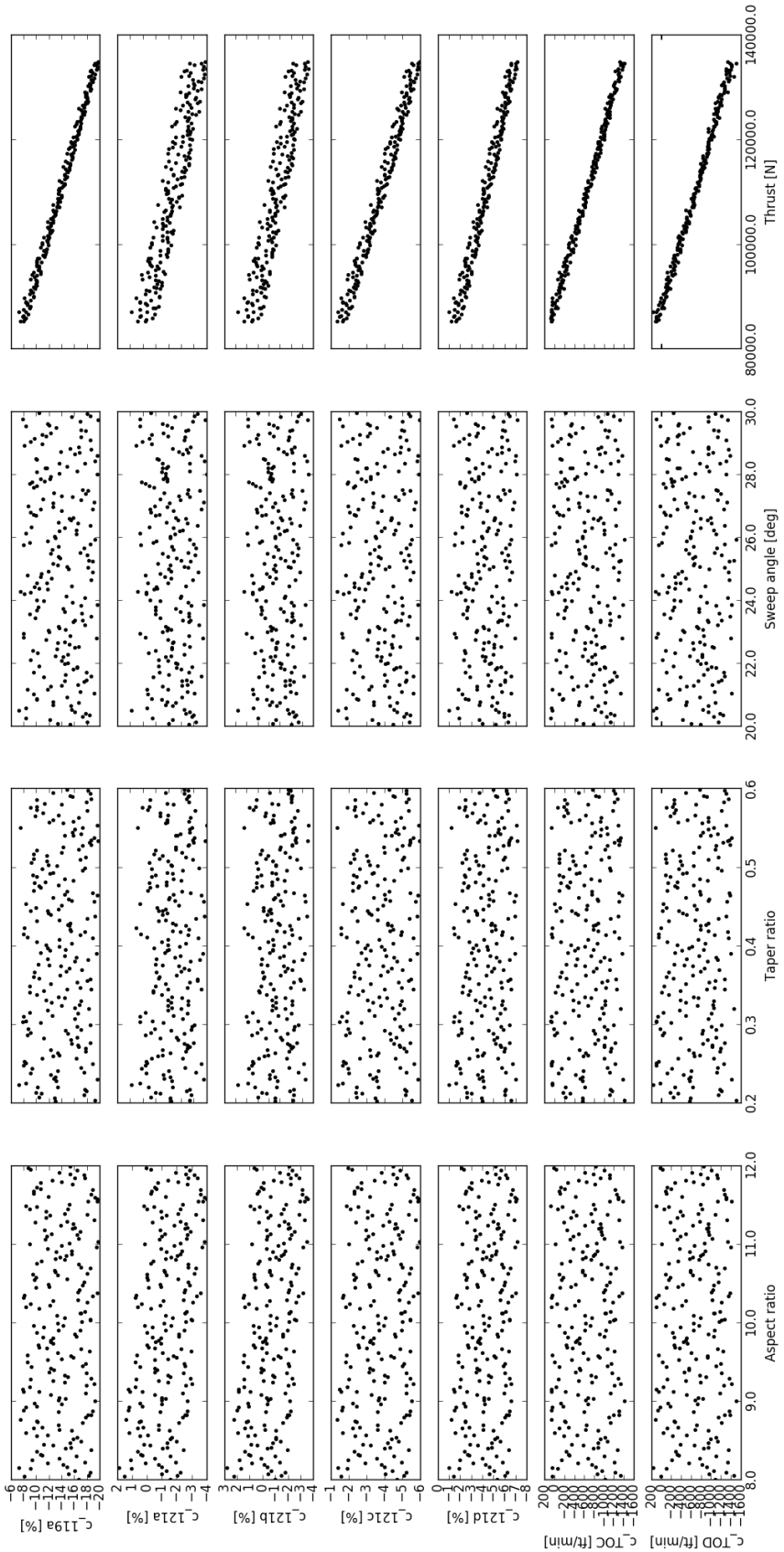

Figure 62: Results of the sensitivity analysis - Part II

- Lift-to-Drag ratio is as expected fully driven by aspect ratio;
- The constraint on Takeoff Field Length (*c_TOFL*) is fully driven by the engine thrust level;
- The constraint on wing span (*c_Span*) is fully driven by the aspect ratio;
- The constraint *c_119a* associated to section CS 25.119(a) [129] is fully driven by the engine thrust level;
- The constraint *c_121a* associated to section CS 25.121(a) [129] is primarily driven by the engine thrust level and the aspect ratio has a slight effect;
- The constraint *c_121b* associated to section CS 25.121(b) [129] is primarily driven by the engine thrust level and the aspect ratio has a slight effect;
- The constraint *c_121c* associated to section CS 25.121(c) [129] is primarily driven by the engine thrust level;
- The constraint *c_121d* associated to section CS 25.121(d) [129] is primarily driven by the engine thrust level and the aspect ratio has a slight effect;
- The constraint *c_TOC* associated to section CAT.POL.A. 410 (a) [201] is fully driven by the engine thrust level (verification at the Top of Climb);
- The constraint *c_TOD* associated to section CAT.POL.A. 410 (a) [201] is fully driven by the engine thrust level (verification at the Top of Descent);
- Taper ratio and sweep angle have secondary effects.

All these key effects follow basic flight physics principles and they highlight the importance of finding the best airframe / propulsion coupling at conceptual stage. One element that must be recalled in this section is that the geometry module of FAST automatically increases the thickness-to-chord ratio of the wing when increasing the sweep angle. Thus, these combined effects diminish the pure effect of wing sweep on performance that could be observed in such sensitivity analysis applied on other sizing codes.

To move from this qualitative analysis to a quantitative one, the computation of Sobol indices [207] for FAST outputs about both performances and outputs is carried out. In such manner, it is possible to identify the portion of variance of a FAST outcome that is caused by each design variables. Following the approach proposed in [208][209][209], the variance based sensitivity analysis is achieved through a sparse polynomial chaos expansion of degree 3. From the 200 points database, 150 points have been used as training sample while 50 were used as validation sample. The resulting first order Sobol indices are reported in Table 11. In this table, the sum of all indices for each outcome of the MDA is reported in the last column. As the value is always very close to 1, it can be said that almost no variance is due to interactions between different design variables. It is then unnecessary to compute the total and cross sensitivity index. Taking for example the Operating Weight Empty (OWE), it can be explained that 32% of its variance is due to Aspect Ratio while 64.8% of its variance is due to engine thrust level. In Table 11, highest indices have been highlighted in red to better visualize the strongest correlations.

Table 11: First order Sobol indices of FAST MDA (strongest correlations are written in red)

	Aspect Ratio (AR)	Taper Ratio (λ)	Sweep angle ($\Lambda_{25\%}$)	Thrust (T_{SL})	Total
MTOW	0.0168	0.0145	0.0193	**0.946**	0.997
OWE	**0.3197**	0.0162	0.015	**0.648**	0.999
M_{fuel} S	**0.8595**	0.0004	0.001	**0.1366**	0.998
M_{fuel} Op	0.0921	0.011	0.0	**0.8533**	0.956
$(L/D)_{max}$	**0.9805**	0.0058	0.005	0.0057	0.997
c_TOFL	0.0133	0.0002	0.007	**0.9734**	0.994
c_Span	**0.9659**	0.0013	0.015	0.0156	0.998
c_119a	0.011	9.49e-05	0.0003	**0.9883**	1.000
c_121a	**0.1638**	0.0001	0.0001	**0.8357**	1.000
c_121b	**0.1669**	0.0001	0.0025	**0.8299**	0.999
c_121c	0.0269	2.81e-05	7.05e-06	**0.9728**	1.000
c_121d	0.0349	1.44e-05	0.0009	**0.9635**	0.999
c_TOC	0.0014	0.0003	0.0039	**0.9909**	0.997
c_TOD	3.74e-06	0.0006	0.0048	**0.9934**	0.999

To better visualize the dominance of aspect ratio and engine thrust level on the outcomes of the FAST MDA, the different Sobol indices are reported in Figure 63 and Figure 64.

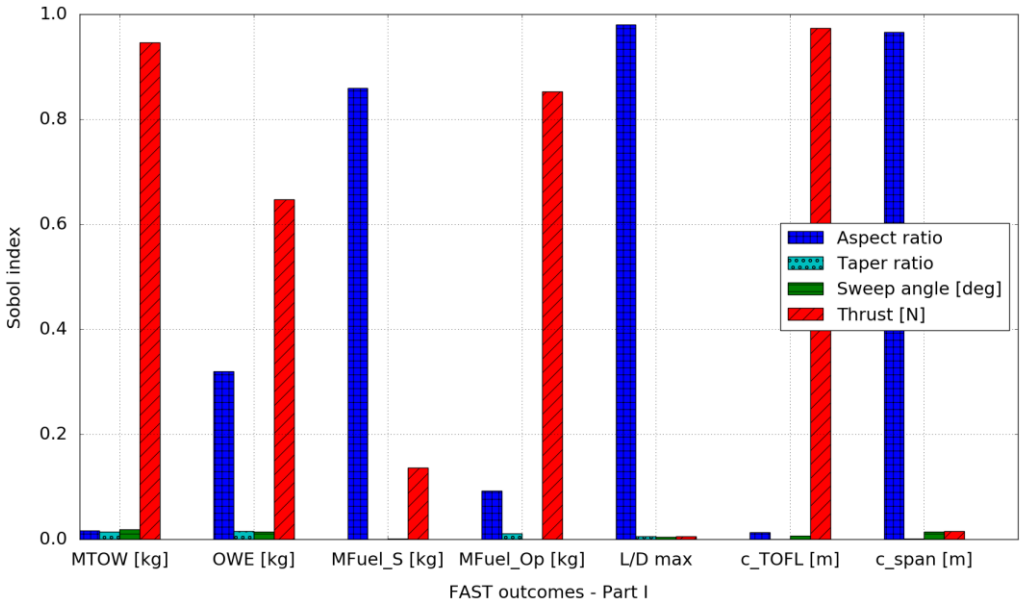

Figure 63: Sobol indices for FAST outcomes (Part I) with respect to design variables

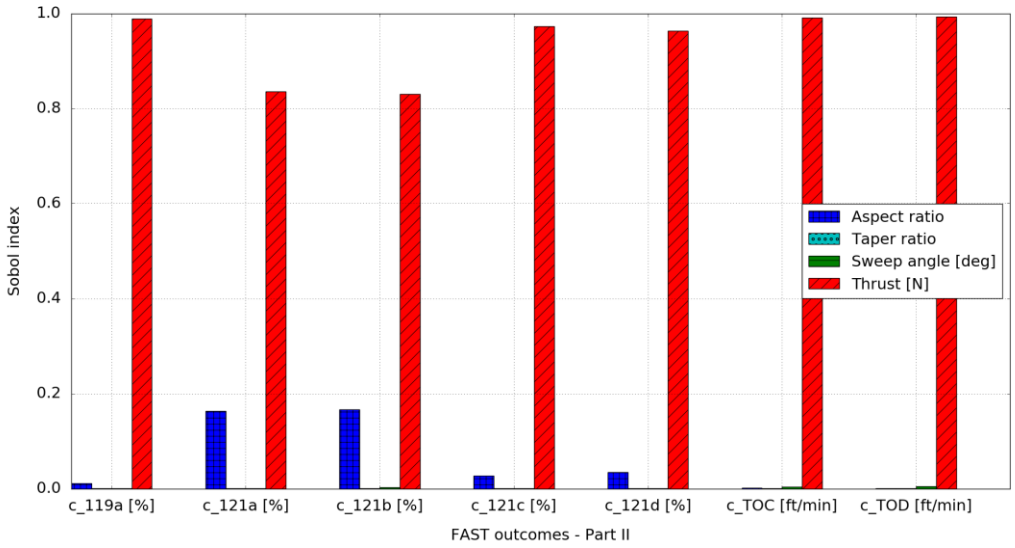

Figure 64: Sobol indices for FAST outcomes (Part II) with respect to design variables

For the subsequent optimization phase, this sensitivity analysis showed that the constraints *c_119a*, *c_121c* and *c_121d* seem always satisfied on the design space. Thus, they will not be considered by the optimizers but their values will be checked at the optimum. Regarding the design variables, the outcomes of FAST are clearly driven by two parameters: Aspect Ratio and Engine thrust level. Nevertheless, at the end of chapter 2, it has been recommended in the case of a multiobjective function to consider OWE. For this output, the sensitivity indices of taper ratio and sweep angle are the highest. Thus, it has been decided to keep all four design variables for the aircraft optimization step. The optimization problem to be described in the next section will consider four design variables and six inequality constraints.

3.4. Aircraft optimization

3.4.1. Problem definition

The results of the GABRIEL MDAO process showed the impact of certification constraints on the best family of aircraft that can be identify during conceptual design. To better manage constraints associated to regulatory texts, the Certification Constraints Module (CCM) has been developed and presented in Section 3.2. In parallel, with the objective of fostering the collaboration between ISAE-SUPAERO and ONERA in Aircraft Design, the aircraft sizing tool FAST has been established (see Section 3.3.). The capabilities of these two tools are then combined to perform aircraft optimizations and better investigate the effects of certification constraints at conceptual level. As the early phases of the design phase are characterized by compromises, the multiobjective approach from chapter 2 is repeated here with different variations. Overall, four optimization problems are carried out to have a complete view (see details in Table 12 for the first three optimizations):

- Optimization 1 - Minimization of MTOW and Sizing mission fuel weight;
- Optimization 2 - Minimization of OWE and Sizing mission fuel weight;
- Optimization 3 - Minimization of OWE and Operational mission fuel weight;
- Optimization 4 - Minimization of OWE and Operational mission fuel weight under more stringent certification constraints (see Table 16).

Table 12: Description of the 3 first MDAO problems

	Function / Variable	Description	Range / Value
minimize	MTOW	Maximum TakeOff Weight	
	or OWE	Operating Weight Empty	
and	Mfuel (sizing)	Mission fuel for the sizing mission	
	or Mfuel (oper.)	Mission fuel for the operational mission	
with respect to 4 design variables			
	AR	Aspect Ratio	[8 : 12]
	λ	Taper ratio	[0.2 : 0.6]
	$\Lambda_{25\%}$	Sweep angle at 25%	[20 : 30] °
	T_{SL}	Maximum Thrust at sea level	[85000 – 135000] N
subject to 6 inequality constraints			
	c_TOFL	Takeoff field length [157]	$c_1 - 2200 \leq 0$
	c_Span	Span **Erreur ! Source du renvoi introuvable.**	$c_2 - 36 \leq 0$
	c_121a	Climb gradient [129]	$- c_4 \leq 0$
	c_121b	Climb gradient [129]	$0.024 - c_5 \leq 0$
	c_TOC	Rate of Climb [201]	$300 - c_8 \leq 0$
	c_TOD	Rate of Climb [201]	$300 - c_9 \leq 0$

3.4.2. FAST Multidisciplinary Design Analysis and Optimization

Given the four optimization problems described in Table 12, an optimization architecture has been implemented on the FAST MDA presented in Figure 57. Based as the GABRIEL study on a MDF formulation, the resulting FAST MDAO is illustrated in Figure 65. According to the XDSM format, the boxes 12 and 13 are recognized as functions to better manage the outcomes and constraints produced by the MDA and to transfer the proper information to the optimizer.

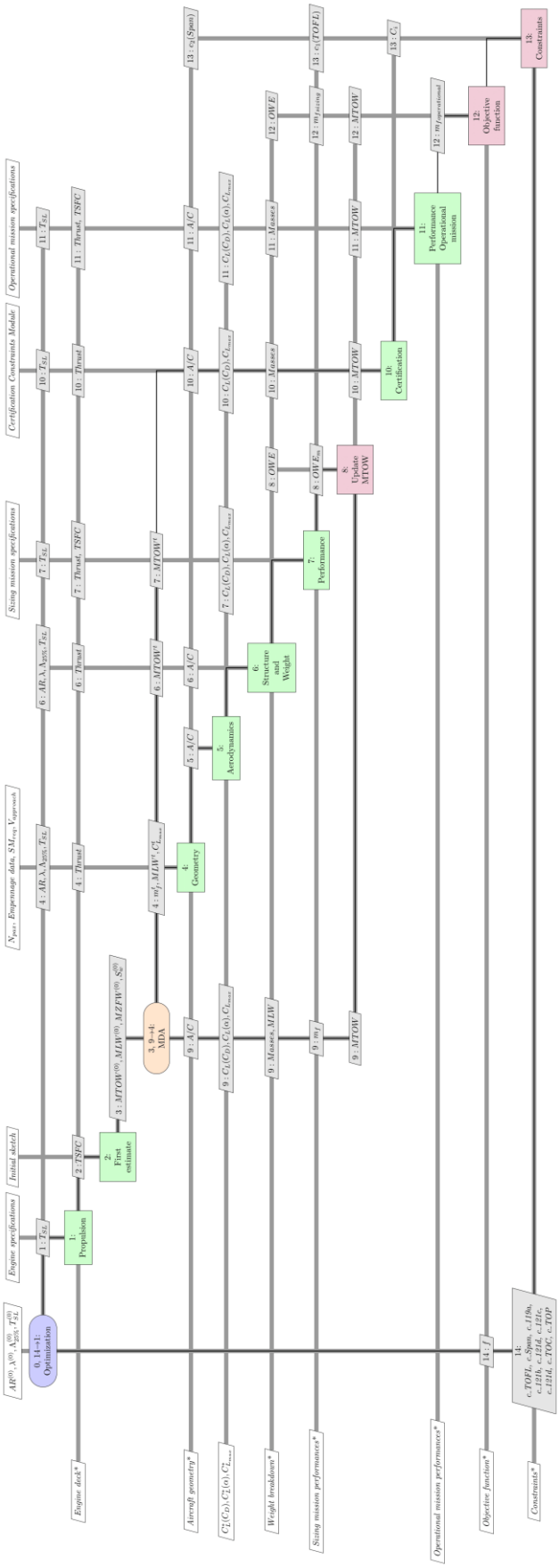

Figure 65: Multidisciplinary Design Analysis and Optimization of FAST (XDSM)

The sequence of operations for the FAST MDAO is detailed below (changes with respect to the FAST MDA are highlighted in red).

Input:	*Initial set of design variables (indicated by $^{(0)}$)*, engine specifications (based on constraint analysis), initial sketch (based on constraint analysis), empennage data (taper ratio and thickness-to-chord ratio), required static margin, approach speed, sizing and operational mission specifications.
Output:	*Optimal design variables, objective function, constraint values and aircraft data*. *The optimal values indicated by (*) concern:* Engine deck, aircraft geometry, aerodynamic characteristics, weight breakdown, sizing and operational mission performances *as well as Certification and operational constraints c_TOFL, c_Span, c_119a, c_121a, c_121b, c_121c, c_121d, c_TOC, c_TOD.*

0. *Initiation of the aircraft optimization*

repeat

1. Propulsion. The propulsion module takes as input the engine specifications and computes its performances in the flight domain for Mach and altitude (Thrust, TSFC).

2. First estimate. With an initial sketch of the vehicle and assumptions on the engine performances and mission segments, a first iterative loop is computed to derive an initial guess for MTOW, MLW, MZFW and the wing area (Breguet approach).

repeat

3. The Multidisciplinary Design Analysis is started;

4. Geometry. In this module, given a certain number of inputs (number of passengers, empennage data, required static margin and approach speed), aircraft parameters (fuel weight, maximum landing weight, maximum lift coefficient) and engine thrust, the complete geometry of the aircraft is computed and the main subsystems are positioned. The wing is sized according to the most critical constraint between approach speed and available fuel quantity. In the generic case, data are stored in the vector identified as A/C but a dedicated CAD model can be used instead [19]. The wing span that can be a constraint is calculated in this module.

5. Aerodynamics. Taking into account the aircraft geometry defined during the previous step, the Aerodynamics module computes the drag polar and other aerodynamics coefficients with respect to the angle of attack, the angle of sideslip and the flight condition.

6. Structure and Weight. Using as input the aircraft geometry, the MTOW value defined at the beginning of the step 2 and the engine thrust calculated by the propulsion module 0, the module "Structure and Weight" sizes the wing and the fuselage and then computes the masses of the different aircraft components.

7. Performance. Based on a point mass analysis, the performance module computes the aircraft fuel consumption for the sizing mission based on the engine performances calculated in step 0, the MTOW value defined at the beginning of the step 2 and the aerodynamics properties of the aircraft calculated in step 4. In this module, the segment simulations based on sizing mission specifications use time step integration to better represent real trajectories. The takeoff field length that can be used as a constraint is calculated in this module.

8. Update MTOW. The objective of this function is to calculate the difference between the Operating Weight Empty taking as input the estimated fuel consumption calculated at step 7 $\left(OWE_m = MTOW - FW - W_{payload}\right)$ and the value of OWE resulting from

the weight breakdown (step 6). If the difference between these 2 values is higher than a given tolerance, MTOW is updated.

9. Iteration loop. All values calculated by the different modules are returned to the MDA so that a comparison with the target values is made (superscript t in Figure 65).

until *9-4 MDA has converged.*

10. Certification and Operational Constraints. Certifications and Operational constraints defined in the CCM are assessed with the aircraft that has been sized through the Multidisciplinary Design Analysis. Thrust is provided by the Propulsion module while masses, aircraft geometric parameters and aerodynamic characteristics are provided during the last loop of the disciplinary module.

11. Performance Operational Mission. The aircraft that has been sized through the Multidisciplinary Design Analysis flies an operational mission to estimate the fuel consumption on a standard route. Thrust and SFC database are provided by the Propulsion module while masses, aircraft geometric parameters and aerodynamic characteristics are provided during the last loop of the disciplinary module.

12. *Objective function. The objective of this function module is simply to manipulate the disciplinary outcomes that are used to compute the objective functions of the problem. In this XDSM scheme, all outcomes of the analyses that can be used for the optimization are illustrated. Following the optimization scenario, the goal is to minimize both MTOW (or OWE) and* $m_{fsizing}$ *(or* $m_{foperational}$*).*

13. *Constraints function. This function gathers the different constraint values (*c_i*) that are computed by the FAST disciplinary modules. The Takeoff Field Length (TOFL) identified as* c_1 *is calculated by the Performance module. The Span, labelled as* c_2*, is determined by the Geometry module. The other relevant constraints* c_i *are computed by the Certification and Operational Constraints. Considering these constraints values and the thresholds from regulatory documents [129][201]****Erreur ! Source du renvoi introuvable.****, the values to be used by the optimizers are computed (c_TOFL, c_Span, c_119a, c_121a, c_121b, c_121c, c_121d, c_TOC, c_TOD).*

14. *Feedback loop for the optimization with objective function (f) and the constraints values computed in step 13.*

until *14-1 Aircraft optimization has converged.*

3.4.3. Optimization algorithms

As the optimization problem has to solve constrained multiobjective problems and FAST does not compute gradients, one solution is to implement the Nondominated Sorting Genetic Algorithm II or NSGAII [110] within the MDAO process as it has been done for the GABRIEL project study. Published in 1995 [210], the first version of the method was characterized by high computational complexity of nondominated sorting, lack of elitism and the need for specifying the sharing parameter [110]. NSGAII proposes improvements regarding these three areas and offers the possibility to solve constrained multiobjective problems efficiently. As FAST is coded in Python, the library Platypus [211] has been considered during this research. However, evolutionary algorithms still require an important number of generations before converging. Thus, other options have also been considered.

Always considering the Python environment, a review of the optimization capabilities offered by SciPy [212] led to the selection of the COBYLA (Constrained Optimization BY Linear Approximation) algorithm invented by Powell [213] as another possibility. This gradient free method approximates at each iteration the constrained problem by a linear programming problem to find the best solution. Subsequently, this candidate solution is assessed with respect to the original objective and constraint functions. The result drives the selection of a new point within the exploration domain. As COBYLA is a local optimizer, a multi start approach is requested. In the present case, a Design of Experiment (LHS [104]) with 5 sampling points has been used.

Due to the collaboration between ONERA and ISAE-SUPAERO, an in-house optimizer has been developed since 2015 [214]. The proposed optimization algorithm SEGOMOE is a constrained Bayesian optimizer where the expensive black boxes (objectives and constraints functions) are approximated by some surrogate models. SEGOMOE stands for Super Efficient Global Optimization using Mixture Of Experts, combining the Efficient Global Optimization proposed by Jones [215] and the constraints handling introduced by Sasena [216]. The idea of SEGOMOE is to use some adaptive mixture of kriging based models to tackle high dimension problems [217][218]. Figure 66 illustrates the adaptive surrogate based process. This optimizer is currently aimed at solving mono-objective problems involving an intermediate number of design variables (up to 100) and potentially constrained by both inequality and equality nonlinear constraints. Its competitiveness essentially relies on the use of a sequential enrichment strategy, performed on adaptive surrogate models.

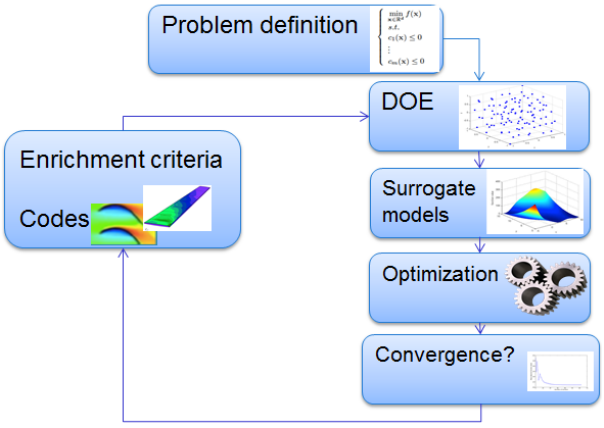

Figure 66: SEGOMOE diagram

SEGOMOE, fully described in [219], has been successfully applied for different applications ranging from analytical problems to aerodynamic shape optimization [220] and nacelle optimization [221]. In order to start the optimization process with SEGOMOE, an initial Design of Experiment is built with $3 \times d$ points where d is the number of design variables.

Because of their structure, SCIPY and SEGOMOE are tailored to solve mono-objective problems. Thus, in order to solve the optimization problems stated in Table 12, a linear scalarization is proposed to combine the two objectives into a single one:

$$\min_{x \in D}(\alpha f_1(x) + (1-\alpha) f_2(x))$$

where x is the design variable vector;
D is the feasible domain;
f_1 is the first objective function to be minimized;
f_2 is the second objective function to be minimized;
$\alpha \in [0,1]$.

With the interval [0,1] discretized with 11 points, 11 mono-objective optimization problems will be solved in order to approximate the Pareto front.

After an initial optimization loop based on NSGAII only, Sections 3.4.5., 3.4.6 and 3.4.7., will compare the different optimizers considering their respective Pareto front, the number of function evaluations (FAST MDA calls in this case) and the associated CPU time:

- For NSGAII, the maximum number of evaluations is a setup parameter to be chosen. To ensure convergence, 10000 individuals have to be computed (unsatisfactory tests with 1000 and 5000 individuals have been made). Given the logic within the algorithm, there is no tolerance criterion for the solution. Simply, if a constraint is negative (<0), it is considered as satisfied.
- About COBYLA, following a multi start approach, 5 different optimization runs are performed for each value of α with a maximum number of iterations fixed to 100. Therefore, in the end, a maximum of $5 \times 11 \times 100$ iterations will be computed. A threshold value of $1e^{-4}$ has been given for the constraint violation.
- Regarding SEGOMOE, a number of maximum iterations must be fixed as a stopping criterion (a budget of 100 iterations in this case). Therefore, considering the 11 values of α, a total of 11×100 iterations will be performed. The same threshold value used for COBYLA is imposed for constraint violation.

3.4.4. Optimization 1 - Minimization of MTOW and Sizing mission fuel weight

As an initial step of this series of optimizations, it has been decided to reproduce as closely as possible the optimization that took place in the GABRIEL project. Thus, Optimization 1 minimizes both MTOW and the sizing mission fuel weight and uses the NSGAII algorithm [110]. The known issue associated to genetic algorithms, regarding the number of required function calls before satisfactory convergence, is confirmed. In this case, after different tests with 100 and 5000 calls to the FAST MDA, the satisfactory optimization requested 10000 calls. The global exploration of the domain space obtained after 144 hours of computational time is illustrated in Figure 67.

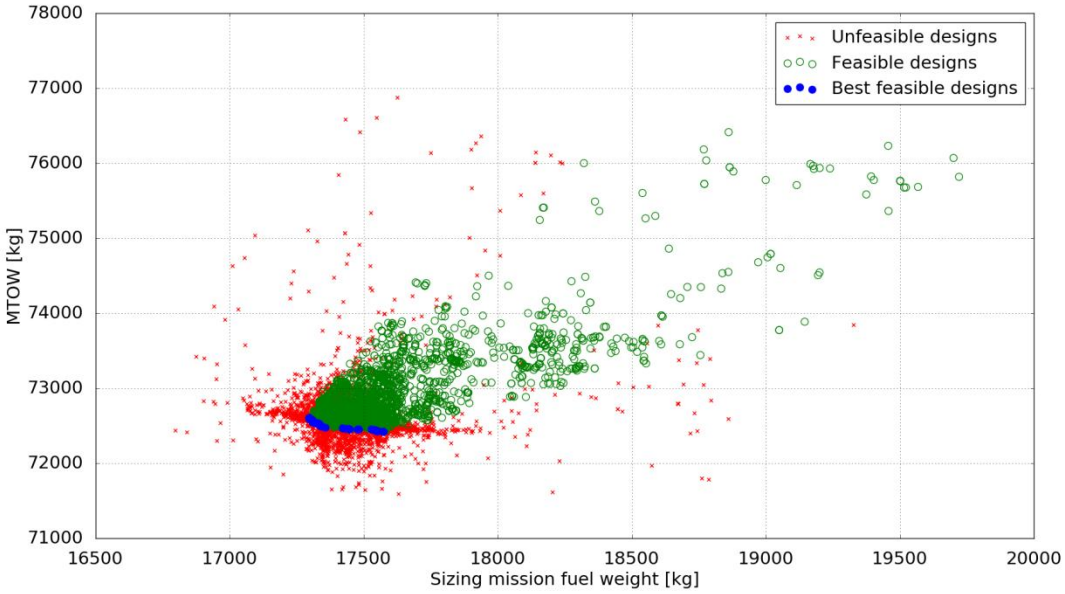

Figure 67: Exploration of the design space during the FAST MDAO process - Optimization 1

As the domain space is very large, a focus on the domain of interest is presented in Figure 68. In this plot, unfeasible designs are identified with a red cross while feasible ones are represented by green circles. More importantly, the optimization process highlighted the Pareto front that defines the family of best possible solutions.

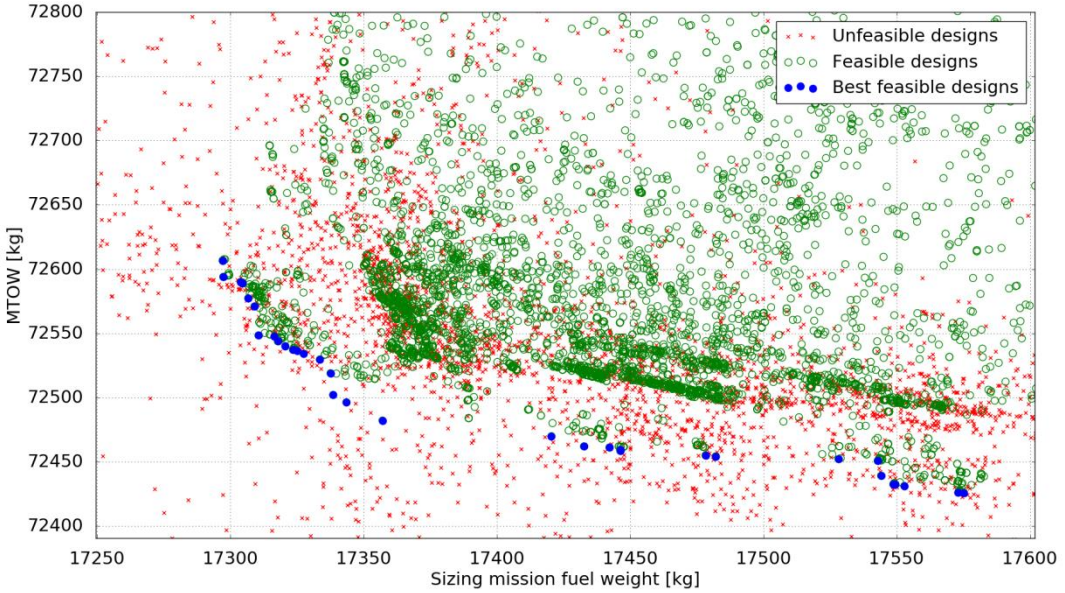

Figure 68: Exploration of the design space during the FAST MDAO process - Optimization 1 (focus on the area of interest)

In order to better assess this Pareto front, it is represented in Figure 69 with the associated evolution of the design variables. The first element to be underlined is that for these best design points, the variations in MTOW (from 72425 kg to 72600 kg) and sizing mission fuel weight (17300 kg to 17575 kg) are limited considering the range of design variables. Regarding the shape of the Pareto front, two

segments can be identified before and after a sizing mission fuel weight of about 17340 kg. Moving away from this intersection point results in a rapid increase of MTOW and sizing mission fuel weight. Among the most promising designs, the aircraft featuring a MTOW of 72500 kg and a sizing mission fuel weight of 17340 kg seems the best option. The corresponding evolution of the design variables offers additional interesting information: as expected, the decrease of aspect ratio leads to both a slight reduction of MTOW (the wing span is reduced) and an increase of fuel consumption (higher induced drag). The variation of aspect ratio is countered by changes on the engine thrust. However, at 17340 kg, it seems that the optimizer cannot increase the aspect ratio (because of the wing span limit) so at geometry level, the only option is to increase the taper ratio. In addition, an increase of thrust is required to satisfy operational constraints. The associated increase of weight generates an offset on the Pareto front.

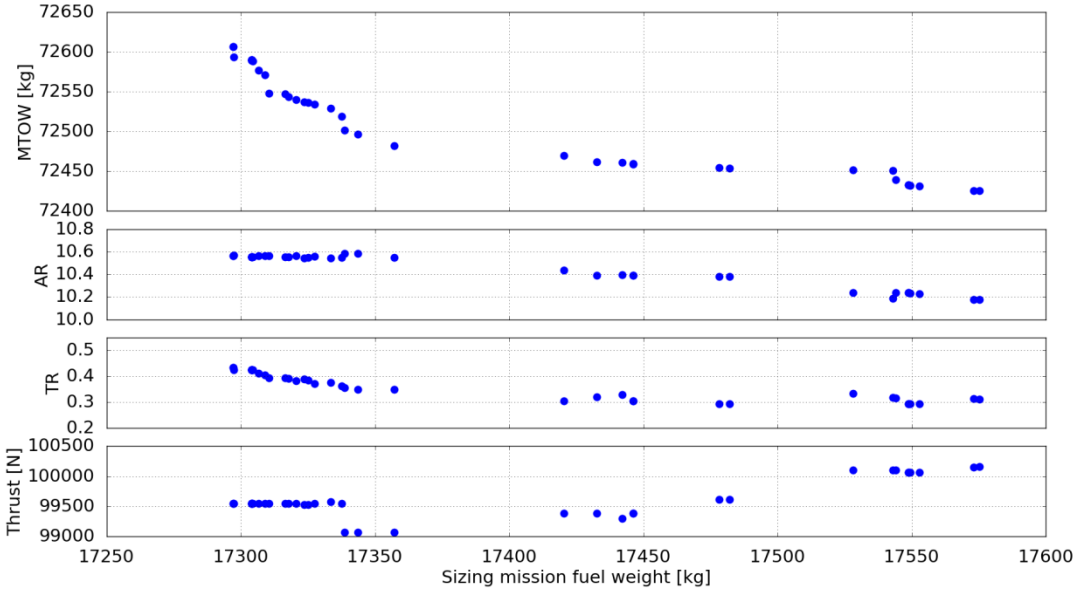

Figure 69: Evolution of key design variables along the Pareto front - Optimization 1

Optimization 1 demonstrated that the FAST MDAO process coupled with the CCM can be used to explore a given design space and to identify a set of optimal designs. However, as concluded in Section 2.2.6., the minimization of both MTOW and mission fuel weight is not a well stated optimization problem because of an obvious dependency. In addition, the computational time required by NSGAII is extremely high. Thus, other optimization algorithms will be tested in the next steps.

3.4.5. Optimization 2 - Minimization of OWE and Sizing mission fuel weight

The problem of performing a multiobjective optimization with MTOW and mission fuel weight is that the second performance metric is included in the first one: there is a high correlation between the two outputs. Thus, if the interest is to observe outcomes affecting acquisition cost and Direct Operating Cost (DOC), a more exact optimization requires the minimization of both Operating Weight Empty and sizing mission fuel weight. This optimization problem solved in Optimization 2 is carried out for

three different optimization algorithms. Details about the algorithm performances are reported in Table 13 and the resulting Pareto fronts are shown in Figure 70.

Table 13: Differences in computational time for Optimization 2

	COBYLA	**SEGOMOE**	**NSGAII**
CPU time [hours]	36	22	110
Evaluation calls [#]	3325 (average)	1100	10000

In Table 13, the number of evaluation calls and the CPU time are reported. For COBYLA, for each value of α, a mean value of 60.45 evaluations to reach convergence has been observed. Thus, considering the multi start approach, an average of $5 \times 11 \times 60.45$ runs is reported (5 numbers of starting points, 11 different values of α). For SEGOMOE and NSGAII, the number provided in the table corresponds to the imposed maximum number of evaluations.

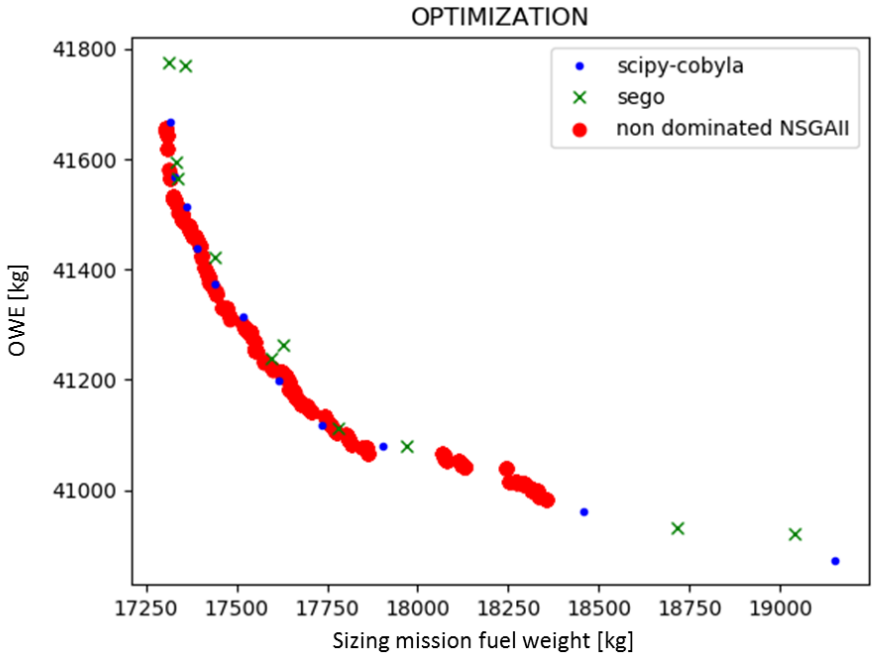

Figure 70: Pareto fronts obtained with the three optimization algorithm for Optimization 2

In Figure 70, it can be observed that the three optimizers converge to an equivalent Pareto front with NSGAII having a limited exploration of the design space. COBYLA and SEGOMOE naturally result in a less dense set of data as it is directly associated to the discretization used in the composite function to be minimized (11 points).

Given its reduced CPU time and its capability to better explore the design space, SEGOMOE is used as the reference algorithm. The total domain space exploration obtained after 11 minimizations of the composite function (corresponding to 22 hours of computational time) is illustrated in Figure 71.

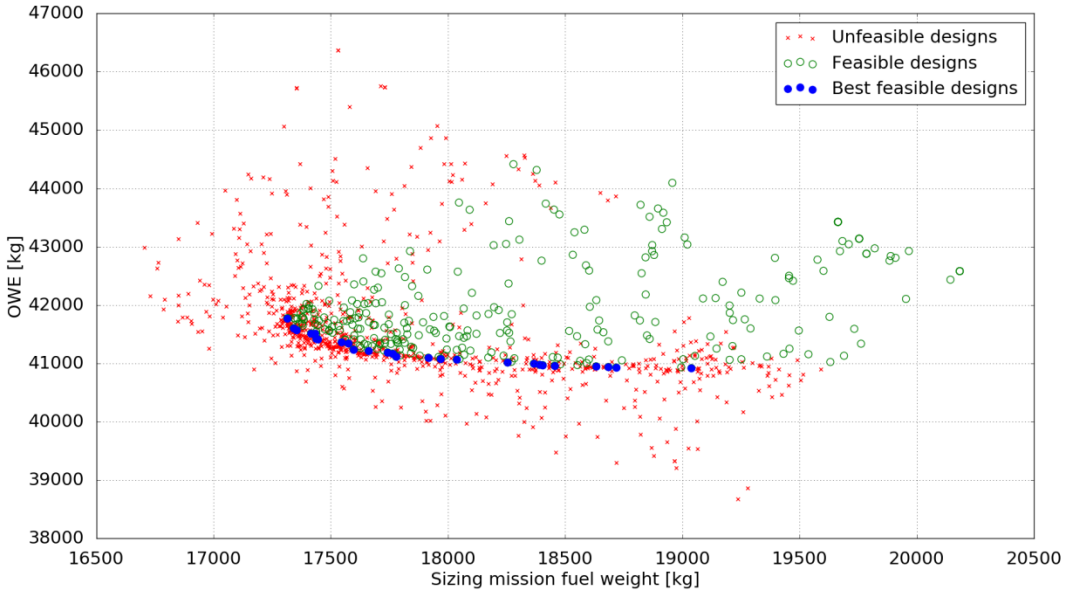

Figure 71: Exploration of the design space during the FAST MDAO process - Optimization 2

During the optimization, all results computed by FAST for the 1100 function calls have been recorded. There is then a large database that is available for post processing. In order to observe Pareto fronts with a higher density of points, the best designs computed for all available FAST calculations are extracted. Such reconstructed Pareto front feature small differences with the one obtained directly with the composite function, as shown in Figure 72.

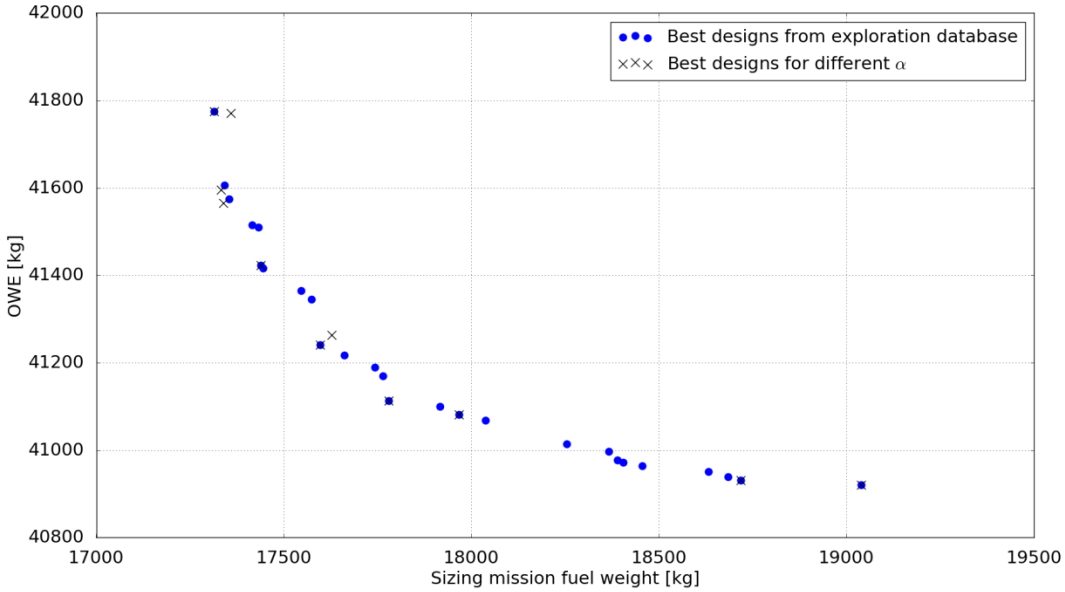

Figure 72: Pareto front verification - Optimization 2

With respect to Optimization 1, the resulting Pareto front is much smoother. Indeed, it is more difficult to rapidly identify a single best solution. This trend is associated with an almost linear effect of the two key design variables (aspect ratio and engine thrust level) on sizing mission fuel weight (see

Figure 73). At aircraft design level, the tradeoff to be considered at this stage is between an aircraft with high aspect ratio wing and smaller engines and an airplane with low aspect ratio wing and larger engines.

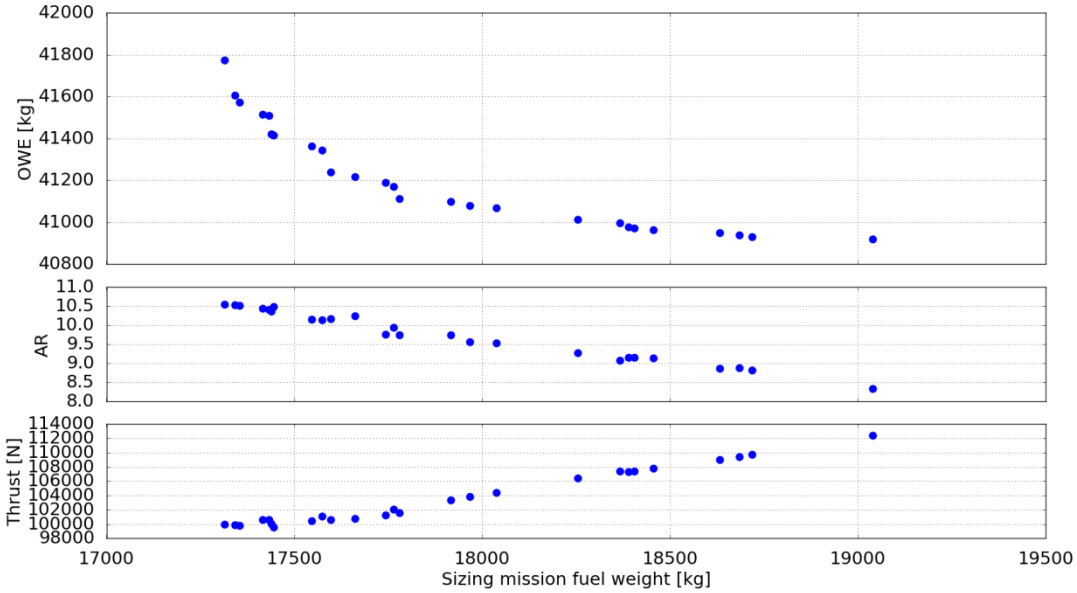

Figure 73: Evolution of key design variables along the Pareto front - Optimization 2

Parsing through the database, it is also possible to identify the best solutions satisfying only operational constraints (black Pareto front in Figure 74) and the best solutions satisfying only the certification constraints (red Pareto front in Figure 74). The feature to be noted is that the feasible solutions cover a smaller range of sizing mission fuel weight domain when considering operational constraints.

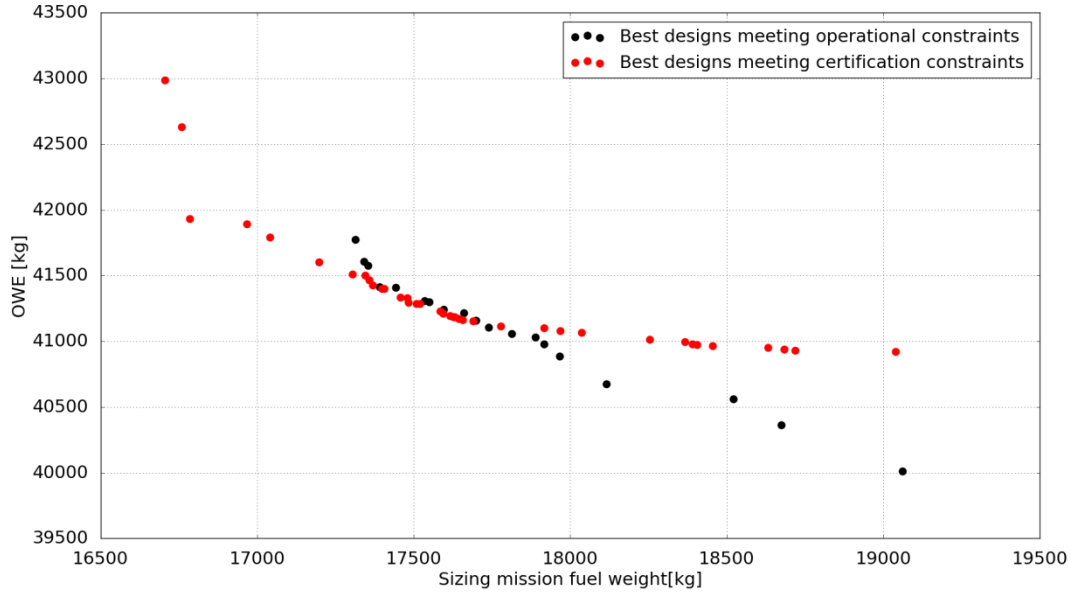

Figure 74: Evolution of the Pareto front depending on the active constraints - Optimization 2

For OWE, on the other hand, the variations are similar independently of the activated constraints. Logically, the Pareto front seen in Figure 73 then corresponds to the worse combination of the black and red Pareto fronts shown in Figure 74. Overall, it is observed that below a mission fuel weight of 17400 kg, operational constraints are key (wing span limit) while above 17900 kg, the certification constraints are keeping the OWE at a higher value (requirements on engine size to maintain climb capabilities).

3.4.6. Optimization 3 - Minimization of OWE and Operational mission fuel weight

The Pareto front obtained through optimization allows design engineers to make better tradeoffs among a family of best vehicles and these compromises are often affected by economical aspects. Naturally, the mission fuel consumption is the primary criterion to estimate the Direct Operating Costs of an aircraft. However, for Optimization 1 and Optimization 2, it is the sizing mission fuel weight that has been considered. From an airline point of view, this outcome may not be the most appropriate one in an assessment phase, as the aircraft is seldom used for missions at the design range. Indeed, for cost evaluations, it is the operational range that is taken into account. Optimization 3 then aims at minimizing both OWE and the operational mission fuel weight. Table 14 reports the performances of the three algorithms while the calculated Pareto fronts are illustrated in Figure 75. In terms of performance, the CPU time has basically doubled with respect to values indicated, as a single FAST MDA takes twice as long because of the computation of the operational mission performance. As for Optimization 2, the capabilities of SEGOMOE stand out since the gain in evaluation calls is very important and the resulting Pareto front captures the main trend.

Table 14: Differences in computational time for Optimization 3

	COBYLA	**SEGOMOE**	**NSGAII**
CPU time [hours]	72	44	221
Evaluation calls [#]	3575 (average)	1100	10000

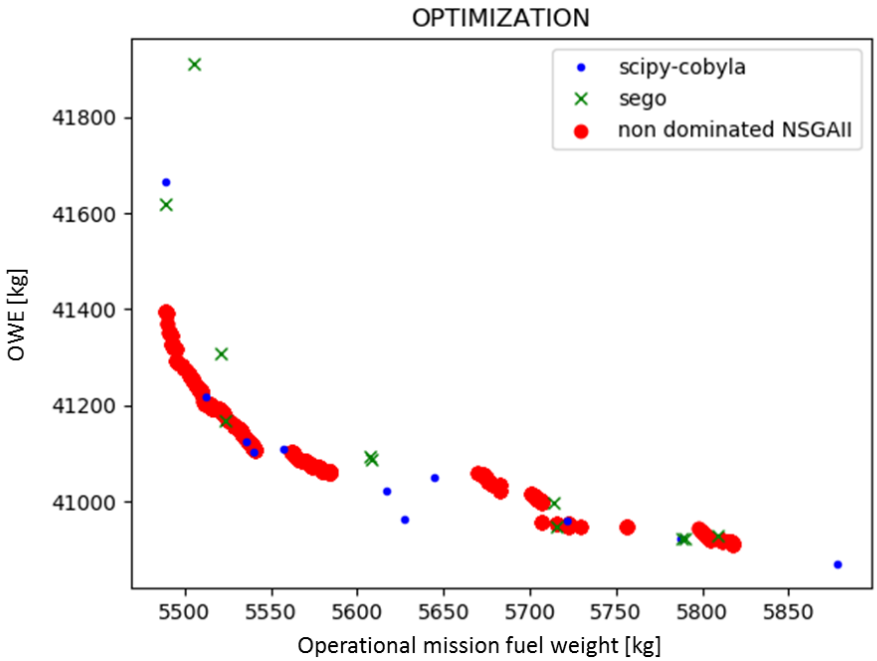

Figure 75: Pareto fronts obtained with the three optimization algorithm for Optimization 3

The post processing of the database generated during the SEGOMOE optimization results in the design space exploration illustrated in Figure 76. With respect to Optimization 2, the range in OWE does not really change while there is an obvious shift with respect to mission fuel weight, as the required fuel for 800 NM is between 5500 kg and 5800 kg.

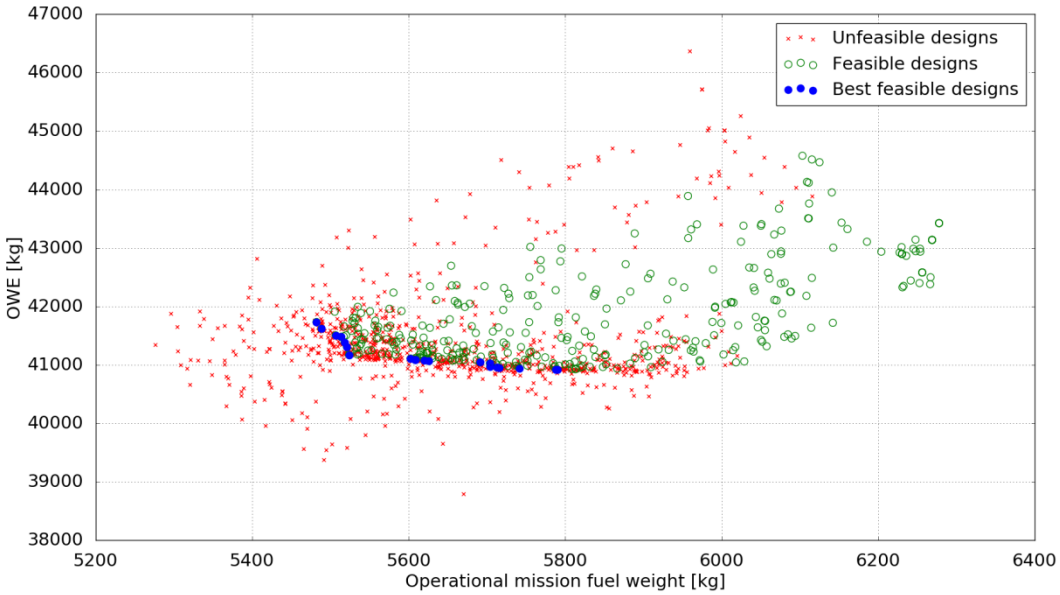

Figure 76: Exploration of the design space during the FAST MDAO process - Optimization 3

A focus on the Pareto front only (see Figure 77) shows overall consistency with the points obtained through the post processing and the ones achieved through the composite function (see Figure 75). More importantly, this Pareto front is characterized by two segments intersecting for an operational

mission fuel weight of 5525 kg. It is at this point that the most promising design can be identified: small variations would indeed lead to a rapid increase of OWE or operational mission fuel weight.

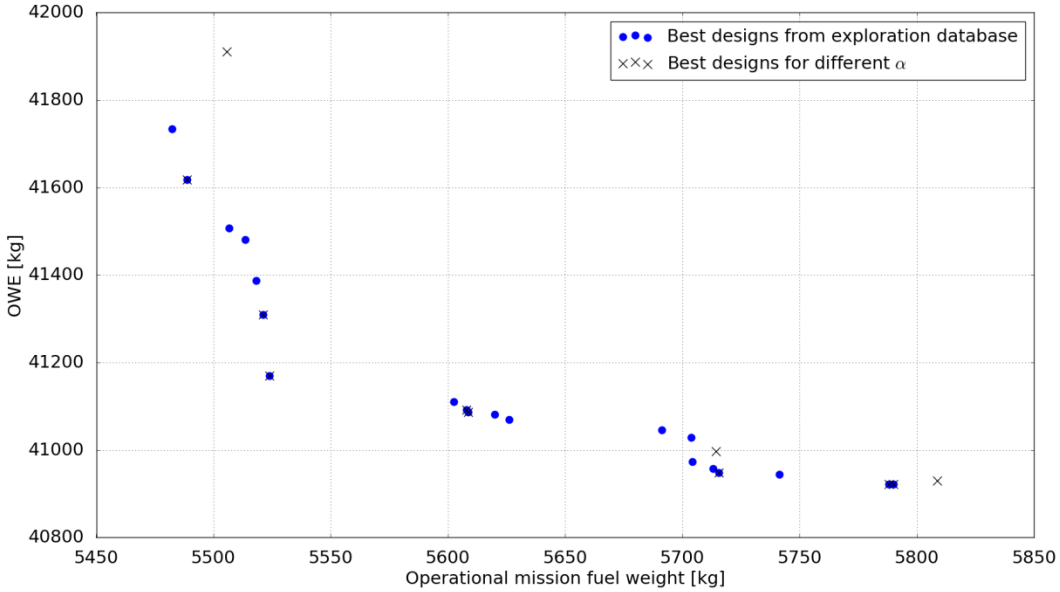

Figure 77: Pareto front verification - Optimization 3

To assess the evolution of the design variables along this Pareto front, it must be recalled that the Sobol indices indicated a similar effect by aspect ratio and taper ratio on OWE variance. Thus, these two design variables as well as the engine thrust level are reported in Figure 78. In this figure, it can be observed that an aircraft prioritizing operational mission fuel weight should have large aspect ratio and taper ratio as well as a small engine. Conversely, an airplane designed to minimize OWE should feature a large engine, low aspect ratio and low taper ratio. However, given the shape of the Pareto front, design engineers have in this case a very limited freedom.

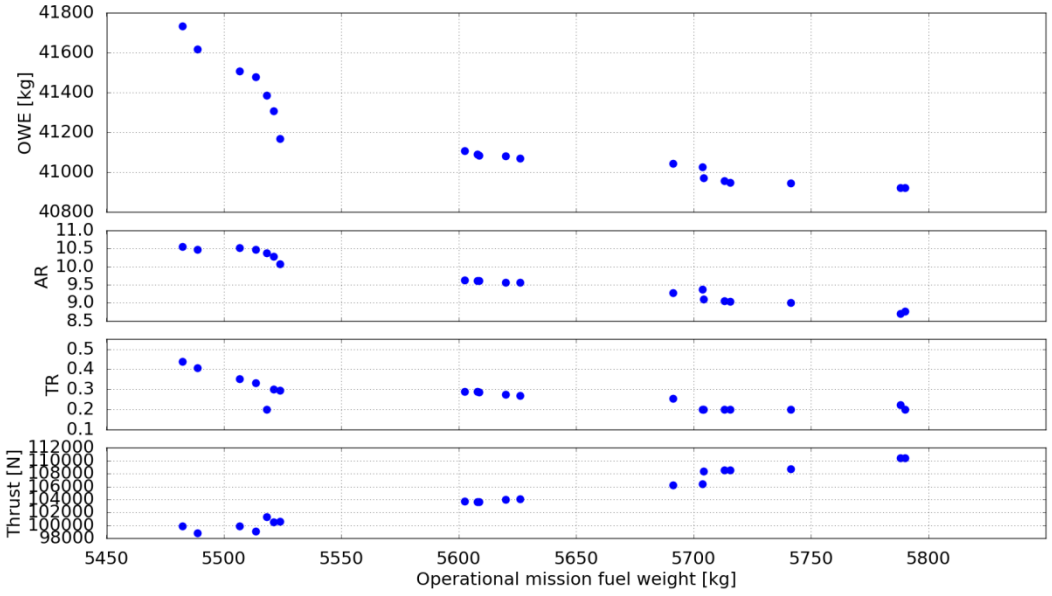

Figure 78: Evolution of key design variables along the Pareto front - Optimization 3

A complementary analysis explaining the evolutions in Figure 78 can be supported by the Pareto fronts illustrated in Figure 79.

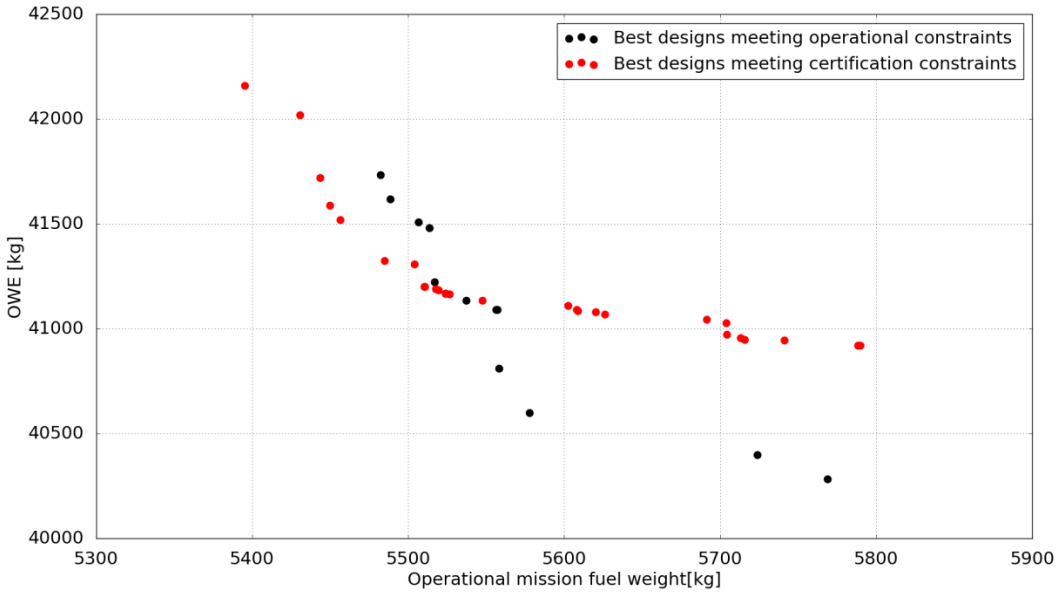

Figure 79: Evolution of the Pareto front depending on the active constraints - Optimization 3

In this plot, best designs satisfying operational constraints only and certification constraints only are represented. The Pareto front shown in Figure 79 naturally corresponds to the worse combination of these two fronts. The crossing of both Pareto fronts is much more evident than in Optimization 2 and the evolution of the design variables for low operational mission fuel weight is fully driven by operational limitations. Thus, with a minimum necessary thrust to achieve a TOFL that is less than 2000 meters and a constraint on aspect ratio because of the 36 meters limit, the only possible way for the optimizer to reduce fuel burn is to modify the taper ratio. This explains the change in slope for taper ratio in Figure 78. Another interesting way to look at Figure 79 is the estimation of a cost associated to a constraint type. Indeed, as the two Pareto fronts intersect and are shifted, the lower right area of the plot indicates a cost of certification that is about 500 kg (1% of OWE) while the upper left area presents a cost of operational constraint that is about 50 kg (1% of fuel).

3.4.7. Optimization 4 - Minimization of OWE and Operational mission fuel weight under more stringent constraints

In terms of multiobjective function, Optimization 3 corresponds to a sound optimization problem as well as a typical tradeoff case to be investigated at conceptual design stage. However, in terms of constraints, the setup still doesn't correspond to the industrial case. The reason is that all regulatory constraints have been verified for International Standard Atmosphere (ISA) conditions and no margins with respects to the threshold values have been taken to consider, for example, a takeoff at high altitude. Looking at the results obtained for the reference aircraft in Section 3.3.3., the FAST MDA provided the values reported in Table 15 for the exit criteria.

Table 15: Exit criteria values for the reference aircraft

Constraint name	Description	Reference value	Exit criteria vale
c_1	TakeOff Field Length	2000 m [157]	1903.5 m
c_4	Climb gradient	0 % [129]	1.87%
c_5	Climb gradient	2.4 % [129]	3.73%
c_8	Vertical speed at TOC	300 ft/min [201]	1236.6 ft/min
c_9	Vertical speed at TOD	300 ft/min [201]	1294.6 ft/min

It has thus been decided to explore in Optimization 4 the design space corresponding to an aircraft meeting the same exit criteria values as the reference aircraft. For clarity, this last optimization problem is detailed in Table 16.

Table 16: Description of the MDAO problem considered in Optimization 4

	Function / Variable	Description	Range / Value
minimize	OWE	Operating Weight Empty	
and	Mfuel (oper.)	Mission fuel for the operational mission	
with respect to 4 design variables			
	AR	Aspect Ratio	[8 : 12]
	λ	Taper ratio	[0.2 : 0.6]
	$\Lambda_{25\%}$	Sweep angle at 25%	[20 : 30] °
	T_{SL}	Maximum Thrust at sea level	[85000 – 135000] N
subject to 6 inequality constraints			
	c_TOFL	Takeoff field length [157]	$c_1 - 1903.5 \leq 0$
	c_Span	Span **Erreur ! Source du renvoi introuvable.**	$c_2 - 36 \leq 0$
	c_121a	Climb gradient [129]	$0.0187 - c_4 \leq 0$
	c_121b	Climb gradient [129]	$0.0373 - c_5 \leq 0$
	c_TOC	Rate of Climb [201]	$1236.6 - c_8 \leq 0$
	c_TOD	Rate of Climb [201]	$1294.6 - c_9 \leq 0$

As for the two previous cases, the optimization convergence has been achieved with various algorithms. Computing performances reported in Table 17 once again highlight the important difference between SEGOMOE or COBYLA and the pure evolutionary algorithm NSGAII. The resulting Pareto fronts are shown in Figure 80, where the red points associated to NSGAII feature some discontinuity. Most likely, the number of generations was not sufficient enough to allow the optimizer further improvements. Nevertheless, all three algorithms recognize the general shape characterized by two steep linear zones.

Table 17: Differences in computational time for Optimization 4

	COBYLA	SEGOMOE	NSGAII
CPU time [hours]	72	38	208
Evaluation calls [#]	3410 (average)	1100	10000

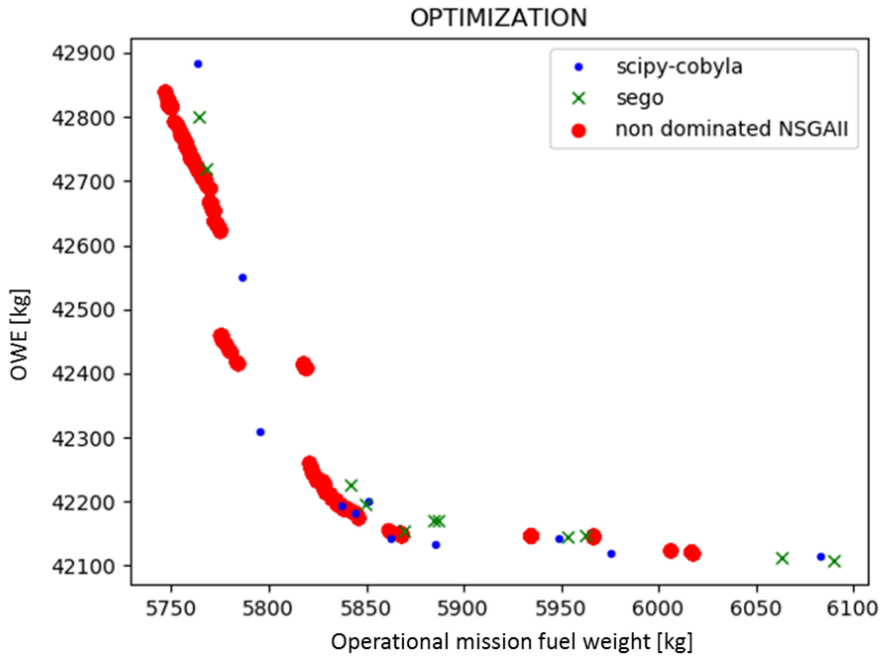

Figure 80: Pareto fronts obtained with the three optimization algorithms for Optimization 4

During the SEGOMOE optimization, all calls to the FAST MDA and the related results are stored in a .csv file. An easy data post processing step allows the visualization of unfeasible, feasible and best designs. The latter correspond to the Pareto front that is obvious in Figure 81 (blue points).

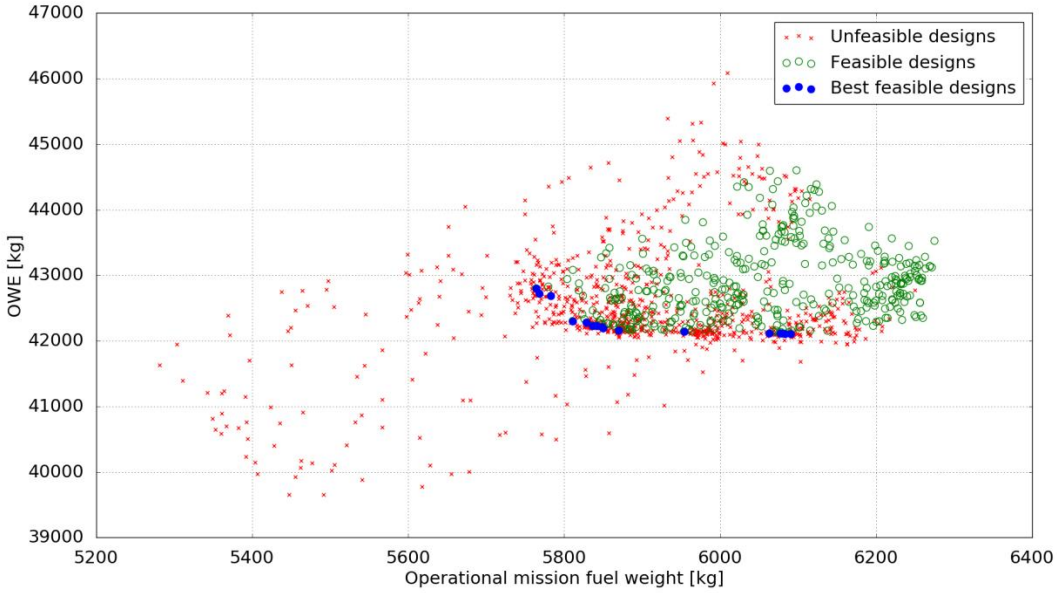

Figure 81: Exploration of the design space during the FAST MDAO process - Optimization 4

With respect to Optimization 3 and the position of the Pareto front within the design space, an important shift of about 1000 kg is noticed for OWE. For the operational mission fuel weight, the range covered by these best designs is very similar to the one in Optimization 3. For better visualization, Figure 82 zooms on this resulting Pareto front. As observed in the previous optimizations, the Pareto front derived from the exploration database is consistent with the one obtained for the 11 best cases with each one corresponding to a value of α. Overall, variations in OWE and operational mission fuel weight follow the tendency identified for Optimization 3: the Pareto front can be approximated by two intersecting segments. However, this time, any reduction in OWE below 42200 kg is associated to a very large increase of mission fuel weight (indeed, the Pareto front features a flat portion on the right in Figure 82). When reporting in Figure 82 the characteristics of the reference aircraft calculated in Section 3.3.3., it can be observed that the airplane is located in the area of the optimal point, which is the intersection between the two segments. Considering the uncertainties associated to the convergence tolerance within FAST and the fact that the reference aircraft is mainly sized according to wing geometry criteria, this result stresses the consistency of the FAST Multidisciplinary Design Analysis and Optimization. Moreover, it confirms that the wing geometry and the engine thrust level selected for the reference aircraft lead to a near optimal aircraft.

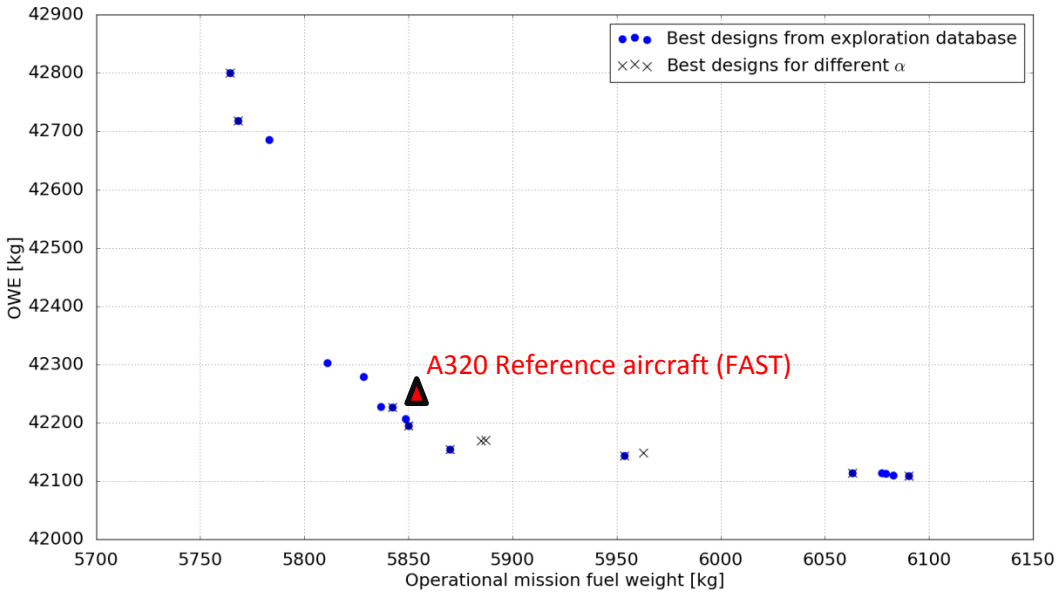

Figure 82: Pareto front verification - Optimization 4

To better understand the key effects that take place in such optimization, best designs meeting operational constraints only and best designs meeting certification constraints only are shown in Figure 83. Contrary to what has been observed during Optimization 2 and Optimization 3 there is no crossing: because of the higher threshold values that have been considered, certification constraints are the only driving factors. The red Pareto front in Figure 83 corresponds in fact to the global Pareto front shown in Figure 82.

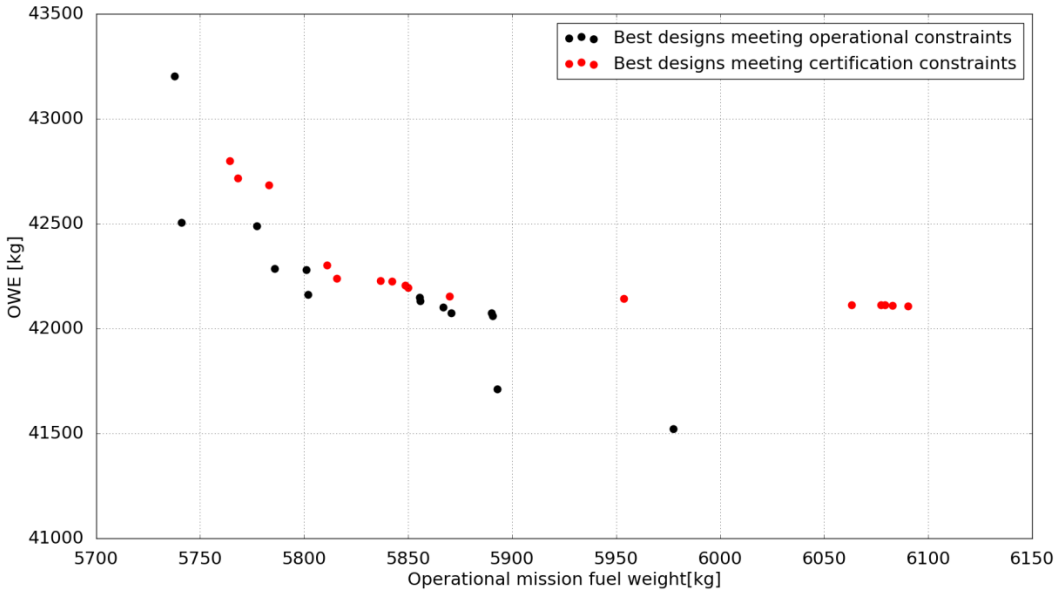

Figure 83: Evolution of the Pareto front depending on the active constraints - Optimization 4

In order to further assess the impact of certification constraints, Figure 84 shows the evolution of not only the design variables but also the four certification constraints that have been used in this problem.

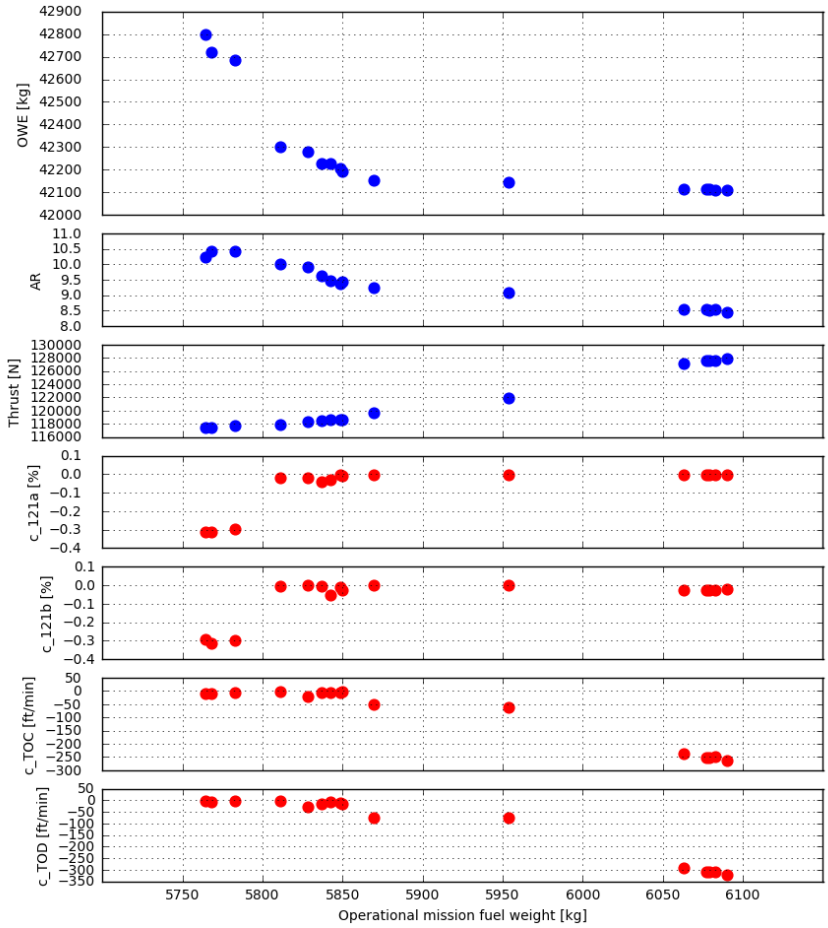

Figure 84: Evolution of key design variables and certification constraints along the Pareto front - Optimization 4

In Figure 84, the constraints have been defined so that a positive value indicates a violation. Thus, it can be seen that sections CS 25.121 (a) and (b) [129] are driving the design space for designs which fuel weight is above 5850 kg. Below this value, it appears that the vertical speed constraints associated to CAT.POL.A.410 [201] also become active.

With the activation of the constraint, there is a change of slope in the aspect ratio variation up to 10.5 that corresponds to the acceptable limit (span constraint of 36 meters). With the aspect ratio fixed, the optimizer keeps the thrust level to a constant value to satify the vertical speed constraints (Top Of Climb, Top Of Descent). The only option to reduce operational mission fuel weight is then the increase of taper ratio, as in previous optimizations.

3.5. Conclusion

The first part of this chapter was dedicated to the development of the Certification Constraints Module (CCM). The initial point of this task was the identification of the logic and overall structure of reference regulatory text from the European Aviation Safety Agency CS-25 [129]. For this first development of the CCM, it has been decided to limit the translation into a digital format of key sections within CS 25 SUBPART B - FLIGHT. From this analysis, a data model of the certification constraints has been defined, also allowing the characterization of constraints related to the Acceptable Means of Compliance. Through the use of the ONERA code GAMME [186], an automatically generated Graphical User Interface related to the data model is generated. With the structure of the constraints well defined, designers can follow a template that guides them in the definition of the test condition. For this step, it is important to note that a particular effort has been made in order to manage reference values that are used for different sections. The result is a robust step-by-step definition of state vector variables, among which users can select these reference values. Finally, the creation of the CCM has been possible thanks to collaboration with Model-Driven Engineering specialists within ONERA. This positive experience should then foster similar future exchanges providing state-of-the-art capabilities to the aircraft Multidisciplinary Design Analysis and Optimization.

To assess the benefits of the CCM for Aircraft Design studies, different optimization problems subject to certification constraints have been solved. To carry out the aircraft sizing iterations within the monolithic optimization architecture, the tool FAST (Fixed-wing Aircraft Sizing Tool) has been used. Developed jointly by ONERA and ISAE-SUPAERO since 2015, this Python code follows a set of specifications aiming at shared development, disruptive configurations evaluation, multifidelity capability and subsystems models refinements. In terms of analysis capabilities, the comparison of FAST results given a set of mission parameters and geometric setting with respect to a corresponding reference aircraft shows little differences on the design point. More importantly, the payload range diagram is consistent with the available data and discrepancies can be explained. Prior to optimizations, a sensitivity analysis is carried out around the reference aircraft to better assess the outcomes variance with respect to design variables. As expected, the calculation of the Sobol indices

confirmed a design space dominated by the wing aspect ratio and the engine thrust. These various verifications provided enough confidence on FAST ability to correctly capture the main tradeoffs within the multidisciplinary analysis including engine sizing. Through an active collaboration between ISAE-SUPAERO and ONERA in the last years, FAST has been continuously improved and is nowadays used as the backbone of Aircraft Design activities including studies on hybrid electric concepts, Blended Wing Body and regional aircraft.

For the optimization, the objective is to gather as much information as possible on the vehicle to be sized. Thus, it is decided to consider a multiobjective problem taking into account certification constraints (climb capability verifications) and also operational constraints (takeoff field length and wing span limitation). With this approach, aircraft designers can obtain Pareto fronts showing the best set of solutions and possible compromises to be made between the functions to be minimized. Regarding the optimization algorithms, it has been decided to use three different ones in order not only to verify the outcomes of the optimization and the Pareto fronts but also to compare CPU time. These algorithms are NSGAII [110], COBYLA [213] and SEGOMOE [219]. Overall, four different optimization problems have been solved with the first one replicating the minimization of MTOW and sizing mission fuel weight performed in chapter 2 on the GABRIEL aircraft. However, as MTOW includes the fuel weight, the other three optimizations have been launched with the goals of minimizing OWE instead. In all cases, SEGOMOE demonstrated superior performances as its outcomes matched the ones found with the other codes but for a much smaller CPU time (5 times faster than NSGAII). Illustrated in Figure 85, these resulting Pareto fronts provide valuable information:

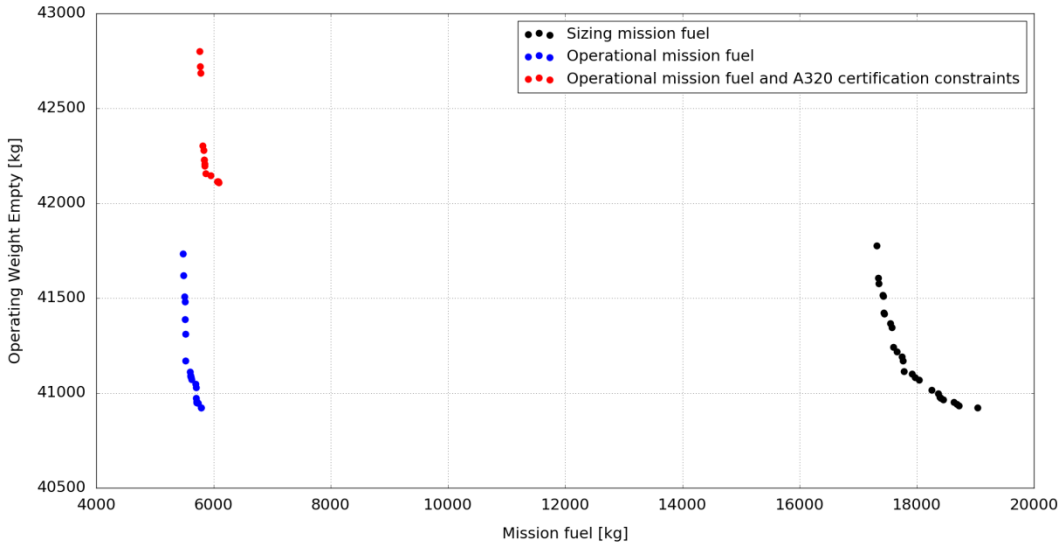

Figure 85: Pareto fronts resulting from different optimization problems

- For Optimization 2, OWE and the Sizing mission fuel weight are minimized. Represented by black dots in Figure 85, the best designs associated to the Pareto front cover a large interval either for OWE or fuel weight. Then, the Pareto front shows no discontinuity which makes it harder for design engineers to pick a single most promising solution.

- For Optimization 3, OWE and the Operational mission fuel weight are minimized. In this case, the best designs associated to the blue Pareto front in Figure 85 cover a smaller interval in fuel weight. More importantly, the shape of the Pareto front is completely changed as it is now characterized by a discontinuity between two linear portions. In such a case, the optimal design corresponds to the intersection.
- For Optimization 4, OWE and the Operational mission fuel weight are minimized considering the same margin on the constraints as the ones calculated on the reference aircraft. In this case, the domain covered by the best designs (red Pareto front in Figure 85) is further reduced. More significantly, it is possible to see a change in the shape and an expected degradation in terms of performances.

In terms of Aircraft Design research, these various optimizations highlighted the strong impact of certification constraints and their thresholds on the families of best designs. At conceptual level, the risk is to eliminate a valuable concept or to select a bad configuration. So, as certification constraints shape the aircraft and define the best airframe / engine combination, it then becomes mandatory to partially mitigate this risk by considering as much certification constraints as possible very early in the design process. In this regard, the Certification Constraints Module offers unique capabilities that surely support designers in their decision making process as illustrated in this work for a conventional aircraft or in the case study of a Blended Wing Body [198].

In chapter 3, the Multidisciplinary Design Analysis and Optimization considered only a few basic certification constraints and the reference mission for sizing is defined by high level indications. In reality, certifications constraints involve flight dynamics aspects and the mission is subject to Air Traffic Management constraints. To prepare such global analysis capability, full simulation capabilities must be included in the Multidisciplinary Design Analysis. The work performed towards this objective is described in chapter 4.

Synthesis of the chapter

- The data model of certification constraints has been defined
- The ONERA tool GAMME has been used to generate the Certification Constraints Module with a Graphical User Interface
- The Certification Constraints Module automatically generates a digital version of the certification constraints following the data model template
- FAST outcomes show good consistency with available data on a reference aircraft
- Setup time for the optimization is reduced through the use of the Certification Constraints Module
- The analyses of the different optimizations detail the impact of certification constraints on the design
- SEGOMOE optimizer provides reliable results with an important reduction of CPU time

➢ Only a few certifications and operational constraints have been considered so far: more can be added but full simulation capabilities are required for the assessment. The addition of such capability is detailed in chapter 4.

Associated conferences

- Schmollgruber P., Bartoli N., Gourinat Y., "Impact of Certification Constraints in a Multi-disciplinary Design Process", 4th EASN Association International Workshop on Flight Physics & Aircraft Design, Aachen, 2014
- Schmollgruber P., Bedouet J., Bartoli N., Gourinat Y., "Development of a certification module tailored to Aircraft Multi-Disciplinary Optimization", 5th CEAS European Air & Space Conference, CEAS 2015-150, Delft, 2015
- Schmollgruber P., Bartoli N., Bedouet J., Defoort S., Gourinat Y., Benard E., Lafage R., Sgueglia A., "Use of a Certification Constraints Module for Aircraft Design Activities", 17th AIAA Aviation Technology, Integration, and Operations Conference, AIAA AVIATION Forum, AIAA 2017-3762, Denver, 2017

Chapter 4

Including full simulation within the aircraft conceptual design process

Roadmap of the chapter

- The FAST Multidisciplinary Design Analysis must be modified in order to add full mission simulation capabilities
- Specific analysis tools required for the development of new modules are presented
- The new Aerodynamics module providing the database for 6 Degrees-of-Freedom models is detailed
- The new module estimating inertia properties of the aircraft is presented
- The full simulation module with the required control laws is explained
- Mission simulations following high level orders are performed
- Trajectories following Air Traffic Management constraints are simulated and compared with real flight data recorded with an ADS-B antenna

Résumé du chapitre

L'implémentation d'un outil de simulation complète au sein du processus de conception est justifiée par la nécessité d'évaluer le comportement dynamique de l'aéronef pour vérifier des contraintes de certification et par le besoin de simuler des trajectoires avion fiables soumises aux contraintes du trafic aérien.

Afin de mettre en place un tel outil d'analyse au sein de FAST, différentes évolutions ont été nécessaires. Tout d'abord, le module Aérodynamique a été modifié et intègre désormais DATCOM+PRO qui est utilisé comme soufflerie numérique. Ainsi, pour une géométrie et des conditions de vol (altitude, vitesse) données, il est possible d'obtenir une base de données complète permettant de calculer les moments et les forces exercés le long et autour des trois axes de l'avion pour différentes déflections des surfaces mobiles. L'étape suivante a été la définition du module d'estimation des inerties. Basé sur le devis de masse de l'avion effectué par FAST et son modèle 3D généré avec OpenVSP, le module va automatiquement affecter les masses à différents volumes au sein de la cellule. En revanche, certains éléments tels que le train d'atterrissage sont considérés comme des masses ponctuelles. Avec ces données supplémentaires, OpenVSP est à nouveau utilisé pour calculer les moments et les produits d'inertie. Enfin, afin de permettre la simulation de trajectoires complètes, des boucles de stabilisation et de pilotage automatique ont été définies. Il était important lors de cette étape de trouver le bon compromis entre efficacité et complexité afin de donner au concepteur la visibilité des effets des différentes boucles de retour sur les déflections des surfaces de contrôle. La base de données aérodynamiques, les moments et produits d'inertie ainsi que les boucles du système de contrôle sont alors intégrés dans le modèle à 6 degrés de liberté JSBSim. En reprenant les consignes de haut niveau utilisées dans FAST pour définir la mission de référence, des simulations de trajectoire sont automatiquement calculées par JSBSim. Dans le cas d'une mission de référence simple, l'évaluation de performances pures par la simulation complète amène peu d'information supplémentaire par rapport à l'approche classique. En revanche, vu le grand nombre de données à disposition, la simulation complète a une valeur ajoutée évidente en termes de capacité de vérification sur toutes les phases du vol.

Suite à ces simulations, la thèse s'est focalisée sur l'évaluation de la qualité des résultats obtenus. Pour atteindre cet objectif, le modèle avion à 6 degrés de liberté obtenu avec FAST a été utilisé pour simuler un plan de vol réel. Une comparaison entre la trajectoire obtenue et des données de vol réelles enregistrées via une antenne ADS-B a mis en valeur le réalisme du modèle de simulation. Cependant, au cours de cette étape de vérification, certaines hypothèses ont dû être faites au niveau de la vitesse de l'aéronef réel. Ainsi, pour compléter l'évaluation, une seconde comparaison utilisant des données réelles supplémentaires fournies par le Mode S a été faite. Les différences minimes entre les simulations ATM basées sur le modèle JSBSim et les données de vol réelles démontrent la capacité de FAST à générer un modèle de simulation complet et fiable pouvant être utilisé dans les études de conception et de gestion du trafic aérien.

4.1. Introduction

In conceptual design, the sizing and assessment of aircraft concepts based on the classical architecture with turbine engines are usually achieved through a performance analysis only. In parallel, stability and control characteristics are taken into account through basic engineering methods. However, as presented in chapter 1, the next generation of airplanes might be characterized by disruptive configurations and innovative technologies. In this case, both longitudinal and lateral - directional responses of the airplane during the different mission phases can directly affect the sizing loop. More importantly, they can drive the overall aircraft viability. Thus, to minimize risk during the concept downselection process, the Multidisciplinary Design Analysis must be able to analyze the movement of the airplane around its Center of Gravity (CoG) along the three reference axes considering Stability Augmentation System. Besides, in the future, new concepts might follow different mission profiles (such as continuous descent, or direct turn before approach…) to cope with new ATM constraints. In that case, a detailed mission simulation is necessary to assess the capability of the new air vehicle to perform the mission.

To answer this need, this research proposes to expand the capabilities of the MDA through the addition of a 6 Degrees-of-Freedom (DoF) aircraft model. However, the integration of such tool in the design process automatically requires the determination of many additional data that were not computed previously. In the case of Aerodynamics for example, the regular FAST MDA computes static coefficients for Drag and Lift for performance analysis. When considering a 6 DoF model, it becomes mandatory to have an Aerodynamics analysis that determines all required additional aerodynamic coefficients including derivatives and control surfaces effectiveness along and around the three axes. In addition, if movements around the CoG are considered, Moments of Inertia (MoI) must now be calculated in order to have correct first order responses of the aircraft after a given control input. Then, knowing that Air Traffic Management research requires automated simulations of flight trajectories, stability, control and navigation laws must be designed and implemented in the Multidisciplinary Design Analysis.

In order to provide a global view of all changes within the design process associated to full simulations integration, chapter 4 begins with the description of the revised FAST XDSM scheme. In this advanced Multidisciplinary Design Analysis, new modules relying on specific analysis tools are required. Thus, the second part of this chapter presents new softwares to be used within FAST. Subsequently, the new Aerodynamics module as well as the Inertia estimation module are detailed. With the disciplinary modules fully explained, the following section focuses on the full simulation module that includes stability and control laws. In this section, the first trajectories obtained through full simulations are presented. Last, in order to assess the quality of the resulting 6 Degrees-of-Freedom aircraft model, a comparison between a simulated trajectory and real flight data recorded with an ADS-B antenna is made.

4.2. The evolution of the Multidisciplinary Design Analysis for full simulation capability

The addition of full simulation capability within the MDA requires the computation of further data and the definition of new system models to fully support the aircraft 6 DoF model. The supplementary information, with respect to the original FAST MDA presented in Section 3.4.2. that must be provided or computed, are: (i) a full aerodynamics dataset with static and dynamic coefficients as well as control surface effectiveness; (ii) Moments of Inertia; (iii) control laws to achieve augmented stability, control and navigation. As illustrated in the revised XDSM diagram of FAST (Figure 86), this extra knowledge about the aircraft feeds the full simulation module that replaces the operational mission.

The resulting sequence of operations for the FAST MDA tailored for full simulation capability is as follows (changes with respect to the FAST MDA are highlighted in red).

Input:	Engine specifications (based on constraint analysis), initial sketch (based on constraint analysis), empennage data (taper ratio and thickness-to-chord ratio), required static margin, approach speed, sizing and operational mission specifications, *control surfaces definition, position of key subsystems along the 3 airframe axes*
Output:	Engine deck, aircraft geometry (including wing span), aerodynamic characteristics, weight breakdown, sizing mission performances (including takeoff field length), Certification constraints 119a, 121a, 121b, 121c, RoC at Top of Climb (TOC), RoC at Top of Descent (ToD), *Moments of Inertia, full simulation of the operational mission*

0. Propulsion. The propulsion module takes as input the engine specifications and computes its performances in the flight domain for Mach and altitude (Thrust, TSFC).

1. First estimate. With an initial sketch of the vehicle and assumptions on the engine performances and mission segments, a first iterative loop is computed to derive an initial guess for MTOW, MLW, MZFW and the wing area (Breguet approach).

repeat

2. The Multidisciplinary Design Analysis is started;

3. Geometry. In this module, given a certain number of inputs (number of passengers, empennage data, required static margin and approach speed), aircraft parameters (fuel weight, maximum landing weight, maximum lift coefficient) and engine thrust, the complete geometry of the aircraft is computed and the main subsystems are positioned. The wing is sized according to the most critical constraint between approach speed and available fuel quantity. In the generic case, data are stored in the vector identified as A/C but a dedicated CAD model can be used instead [19]. The wing span that can be a constraint is calculated in this module.

4. Aerodynamics. Taking into account the aircraft geometry defined during the previous step *and the new information about the control surfaces, the Aerodynamics module computes the complete aerodynamic dataset that is required by the 6 DoF model (static and dynamic coefficients, control surface effectiveness). The classical drag polar required for the sizing loop is extracted from this dataset.*

5. Structure and Weight. Using as input the aircraft geometry, the MTOW value defined at the beginning of the step 2 and the engine thrust calculated by the propulsion module 0, the "Structure and Weight" module sizes the wing and the fuselage and then computes the masses of the different aircraft components.

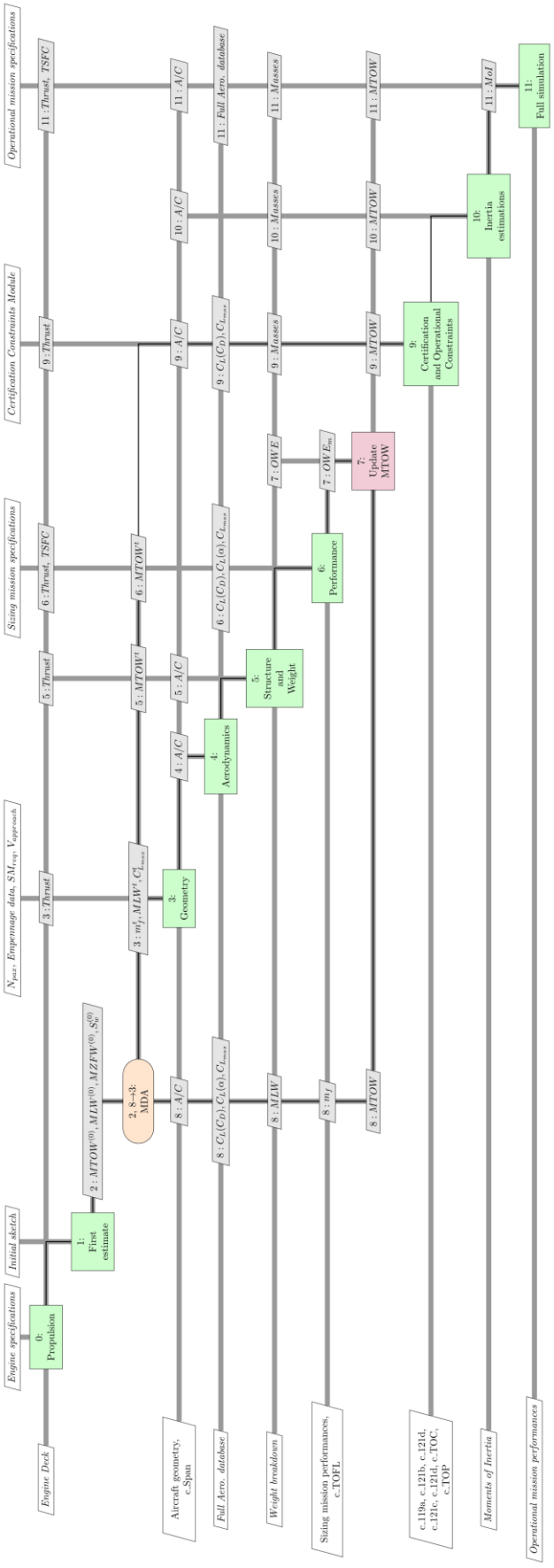

Figure 86: Multidisciplinary Design Analysis of FAST including full simulation capability (XDSM)

6. Performance. Based on a point mass analysis, the performance module computes the aircraft fuel consumption for the sizing mission based on the engine performances calculated in step 0, the MTOW value defined at the beginning of the step 2 and the aerodynamics properties of the aircraft calculated in step 4. In this module, the segment simulations based on sizing mission specifications use time step integration to better represent real trajectories. The takeoff field length that can be used as a constraint is calculated in this module.

7. Update MTOW. The objective of this function is to calculate the difference between the Operating Weight Empty taking as input the estimated fuel consumption calculated at step 6 $\left(\mathrm{OWE_m} = \mathrm{MTOW} - \mathrm{FW} - \mathrm{W_{payload}}\right)$ and the value of OWE resulting from the weight breakdown (step 5). If the difference between these 2 values is higher than a given tolerance, MTOW is updated.

8. Iteration loop. All the values calculated by the different modules are returned to the MDA so that a comparison with the target values is made (superscript t in Figure 86).

until 8-2 MDA has converged.

9. Certification and Operational Constraints. Certifications and Operational constraints defined in the CCM are assessed with the aircraft that has been sized through the Multidisciplinary Design Analysis. Thrust is provided by the Propulsion module while masses, aircraft geometric parameters and aerodynamic characteristics are provided during the last loop of the disciplinary module.

10. *Inertia estimations. Considering inputs about key subsystems position within the aircraft (the subsystem positions must be a percentage of a reference length, as the dimensions of the aircraft evolve during optimization) the geometry of the aircraft computed at step 3 and the various weights calculated during step 5, the Moments of Inertia (MoI) of the aircraft in a zero fuel weight configuration are estimated. Values in the flying configuration with fuel and payload are computed by JSBSim (the simulator used in this work and described in Section 4.3.1.)*

11. *Full simulation. With the new inputs provided by the Aerodynamics and Inertia estimations modules, the 6 DoF model can be used to simulate the aircraft motion. In addition, a Stability Augmentation System is added to increase design freedom. Finally, in order to simulate the flight trajectory, control loops are added to maintain speed, altitude and heading. Performances during the takeoff phase and initial climb are estimated with the classical point mass approach.*

4.3. Description of the new analysis tools

In the initial version of FAST, all the disciplinary analysis tools have been developed following the approaches presented in [151] mostly and also in [5] and [200]. For the new analysis tools that are mandatory to perform aircraft simulations, the choice has been made to rely on existing and available programs even if recent publications suggest newer approaches. Indeed, the objective in this PhD research is to achieve a full coupling of the diverse data to illustrate the benefits of the MDA expansion. Refinements at analysis level could be performed in other contexts. In the next paragraphs, the rationale associated to the tool selection process and a description of the selected one are provided. Naturally, the key component in the new MDA is the full simulation module. Thus, the priority has been to choose the most suitable flight dynamics model.

4.3.1. The flight dynamic model JSBSim

4.3.1.1 Selection of JSBSim

Today, flight dynamics models are available either in commercial packages [222], scientific books [223] or through open source initiatives [224]. From a technical point of view, when considering the results for a rigid aircraft, no solution stood out. Additional requirements have thus been taken into account to choose the full simulator. First, design engineers collaborate with disciplinary experts from other departments (in case of internal research projects) or other companies (in case of international collaborations) to assess or develop new aircraft configurations. Furthermore, with the idea of facilitating exchanges with ISAE-SUPAERO students, it is mandatory that tools must be easily used and installed on all contributors' computers. Naturally, as many studies concentrate on innovative architectures, the full simulator has to be flexible enough to compute the flight trajectories of many aircraft types. Also, if it is considered that the full simulator has to be integrated within an optimization loop, it must be designed to be run in an automated manner, without any Graphical User Interface (batch mode). Finally, as written in Section 1.4.4., many future concept explorations focus on hybrid propulsion systems. The full simulator must then have an open structure allowing designers to add new subsystems models without difficulties.

These specific requirements led to the selection of JSBSim [224] as the full simulator to be used in the MDA process. First of all, it is an open source model that can be installed on any computer without additional cost. Second, its structure is very flexible as it can easily manage all types of aircraft with an impressive number of subsystems. For these reasons, JSBSim has been selected as one of the flight dynamics model that is used in the open source simulator FlightGear [225]. Finally, it can be stressed that this program is fully managed through .XML files that can easily be modified during the analysis or optimization loop. The most important one is the aircraft description containing all data (aerodynamics, weight, inertia, engine name...). The engine name refers to another .XML file where the engine performances with respect to altitude and speed are stored. Last, the script enables the launch of the simulations in an automated manner for a given set of initial conditions. With so many assets, it is not surprising to see various research activities based on JSBSim [136][226].

4.3.1.2 Verification of JSBSim capabilities

In order to illustrate the good results obtained with the JSBSim flight dynamics model, an earlier work performed at ONERA in the frame of the EU project "The Endless Runway" [227] is recalled in this section. For the project goals, takeoff and landing simulations with a large passenger aircraft had to be completed. After a review of available data, the design team decided to model the Boeing B747-100. All data required by JSBSim have been extracted from a NASA report used for simulation purposes [228] and subsequently written in the input .XML file. As experimental data are also provided in [228], it has been possible to compare them with the values provided by the JSBSim simulation. Figure 87 shows the differences in Indicated Air Speed during takeoff.

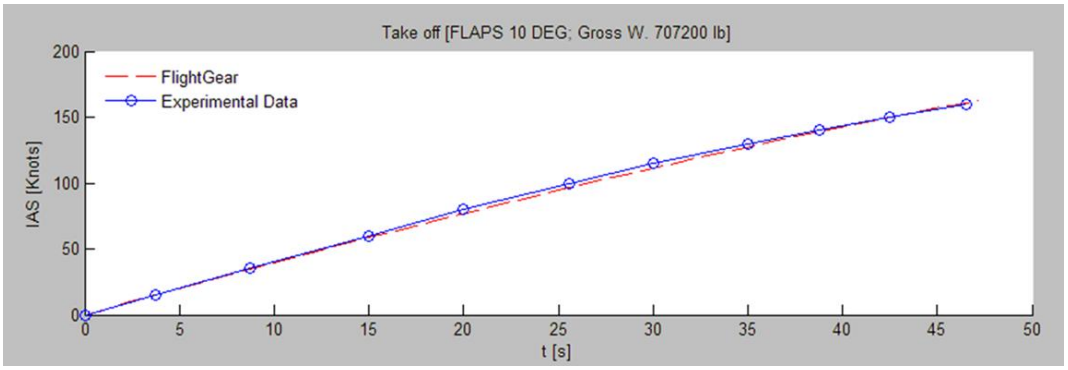

Figure 87: Comparison of Boeing B747-100 experimental data and FlightGear simulations [229]

As there are very little discrepancies on the outputs, this verification provides a positive first assessment of JSBSim capability to simulate a real takeoff. The next step consists in evaluating JSBSim's dynamic responses with respect to known flight test data. As such type of information is scarse, data provided by Hanke and Nordwall [228] on Boeing B747-100 are once again used. In their report, the longitudinal dynamic response of the transport aircraft to an equilibrium perturbation (phugoïd) is documented. It is then decided to simulate this manoeuvre with JSBSim. Using the previously generated .XML file, the conditions of the test described in [228] must be met: the Gross Weight is fixed to 710 000 lbs, the test altitude must be 5000 ft, the reference speed shall be set at 210 kt, the elevator is in a +2° position and the flaps are set up at 10 degrees. In order to achieve these stabilized conditions, two control loops have been implemented in JSBSim: the first one controls the speed through the engines throttle level while the second one controls the altitude through the stabilizer. This second closed loop might be unconventional but it was the simplest solution to match the requested Elevator deflection of +2 degrees. In JSBSim, these controllers are named "fcs/CVCH" (Cruise Vc Hold) and "fcs/CAH" (Cruise Altitude Hold) respectively. The simulator is then set to receive a set of inputs through the .XML script file to launch a given sequence of events. For such standardized simulation, the open structure of the Certification Constraints Module (Section 3.2.) is used so that the different parameters defined in the State Vector window can be associated to their JSBSim name ("AliasJSBSim" in Figure 88). Thus, by defining a list of changes in time of state vector elements (in the "DynamicManoeuvres" table shown in Figure 89), the designer automatically generates a sequence of JSBSim commands. In the end, through a simple read / write function, the .XML generated by the CCM transfers some of its data to the JSBSim script file. In this case (see Figure 89), at t=0 seconds, the elevator is set to +2 degrees, the controller CVCH is activated and it aims for a speed of 210 kt, the controller CAH is running with a target altitude of 5000 ft. At t=250 seconds, the control loops are turned off (to check the natural response of the vehicle) and the elevator is deflected to -6 degrees. Two seconds later, the elevator is back to its original position.

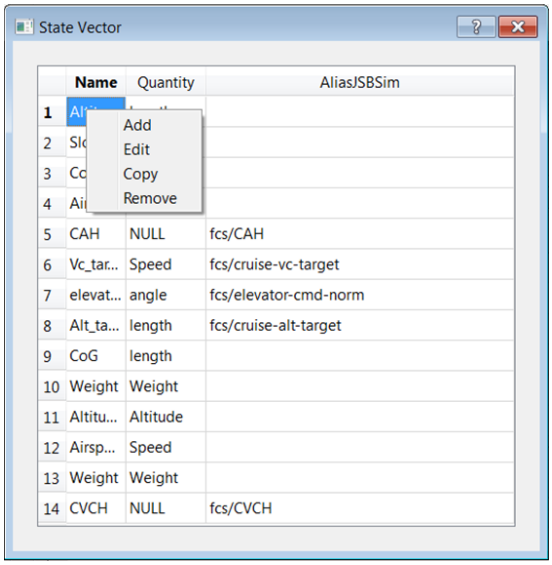

Figure 88: State Vector for the JSBSim test

DynamicManoeuvres

	Variable	Value	T
1	elevator	2	0 s
2	CVCH	1	0 s
3	Vc_target	210	0 s
4	CAH	1	0 s
5	Alt_target	5000	0 s
6	CVCH	0	250 s
7	CAH	0	250 s
8	elevator	-6	250 s
9	elevator	-2	252 s

Figure 89: Flight manoeuvre list from the Certification Constraints Module for JSBSim

The simulation obtained with JSBSim is shown in Figure 90 with a continuous line while the flight test data from NASA [228] are represented by black circles. For the different parameters of interest, there is a good match between the two curves. It can be said that JSBSim, when given a full set of aircraft characteristics, estimates reliable longitudinal responses for conceptual or even preliminary studies.

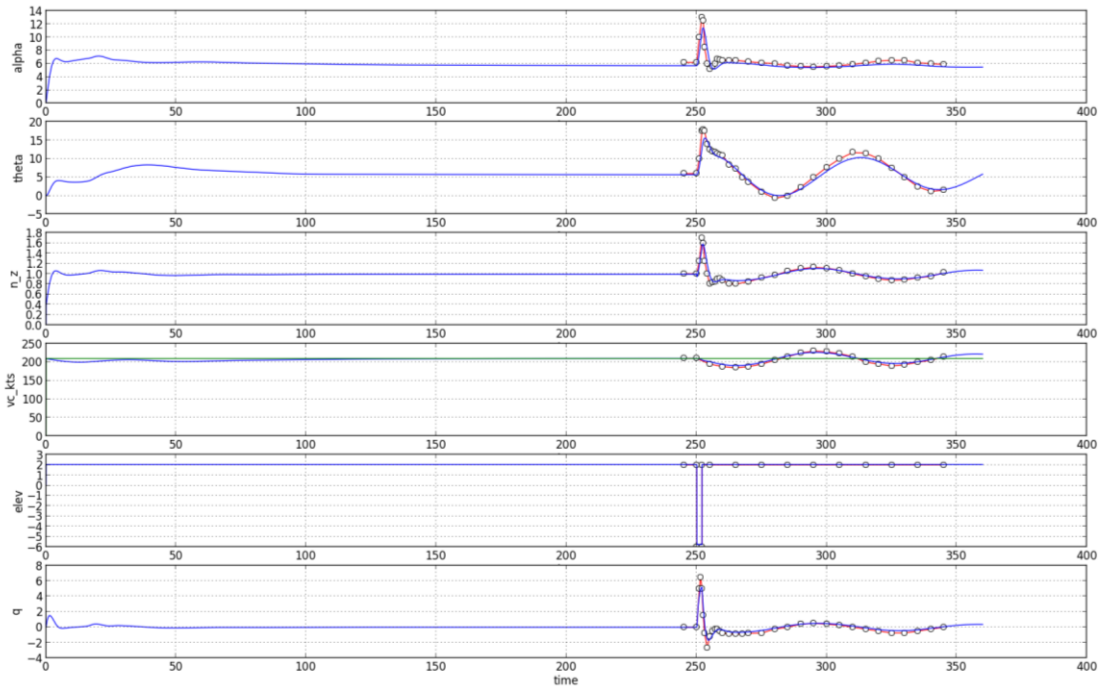

Figure 90: Outputs of JSBSim following a manoeuvre defined within the CCM (in blue) compared to flight test data (black circles)

Finally, a small Python module has been written to automatically analyze the outcomes of JSBSim in an approach that is more associated to Flight Test Engineering than Aircraft Design where data are calculated through a post-processing of flight simulations. For this reference case, the module

calculates a damping ratio for the phugoïd of 0.057 thus indicating that the Boeing B747-100 has Level 1 characteristics according to [130]. This simple example illustrates how JSBSim and the CCM could be used to assess flying qualities of the aircraft directly within the sizing loop.

4.3.2. The Aerodynamics analysis tool DATCOM

In FAST, the basic Aerodynamics analysis module relies on an analytical approach that provides reliable results for classical transport aircraft configurations (see Section 3.3.3.). Unfortunately, it cannot be used for full simulation models where a complete aerodynamic database (three moments, three forces) including dynamic derivatives and control surface effects is needed. In [125], Chudoba identified possible aerodynamics tools that could supply the mandatory data to the 6 DoF aircraft model with a final recommendation for VORSTAB [230]. For conceptual design studies, Digital DATCOM [231], AVL [232] and Tornado [233] are also capable of generating a complete aerodynamic dataset. To better assess the capabilities of these tools and their possible coupling in a MDA process, Cöllen [234] made an extensive comparison of the available codes for different aircraft configurations for which wind tunnel test data were available. Overall, VORSTAB demonstrated high accuracy with respect to experimental data and a very good prediction of nonlinear effects. However, its implementation in an automated design process is very complex. AVL on the other hand provides reliable estimations in the linear domain only (limitation directly associated to the Vortex Lattice method that is implemented). When focusing solely on conventional configurations, DATCOM - a semi-empirical method - demonstrated very good estimations including nonlinear effects (values can diverge after a certain angle of attack), an easy implementation in an automated process and low computational time. As stated previously, the goal of this thesis is to assess the added value of the MDAO expansion capabilities. An assessment on classical configuration as it has been performed in chapter 3 is thus considered sufficient. Taking into account this approach, it is decided to implement Digital DATCOM [231] as the Aerodynamics analysis tool within FAST. To ease the coupling of Digital DATCOM with the existing Python modules of FAST and the flight dynamic model JSBSim, the program DATCOM+PRO [235] has been used. This modified version of the original code has indeed interesting features: first, it offers the possibility to visualize the aircraft model that is actually analyzed in 3D (see Figure 91).

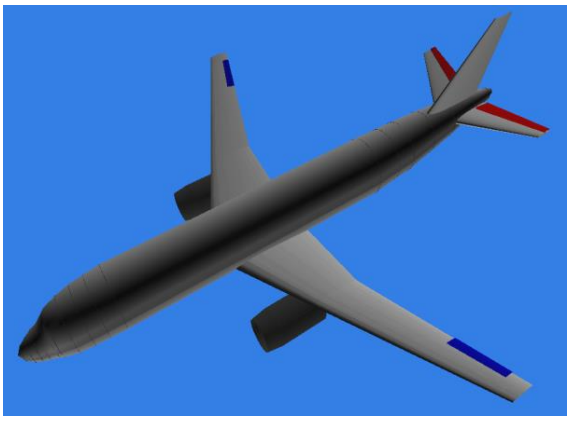

Figure 91: 3D model of the aircraft generated by DATCOM+PRO (control surfaces are highlighted)

Disabled when used in an automated process, this option is useful during the prototyping phase of the complete process to make sure that parameters of the reference .XML file of FAST are correctly transferred to the disciplinary module. Second, DATCOM+PRO automatically generates all aerodynamic properties under the JSBSim structured format. As Python can easily parse an .XML file, the coupling with FAST is straightforward. It is worth noting that the original DATCOM does not compute rudder effects. In DATCOM+PRO, a default value to be used by JSBSim is provided (further verifications should be carried out to assess the resulting value for different types of aircraft).

4.4. The new Aerodynamics module

Regarding the new Aerodynamics module, the idea is to use DATCOM+PRO as a numerical wind tunnel to generate the complete aircraft database. The geometry parameters stored in the reference .XML file including control surfaces geometry and information about the flight domain for the mission of interest (altitude, flight Mach number) are processed by a Python function that automatically generates many DATCOM+PRO input files under the required format (.DCM). The number of files depends on the configurations to be computed. After launching DATCOM+PRO, all results are stored in many .XML files identified by the suffix "_AERO" in the name. This initial sequence is illustrated in Figure 92 where the overall use of DATCOM+PRO is detailed.

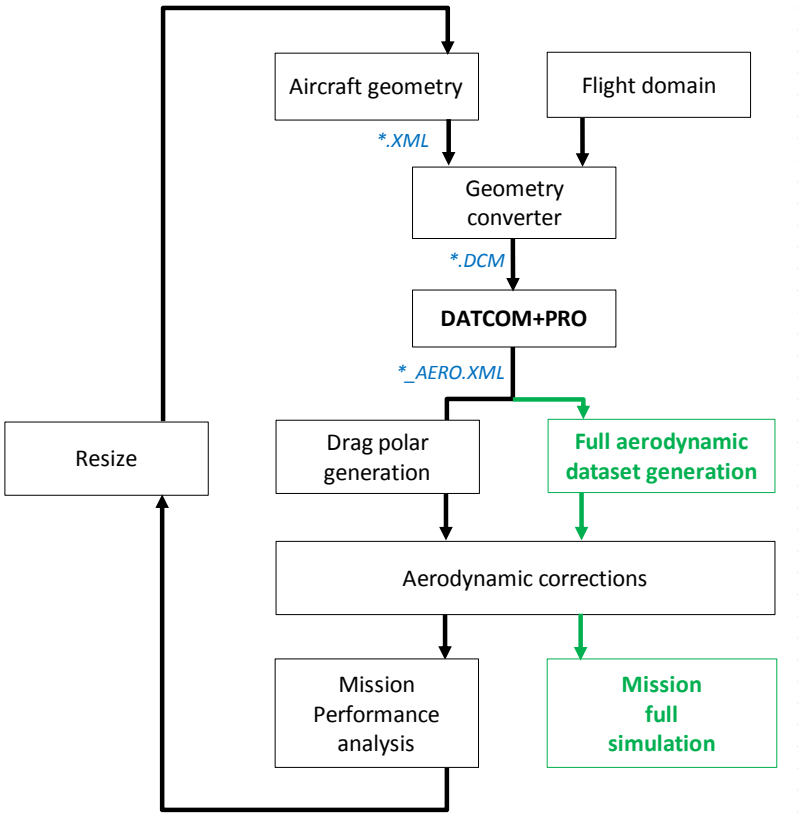

Figure 92: Use of DATCOM+PRO within the MDA (green boxes are performed only after completion of the sizing loop)

The next step consists in post-processing the important aerodynamic database available in these _AERO.XML files. At this stage, it must be noted that the resulting dataset is treated differently if the aircraft sizing is completed or not. This can be seen in Figure 92 where the steps associated to the sizing loop are colored in black while green boxes are performed only for a converged aircraft.

For the sizing loop, the requirement on the new Aerodynamics module is to provide the same type of information as before in order to minimize changes within the different modules of FAST. Thus, as the mission performance module detailed in Section 3.3.2. is based on the use of drag polars, a first post-processing routine extracts a set of drag polars for given altitudes and given Mach numbers from the various _AERO.XML files. In a subsequent step, the drag coefficients are corrected to increase the analysis accuracy. Indeed, DATCOM+PRO computes the aerodynamic coefficients for a configuration made of fuselage, main wing and HTP only. Penalties in terms of zero lift drag associated to the Vertical Tail Plane, the nacelle and the engine pylons must be taken into account. As transonic computations with DATCOM+PRO required additional rare data on the airfoil characteristics, it has been decided in this research to run DATCOM+PRO with subsonic methods only. Thus, an increase of Drag due to compressibility must also be added. Finally, as in the standard FAST aerodynamics module, the effects associated to the aircraft trim are translated into a Drag penalty. In the end, the corrected Drag coefficient can be expressed as follows:

$$C_{D\,Total} = C_{D\,wbh} + C_{D0\,nacelle} + C_{D0\,pylons} + C_{D0\,VTP} + C_{D\,compressibility} + C_{D\,trim}$$

where $C_{D\,Total}$ is the total Drag coefficient to be considered in the performance analysis;

$C_{D\,wbh}$ is the Drag coefficient computed by DATCOM+PRO with subsonic methods;

$C_{D0\,nacelle}$ is the zero lift Drag coefficient associated to the nacelle (computed as in the standard aerodynamics module of FAST according to [151]);

$C_{D0\,pylons}$ is the zero lift Drag coefficient associated to pylons (computed as in the standard aerodynamics module of FAST according to [151]);

$C_{D0\,VTP}$ is the zero lift Drag coefficient associated to the Vertical Tail Plane (computed as in the standard aerodynamics module of FAST according to [151]);

$C_{D\,compressibility}$ is the compressibility Drag coefficient (computed as in the standard aerodynamics module of FAST according to [151]);

$C_{D\,trim}$ is the trim Drag coefficient (computed as in the standard aerodynamics module of FAST according to [151]).

With the Drag coefficients corrected, an interpolation function is created so that the Mission performance analysis can quickly compute the Drag coefficient associated to a certain Lift coefficient for a given Mach and a given altitude. Following the FAST MDA logic detailed in Section 3.3.2., this process is repeated until convergence on the values of Operating Weight Empty is achieved (see left part of Figure 92). To illustrate the results obtained with the new aerodynamics module, Figure 93 shows the computed high speed drag polar and other curves from various references. As expected, the basic computations provided by DATCOM+PRO with subsonic methods do not consider the

compressibility effects. As observed in the figure, the correction $C_{D\ compressibility}$ properly modifies the drag polar shape and the result is very close to the CeRAS data [157] and the values obtained with the classical aerodynamics module of FAST (Section 3.3.2.). Looking at the zero lift Drag coefficient, it can be concluded that DATCOM+PRO is slightly more conservative than the approach proposed in [151] (and coded in FAST) when assessing the wing, body and HTP configuration.

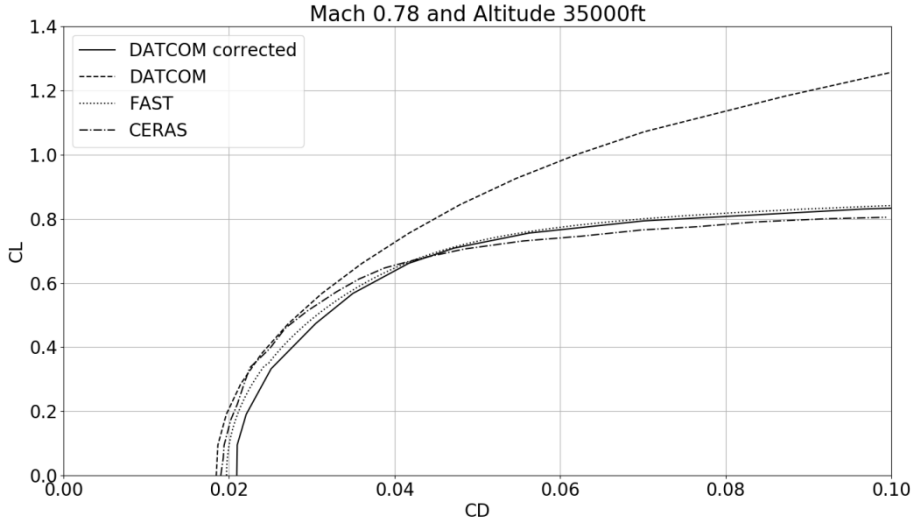

Figure 93: Drag polar comparison showing the curves obtained with the new aerodynamics module (DATCOM corrected) - high speed

When convergence for OWE is reached, the aircraft is considered as sized. The FAST MDA naturally proceeds with the steps 9, 10 and 11 illustrated in Figure 86. For step 11 that corresponds to the full simulation of the operational mission, the new Aerodynamics module merges all the available data in the various _AERO.XML files so that a complete aerodynamic dataset can be provided to JSBSim to carry out the full simulation. Corrections applied for the sizing loop are also applied to this set of data except $C_{D\ trim}$ (see Figure 92). To provide a better understanding of the overall dataset structure, Table 18 and Table 19 detail all coefficients generated through DATCOM+PRO that are used to compute the total force and moment coefficients.

Table 18: Decomposition of the aerodynamic force coefficients provided to JSBSim

Total Lift coefficient C_L	**Total Drag coefficient C_D**	**Total Side force coefficient C_Y**
$C_{L\ wbh} = f(\alpha, h, M, \delta_{stab})$	$C_{D\ wbh} = f(\alpha, h, M)$	$C_{Y\ \beta} = f(\beta)$
$C_{L\ q} = f(\alpha, h, M)$	$C_{D\ gear} = constant$	
$C_{L\ \dot{\alpha}} = f(\alpha, h, M)$	$C_{D\ compressibility} = f(C_L, M)$	
$C_{L\ \delta_e} = f(\delta_e, h, M)$	$C_{D0\ correction} = f(h, M)$	
	$C_{D\ \delta_e} = f(\alpha, \delta_e, h, M)$	

Table 19: Decomposition of the aerodynamic moment coefficients provided to JSBSim

Total Rolling moment coefficient C_l	**Total Pitching moment coefficient C_m**	**Total Yawing moment coefficient C_n**
$C_{l\,\beta} = f(\beta)$	$C_{m\,wbh} = f(\alpha, h, M, \delta_{stab})$	$C_{n\,\beta} = constant$
$C_{l\,p} = constant$	$C_{m\,q} = f(\alpha, h, M)$	$C_{n\,r} = constant$
$C_{l\,r} = constant$	$C_{m\,\dot{\alpha}} = f(\alpha, h, M)$	$C_{n\,\delta_r} = constant$
$C_{l\,\delta_a} = constant$	$C_{m\,\delta_e} = f(\delta_e, h, M)$	
$C_{l\,\delta_r} = constant$		

In the definition of the new Aerodynamics module, efforts have been made in order to achieve consistency between the drag polars used during the sizing loop and the dataset to be used for full simulation. As the classical performance analysis in FAST is carried out in the longitudinal plane, the lateral-directional coefficients have not been a point of study. As shown in Table 18 and Table 19, the result is that only the longitudinal coefficients benefit from the large database computation made with DATCOM+PRO. For Side force, Rolling moment and Yawing moment, the JSBSim model uses the existing aerodynamic data from the Airbus A320 model provided by FlighGear [225].

The standard Aerodynamics module of FAST estimates the high lift characteristics of the airplane through a rapid analytical approach [151]. When DATCOM+PRO has been used to compute maximum lift coefficients for takeoff, approach and landing phases, results were not satisfactory: first, there was a postprocessing error when generating the _AERO.XML file that has been corrected by the software supplier. Second, the code was not providing all necessary effects (variation in zero lift drag generated by slats). After different revisions, a consistent set of drag polars for the high lift devices configurations have been defined (see Appendix D). However, the variations in performance with respect to the original FAST results were too high to use the DATCOM+PRO outcomes in the sizing loop. Indeed, the variations in the maximum lift coefficient for landing configuration would change the size of the wing and initiate a snowball effect affecting the final vehicle. Thus, it has been decided that the new Aerodynamics module would keep the original approach to compute the performance of high lift devices. Nevertheless, for a given aircraft, it would be possible to use the DATCOME+PRO data for detailed simulations of the takeoff and landing phases.

With the new Aerodynamics module finalized, a full sizing of the aircraft has been performed (from step 0 to step 9 in Figure 86). Given the small variations of the Lift and Drag coefficients, very small differences in terms of fuel consumption are noted. Taking into account that the maximum lift coefficient for landing configuration is not modified, the resulting aircraft features negligible differences with the one presented in Section 3.3.3. Therefore, it is possible to use the new Aerodynamic module either for sizing or performance analysis, ensuring a consistent level of fidelity throughout the process.

4.5. The Inertia estimation module

The calculation of inertia properties of a vehicle is a classical step in the aircraft design process. It is usually performed at the beginning of the preliminary design phase, when the architecture is almost frozen for control system assessments [34]. At this point, given the large number of inputs about the different components, industry CAD systems [236] can easily and quickly derive the inertia properties. FAST, on the other hand, is a tool dedicated to early sizing and exploration at conceptual level. Thus, very little information is available in terms of structural architecture and internal layout to estimate moments of inertia. One option could be the use of analytic relationships between key aircraft parameters and statistical data as presented by Risse [136] but the uncertainty could be quite high in the case of disruptive concepts. In this research, it is proposed to follow another approach that relies on designer's inputs, the available FAST mass breakdown (see Appendix E) and a 3D model. In terms of implementation, as OpenVSP [19] is already included within FAST to visualize the aircraft resulting from the sizing process, it is decided to use its capabilities to calculate Moments of Inertia (MoI). The generic method implemented in the Inertia estimation module (written in Python) offers an acceptable compromise between the level of details to be managed during the sizing process and the result accuracy. It is based on an automated allocation of the aircraft component masses identified in FAST to specific volumes (existing or new) or to specific point masses within the OpenVSP model. The programmed generations and placements of elements are based on a large number of variables that are available either in the .XML file of FAST or in the .vsp3 file generated by OpenVSP. The refined parametric digital mock-up of the aircraft and its subsystems is then analyzed by the Mass Properties feature of OpenVSP to determine the Moments of Inertia.

As a first step, seven aircraft components have been identified as point masses for the inertia properties computations (see Table 20). Subsequently, to define their position within the OpenVSP 3D model, the coordinate along the X axis starting from the nose (see Figure 94) is already available in FAST [151]. However, hypothesis on their position with respect to the Y and Z axes (see Figure 94) must be made.

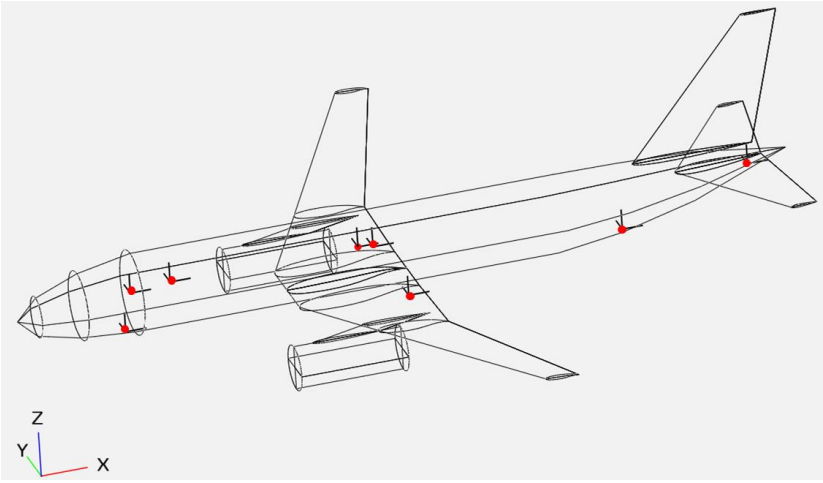

Figure 94: Visualization under OpenVSP of the aircraft point mass elements for a generic Small Medium Range aircraft

Regarding the Main Landing Gear (component A51) its coordinate along the Z axis is associated to the main wing position. Thus, it is assumed that the location along Z is the same as the main wing (the reference point is the leading edge in the symmetry plane, identified as $ZLoc_{wing}$). For the position along the Y axis of the aircraft, the value y_{A51} is taken from the ISAE-SUPAERO design class handout [151].

$$y_{A51} = \pm 1.30 \times D_{nac}$$

where D_{nac} is the maximum diameter of the nacelle.

As the Nose Landing Gear (component A52) is located in the symmetry plane of the aircraft, $y_{A52} = 0$. For the position along Z, this component can be found near the fuselage bottom surface after the cylindrical part. At this station, the diameter is slightly reduced with respect to the reference value used for the cabin. Thus, the coordinate z_{A52} is defined as follows:

$$z_{A52} = -0.95 \times \frac{h_{fuselage}}{2}$$

where $h_{fuselage}$ is the maximum height of the fuselage.

The review of various cutaways related to recent civil transport airplanes [238][239][240][241] and the information available in reference aircraft design books [24][35] confirmed that the Auxiliary Power Unit (APU) is in most cases located in the tail cone within the symmetry plane ($y_{C11} = 0$). For the position along the Z axis (z_{C11}), the valuable variable to be used is the position along the vertical axis of the penultimate section of the fuselage ($z_{fuselage\ section}$), the last one being a point to close the volume. A margin of 20% is taken above this value to make sure that the APU always remains within the external shell of the vehicle. z_{C11} is thus defined by the following equation:

$$z_{C11} = 1.2 \times z_{fuselage\ section}$$

where $z_{fuselage\ section}$ is the coordinate along Z of the penultimate section of the fuselage.

For crew accommodation, some seats have to be installed in the cabin depending on the mission Top Level Aircraft Requirements. Preliminary estimations made within the Inertia estimations module consider that these seats are within the symmetry plane. This leads to fixing y_{C25} to 0. For the position along the Z axis, the proposed hypothesis is to consider the seats at the cabin floor level. This same vertical coordinate is used for item C6 “Flight kit” that has a spanwise coordinate $y_{C6} = 0$. After a review of different fuselage cross sections [29][151], the seats’ position is defined as:

$$z_{C25} = z_{C6} = \frac{h_{fuselage}}{2} + 0.6 + h_{cargo}$$

where $h_{fuselage}$ is the maximum height of the fuselage;
h_{cargo} is the height of the cargo hold within the fuselage.

The last two elements within the mass breakdown of FAST to be considered as point masses are items C3 "Instruments and Navigation" and D3 "Catering equipment, water supply". Equipment as C3 are usually located in front of the cockpit in the lower part of the nose. Thus, the coordinates have been fixed to $y_{C3} = 0$ (in the symmetry plane) and to $z_{C3} = 0$. For D3, the water tank is usually located in the lower rear part of the fuselage (also assuming $y_{D3} = 0$). Once again, the parameter of reference taken in this case is the maximum height of the fuselage which leads to:

$$z_{D3} = -0.7 \times \frac{h_{fuselage}}{2}$$

where $h_{fuselage}$ is the maximum height of the fuselage.

The X, Y and Z coordinates for the different elements considered as point masses in this analysis are reported in Table 20, knowing that L_{AV} is the length of the front part of the fuselage before it becomes cylindrical and $L_{fuselage}$ is the total length of the fuselage.

Table 20: Positions of the point mass elements in the OpenVSP reference frame

Aircraft component		X coordinate	Y coordinate	Z coordinate
A51	Main Landing Gear	Associated to the sizing loop	$\pm 1.30 \times D_{nac}$	$ZLoc_{wing}$
A52	Nose Landing Gear	$0.75 \times L_{av}$	0	$-0.95 \times \frac{h_{fuselage}}{2}$
C11	APU	$0.95 \times L_{fuselage}$	0	$1.2 \times z_{fuselage\ section}$
C25	Seats (crew accommodation)	Depending on cabin layout	0	$-\frac{h_{fuselage}}{2} + 0.6 + h_{cargo}$
C3	Instrument and navigation	$0.8 \times L_{av}$	0	0
C6	Flight Kit	Depending on cabin layout	0	$-\frac{h_{fuselage}}{2} + 0.6 + h_{cargo}$
D3	Catering eq., water supply	Depending on cabin layout	0	$-0.7 \times \frac{h_{fuselage}}{2}$

The second step towards the estimation of the Moments of Inertia is the association of some elements of the mass breakdown to existing geometries and their associated volume within the OpenVSP model generated by FAST. This is the case for the wing (A1), the empennage (A31 for HTP and A32 for VTP) and the pylons (A6). For the propulsive system, it has been decided to affect three elements of

the mass breakdown (B1 Installed engines, B2 Fuel and oil systems, B3 Unusable oil and fuel) to the volume representing the engines in the digital mock-up. As components of B2 (fuel system) are installed within the wing, such choice leads to approximations regarding the Moments of Inertia. However, as explained in the introductory paragraph associated to the Inertia estimations module, the objective is to find a good compromise between accuracy and complexity for conceptual design studies. For B2, it would take a non-negligible effort to derive the mass of each subsystem and then to affect these results to specific geometries in OpenVSP. After the association of masses and component volumes, a density is calculated for each volume representing one or more components. As an example, the density formula for the engine is:

$$\rho_{engine} = \frac{m_{B1} + m_{B2} + m_{B3}}{V_{engine} \times n_{engine}}$$

where ρ_{engine} is the density of the OpenVSP object representing 1 engine in kg/m^3
m_{B1} is the calculated mass by FAST for the installed engines in kg;
m_{B2} is the calculated mass by FAST for the Fuel and oil systems in kg;
m_{B3} is the calculated mass by FAST for the Unusable oil and fuel in kg;
V_{engine} is the volume of the OpenVSP object representing 1 engine in m^3;
n_{engine} is the number of engines.

Another key element of the aircraft that is not yet taken into account is the fuselage. For this component, the structural layout of today's transport aircraft is relying on formers, stringers and outer skin. Therefore, to compute its Moment of Inertia, the fuselage is treated as a hollow element. This translates into activating the "Thin Shell" flag in OpenVSP and calculating an area density instead of the aforementioned density:

$$\rho A_{fuselage} = \frac{m_{A2}}{A_{fuselage}}$$

where $\rho A_{fuselage}$ is the area density of the OpenVSP object representing the fuselage in kg/m^2;
m_{A2} is the calculated mass by FAST for the fuselage in kg;
$A_{fuselage}$ is the total area of the fuselage in m^2.

The following phase towards the computation of the Moments of Inertia is the creation of new volumes in the OpenVSP model to take the remaining components of the mass breakdown into account. After exploring different options, only 8 additional elements have been generated (see Figure 95):

- One volume V_1 representing systems distributed along the fuselage. Elements of the mass breakdown affected to this object are A4, C12 and C13 (see Appendix E);
- Two volumes V_2 and V_3 representing systems distributed from the engine to the fuselage. Elements of the mass breakdown affected to this object are A4, C12 and C13 (see Appendix E);

- Two volumes V_4 and V_5 representing systems distributed along the wing. Elements of the mass breakdown affected to this object are A4, C12, C13 and C23 (see Appendix E);
- Two volumes V_6 and V_7 representing the cargo containers. The element affected to this object is D1;
- One volume V_8 representing systems associated to the cabin. Elements of the mass breakdown affected to this object are C21, C22, C24, C26, C27, C4, C5, D2, D4, D5, E (see Appendix E). It must be noted here that element G of the mass breakdown (the payload) is not considered in this presentation of the module as validation data correspond to an aircraft without payload.

Volumes V_1, V_2 and V_3 are partially representing systems that will distribute electricity (C12), hydraulics (C13) and controls (A4) within the aircraft. Therefore, the Inertia estimations module arranges them within the aircraft through an overall cross shape geometry to cover the distribution along the fuselage (V_1) and the partial distribution from the engines to the fuselage (V_2 and V_3). In this approach, volumes V_4 and V_5 allocate the other portion of C12, C13 and A4 within the geometry of the vehicle. More importantly, they have to assign the de-icing system along the leading edge to increase the accuracy of the Moments of Inertia calculation. Therefore, scripts have been defined in OpenVSP so that these volumes rotate along a reference point to match the leading edge sweep angle.

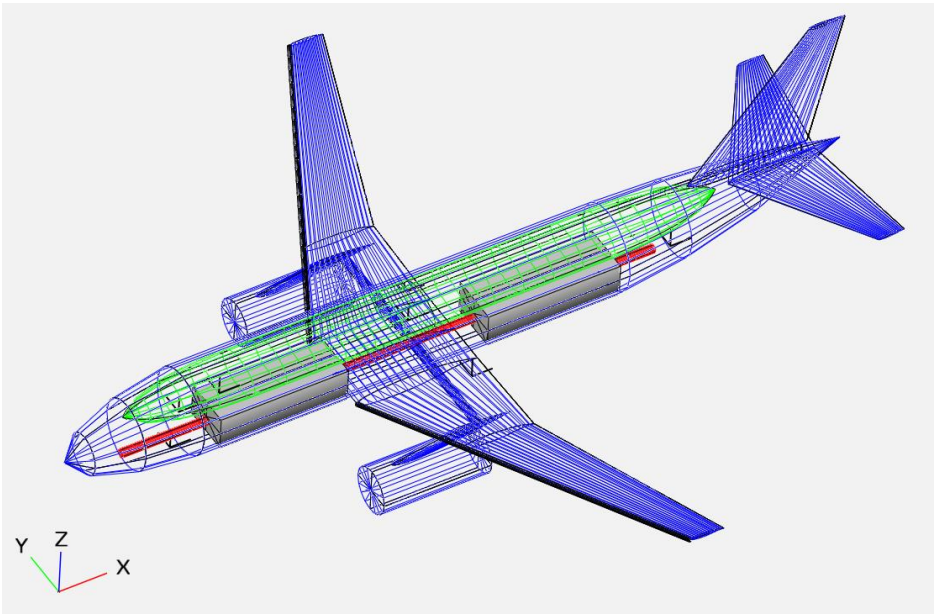

Figure 95: OpenVSP model including the new volumes representing mass distribution (V_1 is highlighted in red, V_2 and V_3 are colored in blue, V_4 and V_5 are represented in black, V_6 and V_7 are the grey blocks while V_8 is shown in green)

For the cargo hold volumes V_6 and V_7, their positions in the longitudinal plan and their sizes are the result of the overall fuselage shape constrained by the cabin sizing and some assumptions concerning the cargo hold floor [29]. The last volume to be considered in this study is V_8 and it is clearly associated to items within the mass breakdown that are located in the vicinity of the cabin. Thus, a specific volume that conforms to the upper half part of the cabin in a parametric manner, so that

changes during the sizing process could be automatically handled, has been defined in OpenVSP. As previously stated, all the reference parameters or variables that have been used to both define these volumes and place them within the aircraft outer shell can be found either in the .XML or the .vsp3 files available in FAST. As soon as the volumes and the associated masses are fixed, the density to be considered for MoI estimations can be computed:

$$\rho_V = \frac{\sum_{i=1}^{n} m_i}{V}$$

where i indicates an element from the mass breakdown;
ρ_V is the density of one OpenVSP object in kg/m^3;
m_i is the mass calculated by FAST for component i that is affected to volume V in kg;
V is the total volume of the OpenVSP objects considered for a given set of elements in m^3.

Of course, the calculation of this density ρ_V has to take into account the fact that elements of the mass breakdown can be affected to various volumes (A4, C12 and C13 for example).

The final step before computing the MoI concerns the priority management within OpenVSP. This feature is available in order to set the density of a volume that is the intersection of two objects. Effectively, when calculating the mass properties, OpenVSP affects the density of the volume with the highest priority to the intersecting volume. In the end, the maximum priority (level 2) has been given to V_1, V_2, V_3, V_4, V_5 and V_8. A priority level of 1 is set for V_6 and V_7. All remaining objects within the OpenVSP model have a priority level of 0. With all the elements of the aircraft mass breakdown represented through volumes or point masses in the 3D mock-up, MoI can be calculated. Table 21 presents the differences calculated between the outcomes of the Inertia estimations module and data from a reference airplane in an Empty Weight configuration (no fuel, no payload) used in the frame of the Clean Sky 2 program [193]. An under estimation of the MoI is noted but the variations are considered acceptable for conceptual design trade studies. Possible changes within the Inertia estimations module have been explored and it has been clearly identified that the current approach is not accurate enough regarding the systems distribution along the fuselage (and the associated volumes). Improvements can be achieved but at the cost of an important increase in complexity: more data to better allocate the items would be required and a more detailed mass breakdown than the one presented in Appendix E would be needed. Moreover, Moments and Products of Inertia only play a role in dynamic aspects. Thus, limited errors in the estimation should not have a strong impact on the outcomes of conceptual studies.

Table 21: Differences regarding Moments of Inertia for a single aisle transport aircraft (with respect to ONERA internal reference)

I_{xx}	-8.7 %
I_{yy}	-14.1%
I_{zz}	-14.6%
I_{xz}	-5.3%

4.6. Full simulation module

4.6.1. Definition of the control system

Before the full simulation can be executed with JSBSim, the Stability Augmentation System and control laws enabling the aircraft to fly automatically a given mission based on high level order must be defined. Usually, these aircraft systems are taken into account much later in the design process and their design is performed by specialists that define robust, efficient but also complex solutions. Within FAST, the control laws must be kept as simple as possible so that aircraft designers can easily understand the impacts of the different feedback loops. For this reason, it was decided to implement very simple laws that are published in reference textbooks by Stevens [242] or Nelson [243].

The first components of the control system that have been defined are Stability Augmentation Systems (SAS). For the stability in Pitch, the selected structure is the one proposed by Stevens [242] with two proportional feedbacks acting directly on the elevator actuator: one related to the angle of attack and one associated to the angular velocity *q* around the aircraft Y axis (see Figure 96). For roll and yaw stability augmentation, the proportional feedback on the angular velocity *p* around the X axis (see Figure 96) is associated to the ailerons deflection while the proportional feedback on the angular velocity *r* around the Z axis (see Figure 96) is affecting rudder movements.

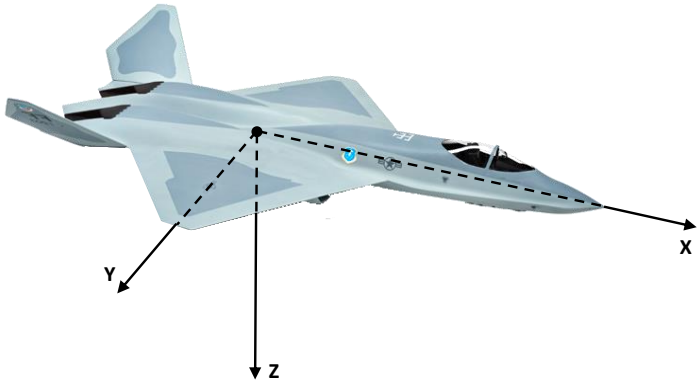

Figure 96: Reference body axes

Autopilot features have been added to this basic system, so that the aircraft can maintain a certain speed while climbing. As the sizing mission defined within FAST considers climb phases at constant CAS (the first one at a CAS of 250 kt and the second one at a CAS of 300 kt), a control loop enabling such speed holding is defined (see Figure 97). The logic is that given a fixed throttle setting and a target CAS, the control system finds the corresponding position of the elevator.

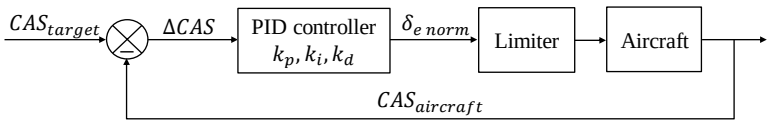

Figure 97: Speed hold control system for climb phases (constant CAS)

Always with the idea of reproducing the climb profile of the sizing mission in FAST, a similar control system is implemented to climb at constant Mach number after passing the crossover altitude up to the cruise altitude. Figure 98 details the selected scheme.

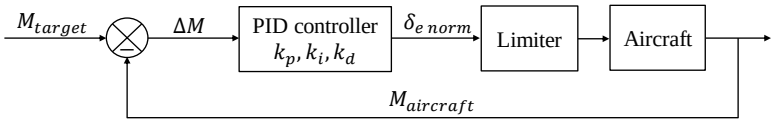

Figure 98: Speed hold control system for climb phases (constant Mach)

As soon as the aircraft reaches this cruise altitude, new holding control loops are implemented. As proposed by Nelson [243], the speed is controlled by the throttle position while the altitude is achieved by elevator deflections. Both control systems that need to be activated concurrently are illustrated in Figure 99. The option to control the cruise speed through CAS has been implemented as this solution proved to be more robust than the same architecture with a control in Mach.

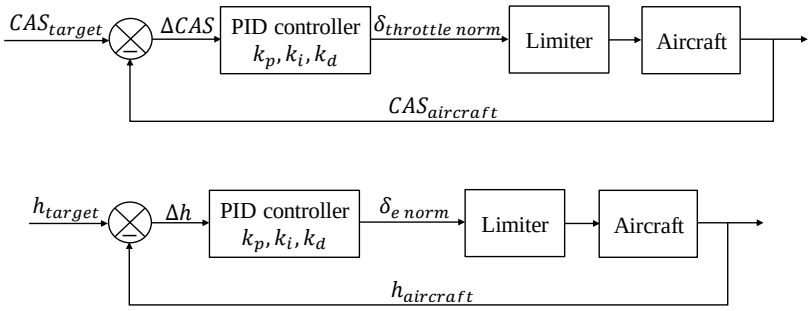

Figure 99: Speed hold (top) and altitude hold (bottom) control systems for cruise phase

Last, ATM simulations require heading hold capabilities to follow specific routes. Therefore, such a control system has been implemented in JSBSim. The idea is to convert a difference in heading into a roll angle target (indicated as ϕ_{target} in Figure 100). The difference between this roll angle target and the actual roll angle of the aircraft is given to the PID controller which provides an aileron deflection. In the architecture proposed by Stevens [242], an additional third step is added so that the ailerons control the angular velocity *p* around the X axis. With such a structure, trajectories are smoother as the angular velocity is controlled but the tuning of the PID controllers for all three layers turned out to be too complex.

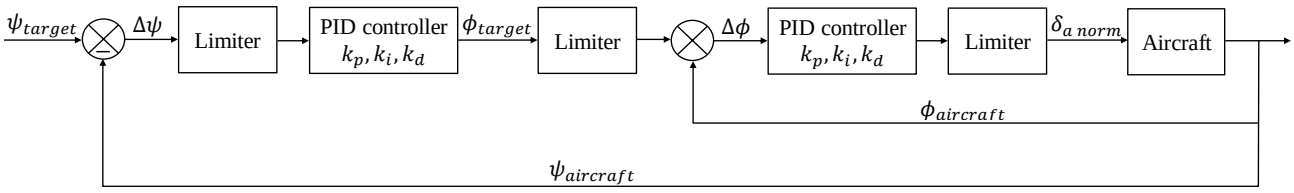

Figure 100: Heading hold control system (for all segments)

With the definition of the control system completed, all the necessary data to build the JSBSim model are available.

4.6.2. Results of the full simulation model

The .XML file defining the JSBSim aircraft model is about 3500 lines. For the reference aircraft that has been generated within the MDA tailored to full simulations, the corresponding file is made of 8 main parts, each defined by a start-tag and an end-tag.

- Fileheader
  The fileheader allows authors of the .XML file to provide information about the aircraft model. Some notes, generally about the sources used to derive the aircraft characteristics, can be also stored.
- Metrics
  In this section, some key geometric values are defined. Also, conversion factors between units can be specified. Such utility can be useful in later sections to convert radians into degrees or vice-versa. More importantly, it is in the geometry section that the reference point for the aerodynamic dataset is written (to avoid issues, the reference point used for DATCOM+PRO computations is automatically reported).
- Mass balance
  This group is dedicated to all information related to masses, position of the center of gravity, moments and products of inertia as well.
- Ground reactions
  In this part, designers indicate at first the characteristics of the landing gears (position along X, Y and Z, friction level…). Second, other points of the aircraft that may touch the ground during operations must be indicated (e.g. the lower part of the fuselage where tail strike could occur). This information is used by the flight dynamics model to assess when the airframe touches the ground, voluntarily or not.
- Propulsion
  This section of the .XML file is dedicated to all data related to the engines. First, the engine name is provided. When the simulation is launched, JSBSim will look for the corresponding engine .XML file that shares this same name. It is in this engine file that the performances in terms of thrust and fuel consumption are indicated. In addition to the engine name, the propulsion section of the aircraft file provides the engine position and orientation (e.g. toe-in or toe-out).
- Flight control
  This set of data regroups all the necessary functions that define the control laws presented in Section 4.6.1. The initial step consists in setting up the various feedback loops that will affect movable deflections to control the aircraft around the three axes. Second, the PID controllers with gains are implemented according to JSBSim structure.

- Aerodynamics
  In this part of the aircraft .XML file, the aerodynamics database generated with DATCOM+PRO is reported. Total coefficients are computed for Lift, Drag and Sideforce as well as for Rolling, Pitching and Yawing moments (see Table 18 and Table 19). Subsequently, the actual forces and moments are computed on the corresponding reference point considering dynamic pressure and the reference wing area. In the case of the reference aircraft computed with FAST, the complete aerodynamic dataset is about 2000 lines.
- Output
  In this last section of the JSBSim aircraft model file, designers can specify all outputs of the simulation that need to be recorded for later analyses. To setup the full simulation capability, about 130 outputs were necessary to make the appropriate verifications, especially to monitor the control system actions.

In this research, the objective is to show that FAST is able to reproduce accurately real flight trajectories. Thus, only the relevant data for this demonstration have been computed by FAST and transferred to these 8 sections of the JSBSim model. Other values among the 3000 lines that do not have an impact on the simulation results have been implemented manually once.

When the aircraft and engine .XML files are completed, the simulation is initiated through a Python module that launches a JSBSim script. Also under the .XML format, this file provides a sequence of high level commands describing the mission profile. It is important to note that with the control laws that have been implemented in JSBSim, it is possible to fly a full simulation with the same inputs as for the sizing mission used for the aircraft sizing loop by FAST (e.g. the aircraft climbs at a constant CAS for a given throttle level). The results of the JSBSim simulations are illustrated in the next two figures. In Figure 101, the resulting trajectory following different climb objectives (constant CAS and constant Mach) and featuring change in altitude during cruise is illustrated. In the trajectory plot, two interesting areas are visible: first, there is the acceleration phase from 250 kt to 300 kt (CAS) between 200 and 300 seconds. Second, it is possible to observe the change in the climb trajectory when the control system switches from a constant CAS law to constant Mach law. For cruise, it can be observed that the altitude is well maintained. In the original FAST mission profile, the acceleration from 250 kt to 300 kt is performed during a very short level flight segment. In case of the full simulation the duration of the level flight caused issues with the control laws. Thus, the acceleration is directly done during climb as in real flights.

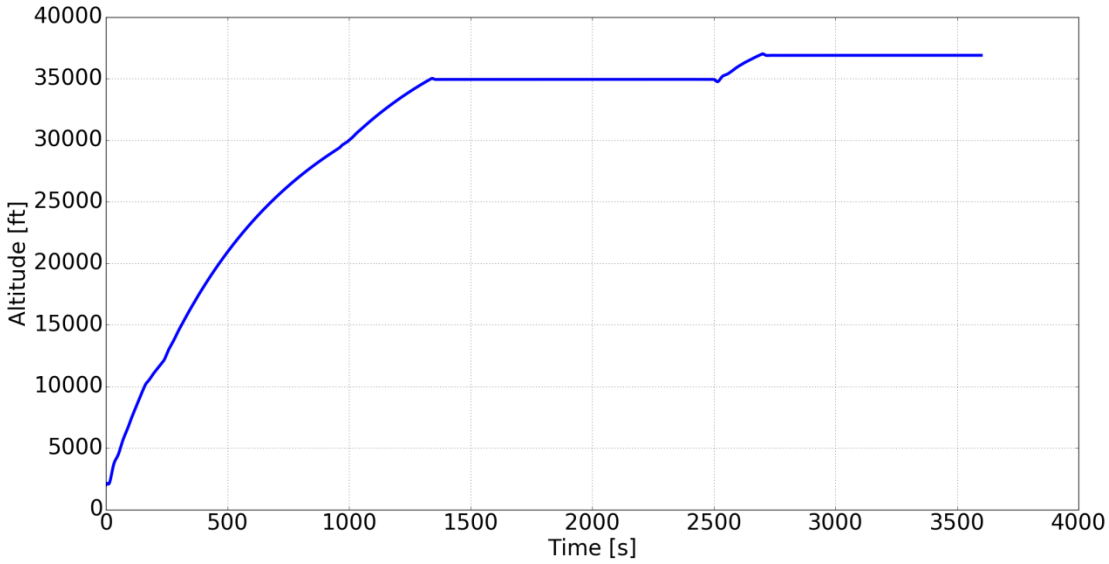

Figure 101: JSBSim simulation to verify the climb speed hold control system (CAS and Mach) and the altitude hold for the cruise segment (FL 350 and FL 370)

For ATM simulations, it is important that the aircraft is able to follow a given heading. Thus, it is interesting to see the efficiency of the heading control law that has been implemented in JSBSim. In Figure 102, the response of the reference aircraft to heading variation requests during the simulation of an operational route is illustrated. On the figure, is can be seen that the response is quite slow to achieve the requested heading because of the bank angle limitation (+/- 30°) that has been implemented. This setup of the control law proved to be the most robust among the tested solutions. Following these verifications, the next step is to use the JSBSim model to perform ATM simulations and to compare the results with real trajectories.

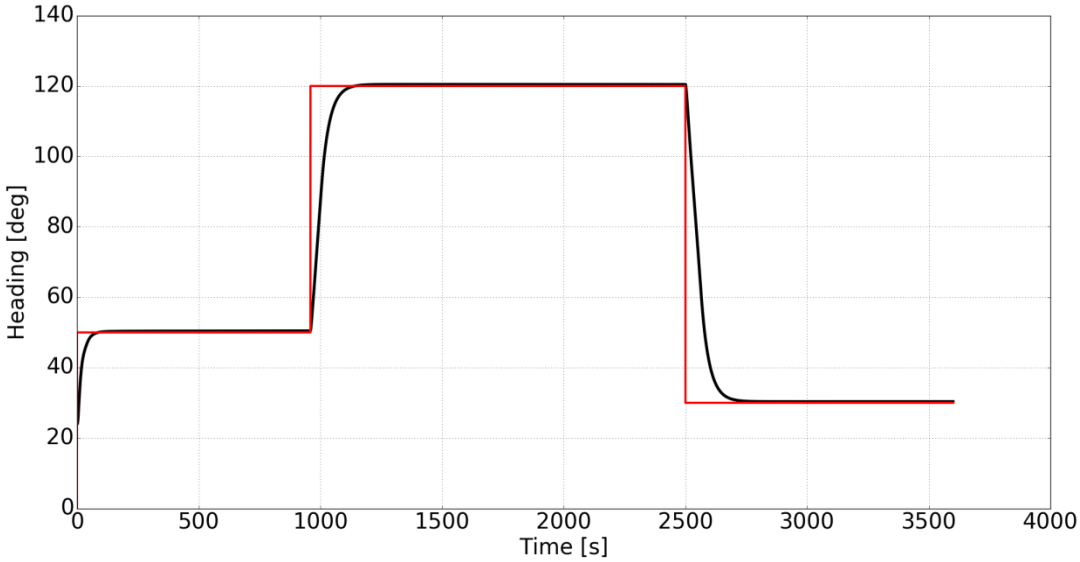

Figure 102: JSBSim simulation to verify the heading hold control system activated during climb and cruise (the red curve is the heading target while the black curve is the actual aircraft heading)

4.7. Validation of the ATM simulation based on FAST aircraft model

In this section, the simulation model generated by FAST is validated through a comparison with real flight trajectories. Several trajectories were captured by an ADS-B receiver located in the ONERA Center of Toulouse during the morning of Monday November 27th, 2017. These trajectories correspond to A320 flights going from the Toulouse-Blagnac airport (LFBO) to the Paris-Orly airport (LFPO) in France. According to the forecast from Meteo France, the weather was quite stable with approximatively a 50 knots headwind at Flight Level 300 (see Appendix E). These conditions are interesting to compare the different trajectories with the aircraft model produced by FAST.

In order to compare the simulation with real trajectories, a basic ATM simulator in Python has been developed to follow a realistic flight plan. A flight plan is provided to air traffic service units and it describes the flight of an aircraft. It contains different pieces of information like the aircraft identification, the departure and arrival airfields, the cruise speed, the requested flight level or the route intended to be followed by the aircraft [244]. The cruise speed corresponds to the intended True Air Speed (TAS). All cruise speeds and requested flight level changes are planned. Table 22 describes a classic route to go from LFBO to LFPO. This route is used to guide the JSBSim model generated with FAST by providing guidance orders on speed, heading and altitude.

Table 22: Example of an ICAO route from LFBO to LFPO

N0400F280 FISTO5B FISTO UY156 PERIG UT210 TUDRA UT158 AMB AMB6W	
N0400	Cruise True Air Speed expressed in knots (Mach number at FL280 is 0.67).
F280	Requested Flight Level
FISTO5B	Standard Instrument Departure procedure to quit LFBO
FISTO	Significant point FISTO (44.461388°, 1.2272222°)
UY156	Name of the airway to go until PERIG
PERIG	Significant point PERIG (45.117222°, 0.96944445°)
UT210	Name of the airway to go until TUDRA
TUDRA	Significant point TUDRA (46.538887°, 0.78083330°)
UT158	Name of the airway until AMB
AMB	Significant point AMB (47.428890°, 1.0644444°)
AMB6W	Standard Instrument Arrival procedure to arrive at LFPO

The ground speed calculated by the real aircraft is extracted from the ONERA ADS-B database. On the day of reference, Meteo France forecast a headwind increasing with the altitude, from 5 kt to 60 kt. Considering the possible wind strength, True Air Speed (TAS) can be computed. Subsequently, the Calibrated Air Speed (CAS) is derived. As presented in Section 4.6.1., this speed is used as target during the first phase of climb. Later, at the crossover altitude, the aircraft follows a given Mach number. In Figure 103, the real and simulated speeds are represented.

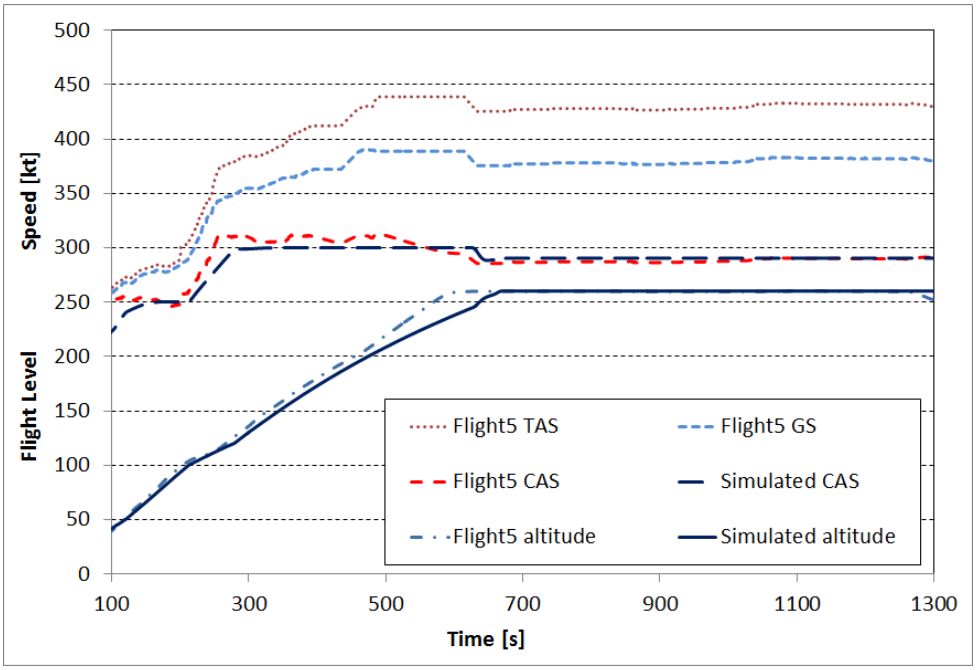

Figure 103: Real and simulated speed and altitude profile for a flight having requested FL260

Due to some uncertainties on the wind strength, the airspeed values are approximated. Still, different phases can be observed. The aircraft climbs at a constant CAS of 250 kt (there is an operational limit under FL100 limiting the CAS to 250 kt) and then at a CAS of 300 kt. The crossover altitude corresponds to the requested flight level. In cruise, CAS is at 290 kt. These values have been used to initialize the ICAO route of the ATM simulator with N0425F260 (cruise TAS is 425 kt and requested flight level is 260) following a climb CAS of 300 kt. The simulated CAS is represented by a long-dashed line in Figure 103. The three previous phases (250 / 300 / 290 kt) can be recognized. In addition, a small inflection around 200 seconds in both real and simulated altitude profiles due to the speed law change is observed. From these comparisons, it can be concluded that the JSBSim model is representative of the aircraft performances. This highlights the accuracy of the overall design and sizing process as all parameters within the JSBSim model have been generated by FAST.

On the day of reference, three A320 flights from LFBO to LFPO requesting FL300 and one requesting FL280 were recorded and are illustrated in Figure 104. The ATM simulator is initialized with a cruise flight level fixed at FL300. The simulation is also represented in Figure 104 (plain line). Overall, it can observed that the simulated climb profile matches the ones of real flights. Regarding Top of Climb (ToC), it is reached between 800 and 980s for real flights. In the simulation, this ToC is reached within this interval at 830s. It can be concluded that the simulation model generated by FAST under the JSBSim format is able to simulate realistic altitude profiles. It must be noted that no rate of climb is given during the simulation. Thus, the rate of climb is clearly the result of a combination of aerodynamics and propulsion at a given target speed.

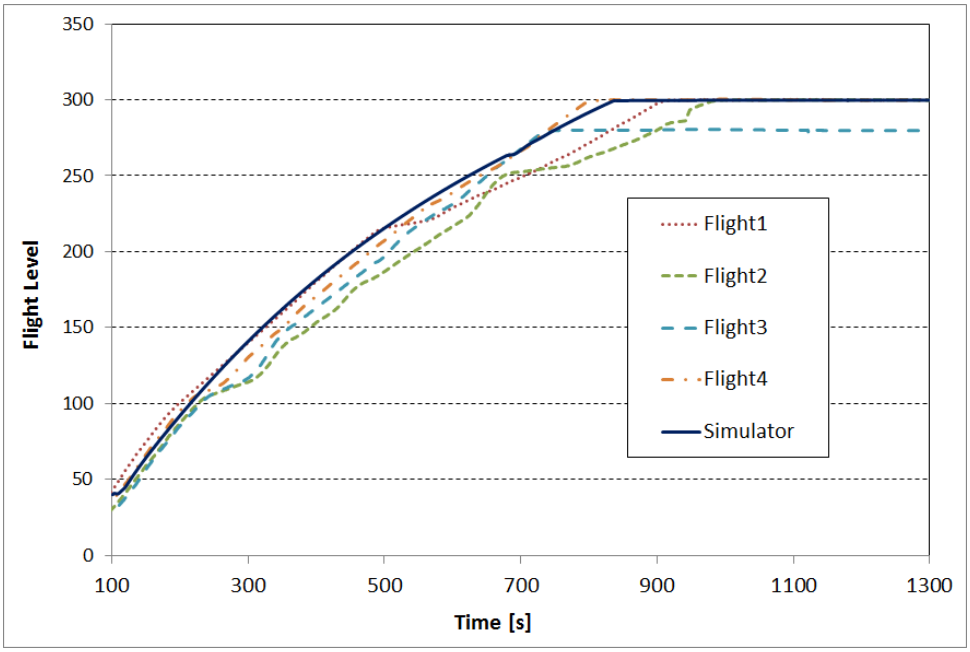

Figure 104: Simulated altitude profile compared to 4 real profiles of A320 going from LFBO to LFPO

The flight plan described in Table 22 is simulated by replacing the airway instructions by DireCT (DCT) instructions (direct route from the previous significant point to the next significant point). In Figure 105, the dotted line represents the heading target, which is regularly recomputed to guide the aircraft along a great circle between two points (orthodromy). The simulated heading is represented by the plain line. It varies between 350° and 10°, which corresponds to a route from South to North. This is natural as the flight goes from LFBO to LFPO. It can be concluded that the heading hold control law implemented in JSBSim is sufficient for basic ATM simulations.

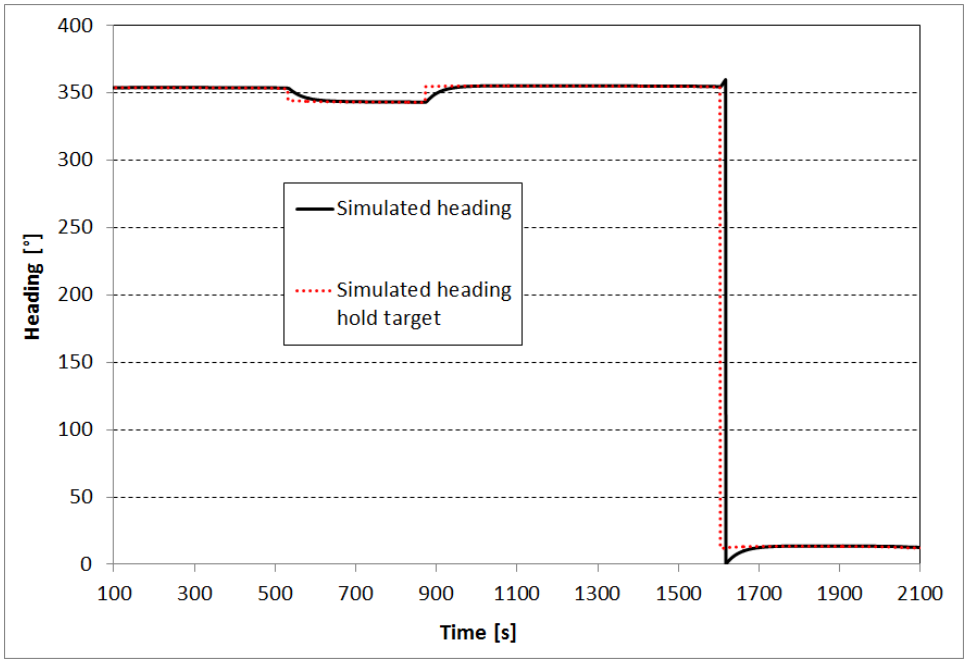

Figure 105: Simulated heading compared to the simulated heading hold target

4.8. Conclusion

The implementation of a full simulation capability within the MDA was driven by the necessity to assess the aircraft dynamic behavior according to certification constraints and the need of more reliable aircraft trajectory to enable Air Traffic Management studies. In addition, this supplementary module that is added at the end of the aircraft sizing loop offers to designers a complete view on the aircraft characteristics during the entire operational mission.

However, the integration of such analysis tool requires specific tailoring of the existing process. To this end, the first part of the work consisted in revising the Multidisciplinary Design Analysis of FAST. Naturally, full simulations based on a 6 Degrees-of-Freedom model require a large amount of additional information that is not useful for classical sizing process. First, the Aerodynamics module must provide a complete database so that moments and forces along and around the three axes can be computed for various movable deflections. Second, it becomes mandatory to determine the inertia properties of the aircraft that has been sized. Finally, for automated flight simulations, various control laws must be defined so that the overall aircraft trajectory can be defined through high level orders subsequently translated to the control surfaces. With the workplan well defined, it became necessary to downselect the analysis tools that would be used to provide the required supplementary data. Based on reviews, past projects and internal ONERA studies, it has been decided to use: (i) JSBSim as the flight dynamic model as it is opensource, flexible and can manage the addition of control laws; (ii) DATCOM+PRO mainly for its capability to compute all necessary coefficients for a 6 DoF aircraft model; (iii) OpenVSP and its mass properties function to estimate Moments of Inertia.

For the new Aerodynamics module, DATCOM+PRO is used as a numerical wind tunnel to generate a complete dataset providing all the required static and dynamic coefficients for various Mach numbers, different altitudes and diverse control surfaces deflections. With this kind of outcomes available, one single data fusion operation is necessary to build the aerodynamic dataset for the full simulator model under the JSBSim format. The challenge is that this dataset must be fully consistent with the type of data used in the performance module of FAST for the sizing loop. Thus, a postprocessing step has been applied in order to extract necessary coefficients to generate Drag polars for different Mach and different altitudes. In this manner, the classical point mass approach can be applied. Because of computational limitations, DATCOM+PRO does not consider all effects on Drag. Therefore, for the Drag polars to be used in the sizing loop as well as for the full dataset used by the 6 DoF model, corrections are provided. The comparison of the resulting aerodynamic data showed very good consistency with available reference data in cruise condition. For low speed, as high lift devices performances affect wing sizing, it has been decided in this research to maintain the original computations for maximum lift coefficient at takeoff and landing. Considering the overall aircraft sizing process, the implementation of the new Aerodynamics module within FAST increased the total CPU time as the numerous calls to DATCOM+PRO are not negligible but did not modify the mission fuel consumption and the overall geometry of the converged aircraft. In the end, FAST now features an Aerodynamics module providing reliable results and generating the necessary outputs to assess the

aircraft motion around its Center of Gravity. In aircraft design, the estimation of inertia properties is usually carried out in later phases of the project when detailed information about the systems location and volume is known. In this research, it is required that FAST computes preliminary values of the Moments and Products of Inertia. To this end, the Inertia estimation module is developed with the idea of maximizing the available data. As detailed in Section 3.3., FAST generates a detailed mass breakdown and an OpenVSP 3D model of the aircraft. Based on these two elements, the module is able to affect different masses to different volumes within the airframe. Depending on the system or the component, the volume is already available in the 3D model (wing, fuselage or engine) or it is automatically generated (e.g. systems distributed along the wing). In addition, some elements of the aircraft are considered simply as point masses with no volume associated (landing gear). With such a refined 3D model, OpenVSP is used to compute the Moments of Inertia and the Products of Inertia. The comparison between the outcomes of the Inertia estimation module and ONERA internal data underlines that the order of magnitude is correctly captured with the simplified approach.

Before implementing full simulations, it was necessary to define various stability and control laws. The difficult part in this task was to find the right balance between the control laws performances (robustness, efficiency) and complexity. After a review of possible options, it has been decided to implement simple feedback loops and PID controllers so that aircraft designers could easily trace any effect of a control law and the movable deflection. Following this logic, Stability Augmentation Systems as well as different control laws for climb, cruise and descent have been implemented. During this part of the research, it has been observed that there are many solutions to control an aircraft. It is clear that the design and optimization of the most efficient and robust option is a specialist task. The work performed in this PhD must thus be seen as a first step to foster the necessary exchanges between control laws experts and aircraft designers, especially in view of the design of unconventional configurations.

With the full aerodynamic dataset, the inertia properties and the control laws defined, full mission simulations with JSBSim have been launched. The results indicated that the aircraft correctly follows the various climb laws and heading control. From a design point of view, the achievement of full simulations is an important step as it can be viewed as a virtual flight test of the aircraft that has just been sized. A performance analysis already provides much information but the full simulation truly adds another layer of additional data. In terms of pure performance assessment, the full simulation does not offer much more than the point mass approach when considering classical missions. However, given the amount of values that can be monitored, full simulation provides a clear added value in terms of verification capability over all the phases of the flight. Such benefits are well described by Altman in [245], especially in an educational context.

Following successful simulations computed with JSBSim, the natural next step in this research has been the quality assessment of these results. In order to meet this objective, the 6 DoF aircraft model generated with FAST has been used to generate a real trajectory following Air Traffic Management routes. The resulting trajectory has been compared with real flight data recorded through an ADS-B

receiver. Results indicated that the simulation model generated by FAST can replicate realistic flights. Still, during this verification step, some assumptions had to be made regarding the speed of the real aircraft. To complete the evaluation, a second comparison using additional real data provided through Mode S has been performed. In this case, the supplementary data allowed a better setup of the same JSBSim model and its control laws. The resulting comparison between the ATM simulations based on the FAST 6 DoF model (continuous line) and real flight data (green points) illustrated in Figure 106 displays very small differences. The ADS-B antenna that is used in this research is located in Toulouse. This is the reason why Figure 106 shows only the arrival to and departure from Blagnac airport of the same aircraft.

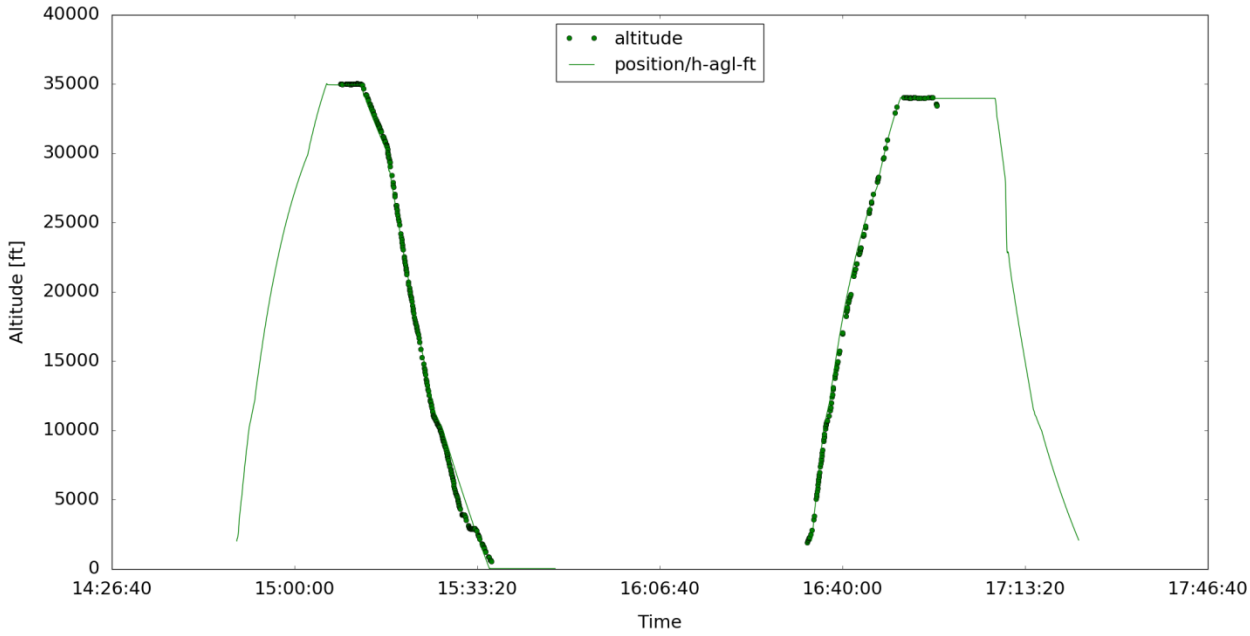

Figure 106: Comparison of simulated trajectories and real flight data (green points represent the real aircraft trajectory while the continuous line is generated by simulation)

From the work completed in chapter 4, it can be then concluded that the modifications of the sizing code FAST allow aircraft designers to generate a reliable full simulation model that can be used in Air Traffic Management studies.

Synthesis of the chapter

- A new Multidisciplinary Design Analyis providing full simulation capability has been defined
- A new Aerodynamics module based on DATCOM+PRO has been implemented within FAST in order to generate the complete set of coefficients needed by the full simulator
- Based on OpenVSP, an Inertia estimation module has been developed enabling the computation of Moments of Inertia and Products of Inertia at conceptual design stage
- Basic control laws have been defined to augment stability and to allow a control of the aircraft speed or altitude with different throttle settings
- With high level mission specifications a full simulation of the mission has been performed using the open source flight dynamics model JSBSim
- An operational mission simulated with the same 6 Degrees of Freedom model has been positively compared to real aircraft trajectories recorded with an ADS-B antenna
- Using supplementary data provided via Mode S, a second comparison between a simulated mission and real flight data demonstrated the capability of the new Multidisciplinary Design analysis to generate very realistic trajectories

Associated conferences

- Schmollgruber P., Bartoli N., Bedouet J., Benard E., Gourinat Y., “Improvement of the Aircraft Design process for Air Traffic Management evaluations”, 2018 AIAA Aerospace Sciences Meeting, AIAA SciTech Forum, AIAA 2018-0283, Kissimmee, 2018

Conclusion and perspectives

With pressure coming from a competitive business and stringent constraints defined by international organizations in terms of environmental impact, the next generation of airplanes must achieve a step change in fuel burn reduction. As the classical “tube and wing” configuration equipped with turbofans has been optimized for the last 60 years, it offers limited possibilities for important gains in efficiency. Within aircraft manufacturers, design engineers involved in the conceptual design must then be capable of exploring and assessing potential benefits of futur concepts that feature innovative configurations (e.g. Blended Wing Body), disruptive technologies (e.g. Distributed Electric Propulsion) or new concepts of operations (e.g. formation flight). In an aircraft program, analyses and decisions made during this initial design phase will commit about 65% of the life cycle costs. There is then the necessity to reduce risk during this fundamental step that can entail the success or failure of a new product. For researchers in Aircraft Design, the goal is then to continuously develop and validate new capabilities paving the way for a reliable design and sizing of these future airplanes.

As the design of an airplane relies on many different disciplines and subsystems, the analysis of the overall aircraft performances is computed through a Multidisciplinary Design Analysis. In this research, a review of the technical challenges imposed by the design and evaluation of unconventional configurations, technologies or operational concepts, highlighted the limitations of today’s tools and overall approach. More precisely, the key question that must be answered in order to support aircraft designers has been pointed out: **“How to add knowledge in the Multidisciplinary Design Analysis at aircraft conceptual design level?”**

A review of studies in various fields associated to the design of future aircraft concepts allowed to identify and classify the different options that can be used by Aircraft designers in order to increase the level of knowledge in conceptual design. First, there is Multidisciplinary Design Optimization, a discipline that allows an unbiased exploration of the design space and the identification of the most promising design or family of designs. Second, there is the quite natural solution to perform disciplinary analyses with higher fidelity tools in order to both increase accuracy as well as reliability and better understand complex phenomena. Third, some advanced technologies to be integrated within an airframe require new analyses with specific inputs and outputs within the MDA. In this case, knowledge is automatically added no matter the level of fidelity as new tradeoffs can be made. The last option that has been considered in this work is uncertainty management. The early phases of a design process are indeed characterized by many unknowns for which assumptions must be made. In addition, disciplinary and system models mimic the behavior of the real phenomena or component but they inherently generate errors. It is then possible through the use of diverse mathematical approaches to quantify, manage and possibly reduce the associated uncertainty so that engineers have more confidence in their design downselection. Part of the aircraft designer activity then becomes the tailoring of the MDA through the implementation of one or many of these available solutions to increase the level of knowledge. The regular other task is naturally the design and evaluation of the future concepts using the revised MDA, knowing that the aircraft has to meet regulatory and

operational constraints. To illustrate such typical work, the sizing of an aircraft adapted to a pioneering ground based takeoff and landing system is carried out. Implemented under ModelCenter, the design process includes higher fidelity modules to estimate the structural mass of the wing and the fuselage. In addition, a monolithic MDO architecture is selected to make a multiobjective optimization. With valuable results used for the EU GABRIEL project in terms of fuel burn reduction, this work also emphasized the strong impact of certification constraints on the selection of the most promising designs. Driven by such a conclusion, the work subsequently concentrated on reviewing key sections of the regulatory text providing Certification Specification for Large Aeroplanes issued by the European Aviation Safety Agency and on finding a solution to better manage such constraints in conceptual design. In parallel, as new aircraft concepts must fly in an environment regulated by Air Traffic Management, research needs in this field have been looked at. The result is that both certification aspects and ATM require the capability to perform full trajectory simulations including the Stability Augmentation system to specially increase the design space. **This research then proposed to add knowledge in conceptual design: it consists in the expansion of the Multidisciplinary Design Analysis and Optimization through the development of a Certification Constraints Module and the implementation of full simulation capabilities.**

Based on the ONERA software GAMME, the Certification Constraints Module or CCM is a tool that generates a digital version of the regulatory text. Under this numerical format, the certification constraints can easily be introduced and managed in the Multidisciplinary Design Analysis and Optimization process. Based on a flexible data model reflecting the structure of the reference documents, the CCM automatically generates a Graphical User Interface with a structured template that allows an easier constraint management. To illustrate the possible benefits of the CCM, the optimization of a classical twin engine transport aircraft, taking into account certification and operational constraints, has been performed with FAST, the aircraft design code jointly developed in Python by ISAE-SUPAERO and ONERA since 2015. Following specifications derived from past experiences and recent trends in aircraft design, FAST has been improved yearly through student projects, ONERA contributions and this research. Today, FAST accurately captures key design sensitivities and it is still evolving in order to size and optimize vehicles such as Blended Wing Body or hybrid electric transport aircraft. Through the use of the CCM, the implementation of the MDAO process based on FAST, taking into account certification constraints, went much faster in comparison to the classical approach used in the EU project GABRIEL. The gain is coming from the Graphical User Interface that guides designers but it is mostly due to the management of values through the data model. Second, the CCM gathers all certification constraints that are used in the optimization in a single interface. For the designers, assessing different constraint scenarios to evaluate the impact of threshold changes on the final design becomes easy. In this research, such variations have been carried out and, as expected, the level of performance of the best designs is strongly affected. More importantly, the study demonstrated that the resulting Pareto front is not only shifted by also modified. For the various optimizations that have been completed, three optimization algorithms (NSGAII, COBYLA and SEGOMOE) have been used in order to validate the Pareto fronts. In addition, the comparison of the necessary computational time to reach valuable solutions between the three

available options identified SEGOMOE (a surrogate-based optimizer) as the faster solution (by a factor of 10). Last but not least, the analysis of both MDAO results and constraint variations with respect to design variables showed that operational and certification requirements dominate different areas of the feasible domain. So, it becomes clear that these constraints drive the overall design. This outcome underlines the usefulness of the CCM within a Multidisciplinary Design Analysis and Optimization, especially in the case of an unconventional configuration. Indeed, this unique capability allows aircraft designers to quickly comprehend the effects of certification constraints and to identify the critical threshold associated to the classical configuration that could be modified (without decreasing safety level) when considering a new radical design.

In this research, the aircraft to be sized and optimized within the FAST MDAO is considered rigid. Thus, full simulations of flight trajectories are based on a 6 Degrees-of-Freedom model. However, such model requires data that are usually not computed during the conceptual design process. Thus, the implementation of full simulations within the FAST Multidisciplinary Design Analysis required at first the modification of the Aerodynamics module in order to generate a complete set of aerodynamic coefficients to be used by the 6 DoF model. Second, Moments of Inertia had to be computed. Last, various control laws enabling Stability Augmentation as well as speed and altitude hold had to be defined. All these data have been subsequently provided to the open source flight dynamics model JSBSim that computes the aircraft motion around and along its three axes. For the aerodynamics analysis, the semi-empirical equations initially [151] proposed in FAST are replaced by the software DATCOM+PRO, an evolution of the historical digital DATCOM that provides outputs under the JSBSim format. To compute the mandatory Moments of Inertia, a new Python module automatically allocates the masses of aircraft components to the corresponding volumes within the aircraft 3D model generated with OpenVSP by FAST. Following the definition of specific point masses such as the landing gear, a native OpenVSP function automatically computes the inertia properties. Regarding control laws, the objective in this research was to find the simplest but still efficient architecture so that aircraft designers could have a clear understanding of the various feedback loops on the aircraft control surfaces deflection. Following basic examples in textbooks, the various laws that have been implemented in JSBSim rely on PID controllers that provide satisfactory stability, control and navigation for a given flight trajectory. In order to assess the quality of the full simulations obtained by the FAST MDA dedicated to conceptual level studies, the simulated trajectories have been compared with real aircraft trajectory data recorded through an ADS-B (Automatic Dependent Surveillance – Broadcast) antenna. As the simulated and real trajectories featured small or justifiable differences, it is considered that FAST now has the capability to accurately simulate flight trajectories following ATM guided routes. This specific characteristic is fundamental for the assessment of future operational concepts such as On Demand Mobility or, to remain in the civil transport domain, formation flights.

With the developments achieved in this research, the sizing tool FAST is now capable to better manage the impact of Certification constraints in a Multidisciplinary Design Analyis and Optimization process and to provide a full simulation model predicting accurate trajectories.

The key contributions made by this work in the field of Aircraft Design are summarized below:

- Knowledge within the Multidisciplinary Design Analysis and Optimization process is usually added through contributions from disciplinary or system experts and also applied mathematics researchers. **In this work, the expansion of the MDAO capabilities is based on new modules that are at the core of the aircraft designer competences** (ensuring certification compliance and safe operations in a given environment).
- Through specification definition, development coordination, new capability implementation and testing, **this research contributed to the development and improvement of the ONERA / ISAE-SUPAERO sizing code FAST.**
- After pointing out a specific need, **the Certification Constraints Module has been specified, designed, developed and tested within an MDAO process**. Based on initial input from designers, this tool automatically generates a digital version of the regulatory text to ease the manipulation of certification constraints during optimizations.
- The different multiobjective optimizations carried out with FAST demonstrated at first the benefits in terms of CPU time associated to the optimization algorithm SEGOMOE. Second, **the analysis of the best designs illustrated the strong impact of certification and operational constraints in different areas of the design space.**
- With the implementation of full simulation within a Multidisciplinary Design Analysis, **this thesis offers aircraft designers the possibility to use a Level 2 physics representation** [67] of the mission as illustrated in Figure 107. A more complete knowledge about the aircraft and its systems for the duration of the mission automatically becomes available.

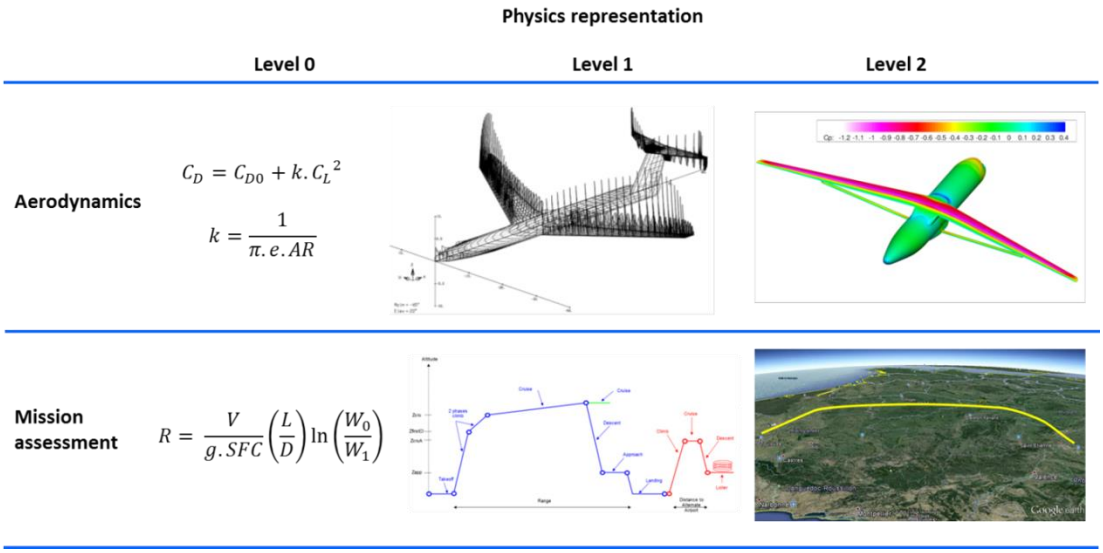

Figure 107: Fidelity levels for mission assessment and aerodynamics

- **The coupling of the conceptual design MDAO with the Certification Constraints Module and an operational mission full simulation provided design engineers with a global assessment environment** from regulatory texts to operations with ATM constraints. Such complete vision is mandatory for the exploration of disruptive operational concepts.

- In an aircraft program, conceptual design studies and flight tests find themselves at opposite ends. On the other hand, **this work has been the opportunity to verify the quality of flight trajectories generated with a conceptual design process through a comparison with real flight data recorded with an ADS-B antenna.**

In parallel to this work, the position as an ONERA Research Engineer has been the opportunity to actively develop the Aircraft Design activity in different manners for the last six years. The most important way is naturally through the teaching of the discipline within university and the various possible options: classes, internships and projects. Second, the co-organization of a Symposium on Collaboration in Aircraft Design (SCAD) fostered European collaboration on the topic with successful results such as the AGILE project. Subsequently, the importance of the overall aircraft analysis has been underlined during participations in ONERA prospective studies including experts from all disciplines. Last, becoming a member of the AIAA Aircraft Design Technical Committee in 2017 allows an active contribution to international student competitions and the preparation of recognized conferences in the field.

In order to achieve more robust evaluations and designs for future Air Transportation Systems, there are two streams of research activity that must jointly progress. The first one aims at enhancing the capability to investigate fully integrated advanced concepts. The second one focuses on the development of multidisciplinary methods enabling faster design space explorations, more robust optimizations and uncertainty management. It is important to always coordinate progresses as the study of an unconventional aircraft could push the development of new methods and original mathematical approaches would pull more robust design space explorations. Following this logic, possible future works based on this research are detailed hereafter:

- It has been demonstrated that FAST is capable of correctly assessing tradeoff trends for conventional transport aircraft. In addition, the full simulation capability allows to fly real routes defined following ATM guidance. Thus, a valuable study would be to extend the design process towards multiple aircraft simulations, and validate the results on the use-case of formation flights [171].
- In this work, a series of simple stability and control laws have been implemented for a conventional aircraft. In the case of unconventional configurations, their design can become a real challenge (see Figure 26). Future research could then focus on the development of robust control laws that would be applied on many different architectures with an automated tuning of the different gains.
- The CCM offers the possibility to investigate regulatory changes that would be associated to unconventional concepts. Knowing that full mission simulations can be also assessed, there is then a complete set of tools to make a thorough evaluation of unconventional operational systems. The optimization of Urban Air Mobility vehicles considering the specific routes and the required changes to regulations would be a valuable use case [180][181]. In terms of research, it would be interesting to investigate the possible implementation of unmanned

systems regulations into the Certification Constraints Module and the impact of considering a fixed probability of failure as a design criterion.

- The coupling of high fidelity tools and the MDAO used in the early design stage is always a topic of interest. A possible future endeavour could be a multifidelity investigation including a Finite Element Analysis within FAST for estimating the structural mass of the wing and fuselage. The innovative element could be the interface between the FEA tool and the CCM that would generate a digital version of the CS 25 SUBPART B - STRUCTURE [129]. In this case, sensitivities to possible regulation changes would be traced.
- In this work, the optimizations that have been carried out featured a limited number of design variables and constraints. In the case of the definition of advanced concepts such as the Blended Wing Body or a Distributed Electric Propulsion aircraft, this number would rapidly increase. In this case, it becomes mandatory to extend the capabilities of existing optimization algorithms to manage large sets of variables and constraints [247].
- In conceptual design, studies will always be affected by uncertainty, whether irreducible or epistemic. In the case of FAST, on top of model errors, the code includes a convergence tolerance on OWE values: the outcomes are affected by uncertainty. Thus, the Pareto fronts obtained at the end of the optimization are in reality thicker bands. In order to support designers in their decision making process, it is then recommended that next studies on advanced concepts should include uncertainty analyses, at the Multidisciplinary Design Analysis level [140] or at Multidisciplinary Design Optimization level [248].

Overall, this research on Aircraft Design pointed out the key issue about the necessity to increase knowledge in the early phases of the project. Following a review of the state-of-the-art in different domains and the consideration of additional needs coming from both certification and Air Traffic Management aspects, it has been proposed to expand the Multidisciplinary Design Analysis and Optimization. This expansion relies on the addition of two new components in the design process that are fully within the core competences of the aircraft designer: the Certification Constraint Module and the full operational mission simulation. Indeed, it is the Aircraft designer that ensures the viability of the aircraft with respect to certification constraints and the consistent behavior of the aircraft along the mission considering ATM requests. With positive results about the use of the CCM and the capability to generate real flight trajectories, it is believed that this proposed expansion will foster the design of innovative configurations, future “tube and wing” architectures with disruptive technology or advanced operational concepts. Naturally, as Aircraft Design remains both art and science [7], this new process has to be tailored according to company policies and aircraft designer’s experience.

References

[1] Roskam J., "Aircraft Design Part VIII: Airplane Cost Estimation: Design, Development, Manufacturing and Operating", DARcorporation, 2002

[2] "Airbus launches Sharklet retrofit for in-service A320 Family aircraft" [website] URL: https://www.airbus.com/newsroom/press-releases/en/2013/10/airbus-launches-sharklet-retrofit-for-in-service-a320-family-aircraft.html, [cited 21 August 2018]

[3] Pardessus T., "Concurrent engineering development and practices for aircraft design at Airbus", 24th Congress of the International Council of the Aeronautical Sciences ICAS, Yokohama, Japan, 2004

[4] Morales J., "The A380 Transport Project and Logistics", 13th Colloquium in Aviation, University of Darmstadt, 2006 [online publication] URL : http://www.aviation.tu-darmstadt.de/media/arbeitskreis_luftverkehr/downloads_6/kolloquien/13kolloquium/05druckvorlage_morales.pdf, [cited 21 July 2018]

[5] Raymer D. P., "Aircraft Design : A Conceptual Approach", 5th Edition, AIAA, 2012

[6] Anderson J. D., "Aircraft performance and design", WCB/Mc Graw-Hill, 1999

[7] Anderson J. D., "The Grand Designers: The Evolution of the Airplane in the 20th Century", Cambridge Centennial of Flight, Cambridge University Press, 2018

[8] Dieter G. E., "Engineering Design", 3rd Edition, Mc Graw Hill, 2000

[9] Mavris D. N., DeLaurentis D., "Methodology for examining the simultaneous impact of requirements, vehicle characteristics, and technologies on military aircraft design", 22nd Congress of the International Council of the Aeronautical Sciences ICAS, Harrogate International Conference Centre, UK, 2000

[10] "System specification for the advanced pilot training (APT) program, aircraft system", PRF APT-ACFT-1001, 2016 [on line database] URL: https://www.fbo.gov/utils/view?id=646b86a7bd46af87a7fc69de9ed306fc, [cited 12 August 2018]

[11] "Commercial Market Outlook 2018-2037", Boeing, 2017

[12] "Virgin Galactic Vision" [website] URL: https://www.virgingalactic.com/vision/ [cited 12 August 2018]

[13] Nicolai L., Carichner G., "Fundamentals of Aircraft and Airship Design Volume I – Aircraft Design", AIAA, 2010

[14] McDonald R., "Welcome & Overview", OpenVSP Workshop, 2014 [online proceedings] URL: http://openvsp.org/wiki/lib/exe/fetch.php?media=workshopv3:welcome_overview_mcdonald.pdf, [cited 11 August 2018]

[15] Whitford R., "Fundamentals of fighter design", The Crowood Press, 2004

[16] Rich B. R., Janos L., "Skunk Works: A Personal Memoir of My Years at Lockheed", Back Bay Books, 1994

[17] Nicolai L., "Lessons learned, a guide to improved Aircraft Design", Library of Flight, AIAA, 2016

[18] Takahashi T., "Aircraft Performance and Sizing, Volume II, Applied Aerodynamic Design", Aerospace Engineering Collection, Momentum Press Engineering, 2016

[19] "OpenVSP, NASA Open Source Parametric Geometry", [website] URL: http://www.openvsp.org/, [cited 27 October 2016]

[20] Raymer D. P., “Advanced Technology Subsonic Transport Study, N+3 Technologies and Design Concepts”, NASA/TM 2011-217130, 2011

[21] J. D. Mattingly, W. H. Heiser, D. T. Pratt, “Aircraft Engine Design”, AIAA, 2002

[22] Roskam J., “Aircraft Design Part V: Component Weight Estimation”, DARcorporation, 1999

[23] Roskam J., Lan C. T., “Airplane Aerodynamics and Performance”, DARcorporation, 2003

[24] Torenbeek E., “Synthesis of Subsonic Airplane Design”, Delft University Press, 1982

[25] Roskam J., “Aircraft Design Part I: Preliminary Sizing of Airplanes”, DARcorporation, 1997

[26] Sforza P., “Commercial Airplane Design Principles”, Elsevier Aerospace Engineering Series, Butterworth-Heinemann, 2014

[27] Takahashi T., “Aircraft Performance and Sizing, Volume I, Fundamentals of Aircraft Performance”, Aerospace Engineering Collection, Momentum Press Engineering, 2016

[28] Kirby M. R., “TIES for Dummies (Technology Identification, Evaluation, and Selection), Basic how to’s to implement the TIES method”, 3rd edition, Aerospace Systems Design Laboratory, Georgia Institute of Technology, 2002

[29] Roskam J., “Aircraft Design Part III: Layout design of cockpit, fuselage, wing and empennage: cutaways and inboard profiles”, DARcorporation, 2002

[30] Kenway G. K. W., Martins J. R. R. A., “Multipoint High-fidelity Aerostructural Optimization of a Transport Aircraft Configuration”, Journal of Aircraft, Volume 51, Issue 1, 2014

[31] Roskam J., “Lessons Learned in Aircraft Design, the devil is in the details”, DARcorporation, 2017

[32] “GSP, Gas Turbine Simulation Program”, [website] URL: https://www.gspteam.com/, [cited 14 August 2018]

[33] “Numerical Propulsion System Simulation (NPSS)”, [website] URL: https://software.nasa.gov/software/LEW-17051-1, [cited 14 August 2018]

[34] Lapins M., Martorella R. P., Klein R. W., Meyer R C., Sturm M. J., “Control Definition Study for Advanced Vehicles”, NASA CR 3738, 1983

[35] Roskam J., “Aircraft Design Part IV: Layout of Landing Gear and Systems”, DARcorporation, 2000

[36] Chakraborty I., Trawick D. R., Mavris D. N., Emeneth M., Schneegans A., “Integrating Subsystem Architecture Sizing and Analysis into the Conceptual Aircraft Design Phase”, 4th Symposium in Collaboration in Aircraft Design, 2014, [online presentation] URL: http://w3.onera.fr/ceas-tcad2014/sites/w3.onera.fr.ceas-tcad2014/files/03_industrial_vision_s1_c_pace.pdf, [cited 14 August 2018]

[37] “Northrop YF-23 ATF”, [website] URL: https://yf-23.net/, [cited 14 August 2018]

[38] Mason W. H., “Some High Alpha and Handling Qualities Aerodynamics”, Configuration Aerodynamics Class, 2018 [online presentation] URL: http://www.dept.aoe.vt.edu/~mason/Mason_f/HiAlphaBasicsPres.pdf, [cited 14 August 2018]

[39] Bartels R.E., Scott R. C., Allen T., Sexton B., “Aeroelastic Analysis of SUGAR Truss-Braced Wing Wind-Tunnel Model Using FUN3D and a Nonlinear Structural Model”, AIAA 2015-1174, 2015

[40] Fualdes C., “Experience and lessons learned of a Composite Aircraft”, 30th Congress of the International Council of the Aeronautical Sciences ICAS, Daejeon, Korea, 2016

[41] Kaufmann M., “Cost/Weight Optimization of Aircraft Structures”, Licentiate Thesis, KTH Engineering Sciences, 2008

[42] "Airbus A350 XWB passes ultimate load wing test", [website] URL: https://www.compositesworld.com/news/airbus-a350-xwb-passes-ultimate-load-wing-test, [cited 19 August 2018]

[43] "Taking flight with the Airbus "Iron Bird"", [website] URL: https://www.airbus.com/newsroom/news/en/2017/05/taking-flight-with-the-airbus-iron-bird.html, [cited 19 August 2018]

[44] "Jigs & Tools Solutions", [website] URL: https://www.ecagroup.com/en/find-your-eca-solutions/aerospace-jigs-tools, [cited 19 August 2018]

[45] Menéndez J.L., Mas F., Serván J., Ríos J., "Virtual Verification of an Aircraft Final Assembly Line Industrialization: An Industrial Case", Key Engineering Materials Vol. 502 pp 139-144, 2012

[46] Torenbeek E., "Advanced Aircraft Design: Conceptual Design, Analysis and Optimization of Subsonic Civil Airplanes", Aerospace Series, Wiley, 2013

[47] Pappalardo J., "Weight Watchers", Air & Space Magazine, 2006 [online article] URL: https://www.airspacemag.com/military-aviation/weight-watchers-13117183/?all, [cited 19 August 2018]

[48] "IATA Fact Sheet Industry Statistics, June 2018", [website] URL: http://www.iata.org/pressroom/facts_figures/fact_sheets/Documents/fact-sheet-industry-facts.pdf, [cited 15 August 2018]

[49] "IATA Fact Sheet Aviation Benefits Beyond Borders, December 2017", [website] URL: https://www.iata.org/pressroom/facts_figures/fact_sheets/Documents/fact-sheet-economic-and-social-benefits-of-air-transport.pdf, [cited 15 August 2018]

[50] "International Civil Aviation, Uniting Aviation", [website] URL: https://www.icao.int/about-icao/Pages/default.aspx, [cited 15 August 2018]

[51] "ICAO Environment, Market-based Measures and Climate Change", [on line publication] URL: https://cfapp.icao.int/tools/38thAssyiKit/story_content/external_files/Flyer_US-Letter_ENV_MBMs_2013-08-30.pdf, [cited 15 August 2018]

[52] "An introduction to market-based measures (MBMs)", [online presentation] URL: https://www.icao.int/Meetings/EnvironmentalWorkshops/Documents/2015-Warsaw/6_1_An-introduction-to-market-based-measures-MBMs.pdf, [cited 21 August 2018]

[53] "Flightpath 2050 Europe's Vision for Aviation", Report of the High Level Group on Aviation Research, European Commission, 2011

[54] Collier F., "NASA Aeronautics Environmentally Responsible Aviation Project", AIAA , 2012 [online presentation] URL: https://www.aiaa.org/uploadedFiles/About-AIAA/Press-Room/Key_Speeches-Reports-and-Presentations/2012/Collier-NASA-AVC-AIAA-GEPC2-2.pdf, [cited 21 August 2018]

[55] Anderson J. D., "Introduction to Flight", 5th Edition, McGraw-Hill International Edition, 2005

[56] "UPS to Upgrade Boeing 757, 767 Cockpits" [website] URL: https://www.aviationtoday.com/2017/05/09/ups-upgrade-boeing-757-767-cockpits/, [cited 21 August 2018]

[57] "A320 neo" [website] URL: https://www.airbus.com/aircraft/passenger-aircraft/a320-family/a320neo.html, [cited 22 August 2018]

[58] "737 MAX" [website] URL: https://www.boeing.com/commercial/737max/, [cited 22 August 2018]

[59] Hensey R., Magdalina A., "A320 NEO vs. CEO comparison study", FPG Amentum, 2018 [online publication] URL: http://www.fpg-amentum.aero/wp-content/uploads/2018/07/180719-FPG-Amentum-research-A320-NEO-vs-CEO-comparison-study.pdf, [cited 25 August 2018]

[60] Martins J. R. R. A., "A Short Course on Multidisciplinary Design Optimization", Aerospace Engineering, University of Michigan, 2012

[61] Carichner G. E., Nicolai L. M., "Fundamentals of Aircraft and Airship Design, Volume 2 – Airship Design and Case Studies", AIAA, 2013

[62] La Rocca G., Krakers L., Van Tooren M. J. L., "Development of an ICAD generative model for Blended Wing Body aircraft design", AIAA 2002-5447, 2002

[63] Lambe A. B., Martins J. R. R. A., "Extensions to the design structure matrix for the description of multidisciplinary design, analysis, and optimization processes", Structural and Multidisciplinary Optimization, 46(2), pp.273-284, 2012

[64] Raymer D. P., "RDSwin : Seamlessly-Integrated Aircraft Conceptual Design for Students & Professionals", AIAA 2016-1277, 2016

[65] "Advanced Aircraft Analysis" [website] URL: http://darcorp.com/Software/AAA/, [cited 21 August 2018]

[66] Sadraey M. H., "Aircraft Design, a Systems Engineering Approach", Aerospace Series, Wiley, 2013

[67] Ciampa P., Nagel B., "Towards the 3rd generation MDO collaborative environment", 30th Congress of the International Council of the Aeronautical Sciences ICAS, Daejeon, Korea, 2016

[68] Roskam J., "Aircraft Design Part II: Preliminary Configuration Design and Integration of the Propulsion System", DARcorporation, 1997

[69] Hoerner S. F., "Fluid Dynamic Drag", Hoerner Fluid Dynamics, 1993

[70] Jenkinson L. R., Simpkin P., Rhodes D., "Civil Jet Aircraft Design", Butterworth-Heinemann, 1999

[71] Roskam J., "Aircraft Design Part VI: Preliminary Calculation of Aerodynamics, Thrust and Power Characterisitcs, DARcorporation, 2000

[72] Howe D., "Aircraft conceptual design synthesis", Professional Engineering Publishing, 2000

[73] Babikian R., "The historical fuel efficiency characteristics of regional aircraft from technological, operational, and cost perspectives", Massachusetts Institute of Technology, 2001

[74] "The LEAP engine" [website] URL: https://www.cfmaeroengines.com/engines/leap/, [cited 26 August 2018]

[75] Anderson J. D., "The Airplane: A History of Its Technology", Library of Flight, AIAA, 2003

[76] Lee J.J., "Historical and Future Trends in Aircraft Performance, Cost and Emissions", Massachusetts Institute of Technology, 2000

[77] "Boeing 787-8 (Dreamliner) sample analysis" [website] URL: http://www.lissys.demon.co.uk/samp1/index.html, [cited 26 August 2018]

[78] "787 Dreamliner by design" [website] URL: https://www.boeing.com/commercial/787/by-design/#/advanced-composite-use, [cited 27 August 2018]

[79] "Wikipedia" [website] URL: https://www.wikipedia.org/, [cited 27 August 2018]

[80] Kennedy G. J., Martins J. R. R. A., "A Comparison of Metallic and Composite Aircraft Wings Using Aerostructural Design Optimization", AIAA 2012-5475, 2012

[81] Kharina A., Rutherford D., "Fuel efficiency trends for new commercial jet aircraft: 1960 to 2014", International Council on Clean Transportation, 2015

[82] Hughes C., "The Promise And Challenges Of Ultra High Bypass Ratio Engine Technology and Integration", AIAA, 2011 [online presentation] URL: https://ntrs.nasa.gov/archive/nasa/casi.ntrs.nasa.gov/20110011737.pdf, [cited 28 August 2018]

[83] "Industry Provides NASA with Ideas for Next X-Plane" [website] URL: https://www.nasa.gov/aero/industry-provides-nasa-with-ideas-for-next-x-plane, [cited 29 August 2018]

[84] Jansen R., Bowman C., Jankovsky A., Dyson R., Felder J., "Overview of NASA Electrified Aircraft Propulsion (EAP) Research for Large Subsonic Transports", AIAA 2017-4701, 2017

[85] Warwick G., "ESAero Refines Turboelectric Airliner Design For NASA" [on line article] URL: http://aviationweek.com/technology/esaero-refines-turboelectric-airliner-design-nasa-0, [cited 30 August 2018]

[86] "Aviation Renaissance: NASA Advances Concepts for Next-gen Aircraft" [website] URL: https://www.nasa.gov/feature/aviation-renaissance-nasa-advances-concepts-for-next-gen-aircraft, [cited 30 August 2018]

[87] Hooker J. R., Wick A., "Design of the Hybrid Wing Body for Fuel Efficient Air Mobility Operations", AIAA 2014-1285, 2014

[88] Bradley K. R., "A Sizing Methodology for the Conceptual Design of Blended-Wing-Body Transports", NASA/CR-2004-213016, 2004

[89] Gauvrit-Ledogar J., Defoort S., Tremolet A., Morel F., "Multidisciplinary Overall Aircraft Design Process Dedicated to Blended Wing Body Configurations", AIAA 2018- 3025, 2018

[90] Chakraborty I. *et al.*, "Comparative Assessment of Strut-Braced and Truss-Braced Wing Configurations Using Multidisciplinary Design Optimization", AIAA Journal of Aircraft, Vol. 52, No. 6, 2015

[91] Gur O., Bhatia M., Mason W. H., Schetz J. A., Kapania R. K., Nam T., "Development of Framework for Truss-Braced Wing Conceptual MDO", AIAA 2010-2754, 2010

[92] Carrier G., Atinault O., Dequand S., Hantrais-Gervois J.-L., Liauzun C., Paluch B., Rodde A.-M., Toussaint C., "Investigation of a strut-braced wing configuration for future commercial transport", 28th Congress of the International Council of the Aeronautical Sciences ICAS, Brisbane, Australia, 2012

[93] Schiltgen, B. T., Freeman, J. L., Hall, D. W., "Aeropropulsive Interaction and Thermal System Integration within the ECO-150: A Turboelectric Distributed Propulsion Airliner with Conventional Electric Machines," AIAA 2016-4064, 2016

[94] Welstead J., Felder J. L., "Conceptual Design of a Single-Aisle Turboelectric Commercial Transport with Fuselage Boundary Layer Ingestion", AIAA 2016-1027, 2016

[95] Uranga, A., Drela, M., Greitzer, E., "Power Balance Assessment of BLI Benefits for Civil Aircraft", Oral presentation, 2015 [online presentation] URL: http://uranga.usc.edu/presentations/Uranga2015_AIAA-SciTech_BLI_presentation.pdf, [cited 31 August 2018]

[96] Gray J. S., Kenway G. K., Mader C. A., Martins J. R. R. A., "Aero-propulsive Design Optimization of a Turboelectric Boundary Layer Ingestion Propulsion System", AIAA 2018-3976, 2018

[97] Wood R., Bauer S., "A discussion of knowledge based design", AIAA 1998-4944, 1998

[98] Gazaix A., Gendre P., Chaput E., Blondeau C., Carrier G., Schmollgruber P., Brezillon J., Kier T., "Investigation of Multi-Disciplinary Optimisation for Aircraft Preliminary Design", SAE Technical Paper 2011-01-2761, 2011

[99] "What is Moore's law?" [website] URL: https://www.extremetech.com/extreme/210872-extremetech-explains-what-is-moores-law, [cited 3 September 2018]

[100] Sobieszczanski-Sobieski, J., "Multidisciplinary design optimization: An emerging new engineering discipline", NASA-TM-107761, 1993

[101] "The AIAA Multidisciplinary Design Optimization Technical Committee, White Paper on Industrial Experience with MDO" [online publication] URL: http://web.ift.uib.no/~antonych/concur3.html, [cited 10 September 2018]

[102] Raymer D. P., "Enhancing Aircraft Conceptual Design using Multidisciplinary Optimization", Doctoral Thesis, Royal Institute of Technology, 2002

[103] Martins J. R. R. A., "A Short Course on Multidisciplinary Design Optimization", University of Michigan, 2012

[104] Keane A. J., Nair P. B., "Computational Approaches for Aerospace Design, The pursuit of Excellence", John Wiley & Sons Ltd, 2005

[105] Martins J. R. R. A., "High-Fidelity Multidisciplinary Design Optimization for the Next Generation of Aircraft" [online presentation] URL: https://websites.isae-supaero.fr/IMG/pdf/martins-keynote-2015-06-cmn-lisbon.pdf, [cited 10 September 2018]

[106] Martins J. R. R. A., Lambe A. B., "Multidisciplinary Design Optimization: A Survey of Architectures", AIAA Journal, Vol. 51, No. 9, 2013

[107] Forrester A., Sobester A., Keane A., "Engineering Design via Surrogate Modelling", John Wiley & Sons Ltd, 2008

[108] Bettebghor D., Bartoli N., "Approximation of the critical buckling factor for composite panels", Structural and Multidisciplinary Optimization, Vol. 46, No. 4, 2012

[109] Alonso J. J., LeGresley P., Pereyra V., "Aircraft design optimization", Mathematics and Computers in Simulation, Volume 79, Issue 6, 2009

[110] Deb K., Pratap A., Agrawal S., Meyarivan T., "A fast and elitist multiobjective genetic algorithm: NSGA-II", Technical Report No. 2000001, Indian Institute of Technology Kanpur, 2000

[111] Mukhopadhyay V., McMillin M. L., Ozoroski T. A., "Structural Configuration Analysis of Advanced Flight Vehicle Concepts with Distributed Hybrid-Electric Propulsion", AIAA 2018-1747, 2018

[112] Cristofaro M., "Elements of computational flight dynamics for complete aircraft", Doctoral Thesis, Politecnico di Torino, 2014

[113] Lyu Z., Martins J. R. R. A., "Aerodynamic Design Optimization Studies of a Blended Wing Body Aircraft", Journal of Aircraft, Vol. 51, No. 5, 2014

[114] "The challenge of present and future industrial CFD" [online presentation] URL: https://www.grc.nasa.gov/hiocfd/wp-content/uploads/sites/22/AIAA2015_Challenges_for_CFD_NUMECA_Hirsch.pdf, [cited 5 September 2018]

[115] Jameson A., "Computational Fluid Dynamics and Airplane Design: Its Current and Future Impact" [online presentation] URL: http://aero-comlab.stanford.edu/Papers/jameson-cincin-pm.pdf, [cited 5 September 2018]

[116] Defoort S., Méheut M., Paluch B., Liaboeuf R., Murray R., Mincu D. C., David J. M., "Conceptual design of disruptive aircraft configurations based on High-Fidelity OAD process", AIAA 2018-3663 , 2018

[117] Economon T. D., Palacios F., Copeland S. R., Lukaczyk T. W., Alonso J. J., "SU2: An open-source suite for multiphysics simulation and design", AIAA Journal, Vol. 54, No. 3, 2016

[118] Si H., "TetGen, a Delaunay-Based Quality Tetrahedral Mesh Generator", ACM Transactions on Mathematical Software, Volume 41, Issue 2, 2015

[119] Dodt T., "Introducing the 787" [online presentation] URL: http://www.ata-divisions.org/S_TD/pdf/other/IntroducingtheB-787.pdf, [cited 5 September 2018]

[120] Mader C. A., Kenway G. K., Martins J. R. R. A., Uranga A., "Aerostructural Optimization of the D8 Wing with Varying Cruise Mach Numbers", AIAA 2017-4436, 2017

[121] Greitzer E. M., Bonnefoy P. A., De la Rosa Blanco E., Dorbian C. S., Drela M., Hall D. K., Hansman R. J., Hileman J. I., Liebeck R. H., Lovegren J., Mody P., Pertuze J. A., Sato S., Spakovszky Z. S., Tan C. S., Hollman J. S., Duda J. E., Fitzgerald N., Houghton J., Kerrebrock J. L., Kiwada G. F., Kordonowy D., Parrish J. C., Tylko J., Wen E. A., Lord W. K., "N+3 Aircraft Concept Designs and Trade Studies, Volume 2," Final Report NASA/CR-2010-216794/VOL2, 2010.

[122] Lefebvre T., Schmollgruber P., Blondeau C. and Carrier G., "Aircraft conceptual design in a multi-level, multi-fidelity, multi-disciplinary optimization process", 28th Congress of the International Council of the Aeronautical Sciences ICAS, Brisbane, Australia, 2012

[123] Variyar A., Economon T. D., Alonso J. J., "Multifdelity Conceptual Design and Optimization of Strut-Braced Wing Aircraft using Physics-Based Methods", AIAA 2016-2000, 2016

[124] Moerland E., Pfeiffer T., Böhnke D., Jepsen J., Freund S., Liersch C. M., Chiozzotto G. P., Klein C., Scherer J., Hasan Y. J., Flink J., "On the Design of a Strut-Braced Wing Configuration in a Collaborative Design Environment", AIAA 2017-4397, 2017

[125] Chudoba B., "Stability and Control of Conventional and Unconventional Aircraft Configurations: A Generic Approach", BoD–Books on Demand, 2001

[126] Landman D., Dominion O., Simpson J., Vicroy D., Parker P., "Response Surface Methods for Efficient Complex Aircraft Configuration Aerodynamic Characterization", Journal of Aircraft, Vol. 44, No. 4, 2007

[127] Kay J., Mason W. H., Durham W., Lutze F. and Benoliel A., "Control Authority Issues in Aircraft Conceptual Design: Critical Conditions, Estimation Methodology, Spreadsheet Assessment, Trim and Bibliography", Virginia Polytechnic Institute, 1993

[128] "Control Power Assessment" [online databse] URL: http://www.dept.aoe.vt.edu/~mason/Mason_f/MRsoft.html, [cited 1 September 2018]

[129] "CS-25 Large Aeroplanes" [online database] URL: https://www.easa.europa.eu/certification-specifications/cs-25-large-aeroplanes, [cited 1 September 2018]

[130] "MIL-STD-1797A, Flying Qualities of Piloted Aircraft", Department of Defense Handbook, 1997

[131] Lan, C. E., "VORSTAB: A computer program for calculating lateral-directional stability derivatives with vortex flow effect", NASA-CR-172501, 1985

[132] "Impact of Active Control Technology on Airplane Design", AGARD Conference Proceedings No. 157, 1975

[133] Carpenter C., "Flightwise Volume 2, Aircraft Stability and Control", Airlife Publishing Ltd, 2002

[134] Sauvinet F., "Longitudinal active stability: key issues for future large transport aircraft", 22nd Congress of the International Council of the Aeronautical Sciences ICAS, Harrogate International Conference Centre, UK, 2000

[135] Perez R. E., Liu H. T., Behdinan K., "Multidisciplinary Optimization Framework for Control-Configuration Integration in Aircraft Conceptual Design", Journal of Aircraft, Vol. 43, No. 6, AIAA, 2006

[136] Risse K., Anton E., "Methodology for Flying Qualities Prediction and Assessment in Preliminary Aircraft Design", AIAA 2010-9261, 2010

[137] Verseux O., Sommerer Y., "New challenges for engine nacelle compartments pressure and thermal loads management with aircraft engine evolution", 24th Congress of the International Council of the Aeronautical Sciences ICAS, St. Petersburg, Russia, 2014

[138] "NASA Armstrong Fact Sheet: NASA X-57 Maxwell" [website] URL: https://www.nasa.gov/centers/armstrong/news/FactSheets/FS-109.html, [cited 2 October 2018]

[139] Falck R. D., Chin J. C., Schnulo S. L., Burt J. M., Gray J. S., "Trajectory Optimization of Electric Aircraft Subject to Subsystem Thermal Constraints", AIAA 2017-4002, 2017

[140] Dubreuil S., Bartoli N., Gogu C., Lefebvre T., "Propagation of Modeling Uncertainty by Polynomial Chaos Expansion in Multidisciplinary Analysis", Journal of Mechanical Design, Vol. 138, Issue 11, 2016

[141] Sudret B., "Uncertainty propagation and sensitivity analysis in mechanical models, Contribution to structural reliability and stochastic spectral methods", Université Blaise Pascal – Clermont II, 2008

[142] Kirby M. R., Mavris D. N., "Forecasting Technology Uncertainty in Preliminary Aircraft Design", SAE Technical Paper 1999-01-5631, 1999

[143] Chakraborty I., Mavris D. N., "Assessing Impact of Epistemic and Technological Uncertainty on Aircraft Subsystem Architectures", Journal of Aircraft, Vol. 54, No. 4, 2017

[144] "GABRIEL" [website] URL: http://www.gabriel-project.eu/, [cited 1 September 2018]

[145] "Description of Work", GABRIEL Project, Grant agreement n°284884, 2011

[146] Schmollgruber P., "Preliminary Definition of the GABRIEL concept", Deliverable D2.8, GABRIEL EU Project, Grant agreement n°284884, 2012

[147] Rogg, D., "Conceptual design of the ground-based system related to the GABRIEL concept", Deliverable D3.5, GABRIEL Project, Grant Agreement no. 284884, 2013

[148] Rohacs, J., Rohacs D., "The Potential Application Method of Magnetic Levitation Technology – as a Ground-Based Power – to Assist the Aircraft Take-Off and Landing Processes", Aircraft Engineering and Aerospace Technology, Vol. 86, Issue 3, 2014

[149] E. Roux, "Pour une approche analytique de la dynamique du vol", Doctoral Thesis, ISAE-Supaero, 2005

[150] E. Roux, "Turbofan and Turbojet Engines: database handbook", Editions Elodie Roux, 2007

[151] Dupont W. P., Colongo C., "Preliminary design of commercial transport aircraft", ISAE-Supaero, 2012

[152] Michaut C., Cavalli D., Huynh H. T., "Conceptual design of civil transport aircraft by a numerical optimization technique", 17th Congress of the International Council of the Aeronautical Sciences ICAS, Stockholm, Sweden, 1990

[153] F. Morel, "Multivariate optimization applied to conceptual design of high capacity long range aircraft", 19th Congress of the International Council of the Aeronautical Sciences ICAS, Anaheim (CA), USA, 1994

[154] Airbus Flight Operations Support and Line Assistance, "Getting the Grips with Aircraft Performance", Airbus, 2002

[155] “Climbing Flight Performance” [online publication] URL: http://www.dept.aoe.vt.edu/~lutze/AOE3104/climb.pdf, [cited 2 September 2018]

[156] “ModelCenter Integrate” [website] URL: https://www.phoenix-int.com/product/modelcenter-integrate/, [cited 2 September 2018]

[157] “CeRAS, Central Reference Aircraft data System” [website] URL: http://ceras.ilr.rwth-aachen.de/trac/wiki/CeRAS/AircraftDesigns/CSR01, [cited 11 September 2018]

[158] “Electronic Code of Federal Regulations”, Title 14, Chapter I, Subchapter C, Part 25 [Website] URL: https://www.ecfr.gov/, [cited 13 September 2018]

[159] Schmitt D., Gollnick V., “Air Transport System”, Springer-Verlag Wien, 2016

[160] “SESAR 2020: developing the next generation of European Air Traffic Management” [online publication] URL: https://ec.europa.eu/research/press/jti/factsheet_sesar-web.pdf, [cited 14 September 2018]

[161] Jacquemart D., Morio J., “Adaptive interacting particle system algorithm for aircraft conflict probability estimation”, Aerospace Science and Technology, vol. 55, pp.431-438, 2016

[162] Sarrat C., Aubry S., Chaboud T., Lac C., “Modelling Airport Pollutants Dispersion at High Resolution”, Aerospace 2017, 4(3), 46, 2017

[163] Bedouet J., Dubot T., Basora L., “Towards an Operational Sectorisation based on Deterministic and Stochastic Partitioning Algorithms”, 6th SESAR Innovation Days, 2016

[164] “Eurocontrol”, [website] URL: http://www.eurocontrol.int/, [cited 14 September 2018]

[165] “Base of Aircraft DAta (BADA), Aircraft Performance Modelling Report”, EEC Technical/Scientific Report No. 2009-009, 2009

[166] Nuic A., Poles D., Mouillet V., “BADA: An advanced aircraft performance model for present and future ATM systems”, International Journal of Adaptive Control and Signal Processing, vol. 24, 2010

[167] Hermetz J., Ridel M., Doll C., “Distributed electric propulsion for small business aircraft, a concept-plane for key-technologies investigations”, 30th Congress of the International Council of the Aeronautical Sciences ICAS, Daejeon, Korea, 2016

[168] Sgueglia A., Schmollgruber P., Bartoli N., Atinault O., Benard E., Morlier J., “Exploration and Sizing of a Large Passenger Aircraft with Distributed Ducted Electric Fans”, AIAA 2018-1745, 2018

[169] Walker S. A., “Design of a control configured tanker aircraft”, NASA 76N31158, 1976

[170] Hummel D., “The Use of Aircraft Wakes to Achieve Power Reductions in Formation Flight”, AGARD Conference Proceedings No. 584, 1996

[171] Xu J., Ning S. A., Bower G, Kroo I., “Aircraft Route Optimization for Formation Flight”, Journal of Aircraft, Vol. 51, No. 2, 2014

[172] Durango G., Lawson C., Shahneh A. Z., “Formation flight investigation for highly efficient future civil transport aircraft”, The Aeronautical Journal, Volume 120, Issue 1229, 2016

[173] Ledogar J., Hermetz J., Sohier H., Oswald J., Rantet E., “EOLE, an innovative flying scale demonstrator for air-launch-to-orbit automatic systems”, 28th Congress of the International Council of the Aeronautical Sciences ICAS, Brisbane, Australia, 2012

[174] “CNES / ONERA EOLE Program” [website] URL: http://aviation-design-uav.fr/en/sub-scale-demonstrator-cnes-onera-eole/, [cited 15 September 2018]

[175] Schmollgruber P., Bedouet J., Dubot T., Joulia A., Lefèbvre T., “Unmanned Aircraft: from Design to Operations”, ONERA-DLR Aerospace Symposium, Toulouse, 2015

[176] Warwick G., “ESAero Refines Turboelectric Airliner Design For NASA”, [on line article] URL: http://aviationweek.com/technology/esaero-refines-turboelectric-airliner-design-nasa-0, [cited 15 September 2018]

[177] Takahashi T. T., “Regulatory Changes to Enable the Development of More Efficient Transport Category Aircraft”, Journal of Aircraft, Vol. 50, No. 5, 2013

[178] “The new CS-23 – smart and flexible rules that support innovation” [website] URL: https://www.easa.europa.eu/new-cs-23-%E2%80%93-smart-and-flexible-rules-support-innovation, [cited 15 September 2018]

[179] Hwang J.T., Martins J. R. R. A., “Allocation-mission-design optimization of next-generation aircraft using a parallel computational framework”, AIAA 2016-1662, 2016

[180] “Blueprint for the sky, The roadmap for the safe integration of autonomous aircraft” [online publication] URL: https://storage.googleapis.com/blueprint/Airbus_UTM_Blueprint.pdf, [cited 15 September 2018]

[181] “UBER Elevate, Fast-Forwarding to a Future of On-Demand Urban Air Transportation”, UBER, 2016

[182] “Uber's Flying-Car Plan Meets the Regulator It Can't Ignore” [online article] URL: https://www.wired.com/story/uber-flying-cars-faa-regulation/, [cited 15 September 2018]

[183] Goold I., “Waiting for the ’bus”, Aerospace Testing International, UKIP Media & Events LTD, Dorkin, United Kingdom, 2014

[184] Kirkman J., Wood D., Knight T., Gurczak M., Rothlisberger C., Pan Z., Takahashi T., “Design Study for a Highly Fuel Efficient Regional Transport”, AIAA 2016-1029, 2016

[185] “AMC-20 General Acceptable Means of Compliance for Airworthiness of Products, Parts and Appliances” [online databse] URL: https://www.easa.europa.eu/certification-specifications/amc-20-general-acceptable-means-compliance-airworthiness-products-parts, [cited 17 September 2018]

[186] Bedouet J., Huynh N., Kervarc R., “GAMME, a meta-model to unify data needs in simulation modeling”, Symposium on Theory of Modeling & Simulation-DEVS Integrative M&S Symposium, Society for Computer Simulation International, 2013

[187] Klatt B., “Xpand: A closer look at the model2text transformation language”, Language, 10, No. 16, 2008.

[188] Coleman G. J., “Aircraft Conceptual Design – an adaptable parametric sizing methodology”, Doctoral Thesis, the University of Texas at Arlington, 2010

[189] Goraj Z., Frydrychewicz A., Hermetz J., Le Tallec C., “HALE UAV platform optimized for a specialized 20-km altitude patrol mission”, 24th Congress of the International Council of the Aeronautical Sciences ICAS, Yokohama, Japan, 2004

[190] “OpenMDAO” [website] URL: http://openmdao.org/, [cited 18 September 2018]

[191] “SUAVE, An Aerospace Vehicle Environment for Designing Future Aircraft”, [website] URL: http://suave.stanford.edu/, [cited 18 September 2018]

[192] “AGILE project, Aircraft 3rd Generation MDO for Innovative Collaboration of Heterogeneous Teams of Experts” [website] URL: https://www.agile-project.eu/, [cited 18 September 2018]

[193] Pagnano G., “Sustainable development - Clean Sky and the technology challenges”, Second annual Aerospace Symposium “The Aerospace Ecosystem”, University of Glasgow, 2015 [online presentation] URL: https://www.gla.ac.uk/media/media_432749_en.pdf, [cited 18 September 2018]

[194] Nagel B., Böhnke D., Gollnick V., Schmollgruber P., Rizzi A., La Rocca G., Alonso J. J., "Communication in Aircraft Design: can we establish a common language?", 28th Congress of the International Council of the Aeronautical Sciences ICAS, Brisbane, Australia, 2012

[195] Schmollgruber P., Bartoli N., Bedouet J., Defoort S., Gourinat Y., Benard E., Lafage R., Sgueglia A., "Use of a Certification Constraints Module for Aircraft Design Activities", AIAA 2017-3762, 2017

[196] Schmollgruber P., Bartoli N., Bedouet J., Benard E., Gourinat Y., "Improvement of the Aircraft Design process for Air Traffic Management evaluations", AIAA 2018-0283, 2018

[197] Bohari B., Borlon Q., Mendoza-Santos P. B., Sgueglia A., Benard E., Bronz M., Defoort S., "Conceptual Design of Distributed Propellers Aircraft: Non-Linear Aerodynamic Model Verification of Propeller-Wing Interaction in High-Lifting Configuration", AIAA 2018-1742, 2018

[198] Sgueglia A., Schmollgruber P., Benard E., Bartoli N., Morlier J., "Preliminary Sizing of a Medium Range Blended Wing-Body Using a Multidisciplinary Design Analysis Approach", 8th EASN-CEAS International Workshop on Manufacturing for Growth & Innovation, Glasgow, UK, 2018

[199] Nita M., Scholz D., "Estimating the Oswald factor from basic aircraft geometrical parameters", Hamburg University of Applied Sciences, 2012

[200] Kroo I., "Aircraft Design: Synthesis and Analysis" [website] URL: http://rahauav.com/Library/Design-performance/Aircraft%20Design,%20synthesis%20and%20analysis.pdf, [cited 19 September 2018]

[201] "Commission Regulation (EU) No 965/2012", Official Journal of the European Union, 2012

[202] "Airbus A32X FAMILY" [online image] URL: https://fr.wikipedia.org/wiki/Fichier:A32XFAMILYv1.0.png, [cited 23 September 2018]

[203] E. Roux, "Avions civils à réaction", Editions Elodie Roux, 2007

[204] "Commission Regulation (EU) No 8/2008", Official Journal of the European Union, 2007

[205] "A320 Aircraft Characteristics, Airport and Maintenance Planning", Airbus, 2018

[206] Airbus aircraft classification [online document] URL: https://www.airbus.com/content/dam/corporate-topics/publications/backgrounders/techdata/general-information/Airbus-Commercial-Aircraft-ICAO-ARC-FAA-ADG-App-Cat.pdf, [cited 24 September 2018]

[207] Sobol' I.M., "Sensitivity estimates for nonlinear mathematical models", Mathematical modelling and computational experiments", 1(4), 407-414, 1993

[208] Sudret B., "Global Sensitivity Analysis Using Polynomial Chaos Expansions", Reliability Engineering & System Safety, Volume 93, Issue 7, 2008

[209] Blatman G., Sudret B., "Efficient Computational of Global Sensitivity Indices Using Sparse Polynomial Chaos Expansions", Reliability Engineering & System Safety, Vol. 95, Issue 11, 2010

[210] Srinivas N., Deb K., "Multiobjective function optimization using nondominated sorting genetic algorithms" Evolutionay Computation, Vol. 2, No. 3, 1995

[211] "A Free and Open Source Python Library for Multiobjective Optimization" [website] URL: https://github.com/Project-Platypus/Platypus, [cited 24 September 2018]

[212] "SciPy" [website] URL: https://www.scipy.org/index.html, [cited 24 September 2018]

[213] Powell M., "A Direct Search Optimization Method that Models the Objective and Constraint Functions by Linear Interpolation", Advances in Optimization and Numerical Analysis. Mathematics and Its Applications, Vol. 275, Springer, Dordrecht, 1994

[214] Bouhlel M.-A., Bartoli N., Regis R. G., Otsmane A., Morlier, J., "Efficient global optimization for high-dimensional constrained problems by using the Kriging models combined with the partial least squares method", Engineering Optimization, 2018

[215] Jones D. R., Schonlau M., Welch W. J. "Efficient global optimization of expensive black-box functions", Journal of Global optimization, Vol. 13, Issue 4, 1998

[216] Sasena M. J., "Flexibility and efficiency enhancements for constrained global design optimization with kriging approximations", Doctoral Thesis, University of Michigan, 2002

[217] Bouhlel M. A., Bartoli N., Otsmane A., Morlier, J., "Improving Kriging surrogates of high-dimensional design models by Partial Least Squares dimension reduction", Structural and Multidisciplinary Optimization, Vol. 53, Issue 5, 2016

[218] Bouhlel M. A., Bartoli N., Otsmane A., Morlier J., "An improved approach for estimating the hyperparameters of the Kriging model for high-dimensional problems through the partial least squares method", Mathematical Problems in Engineering, 2016

[219] Bartoli N., Bouhlel M. A., Kurek I., Lafage R., Lefebvre T., Morlier J., Regis R., Priem R., Stilz V., "Improvement of efficient global optimization with application to aircraft wing design", AIAA 2016-4001, 2016

[220] Bartoli N., Lefebvre T., Dubreuil S., Olivanti R., Bons N., Martins J. R. R. A., Bouhlel M.-A., Morlier J., "An adaptive optimization strategy based on mixture of experts for wing aerodynamic design optimization", AIAA 2017-4433, 2017

[221] Bartoli N., Lefebvre T., Dubreuil S., Panzeri M., D'Ippolito R., Anisimov K., Savelyev A., "Robust Nacelle Optimization Design investigated in the AGILE European project", AIAA 2018-3250, 2018

[222] "Aerospace Toolbox" [website] URL: https://www.mathworks.com/products/aerotb.html, [cited 16 October 2018]

[223] Zipfel P. H., "Modeling and Simulation of Aerospace Vehicle Dynamics", 3rd Edition, AIAA, 2014

[224] "JSBSim" [website] URL: http://jsbsim.sourceforge.net/, [cited 16 October 2018]

[225] "FlightGear Flight Simulator" [website] URL: http://home.flightgear.org/, [cited 16 October 2018]

[226] Kim J. P., "Evaluation of Unmanned Aircraft Flying Qualities Using JSBSim", Master Thesis, AFIT-ENY-MS-16-M-221, 2016

[227] "The Endless Runway" [website] URL: https://endlessrunway-project.eu/, [cited 16 October 2018]

[228] Hanke C. R., Nordwall D. R., "The simulation of a Jumbo Jet Transport Aircraft – Volume II : Modeling data", NASA-CR-114494, 1970

[229] Schmollgruber P., De Giuseppe A., Dupeyrat M., "Aircraft aspects of the Endless Runway", Deliverable D3.2 of the EU project "The Endless Runway" (Contract N° 308292), 2013

[230] Lan C. E., "VORSTAB: A computer program for calculating lateral-directional stability derivatives with vortex flow effect", NASA-CR-172501, 1985

[231] "The USAF Stability And Control Digital Datcom, Volume I, Users Manual", USAF Technical Report AFFDL-TR-79-3032, 1979.

[232] “AVL – Athena Vortex Lattice” [website] URL: http://web.mit.edu/drela/Public/web/avl/, [cited 17 October 2018]

[233] “Tornado, a Vortex Lattice method implemented in Matlab” [website] URL: http://tornado.redhammer.se/, [cited 17 October 2018]

[234] Cöllen L., “Development of a Hybrid Aerodynamic Module for Aircraft Conceptual Design”, Diploma Thesis, Technische Universität Hamburg-Harburg / ONERA, 2012

[235] “Datcom by Holy Cows, Inc.” [website] URL: http://www.holycows.net/datcom/, [cited 17 October 2018]

[236] “CATIA” [website] URL: https://www.3ds.com/products-services/catia/, [cited 18 October 2018]

[237] “Devis de masse des avions”, AIR 2001/D, Edition N°5, Direction Générale de l’Armement, 1984

[238] “Airbus A350-900 Cutaway” [website] URL: https://www.flightglobalimages.com/airbus-a350-900-cutaway/print/10861182.html [cited 18 October 2018]

[239] “Boeing 787-9 Cutaway” [website] URL: https://www.flightglobalimages.com/boeing-787-9/print/10044478.html [cited 18 October 2018]

[240] “Embraer 175 Cutaway” [website] URL: https://www.flightglobalimages.com/embraer-175-cutaway-drawing/print/4522874.html [cited 18 October 2018]

[241] “Embraer 195 Cutaway” [website] URL: https://www.flightglobalimages.com/embraer-195-cutaway-poster/print/1571197.html [cited 18 October 2018]

[242] Stevens B. L., Lewis F. L., “Aircraft Control and Simulation”, 2nd edition, Wiley, 2003

[243] Nelson R. C., “Flight Stability and Automatic Control”, 2nd Edition, McGraw-Hill Education, 1997

[244] “Procedures for Navigation Services - Air Traffic Management”, Document 4444, 16th edition, 2016

[245] Altman A., “Closing the Loop on Aircraft Conceptual Sizing using the Merlin Flight Simulator”, AIAA 2015-1012, 2015

[246] “Technical Provisions for Mode S Services and Extended Squitter”, Doc 9871, 2nd edition, ICAO, 2012

[247] Priem R., Bartoli N., Diouane Y., Dubreuil S., Lefebvre T., “An adaptive feasibility approach for constrained Bayesian optimization with application in aircraft design”, EngOpt 2018, 6th International Conference on Engineering Optimization, 2018

[248] Dubreuil S., Bartoli N., Gogu C., Lefebvre T., Colomer J. M., “Extreme value oriented random field discretization based on an hybrid polynomial chaos expansion - Kriging approach”, Computer Methods in Applied Mechanics and Engineering, Vol. 332, 2018

Appendix A – Overview of aircraft conceptual design processes

Related to Section 1.4.3., Figure 108 illustrates the aircraft conceptual design process proposed by Roskam [1].

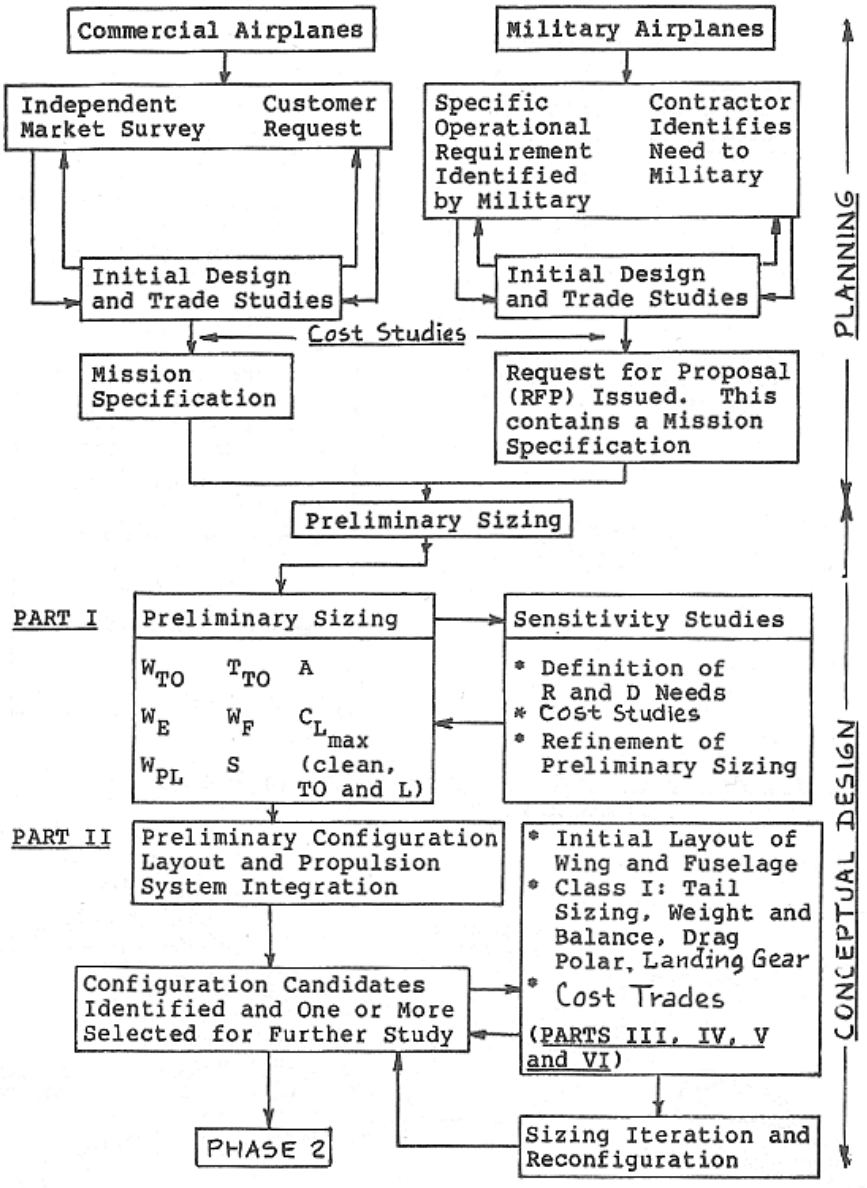

Figure 108: Planning and conceptual design [1]

Also related to Section 1.4.3., Figure 109 illustrates the aircraft conceptual design process proposed by Raymer [5].

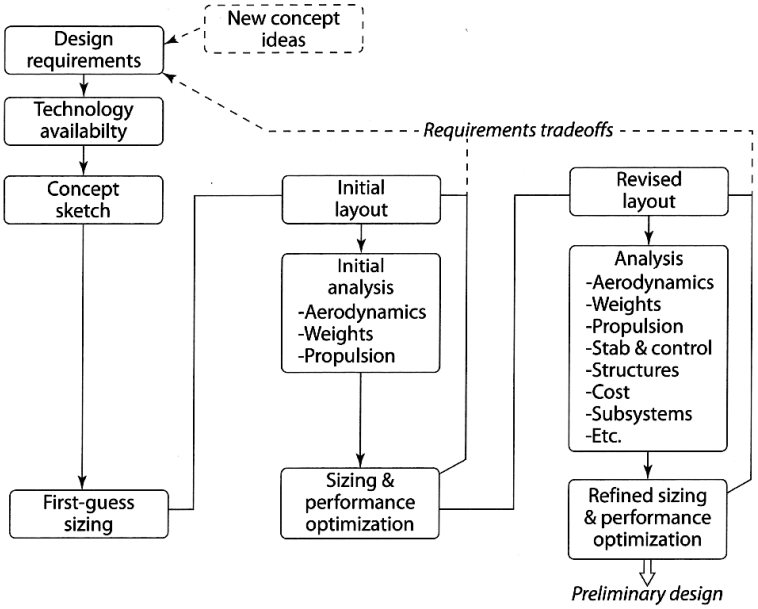

Figure 109: Aircraft conceptual design process [5]

Always with the idea to illustrate various visions of the conceptual desing process (Section 1.4.3.), Figure 110 illustrates the aircraft conceptual design process proposed by Nicolai [13].

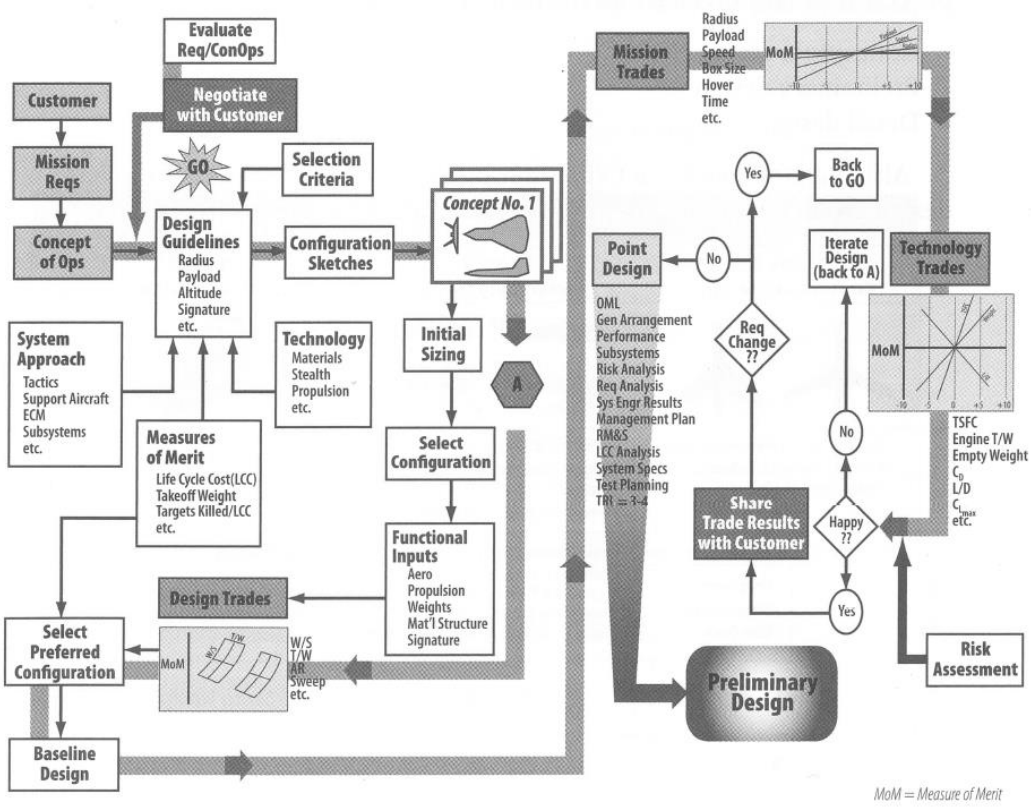

Figure 110: The conceptual design process [13]

To complement discussion in Section 1.4.3., Figure 111 shows the jetliner baseline design process by Torenbeek [46].

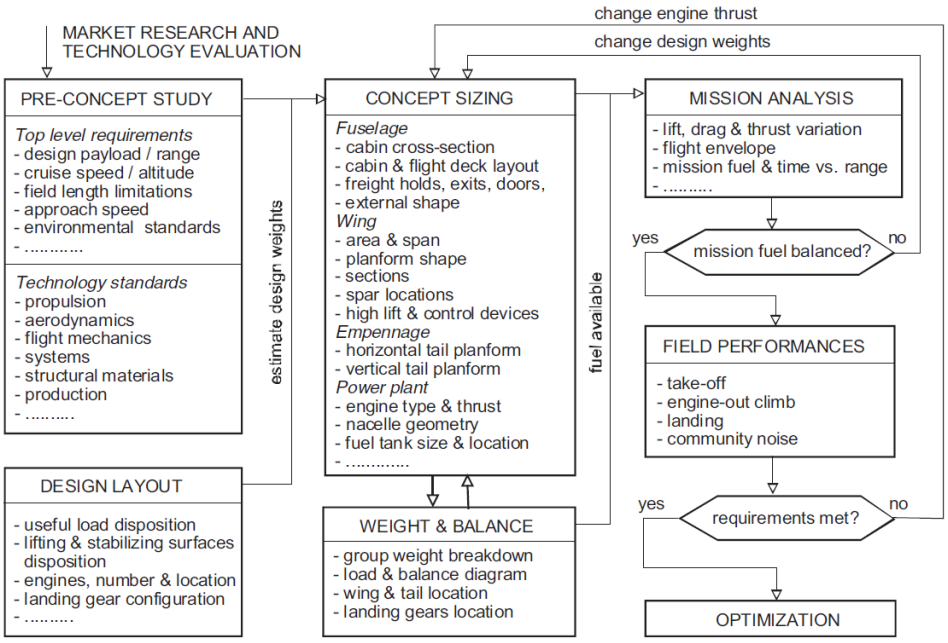

Figure 111: Jetliner baseline design process [46]

Appendix B – Main Inputs and Outputs of FAST

This table provides a detailed description of the modules included in FAST (see Section 3.3.2.).

Table 23: Description, Input and Output of the different Python modules to be found in FAST

MODULE	DESCRIPTION	INPUT	OUTPUT
aerodynamics.py	Compute the aircraft polars for different configurations	Aircraft	C_L
		Mach number	C_D
		Altitude	ΔC_L due to flap and slat
		High lift configurations	ΔC_D due to flap and slat
atmosphere.py	Compute atmospheric conditions	Altitude	Local temperature
		ΔT with respect to ISA	Local density
			Local pressure
			Dynamic viscosity coeff.
			Local speed of sound
ceras_engine.py	Compute the engine parameters according to CeRAS model	Mach number	Thrust
		Altitude	Specific Fuel Consumption
		Throttle setting	
		Flight phase	
consumption_breakdown.py	Compute the fuel consumed for the sizing mission	Mission profile (output of simulation)	Fuel breakdown
			Weight after Take-Off
doc.py	Compute DOC	Common xml file	Direct Operating Costs
geometry.py	Compute the aircraft geometry, sizing and positioning all the components	Common xml file	Aircraft geometry
			Center of gravity, both global and of all the components
initiator.py	Estimate initial values	Number of passengers	Payload
		Design range	Max payload
		Cruise altitude	Maximum Take-Off Weight
		Cruise Mach number	Maximum Landing Weight
		Approach speed	Maximum Zero Fuel Weight
			Wing surface
mass_breakdown.py	Compute the components' weight	Aircraft	Components' weight
		Load conditions	Operating Weight Empty
performance.py	Compute the Sizing mission (made of taxi out, climb, cruise, descent and taxi in) As well as the operational mission	Design range	Mission levels
		Thrust	Mission distances
		Maximum Take-Off Weight	Zero Fuel Weight
		Rotation speed at Take-Off	Landing Weight
			Mission fuel
			Flight time
propulsion_sfc.py	Compute the specific fuel consumption and some thrust conditions	Aircraft	Specific Fuel Consumption
		Altitude	Thrust for one inoperative engine
		Mach number	Take-Off thrust
		Thrust at sea level	
		Net thrust	
rubber_engine.py	Compute the engine parameters according to a parametric model developed by ISAE-SUPAERO and ONERA	Mach number	Specific Fuel Consumption
		Altitude	Max thrust
		Thrust	Engine's weight
		Pressure ratio	Engine's installed weight
		By-Pass ratio	
takeoff.py	Compute the Take-Off parameters with all operative engines	Maximum Take-Off Weight	Engine failure speed
		Take-Off weight	Rotation speed
		Take-Off altitude	Decision speed
		Take-Off ΔT respect to ISA	Lift-Off speed
		Derate ratio	Take-Off climb speed
			Take-Off length
			Take-Off time
			Take-Off consu-ed fuel
wing_sizing.py	Size the wing according to approach speed and mission fuel	Mission fuel	Wing surface
		Maximum Fuel Weight	
		Maximum Landing Weight	
		Approach speed	

Appendix C – Mission plots produced by FAST

The following figures show the plots that are generated by FAST at the end of the Multidisciplinary Design Analysis (see Section 3.3.3.).

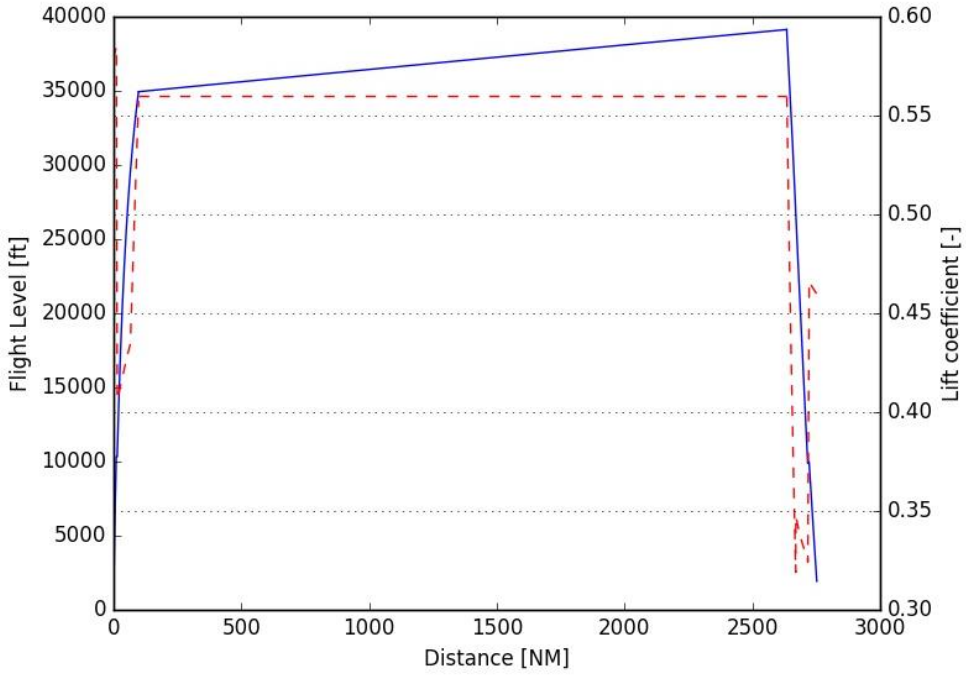

Figure 112: Evolution of Altitude (in blue) and Lift coefficient (in red) for the entire mission (FAST output)

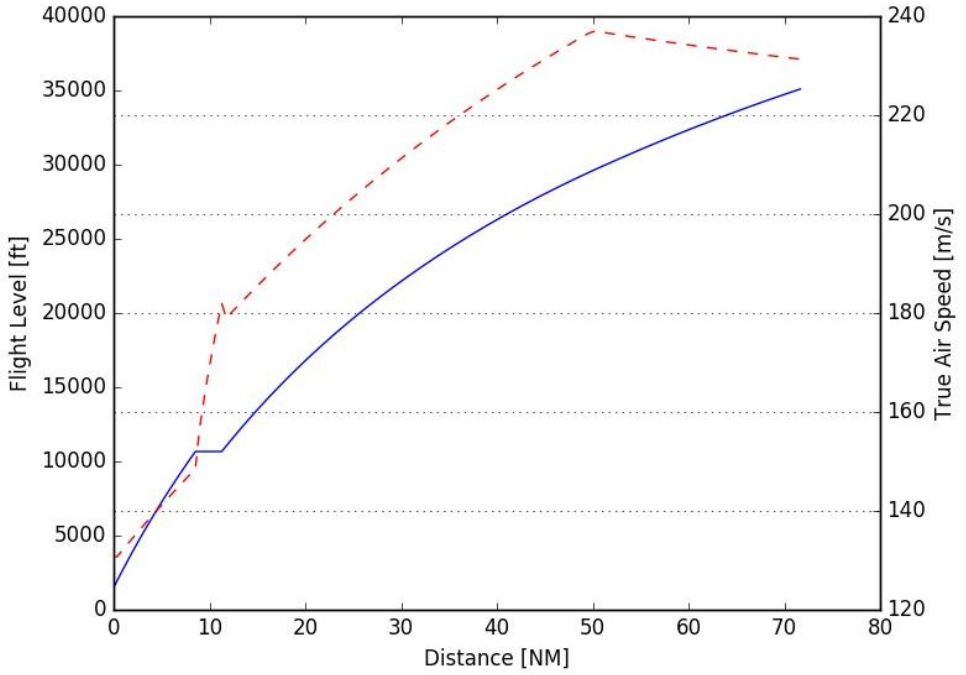

Figure 113: Evolution of Altitude (in blue) and True Air Speed (in red) during climb (FAST output)

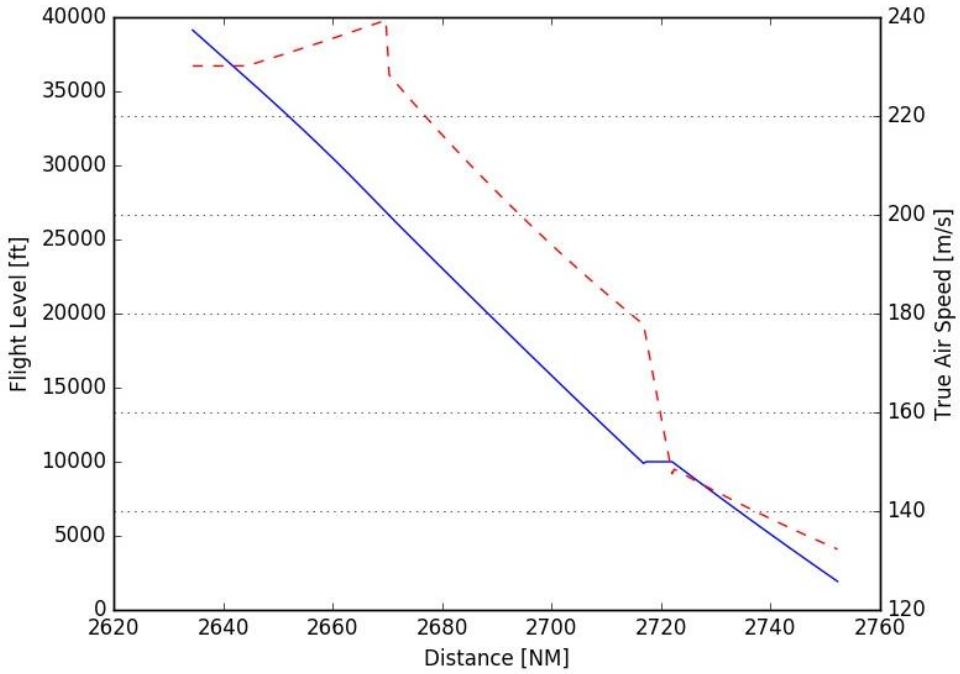

Figure 114: Evolution of Altitude (in blue) and True Air Speed (in red) during descent (FAST output)

Appendix D – High Lift devices performances

The Drag polars computed with DATCOM+PRO (including corrections) discussed in Section 4.4. are presented in Figure 115.

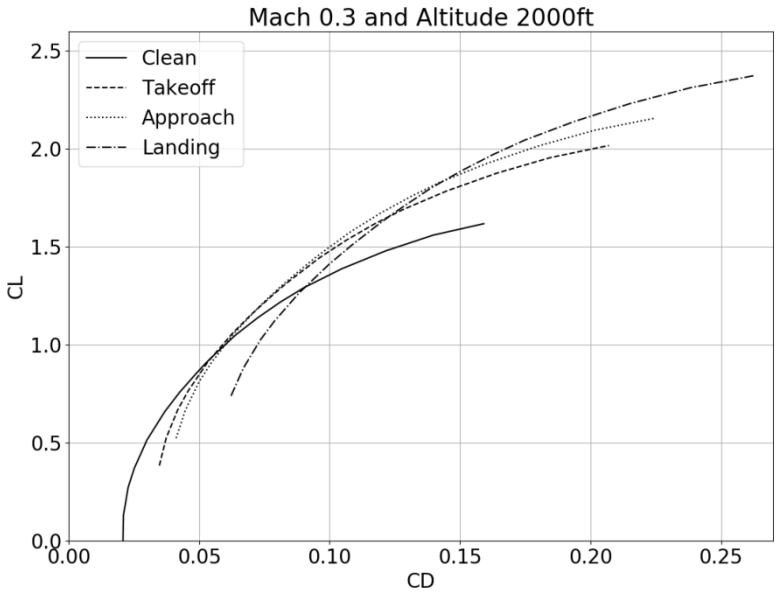

Figure 115: Drag polars obtained with DATCOM+PRO (including correction) for different high lift devices configurations

Appendix E – Mass breakdown within FAST

The mass breakdown implemented within FAST based on the French norm AIR 2001/D [237] is presented in Table 24.

Table 24: Details of the FAST Mass breakdown

A Airframe
A1 Wing
A2 Fuselage
A3 Empennage
A31 Horizontal Tail
A32 Vertical Tail
A4 Flight controls
A5 Landing gear
A51 Main Landing Gear
A52 Nose Landing Gear
A6 Pylons
A7 Paint
B Propulsion
B1 Installed engines
B2 Fuel and oil systems
B3 Unusable oil and fuel
C Systems and fixed installations
C1 Power systems
C11 APU
C12 Electrical Systems
C13 Hydraulical Systems
C2 Life support systems
C21 Insulation, heat shielding
C22 Air conditioning and pressurization
C23 De-icing
C24 Cabin lightning
C25 Seats, crew accommodation
C26 Oxygen system
C27 Safety equipments
C3 Instrument and navigation
C4 Transmissions
C5 Fixed operational systems
C6 Flight kit
D Operational items
D1 Containers and Pallets
D2 Passenger seats
D3 Catering equipment, drinking water
D4 Passenger safety equipment
D5 Cabin toilet equipment
E Crew
F Fuel
G Payload

Appendix F – Wind forecast

Figure 116 illustrates the weather forecast on the day of interest with a map of wind barbs: the long line represents the wind direction while the short barbs indicate the speed (a short barb represents 5 kt, a long barb corresponds to 10 kt and a pennant is associated to 50 kt).

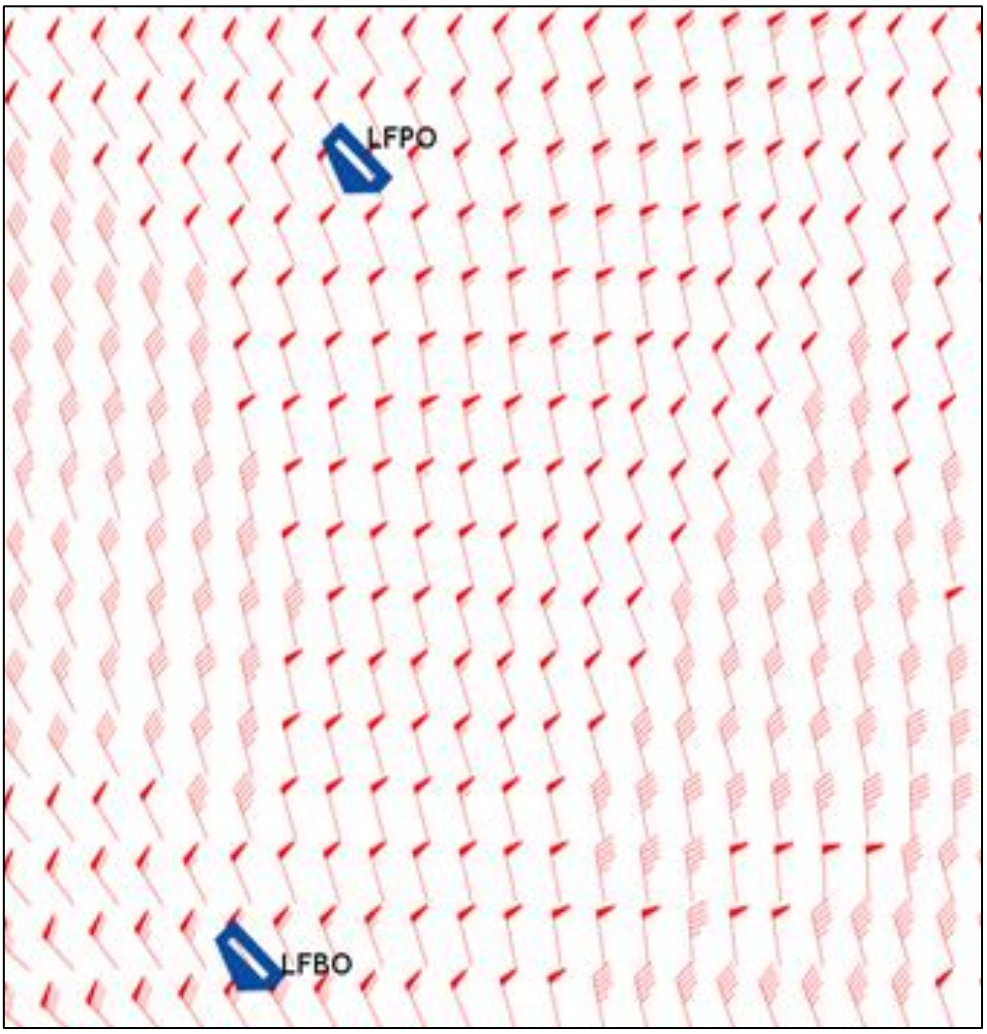

Figure 116: Wind forecast from Meteo France - November 27th, 2017 - 06h00 - 300 hPa - FL300